

**Investigating the role of the JAK/STAT and
MAPK Pathways in Ischaemia/Reperfusion
Injury and Inflammation**

Seán Pío Barry
Medical Molecular Biology Unit
Institute of Child Health
University College London

A thesis submitted for the degree of Doctor of Philosophy (PhD)

at University College London

2009

*“And the newness that was in every stale thing when we
looked at it as children”*

Patrick Kavanagh

*“You got to know when to hold em, know when to fold em,
know when to walk away and know when to run”*

Kenny Rogers

Abstract

The signal transducer and activator of transcription (STAT) proteins are a family of transcription factors which transduce extracellular signals from cytokines, growth factors and G-proteins to the nucleus. STATs become activated by phosphorylation and translocate to the nucleus where they bind to specific target promoters. STAT1 has previously been shown to have a role in inducing apoptosis in the myocardium following ischaemia/reperfusion injury (I/R), however the role of STAT3 in myocardial apoptosis is less clear. Here it is shown that STAT3 is phosphorylated in cardiac cells both *in vitro* and *in vivo* in response to I/R injury and plays a protective role by reducing the levels of apoptosis. Several modulators of STAT3 activity were found to be upregulated following I/R, including JAK2, SOCS3 and GRIM-19. STAT3 was also found to be important in regulating DNA damage and repair through altered activity of DNA damage response proteins. Administration of the antioxidant tempol *in vivo*, reduced infarct size in a rat model of I/R injury and this was accompanied by a reduction in STAT1 and STAT3 phosphorylation. Increasing STAT1 phosphorylation with IFN- γ treatment abolished the protective effect of tempol, suggesting that inhibition of STAT1 phosphorylation may be a key protective effect of tempol infusion. Affymetrix microarray analysis of hearts from the *in vivo* I/R model identified several novel gene expression changes and uncovered transcriptional reduction in large numbers of genes involved in mitochondrial respiration and transport. In addition, this approach identified several possible new regulators of cardiac protection mediated by tempol and the urocortin hormones.

The mitogen activated protein kinase (MAPK) family is involved in sensing cellular stress and play key roles in I/R injury and inflammation. MAPK activity is balanced by MAPK phosphatases (MKPs) such as MKP-1 and the role of MKP-1 in modulating the immune response was investigated. Mice deficient in MKP-1 were more susceptible to endotoxic shock and had elevated levels of serum cytokines. MKP-1 was found to be upregulated following toll-like receptor (TLR) stimulation and this was dependent on the signaling adaptors MyD88 and Trif. Macrophages deficient in MKP-1 had increased phosphorylation of p38 MAPK and JNK following TLR stimulation and secreted elevated amounts of the pro-inflammatory cytokines TNF- α , IL-12 and the anti-inflammatory cytokine IL-10. The temporal control and regulation of cytokine production in response to TLR stimulation was dissected using pharmacological inhibition of MAPKs. MKP-1 was not found to contribute to T cell differentiation but did have a role to play in the adaptive immune response as MKP-1-deficient mice failed to recover from an experimental model of multiple sclerosis.

This thesis is dedicated to my parents

Acknowledgements

First and foremost I would like to thank my parents who throughout my life always told me I could be whatever I wanted to and for their constant love and support. All those years of encouragement really paid off!

I would like to thank Prof. David Latchman for giving me the opportunity to work in his lab and letting me have the freedom to pursue my scientific interests. My appreciation goes to Paul Townsend for his support and insight over the last few years and also to Steph and Dicko. Thanks to the Bogue foundation for providing me with a fellowship to travel to Yale and to Richard Flavell for giving me the opportunity to work in his lab there. Special thanks to Hongbo Chi for really looking after me at Yale and for all he taught me there.

The journey over the last few years would have been far less fun and interesting without all the wonderful people who have been part of MMBU, both past and present. Jimmy, Mattia, Naushaad, Dan, Charis, Emma, because of you guys I got to a rare thing; spend each day working with friends rather than colleagues. My thanks aswell to our tireless lab manager John, who keeps the whole thing together.

Finally I would like to thank Sam for her love and support, you make it all worthwhile. Is tú grá mo chroí.

Declaration: The work described in this thesis was carried out by the author unless otherwise stated

Publications in the course of this work:

Barry SP, Lawrence KM, Townsend PA, Soond SM, McCormick J, Hubank M, Eaton S, Sivarajah A, Knight RA, Thiernemann C, Latchman D and Stephanou A. Gene expression profiling reveals novel targets of urocortin mediated cardioprotection and free radical inhibition. *Physiological Genomics*, 2009; *Accepted subject to revision*.

Barry SP, Townsend PA, McCormick J, Knight RA, Scarabelli TM, Latchman DS and Stephanou A. Genetic Manipulation of STAT3 Sensitizes Cells to Oxidative Stress. *Biochem Biophys Res Commun*. 2009, 385:324-9.

Soond SM, **Barry SP**, Melino G, Knight RA, Latchman DS and Stephanou AS. p73-mediated transcriptional activity is negatively regulated by polo-like kinase 1. *Cell Cycle* 2008, 7(9):1214-23.

Soond SM, Townsend PA, **Barry SP**, Knight RA, Latchman DS and Stephanou A. ERK and the F-box protein betaTRCP target STAT1 for degradation. *J Biol Chem* 2008, 283(23):16077-83.

Barry SP, Jayasinghe SN, Latchman DS and Stephanou A. Gene expression studies on bio-electrosprayed primary cardiac myocytes. *Biotechnology Journal* 2008, 3(4):530-5.

Barry SP, Davidson SM and Townsend PA. Molecular regulation of cardiac hypertrophy. *International Journal of Biochemistry and Cell Biology* 2008, 40(10):2023-39.

Barry SP, Jayasinghe SN, Latchman DS and Stephanou A. Bio-electrospraying primary neonatal cardiac myocytes. *Bioprocessing Journal* 2007, 6(1):5-8.

Barry SP, Townsend PA, Latchman DS and Stephanou A. Role of the JAK-STAT pathway in myocardial injury. *Trends in Molecular Medicine* 2007, 13(2):82-89.

McCormick J*, **Barry***, Sivarajah A, Stefanutti G, Townsend PA, Lawrence KM, Eaton S, Knight RA, Thiernemann C, Latchman DS, Stephanou A. Free radical scavenging inhibits STAT phosphorylation following in vivo ischaemia/reperfusion injury. *FASEB J*. 2006, 20(12):2115-7
*Joint first author.

Chi H, **Barry SP**, Roth R, Wu J, Jones EA, Bennett AM and Flavell RA. Dynamic regulation of pro- and anti-inflammatory cytokines by MKP-1 in innate immune responses. *Proc Natl Acad Sci U S A* 2006, 103(7):2274-9.

Townsend PA, Craig MS, Davidson SM, McCormick J, **Barry S** et al. STAT1 facilitates the ATM activated checkpoint pathway following DNA damage. *Journal of Cell Science* 2005, 118:1629-39.

Table of Contents

Abstract	3
Dedication	4
Acknowledgements	5
Publications in the course of this work	6
Table of contents	7
List of figures	12
List of Tables	16
Abbreviations	17
Chapter 1: Introduction	20
1.1 Myocardial Infarction	21
1.2 Ischaemia/Reperfusion Injury	22
1.2.1 Mechanisms of I/R Induced Cell Death	24
1.2.2 <i>Caspases</i>	24
1.2.3 <i>Bcl-2 Proteins</i>	27
1.2.4 <i>Inhibitors of Apoptosis (IAPs)</i>	28
1.2.5 <i>Evidence for Apoptosis Mediated Cell Death During I/R Injury</i>	29
1.2.6 <i>The Mitochondrial Permeability Transition Pore</i>	31
1.2.7 <i>Reactive Oxygen Species (ROS) in Myocardial Cell Death</i>	32
1.2.8 <i>Ca²⁺ Overload and Contracture</i>	34
1.3 The JAK/STAT Pathway	35
1.3.1 <i>JAK/STAT Family Members</i>	35
1.3.2 <i>STAT Activation</i>	36
1.3.3 <i>STAT Nuclear Import</i>	39
1.3.4 <i>STAT Nuclear Export</i>	40
1.3.5 <i>STAT Serine Phosphorylation</i>	41
1.3.6 <i>STAT Dephosphorylation</i>	43
1.3.7 <i>Negative Regulation of STATs by SOCS</i>	44
1.3.8 <i>Inhibition of STAT DNA Binding by PIAS</i>	47
1.3.9 <i>Inhibition of STAT3 Nuclear Translocation by GRIM-19</i>	47
1.3.10 <i>Non-Transcriptional Regulation of Gene Expression by STATs</i>	48
1.4 The JAK/STAT Pathway and Cardiac Injury	50
1.4.1 <i>JAK/STAT Signalling– A Key Player in Apoptosis</i>	50
1.4.2 <i>STATs as Mediators of Myocardial Cell Death</i>	51
1.4.3 <i>JAK/STAT Pathway in Ischaemic Preconditioning</i>	52
1.4.4 <i>Role of STAT1 and 3 in Hypertrophy and Angiogenesis</i>	53
1.5 Urocortins	56
1.5.1 <i>The Urocortin Family</i>	56
1.5.2 <i>Urocortins and Heart Failure</i>	56
1.5.3 <i>Urocortins and Ischaemia</i>	57
1.6 Mitochondrial Transport	58

1.6.1 Import into the Mitochondria	58
1.6.2 The TOM Complex	58
1.6.3 The TIM22/TIM23 Complex	60
1.6.4 The SAM Complex	61
1.7 The DNA Damage Response	61
1.7.1 Double Strand Breaks	61
1.7.2 Initiation of the DNA Damage Response: ATM and H2AX	61
1.7.3 Amplification of the DNA Damage Response: MDC1	64
1.8 The Innate Immune System	65
1.8.1 Inflammation	65
1.8.2 Toll-Like Receptors (TLR)	66
1.8.3 TLR Adaptors	67
1.9 The Adaptive Immune System	69
1.9.1 Antigen Presentation	69
1.9.2 CD8 Cells	69
1.9.3 CD4 Cells and Th1/Th2/Th17 Differentiation	69
1.10 Cytokines	71
1.10.1 TNF	71
1.10.2 IL-10	73
1.10.3 IL-12	73
1.11 MAPK Signalling in the Innate Immune System	73
1.11.1 Upstream Signals	73
1.11.2 p38 MAPK	75
1.11.3 c-Jun N-terminal Kinase (JNK)	76
1.11.4 Extracellular Regulated Kinase (ERK)	77
1.11.5 MAPK Phosphatase -1 (MKP-1)	77
1.12 Inflammatory Diseases	79
1.12.1 Multiple Sclerosis	79
1.12.2 Inflammatory Bowel Disease (IBD)	80
Chapter 2: Materials and Methods	82
2.1 Reagents	83
2.2 Animals	83
2.3 In Vivo Procedures	84
2.3.1 Myocardial Ischaemia and Reperfusion in the Rat	84
2.3.2 Endotoxic shock	85
2.3.3 Listeria Infection	85
2.3.4 Experimental Autoimmune Encephalomyelitis (EAE)	85
2.3.5 Dextran Sulphate Sodium (DSS) Induced Colitis	86
2.3.6 Middle Cerebral Artery Occlusion (MCAO)	86
2.4 Cell Culture	86
2.4.1 Freezing and Recovery of Cell Lines	86
2.4.2 Preparation of Neonatal Rat Ventricular Cardiac Myocytes	87

2.4.3 Hypoxia/Reoxygenation of Neonatal Rat Ventricular Cardiac Myocytes	87
2.4.4 Isolation of Bone Marrow Derived Macrophages	87
2.4.5 Isolation of Bone Marrow Derived Dendritic Cells	88
2.4.6 T Cell Isolation from Mouse Spleen and Lymph Node	88
2.4.7 T cell Differentiation	89
2.4.8 Preparation of High Titre Adenoviral Stocks	89
2.5 Analysis of Protein Levels	90
2.5.1 Western Blotting	90
2.5.2 ELISA	90
2.5.3 Immunohistochemistry	91
2.5.4 Intracellular staining	91
2.5.6 Determination of tissue malondialdehyde concentration	91
2.5.7 Nuclear Extract	92
2.5.8 Electromobility Shift Assay (EMSA)	92
2.6 Gene Expression Analysis	93
2.6.1 RNA Extraction	93
2.6.2 cDNA Synthesis	94
2.6.3 Quantitative Real Time PCR (qPCR)	94
2.6.4 Luciferase Promoter Assay	95
2.7 Affymetrix Microarray Analysis	95
2.7.1 cDNA Preparation	95
2.7.2 Preparation of Biotinylated cRNA Target by In Vitro Transcription	96
2.7.3 Target cRNA Fragmentation and Hybridisation	96
2.7.4 Fluidics Protocol for Microarray Staining	97
2.7.5 Microarray Data Analysis	97
2.7.6 Ingenuity Pathway Analysis	98
2.8 Propagation and Purification of Plasmid DNA	98
2.8.1 Preparation of Competent JM109	98
2.8.2 Transformation of JM109	99
2.8.3 Large Scale plasmid DNA Extraction from E.Coli	99
2.8.4 DNA Restriction Digest and Agarose Gel Electrophoresis	100
2.8.5 DNA Transfection	100
2.9 Cell Death Measurements	100
2.9.1 TdT mediated dUTP nick end labeling (TUNEL)	100
2.9.2 Exclusion of Trypan Blue	101
2.9.3 Annexin V Staining	101
2.9.4 Quantification of Infarct Size in the Heart	102
2.9.5 Statistical Analysis	102
Chapter 3: Role of STAT1 and STAT3 in I/R Injury	103
3.1 Aims	104
3.2 Overexpression of STAT3 Protects Cardiac Myocytes from Hypoxia/Reoxygenation	105
3.3 Adenoviral Delivery of Dominant Negative STAT3 Increases I/R mediated Cell Death in	108

<i>Cardiac Myocytes</i>	
3.4 <i>Deletion of STAT3 Sensitises Cells to Oxidative Stress and I/R Injury</i>	113
3.5 <i>STAT3 becomes Phosphorylated and Transcriptionally Active Following Ischaemia/Reperfusion in vitro</i>	116
3.6 <i>Oxidative stress induces STAT3 serine phosphorylation through an ERK-dependent pathway</i>	124
3.7 <i>Activation of STAT1 and STAT3 following in vivo ischaemia/reperfusion injury</i>	126
3.8 <i>Increased Expression of STAT3 Target Genes Following in vivo I/R injury</i>	131
3.9 <i>I/R injury in the brain induces distinct kinetics of STAT activity</i>	132
3.10 <i>Reperfusion Induced Myocardial STAT Tyrosine Phosphorylation is Mediated by ROS</i>	134
3.11 <i>Increased Phosphorylation Following IFN-γ Treatment Increases Infarct Size and Reduces the Protective Effect of Tempol</i>	139
3.12 <i>Discussion</i>	142
Chapter 4: Investigating Gene Expression Changes in Myocardial Infarction using Microarray Analysis	147
4.1 <i>Aims</i>	148
4.2 <i>Drug Infusion, Gene Array Procedure and Quality Control</i>	149
4.3 <i>Parameters for Differential Expression</i>	153
4.4 <i>Gene Ontology Analysis of Genes Differentially Expressed by I/R Injury</i>	155
4.5 <i>Differential Expression mediated by Tempol Infusion During I/R</i>	163
4.6 <i>Differential Expression mediated by Ucn1 and Ucn2 Infusion During I/R</i>	166
4.7 <i>Validation of Microarray Data by qPCR</i>	171
4.8 <i>Activation of a STAT3 Transcriptional Programme Following I/R Injury</i>	173
4.9 <i>IL-17 Regulation in I/R injury</i>	179
4.10 <i>Differential Regulation of MAPKs and MKP-1 during I/R Injury</i>	182
4.11 <i>Uracil Metabolism is Altered by I/R Injury</i>	184
4.12 <i>Reduced Expression of Mitochondrial Translation Genes Following I/R Injury</i>	186
4.13 <i>Reduced Expression of Mitochondrial and Respiratory Chain Genes Following I/R Injury</i>	187
4.14 <i>Reduced Expression of Mitochondrial Import Machinery Genes Following I/R Injury</i>	190
4.15 <i>Cardioprotective Genes Induced by Ucn1 and Ucn2</i>	193
4.16 <i>Discussion</i>	197
Chapter 5: Regulation of the DNA Damage Response by STAT3	203
5.1 <i>Aims</i>	204
5.2 <i>STAT3^{-/-} MEFs Repair DNA Less Efficiently Than Wild Type Cells</i>	204
5.3 <i>STAT3^{-/-} MEFs Show Reduced Activity of the ATM/H2AX Pathway</i>	207
5.4 <i>STAT3 Facilitates DNA Damage Mediated Upregulation of MDC1</i>	210
5.5 <i>Discussion</i>	214

Chapter 6: Regulation of the MAPK Pathway in Inflammation	220
6.1 Aims	221
6.2 <i>MKP-1 Deficient Mice have Elevated Cytokine Production, are Hyperresponsive to Endotoxic Shock and are Less Susceptible to Listeria Monocytogenes Infection in vivo</i>	221
6.3 <i>MKP-1 Negatively Regulates p38 MAPK, JNK and AP-1 Activity and iNOS expression</i>	226
6.4 <i>TLR Mediated MKP-1 Expression Proceeds Through TRIF and MyD88</i>	229
6.5 <i>Regulation of IL-10 by MKP-1</i>	232
6.6 <i>Dynamic Regulation of TNF-α is Mediated Through IL-10 in MKP-1^{-/-} Macrophages</i>	238
6.7 <i>MKP-1 Activity Promotes IL-12 Expression</i>	244
6.8 <i>MKP-1 Deficiency has no Effect on the Outcome of DSS Induced Colitis</i>	249
6.9 <i>MKP-1 Deficiency Impairs Recovery from Experimental Autoimmune Encephalomyelitis</i>	250
6.10 <i>Loss of MKP-1 does not Effect T Cell Differentiation</i>	252
6.11 <i>Discussion</i>	257
Chapter 7: General Discussion and Future Work	263
Appendix 1	272
Appendix 2	273
Appendix 3A - Microarray: IR Vs Sham	273
Appendix 3B - Microarray: Tempol Vs IR	293
Appendix 3C - Microarray: Ucn1 Vs IR	295
Appendix 3D - Microarray: Ucn2 Vs IR	297
References	300

List of Figures

Figure 1.1 - Lethal reperfusion injury increases myocardial infarct size	23
Figure 1.2 - The three main pathways of apoptosis	26
Figure 1.3 - Model of STAT protein structure	36
Figure 1.4 - Outline of the JAK/STAT pathway	37
Figure 1.5 - JAK usage by cytokines	38
Figure 1.6 - STAT1 conformations	39
Figure 1.7 - STAT import/export cycle	41
Figure 1.8 - Inhibition of STAT signaling by SOCS	46
Figure 1.9 - Roles of the JAK/STAT pathway in cardiac pathology	55
Figure 1.10 - The mitochondrial import Machinery	59
Figure 1.11 - Schematic of the DNA damage response	63
Figure 1.12 - TLRs and their cognate ligands	66
Figure 1.13 - Signalling pathways initiated by TLR stimulation	68
Figure 1.14 - Outline of T-helper cell differentiation	71
Figure 1.15 - The MAPK signaling cascade	74
Figure 3.1 - Murine STAT3 is transcriptionally active in neonatal rat ventricular myocytes	105
Figure 3.2 - Transfection of STAT3 into cardiac myocytes confers protection from ischaemia/reperfusion injury	107
Figure 3.3 - Adenoviral transduction of cardiac myocytes	110
Figure 3.4 - Dominant negative STAT3 increases I/R induced cell death in cardiac myocytes	111
Figure 3.5 - STAT3 Protects Cardiac Myocytes From Oxidative Stress	112
Figure 3.6 - STAT3 ^{-/-} MEFs are highly sensitive to I/R damage	114
Figure 3.7 - STAT3 ^{-/-} MEFs undergo enhanced cell death following oxidative stress	115
Figure 3.8 - Activation of STAT3 and STAT1 following I/R Injury	117
Figure 3.9 - Testing qPCR efficiency	119
Figure 3.10 - Characterisation of STAT3 dependent gene expression in cardiac myocytes	120

Figure 3.11 - STAT3 mRNA expression is decreased and STAT3-dependent gene expression is increased by I/R injury	122
Figure 3.12 - STAT3 dependent luciferase reporter activity is enhanced by I/R injury	123
Figure 3.13 - STAT3 serine 727 phosphorylation is ERK1/2 dependent	125
Figure 3.14 - Parameters of the in vivo ischaemia/reperfusion model	127
Figure 3.15 - Reperfusion activates the DNA damage and apoptotic pathways	128
Figure 3.16 - Time course of STAT1 and STAT3 activation following I/R injury	130
Figure 3.17 - Expression of STAT3 target genes are increased following I/R injury in viv	131
Figure 3.18 - STAT activation following cerebral I/R injury	133
Figure 3.19 - Infusion of tempol inhibits ROS production and lowers infarct size	135
Figure 3.20 - Tempol infusion reduces JAK/STAT activation and increases GRIM-19	137
Figure 3.21 - Immunohistochemical Staining of STAT Phosphorylation Following Tempol Infusion	138
Figure 3.22 - Effect of I/R and drug infusion on blood pressure, heart rate and pressure rate index	140
Figure 3.23 - IFN- γ induced STAT1 increases infarct size and abrogates the protective effect of tempol.	141
Figure 4.1 - GCRMA normalisation, probe intensity and RNA degradation plots	152
Figure 4.2 - Volcano plots and numbers of differentially expressed genes	154
Figure 4.3 - Manual Gene Ontology analysis of genes differentially expressed by I/R compared to sham	156
Figure 4.4 - Ingenuity analysis of genes differentially expressed by I/R	158
Figure 4.5 - Ingenuity network analysis of genes differentially expressed during I/R	160
Figure 4.6 - Gene Ontology analysis of genes differentially expressed by tempol when compared to saline infusion during I/R	164
Figure 4.7 - Ingenuity functional and network analysis of genes differentially expressed by between tempol and I/R	165
Figure 4.8 - Manual GO analysis of genes differentially expressed by Ucn1 and Ucn2 when compared to saline infusion during I/R	168

Figure 4.9 - Ingenuity analysis of genes differentially expressed by Ucn1 and Ucn2 infusion compared to saline infusion during I/R	169
Figure 4.10 - Network analysis of the Ucn1 and Ucn2 groups	170
Figure 4.11 - Comparison of fold changes obtained by three separate normalisation methods compared with qPCR	172
Figure 4.12 - The IL-6/STAT3/SOCS3 axis is induced by I/R and enhanced by Ucn1	176
Figure 4.13 - Regulation of the Nitric Oxide pathway by I/R injury	178
Figure 4.14 - The IL-17 axis is regulated by I/R injury	181
Figure 4.15 - MAPK activity during I/R injury	183
Figure 4.16 - dUTPase levels are reduced by I/R and partially restored by tempol	185
Figure 4.17 - I/R injury represses the expression of mitochondrial transport genes	192
Figure 4.18 - Tim23 and Tim44 are repressed in an ex vivo model of I/R injury	193
Figure 4.19 - Tempol and Ucn1 upregulate XIAP expression	194
Figure 4.20 - Ucn1 and Ucn2 inhibit free radical formation following I/R injury	196
Figure 5.1 - Rate of HCR in MEF cells with a dose response of UV irradiation	206
Figure 5.2 - STAT3 ^{-/-} MEFs have reduced capacity to repair damaged DNA	207
Figure 5.3 - STAT3 increases the rate of DNA repair	208
Figure 5.4 - Phosphorylation of ATM and H2AX are reduced in STAT3 ^{-/-} MEFs	210
Figure 5.5 - Phosphorylation of Chk1 but not p53 is reduced in STAT3 ^{-/-} MEFs	211
Figure 5.6 - DNA damage mediated increase in MDC1 expression is compromised in STAT3 ^{-/-} MEFs	213
Figure 5.7 - STAT3 regulates the MDC1 promoter	215
Figure 6.1 - MKP-1 genotyping	222
Figure 6.2 - MKP-1 ^{-/-} mice show enhanced cytokine production following LPS challenge	222
Figure 6.3 - Flow cytometry analysis of myeloid cells markers in MKP-1 ^{+/+} and MKP-1 ^{-/-} mice	220
Figure 6.4 - MKP-1 ^{-/-} mice are hyperresponsive to endotoxic shock in vivo	224
Figure 6.5 - MKP-1 ^{-/-} mice are less susceptible to Listeria infection	225

Figure 6.6 - Prolonged MAPK activity in MKP-1 ^{-/-} BMDM in response to LPS	226
Figure 6.7 - Increased AP-1 DNA binding activity in MKP-1 ^{-/-} BMDM	228
Figure 6.8 - MKP-1 Expression can be Stimulated Through both the MyD88 Dependent and Independent Pathways	230
Figure 6.9 - MKP-1 upregulation by LPS is dependent on MAPKs and NF- κ B	232
Figure 6.10 - LPS induced MKP-1 expression in dendritic cells	233
Figure 6.11 - MKP-1 inhibits TLR induced IL-10 expression and has gene dosage effects	234
Figure 6.12 - Temporal regulation of IL-10 by MKP-1	236
Figure 6.13 - MKP-1 inhibition of IL-10 is controlled through MAPK	237
Figure 6.14 - Temporal regulation of TNF- α in MKP-1 deficient cells	239
Figure 6.15 - TNF- α expression in MKP-1 ^{-/-} macrophages is controlled through IL-10 upregulation	241
Figure 6.16 - Increased IL-10 in MKP-1 ^{-/-} macrophages leads to overproduction of Bcl-3 through increased STAT3 activation	243
Figure 6.17 - IL-12p40 expression is repressed in MKP-1 ^{-/-} mice following TLR stimulation	245
Figure 6.18 - Time course of IL-12 expression in MKP-1 ^{-/-} mice	246
Figure 6.19 - Effect of MAPK inhibition on IL-12p40 levels	247
Figure 6.20 - Reduced IL-10 expression in MKP-1 ^{-/-} macrophages may not be responsible for the increased levels of IL-12	248
Figure 6.21 - Loss of MKP-1 does not affect outcome of DSS induced colitis	250
Figure 6.22 - MKP-1 null mice show impaired recovery from EAE	251
Figure 6.23 - Flow Cytometry analysis of lymphoid cell Markers in MKP-1 ^{+/+} and MKP-1 ^{-/-} mice	252
Figure 6.24 - MKP-1 does not affect IL-10 expression from Th2 cells or IFN- γ expression from Th1 cells	255
Figure 6.25 - MKP-1 expression in activated T cells	256
Figure 6.26 - Model of MKP-1 mediated temporal regulation of cytokine production in TLR signaling	260

List of Tables

Table 1.1 - List of kinases which have been shown to phosphorylate STAT3 at ser727	43
Table 4.1 - Quality control statistics for microarrays	150
Table 4.2 - Top 20 differentially expressed genes between I/R and Sham	156
Table 4.3 - Top 20 differentially expressed genes between tempol and I/R	164
Table 4.4 - Top 20 differentially expressed genes between Ucn1, Ucn2 and I/R.	167
Table 4.5 - Genes differentially regulated by I/R previously been shown to be targets of STAT3	174
Table 4.6 - Mitochondrial respiratory complex genes differentially expressed during I/R injury.	188
Table 4.7 - Mitochondrial import genes are differentially regulated during I/R injury	191
Table 6.1 - EAE clinical score measurement	251

Abbreviations

7-AAD	7-amino-actinomycin
AIF	Apoptosis inducing factor
AP-1	Activator protein-1
APAF1	Apoptotic protease activating factor 1
ARE	AU rich element
ASK1	Apoptosis signal-regulating kinase 1
ATF	Activating transcription factor
ATM	Ataxia-telangiectasia mutated gene
ATP	Adenosine-5'-triphosphate
Bcl-2	B-Cell lymphoma
BMDC	Bone marrow derived dendritic cells
BMDM	Bone marrow derived macrophages
BRCA1	Breast cancer, type 1, included
cAMP	Cyclic adenosine monophosphate
Cdk	Cell division kinase
Chk	Cell cycle checkpoint kinase 1
COX	Cyclooxygenase
CT-1	Cardiotrophin 1
DC	Dendritic cell
DDR	DNA damage response
DIABLO	Direct IAP binding protein with low PI
DMEM	Dulbecco's modified eagles medium
DMSO	Dimethylsulfoxide
DSB	Double strand break
DUSP	Dual specificity phosphate
EAE	Experimental autoimmune encephalomyelitis
EGF	Epidermal growth factor
ELK-1	E-26-like protein 1
ERK	Extracellular regulated kinase
FADD	FAS associated death domain
FBS	Foetal Bovine Serum
GAS	IFN- γ activated sequence
GFP	Green fluorescent protein
gp130	glycoprotein 130
GRIM19	Gene associated with retinoid and interferon induced mortality 19
GTP	Guanosine-5'-triphosphate
H2AX	Histone 2AX
I/R	Ischemia/Reperfusion
IBD	Inflammatory bowel disease
IFN	Interferon
IKK	I κ B kinase
IMS	Inner mitochondrial space
iNOS	Inducible nitric oxide synthase

IRAK	Interleukin-1 receptor-associated kinase
IRF	Interferon regulatory factor
IκB	Inhibitor of Nf- κ B
JAK	Janus activated kinase
JNK	c-Jun N-terminal kinase
LIF	Leukaemia inhibitory factor
LPS	Lipopolysaccharide
MAL	MyD88 adapter-like
MAPK	Mitogen activated protein kinase
MCC1	Mediator of DNA damage checkpoint protein 1
MDA	Malondialdehyde
MEF	Mouse embryonic fibroblast
MEK/MKK	MAPK or ERK kinase/MAPK kinase
MEKK/MKKK	MEK kinase/MAPK kinase kinase
MHC	Major histocompatibility complex
MI	Myocardial infarction
MK2	MAPK activated protein kinase 2
MKP	MAPK phosphatase
MLK1	Mixed lineage kinase-1
MNK1	MAPK interacting kinase-1
MOI	Multiplicity of Infection
MOMP	Mitochondrial outer membrane potential
Mre11	meiotic recombination 11
MRN	Mre11/Rad50/Nbs1
MS	Multiple Sclerosis
MSK1	Mitogen and stress activated protein kinase
mTOR	Mammalian target of rapamycin
MyD88	Myeloid differentiation factor 88
Nbs1	Nijmegen breakage syndrome 1
Nemo	Nf- κ B essential modifier
NFAT	Nuclear factor of activated T cells
NF-κB	Nuclear factor kappa B
NIK	Nemo-like kinase
NOS	Nitric oxide synthase
NRVM	Neonatal rat ventricular cardiac myocytes
OSM	Oncostatin M
PIAS	Protein inhibitor of activated STAT
PKC	Protein kinase C
PMN	Polymorphonuclear cell
Rad50	Homolog of yeast radiation 50
ROS	Reactive oxygen species
RSK	Ribosomal S6 kinase
RT	Room temperature
SAM	Sorting and assembly machinery
Skp2	S-phase kinase-associated protein 2
Smac	Second mitochondrial derived activator of caspases

SOCS	Supressor of cytokine signalling
SOD	Superoxide dismutase
Sp1	Specificity protein 1
STAT	Signal transducer and activator of transcription
STEMI	ST-elevated myocardial infarction
TAK1	TGF- β activating kinase 1
TBK1	TRAF family member-associated NF-kappa B activator (TANK)-binding kinase 1
TBK1	TANK binding kinase 1
TCR	T cell receptor
TdT	Terminal tranferase
TFAF6	TNF receptor-associated factor 6
TGF	Transforming growth factor
TIM	Translocase of inner mitochondrial membrane
TIR	translocated intimin receptor
TIRAP	Toll-interleukin 1 receptor (TIR) domain-containing adapter protein
TIRAP	TIR domain-containing adaptor protein
TLR	Toll-like receptor
TNF	Tumor necrosis factor
TNFR1	TNF receptor 1
TOM	Translocase of outer mitochondrial membrane
Tpl2	Tumor progression locus 1
TRAF6	TNF receptor-associated factor 6
TRIF	Toll/IL-1 receptor (TIR) domain-containing adaptor
TRIF	TIR domain containing adaptor inducing IFN- β
TUNEL	TdT-mediated mediated dUTP nick end labeling
Tyk	Protein-tyrosine kinase 2
UV	Ultraviolet
VDAC	Voltage dependent anion channel
XIAP	X-linked inhibitor of apoptosis
γIR	Gamma irradiation

Chapter 1: Introduction

1.1 Myocardial Infarction

Coronary heart disease (CHD) is one of the leading causes of mortality and morbidity in the world, displaying an aetiology that is both varied and complex. The latest World Health Organisation (WHO) estimates suggest that 7.6 million people die annually from CHD, which represents 13% of all global deaths. In patients with CHD, coronary vessel occlusion occurs following rupture of an atherosclerotic plaque, a lesion consisting of a lipid-rich core surrounded by a fibrotic cap (Hansson and Libby, 2006). Atherosclerotic plaque growth is increased by hypercholesterolemia which leads to the accumulation of oxidised modified low-density lipoprotein (oxLDL) in arterial walls, this causes endothelial cell dysfunction, upregulation of inflammatory mediators and leukocyte recruitment, all contributing to plaque growth (Stambler et al., 1988). Macrophage accumulation inside the plaque generates proteolytic and thrombogenic mediators which ultimately lead to plaque rupture (Aikawa and Libby, 2004).

Plaque rupture results in pro-thrombotic conditions inside the vessel, resulting in a rapid thrombotic occlusion; this can cause severely restricted blood flow to the heart, depriving myocardial tissue of oxygen and nutrients which is known as ischaemia. Ischaemic heart damage directly results in cardiac myocyte cell death and the subsequent formation of an area of dead tissue known as an infarct, this process is therefore referred to as myocardial infarction (MI). The INTERHEART study published in 2004 has suggested that over 90% of myocardial infarctions are attributed to modifiable risk factors such as hypertension, smoking, obesity, dyslipidemia and diabetes (Yusuf et al., 2004). Once myocardial infarction is diagnosed, patients are separated into two categories based on ECG measurements; ST elevation MI (STEMI) or non- ST elevation MI (NSTEMI). NSTEMI presents in a similar fashion to unstable angina and is normally treated medically with drugs such as aspirin and heparin (Braunwald, 2003). Patients presenting with STEMI are treated with percutaneous coronary intervention (PCI) which involves an angioplasty and insertion of a stent or through the use of thrombolytic drugs (Sanchez et al., 2005, Shah, 2007). Fibrinolytic drugs such as tissue plasminogen activator (tPA) and streptokinase currently represent the optimal treatment for improving survival after STEMI (Kaul et al., 2004). Even given the current treatments, it is estimated that one third of people suffering from MI will die within the first year after the primary event (Rosamond et al., 2008). In addition many of the survivors

develop systolic dysfunction eventually resulting in congestive heart failure which can lead to further hospitalisation or mortality.

1.2 Ischaemia/Reperfusion Injury

Following MI, interventions are aimed at restoring blood flow to the previously ischaemic vascular bed. In a seemingly contradictory process however, restoration of blood flow, while obviously being essential to restore cardiac function, can actually result in enhanced levels of myocardial damage and increased infarct size (Eefting, 2004). This phenomenon of reperfusion-induced damage, known as ischaemia/reperfusion (I/R) injury was first described in 1960 and is caused by exacerbated death of cardiac myocytes which were viable until immediately before reperfusion (Jennings et al., 1960). Despite successful medical reperfusion following ischaemia, the incidence of cardiac failure after reperfusion stands at 25% and mortality rates at almost 10% which can be attributed to I/R injury (Keeley et al., 2003) and myocardial I/R thus represents an important target for therapeutic intervention. The publication of the AMISTAD (Acute Myocardial Infarction Study of Adenosine) study, demonstrated for the first time that a drug could reduce infarct size in a multi-centre trial (Mahaffey et al., 1999), however translation of positive pre-clinical results from other potential therapies has been disappointing (Bolli et al., 2004).

I/R injury encompasses several types of myocardial dysfunction, including myocardial stunning, no-reflow ischaemia, reperfusion induced arrhythmias and lethal reperfusion injury (Yellon and Hausenloy, 2007). Myocardial stunning, also called post-ischaemic left-ventricular dysfunction, is manifested by mechanical dysfunction after ischaemia, even though blood flow has been restored and there is no evidence of cellular necrosis (Heyndrickx et al., 1975). The time taken to recover contractile performance varies but damage to the heart is reversible and patients usually recover after several weeks (Barnes and Khan, 2003). No-reflow ischaemia occurs when the microvasculature is obstructed after ischaemia, pathologically this manifests as tissue compression, endothelial swelling, myocyte oedema and neutrophil infiltration, all resulting in an inability to fully perfuse a previously ischaemic area (Kloner et al., 1980). No-reflow occurs after the myocytes are already dead and is associated with reduced left ventricular function, ventricular arrhythmia and cardiac rupture; patients diagnosed with no-reflow therefore have a poor prognosis (Ito et al., 1996).

Reperfusion induced arrhythmias are caused by dysregulated Ca^{2+} release from the sarcoplasmic reticulum and are potentially life threatening (Prunier et al., 2008).

Lethal reperfusion injury is the most damaging form of I/R injury and since its discovery it has been highly debated as to whether lethal reperfusion independently contributes to cardiac myocyte cell death or merely exacerbates cell death due to the ischaemic episode (Kloner, 1993). However, the numerous studies in animal models which show that therapeutic intervention before the onset of reperfusion reduces infarct size strongly support a role for lethal reperfusion mediated cell death and current thinking posits that lethal reperfusion injury accounts for up to 50% of the final infarct size (Piper et al., 1998, Yallon and Hausenloy, 2007). Fig 1.1 depicts the reduction in infarct size that can be achieved by preventing lethal reperfusion injury.

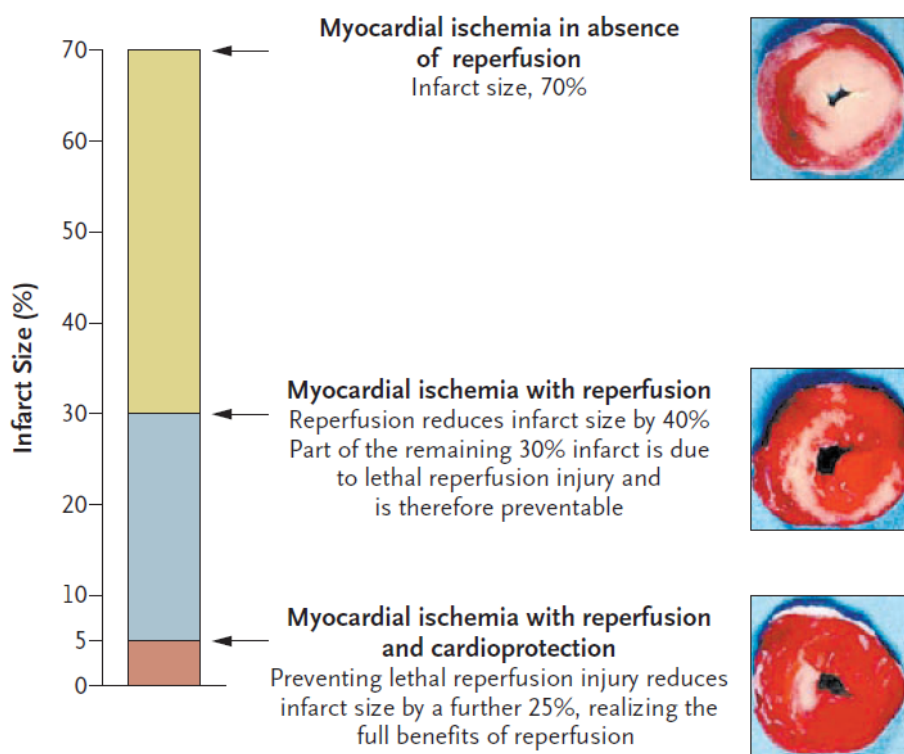


Fig 1.1. Lethal reperfusion injury increases myocardial infarct size. Hearts are stained with triphenyl tetrazolium chloride (TTC), infarcted tissue appears white and viable tissue is stained red. On the left, infarct size is shown as a percentage of the area at risk. Following ischaemia, successful reperfusion substantially lowers infarct size; however lethal reperfusion injury diminishes the magnitude of reduction. Preventing lethal reperfusion injury through cardioprotective intervention at the time of reperfusion further reduces the infarct size (Taken from Yallon and Hausenloy, 2007).

1.2.1 Mechanisms of I/R Induced Cell Death

During I/R injury, cell death can occur through apoptosis, necrosis and autophagy. Necrosis is uncontrolled cellular destruction; necrotic cells rapidly lose membrane integrity and release their contents into the extracellular space. Among the proteins released from necrotic cells are danger associated molecular patterns (DAMPs) such as high mobility group protein B1, uric acid, heat shock proteins (HSPs) and genomic DNA which are recognised by receptors on dendritic cells and lead to the mounting of an inflammatory response (Scaffidi et al., 2002, Shi et al., 2003, Muruve et al., 2008). Apoptosis on the other hand is a form of controlled cellular suicide, distinct from necrosis which does not lead to activation of the immune system. During apoptosis, cells become rounded, retract from neighbouring cells, undergo nuclear fragmentation and membrane blebbing and eventually are engulfed by phagocytes (Taylor et al., 2008). Apoptosis is initiated and controlled through a precisely ordered signalling cascade that contains multiple checks and balances; at the same time that apoptosis is initiated, an anti-apoptotic programme is also induced. The significance of this is that apoptosis is not irreversible, activation of the apoptotic cascade does not guarantee cell death and thus apoptosis is a highly regulated fluidic process. Autophagy involves formation of autophagosomes which degrade and recycle proteins and organelles allowing them to be reused in order to maintain metabolic function. Autophagy has been shown to occur in the myocardium during I/R injury, however the study of autophagy in this context is still at an early stage and it is not yet fully understood how it contributes to cell survival following reperfusion (Yan et al., 2005, Gustafsson and Gottlieb, 2008).

1.2.2 Caspases

Apoptosis is regulated by an ordered signalling cascade which converges on a family of cysteine proteases called caspases which are responsible for controlling the organised cellular destruction. Caspases are present in the cell as inactive precursors and are activated following cleavage; caspase activation can occur through three main routes which are depicted in Fig 1.2. Apoptogenic mediators such as granzyme B released from cytotoxic T cells can induce apoptosis in target cells by directly activating caspase-3, this is a common form of cell death in virally infected cells which display viral epitopes on their MHC for recognition by cytotoxic T cells (Darmon et al., 1995). The extrinsic pathway on the other hand involves recognition of extracellular ligands such as FasL and TNF- α by the corresponding death

receptors such as Fas or TNFR1; these directly activate caspase-8 through binding the adapter protein Fas associated death domain (FADD) (Srinivasula et al., 1996). The intrinsic pathway involves regulation of the Bcl-2 family of proteins, ultimately resulting in activation of the pore forming Bax and Bak which cause mitochondrial membrane opening and release of apoptogenic mediators such as cytochrome c (Rosse et al., 1998). The function of cytochrome c in healthy cells is to shuttle electrons from complex III to complex IV in the mitochondrial respiratory chain. During apoptosis however, cytochrome c is released from the mitochondria and translocates to the cytosol where it binds to apoptotic converting protease-activating factor (APAF-1) and dATP in a heptameric protein complex called the apoptosome which is responsible for caspase-9 activation (Li et al., 1997). In a series of cleavage events, downstream caspases are further activated in a precise order, eventually resulting in activation of the effector caspases, caspase-3, caspase-6 and caspase-7 (Slee et al., 1999). Together these caspases are responsible for cleavage of a host of cellular substrates which result in demolition of the cell. For example, cleavage of cytoskeletal proteins such as actin, myosin and filamin lead to dissolution of the actin cytoskeleton network and contribute to the rounding, retraction and membrane blebbing of cells characteristic of apoptosis (Taylor et al., 2008). Cleavage of the inhibitor of caspase activated DNase II (ICAD) allows activation of the CAD endonuclease and subsequent DNA degradation and chromatin condensation (Enari et al., 1998).

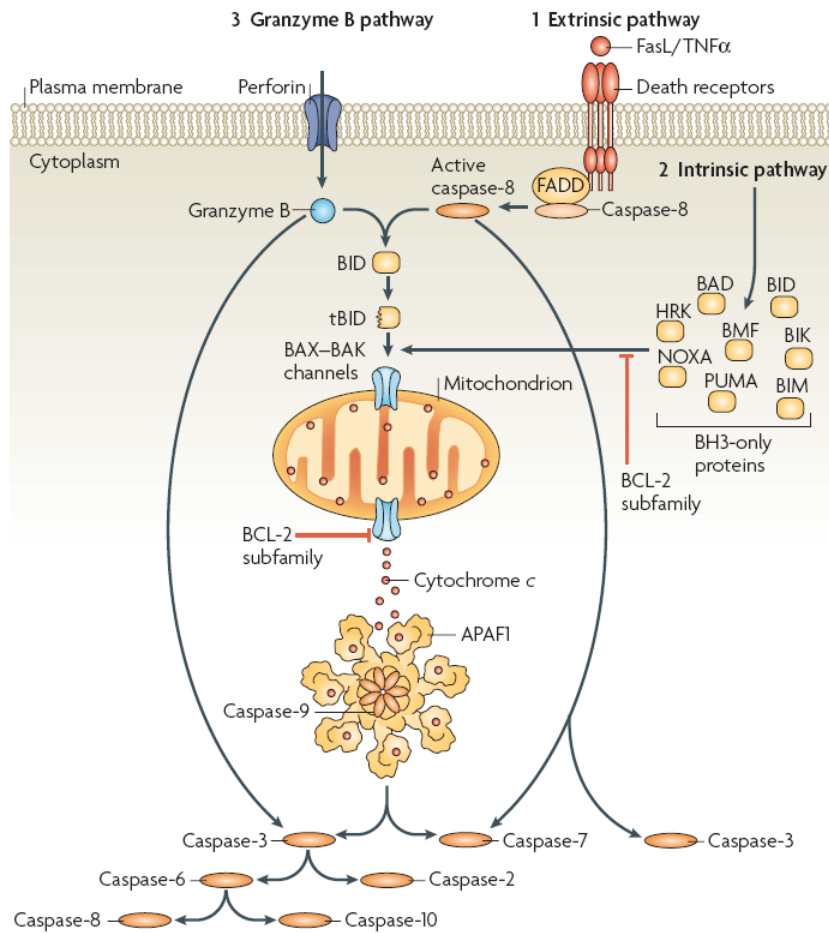


Fig 1.2. The three main pathways of apoptosis. The extrinsic pathway (1) is mediated through extracellular ligands such as FasL and TNF- α , these bind to death receptors such as FAS and TNF-R and induce caspase-8 activity via the adaptor protein FADD. Caspase-8 can directly activate caspase-3 and caspase-7 and can cleave BID to tBID which directly induces BAX and BAK activity. The intrinsic pathway (2) is controlled by the Bcl-2 family, BAX and BAK activity are held in check by anti-apoptotic Bcl-2 proteins, this is antagonized by BH3-only proteins. BAX and BAK oligomerization and insertion into the mitochondrial membrane promote the release of cytochrome c into the cytosol where it binds to APAF-1 and Caspase-9 in the apoptosome. The apoptosome can directly activate caspase-3 and caspase-7 which in turn cases downstream activation of the other caspases. Apoptosis can also be induced directly by the granzyme B pathway (3), cytotoxic T cells release granzyme B through the pore forming perforin which directly activates caspase-3 and tBID. Taken from Taylor et al., 2008.

1.2.3 Bcl-2 Proteins

The intrinsic pathway of apoptosis is co-ordinately regulated by the Bcl-2 family of proteins. Bcl-2, the founder member of this family was first identified as an oncogene at the breakpoint of the t[14:18] chromosomal translocation found in B-cell follicular lymphoma (Bakhshi et al., 1985). Subsequently it was found that transduction of Bcl-2 into B cells could rescue them from cell death, clearly identifying Bcl-2 as an anti-apoptotic protein (Vaux et al., 1998). The Bcl-2 family are normally grouped into three categories; pro-apoptotic (Bax, Bak and Bok), anti-apoptotic (Bcl-2, Bcl-, Mcl-1, Bcl-W, Bcl-2A1 and Bcl-B) and BH3-only proteins, which are homologous only in their BH3 domain (Bik, Hrk, Bim, Bad, Bid, Puma, Noxa and Bmf). BAX and BAK are a focal point for apoptotic induction by the intrinsic pathway; they are kept inactive through direct binding and inhibition by the anti-apoptotic Bcl-2 proteins, the BH-3 only proteins disrupt this interaction and allow BAX and BAK to oligomerize and exert their pro-apoptotic effect on the mitochondria (Taylor et al., 2008). Other BH3 only proteins such as BIM, PUMA and tBID can directly activate BAK and BAX; p53 has also been shown to be capable of directly activating BAX in the cytosol (Chipuk et al., 2004, Ming et al., 2006, Terrones et al., 2008). Generation of BAX/BAK double knockout mice has shown that BAX and BAK are essential for stress induced apoptosis; a high proportion of the double knockouts die during embryogenesis and neonates have various defects, including elevated numbers of lymphocytes and myeloid cells (Lindsten et al., 2000, Rathmell et al., 2002). The intrinsic and extrinsic pathways are not entirely separate and in certain circumstances can intersect. For example, caspase-8 cleaves BID to generate a truncated C-terminal fragment called tBID, tBID activity triggers BAX oligomerisation and translocation to the mitochondria while BCL- is responsible for inhibiting this BAX-tBID interaction (Roucou et al., 2002).

BAX and BAK oligomerisation appears to be essential for inducing mitochondrial outer membrane permeabilisation (MOMP). This may occur through direct pore forming activity of BAK and BAX, although the precise nature of this mechanism remains controversial (Chipuk et al., 2006). MOMP allows the diffusion to the cytosol of apoptogenic proteins such as cytochrome c, Smac/DIABLO, apoptosis-inducing factor (AIF), Tim8a, and endonuclease G, which normally reside in the intermembrane space between the inner and the outer membrane of the mitochondria (Arnoult et al, 2003, 2005). Although BAX and BAK are constitutively expressed, they only induce MOMP following apoptotic stimuli, a process which is

dependent on their oligomerization and stable insertion into the outer membrane (Chipuk and Green, 2008).

The most favoured model for BAX and BAK activation suggests that they require both direct activation by BH3-only proteins and repression of anti-apoptotic Bcl-2 proteins by additional BH3-only members (Kuwana et al., 2005). Recently, Green and colleagues have proposed what they call the innocent bystander scenario where they suggest that control of the intrinsic pathway of apoptosis rests solely with Bcl-2 family mediated MOMP and lacks any input in terms of signalling mechanisms from within the mitochondria themselves (Chipuk et al., 2006). Importantly, Bcl-2 proteins are controlled both transcriptionally and post-translationally, allowing multiple levels of regulation of the apoptotic process. The BH3-only proteins NOXA and PUMA are transcriptionally regulated by p53, BIM is induced by FOXO3A and STAT3 upregulates Bcl- and BIM (Oda et al., 2000, Nakano et al., 2001, Catlett-Falcone et al., 1999, Epling-Burnette et al., 2001). Examples of post-translational control include BAD and BIM; BAD is normally sequestered in the cytosol by 14-3-3 and dephosphorylation of BAD following growth factor withdrawal allows it to interact with Bcl- (Zhou et al., 2000) , BIM can be phosphorylated by ERK which targets it for ubiquitin mediated proteasomal degradation (Ley et al., 2003).

1.2.4 Inhibitors of Apoptosis (IAPs)

The intrinsic pathway of apoptosis is antagonised by the inhibitor of apoptosis (IAP) family of proteins including X-linked IAP (XIAP), IAP1 and IAP2 which block cytochrome c induced apoptosis by inhibiting caspase activity. XIAP is a major constituent of native apoptosomes where it binds to and inhibits caspase-3, caspase-7 and caspase-9 (Deveraux et al., 1997, Hill et al., 2004). XIAP is an E3 ubiquitin ligase and cells from mice deficient in XIAP or harbouring a XIAP protein without the ring finger domain have been shown to have elevated caspase-3 activity, demonstrating that this ubiquitin ligase activity is essential for inhibition of caspases (Schile et al., 2008). Following treatment with or TNF-•, XIAP-deficient MEFs show elevated levels of ROS due to reduced expression of anti-oxidant genes such as superoxide dismutase 1 (SOD1), SOD2, haem oxygenase 1 (HO-1) and glutathione peroxidase (Gpx-1) (Resch et al., 2008). This was associated with prolonged activation of JNK and increased susceptibility to apoptosis, suggesting that XIAP may have functions in

addition to caspase inhibition. XIAP deficient mice however were found to be similar to wild type mice in the ability to induce apoptosis and this was attributed to elevated levels of IAP1 and IAP2 which may compensate for loss of XIAP (Harlin et al., 2001). IAPs themselves are regulated by Smac/DIABLO and HtrA2/Omi which are released from the mitochondria to the cytosol and bind directly to IAPs, thereby relieving their inhibitory effect on caspases (Du et al., 2000, Verhagen et al., 2000, Suzuki et al., 2001), Smac/DIABLO achieves this by both blocking caspase-IAP association and also by repressing IAP ubiquitin ligase activity, thus promoting increased caspase activity (Ekert et al., 2001, Creagh et al., 2004).

1.2.5 Evidence for Apoptosis Mediated Cell Death During I/R Injury

Although the precise contribution of apoptosis to I/R induced cell death is controversial, several studies have provided compelling evidence for a fundamental role of apoptosis in cardiac pathology following I/R injury (Eefting, 2004). In caspase 8 transgenic mice, a cardiac myocyte apoptotic rate of 0.2% was sufficient to induce cardiac dysfunction and heart failure by six months, while in human patients, rates of cardiac myocyte apoptosis of the order of 0.1-0.25% have been associated with end stage dilated cardiomyopathy (Wencker et al., 2003, Zorc et al., 2003). Several early studies measured levels apoptosis in autopsy samples from patients with acute myocardial infarction and compared them to samples from patients who died of non-cardiac related disease. Saraste et al., detected apoptosis by both DNA laddering and TUNEL assay and found levels of 0.04% apoptosis in the central infarct area and higher rates of 0.8% in the border area around the infarct compared to 0.005% in the non-infarcted region or control hearts (Saraste et al., 1997). A similar study from Anversa's group identified an average of 12% apoptotic cells in the border region and 1% in control samples (Olivetti et al., 1996). Even higher rates of apoptosis (26%) were noted by Abbate et al., who used the TUNEL assay (TdT-mediated mediated dUTP nick end labeling) in combination with cleaved caspase-3 immunostaining (Abbate et al., 2002). While these studies report differing levels of apoptosis, presumably due to heterogeneity in patient samples, confounding medical treatment in each patient and the fact that the findings represent a level of apoptosis at a fixed time point rather than the cumulative loss of cardiac myocytes, they nonetheless demonstrate that MI is associated with elevated levels of apoptosis in human patients. Even a small loss of cells from the heart could have a profound impact on myocardial function and contractility. For example, an apoptotic rate of 0.1%

would be expected to result in a ~37% loss in cardiac myocyte number over a year given that myocytes have a limited ability to replenish themselves (Mani, 2008). Thus a greater understanding of MI mediated apoptosis is essential for preserving cardiac integrity following MI.

Further support for the relevance of apoptosis in I/R injury comes from studies which show that administration of pharmacological inhibitors of caspases-3, -8 and -9 during ischaemia and at the onset of reperfusion all significantly lower infarct size in *ex vivo* and *in vivo* models of I/R injury (Yaoita et al., 1998, Holly et al., 1999, Mocanu et al., 2000, Huang et al., 2000). In studies of human cardiomyopathy, the cleaved forms of caspases -3, -8 and -9 have been detected as well as the release of cytochrome c (Narula et al., 1999, Scheubel et al., 2002). In culture, cardiac myocytes exposed to simulated I/R, hypoxia and oxidative stress show caspase activation, PARP cleavage, cytochrome C release and BAD/BAX mitochondrial translocation (Cook et al., 1999, Kang, 2000). Other studies demonstrate that genetic manipulation of components of the apoptotic machinery can greatly influence I/R injury. Transgenic overexpression of Bcl-2 leads to reduced apoptosis, improved left ventricular ejection fraction and decreased infarct size after left coronary ligation (Brocherion et al., 2000). Likewise, following I/R injury, Bax-deficient mice have reduced apoptotic indexes and superior cardiac function compared to wild type controls (Hochhauser et al., 2003). Deletion of the p53 target gene PUMA has also been shown to reduce infarct sizes by 50% (Toth et al., 2006). In addition, modulation of the extrinsic pathway has also provided supporting evidence. Adenoviral administration of FasL induces apoptosis in the myocardium of adult rats and Fas-deficient mice suffer significantly less apoptosis after MI, resulting in reduced infarct sizes (Lee et al., 2002).

Although it is clear that the entire cellular machinery of apoptosis is present in cardiac myocytes, apoptotic regulation in these terminally differentiated cells is distinct from that of other dividing cell types. Since loss of myocytes is so detrimental to the heart, the threshold for apoptosis is elevated in cardiac myocytes compared to other cell types. One of the ways this is achieved is through reduced availability of components of the intrinsic pathway. Sanchis et al. found that treating cardiac myocytes with staurosporine caused the release of cytochrome c into the cytosol but did not lead to caspase-3 activation or DNA fragmentation (Sanchis et al., 2003). They attributed this finding to the lack of Apaf-1 expression in cardiac myocytes and showed that transfecting cardiac myocytes with Apaf-1 restored sensitivity to

staurosporine induced cell death. Likewise, Potts et al., found that cardiac myocytes were resistant to apoptosis induced by micro-injection of cytochrome c (Potts et al., 2005). In contrast to Sanchis et al., their study detected Apaf-1 expression but found that it was greatly reduced in comparison to other cell types. In support of these findings it has also been shown that cytosolic cytochrome c and caspase-9 activity was present in the absence of caspase-3 activity and apoptosis in failing human hearts (Scheubel et al., 2002). In addition, the expression of several caspases, Bcl-2 and Bax have been shown to be repressed postnatally which was associated with reduced caspase-3 activity and DNA fragmentation following ischaemia (Bahi et al., 2006). These studies demonstrate that although apoptosis certainly takes place in cardiac myocytes, it may be more tightly controlled and limited expression of Apaf-1 and caspases may thus serve as a break on apoptosis where a higher critical threshold must be reached before initiating irreversible cell death signals.

1.2.6 The Mitochondrial Permeability Transition Pore

The proton gradient which is required for energy production in the cell is maintained by the inner membrane of the mitochondria. Mitochondrial membrane potential is controlled through the mitochondrial permeability transition pore (MPTP). This is a large non-specific pore spanning both the inner and outer mitochondrial membranes which is formed through the association of the voltage-dependent anion channel (VDAC), the adenine nuclear translocase (ANT) and cyclophilin D (Clerk et al, 2003, Baines, 2007). The MPTP is $^{+}$, redox, voltage and pH sensitive and remains closed during ischaemia due to the low pH within the cell. In the first few minutes of reperfusion however, the pore opens due to a restoration of pH, increases in $^{+}$ levels, free radical production and inhibition of ATP synthesis (Griffiths and Halestrap, 1995, Kim et al., 2006). MPTP opening is associated with increases in mitochondrial volume and permeability which can ultimately lead to a reduction in membrane potential ($\Delta\psi$) and inhibition of ATP synthesis, causing defects in energy production needed to sustain heart muscle contraction (Baines, 2007). Sustained opening of the pore leads to a collapse in the proton gradient and electrical potential across the inner membrane and this in turn causes oxidative phosphorylation uncoupling. Under the force of osmotic pressure, the matrix begins to swell and while the inner mitochondrial membrane can undergo cristae remodelling to adapt to the expansion, the outer membrane is unable to do so and eventually ruptures (Gustafsson and Gottlieb, 2008). This allows the release of pro-

apoptotic mediators such as cytochrome c, AIF and endonuclease G into the cytosol which may further the apoptotic process (Yang and Cortopassi, 1998). This is supported by studies which show that pharmacological inhibition of MPTP opening with cyclosporine, sangliferin A or preconditioning reduce infarct size in rodents by 50%, suggesting that high levels of MPTP opening is a detrimental event during I/R injury (Hausenloy et al., 2003, Javadov et al., 2003). In agreement with this, gene targeted mice deficient in cyclophilin D, an essential component of the MPTP, were resistant to mitochondrial permeability transition and had a 40% reduction in infarct size following I/R injury (Baines et al., 2005, Nakagawa et al., 2005). This has recently been confirmed in humans where a small clinical study showed that a single intravenous bolus of cyclosporine in patients with acute ST-elevation myocardial infarction undergoing primary PCI reduced biochemical markers of cardiac dysfunction and decreased infarct size by 20% (Piot et al., 2008). It must be noted however that MPTP may actually be dispensable for activation of apoptosis via the mitochondrial pathway since cyclophilin D deficient cells were found to respond normally to apoptotic stimuli (Baines et al., 2005).

1.2.7 Reactive Oxygen Species (ROS) in Myocardial Cell Death

Another mechanism whereby reperfusion induces cell death in the myocardium is through the generation of ROS. ROS consist of hydrogen peroxide (H_2O_2), the superoxide anion ($O_2^{\cdot-}$) and the hydroxyl radical ($\cdot OH$) amongst others. ROS can cause cellular damage in several ways, including DNA strand breaks, lipid peroxidation and reduction of protein sulfhydryl bonds (Goswami et al., 2007). In addition, ROS can induce apoptosis directly via peroxidation of cardiolipin which disrupts the cytochrome c-cardiolipin interaction, thereby releasing cytochrome c into the cytosol where it induces apoptosome formation (Shidoji et al., 1999). Under normal cellular conditions in the myocardium, 95% of oxygen is reduced to H_2O via the mitochondrial electron transport chain. However the remaining 5% of oxygen is reduced via the univalent pathway in which free radicals are produced, namely the superoxide anion ($O_2^{\cdot-}$) and its protonated form HO_2^{\cdot} , these are in turn converted by superoxide dismutase (SOD) into H_2O_2 which is toxic at high concentrations. H_2O_2 is further reduced to H_2O via catalase or glutathione peroxidase, therefore the toxic superoxide radical can be safely metabolised to water (Becker, 2004). During ischaemia however, the increasing concentration of $O_2^{\cdot-}$ can lead to the generation of the damaging hydroxyl radical ($\cdot OH$) via the fenton reaction (Mao et al., 1993). Oxidative

stress thus occurs when excess ROS generation cannot be adequately removed by antioxidants.

Zweier et al., measured free radical production using paramagnetic resonance spectroscopy in isolated Langendorff perfused rabbit hearts and found generation of free radicals during ischaemia was accompanied by a further burst within 10 seconds of reperfusion (Zweier et al., 1987). This finding was recapitulated in cardiac myocyte culture using the fluorescent oxidant probe 2',7'-dichlorofluorescein diacetate which is converted to the fluorescent probe DCF by oxidation. Using DCF, Vanden-Hoek et al. demonstrated that ROS are produced in cultured cardiac myocytes during ischaemia and similarly to the isolated heart model, this was followed by a dramatic burst of ROS generation during reperfusion which reached a peak after 5 min (Vanden-Hoek et al., 1997).

The generation of ROS during ischaemia can be abolished by pharmacological inhibitors of mitochondrial electron transport, and several studies suggest that complex III is the main site of ROS generation during ischaemia (Chen et al., 2003, Becker et al., 1999). Intriguingly, these same inhibitors appear to have little effect on the ROS burst which occurs following reperfusion, suggesting that ROS production occurs through distinct mechanisms in ischaemia and reperfusion (Becker, 2004). Further ROS production occurs through a mechanism known as ROS induced ROS release. In this phenomenon, initial ROS production leads to the opening of the MPTP and decreased followed by disruption and redox reduction of the electron transport chain, this increases the rate of electron transfer to molecular oxygen accompanied by a concomitant increase in superoxide production. (Zorov et al., 2000). Treatment of cardiac myocytes with bongkrekic acid, an inhibitor of MPTP opening, inhibited this second burst of ROS from the mitochondria (Zorov et al., 2000). The contribution of ROS to myocardial damage during I/R injury is highlighted in studies of transgenic mice overexpressing SOD1 or SOD2, both of which have reduced infarct size following I/R injury (Chen et al., 1996, Chen et al., 1998). Infusion of membrane permeable free radical scavengers such as tempol have also been shown to reduce infarct size in rats and rabbits by up to 60% (McDonald et al., 1999). Although ROS inhibition has been shown to reduce infarct size in animal models, clinical trials of antioxidant therapies such as SOD, vitamin E and α -carotene have all proved disappointing (Flaherty et al., 1994, Rapola et al., 1997).

While ROS production can be highly toxic and damaging to cellular structures, they also play a role in cell signaling. A pertinent example of this is the finding that the cardioprotection afforded by ischaemic preconditioning (brief periods of repeated ischaemia before the onset of reperfusion) is lost in the presence of anti-oxidants and preconditioning can be mimicked by pro-oxidants both *in vitro* and *in vivo* (Vanden-Hoek et al., 2000, Tang et al., 2002). Therefore ROS production in cardiac myocytes can have both detrimental and beneficial effects during I/R injury.

1.2.8 ⁺ Overload and Contracture

In addition to apoptosis and ROS production, myocardial damage can occur via hypercontracture following reperfusion. During ischaemia, the lack of oxygen leads to lowered production of ATP, increased lactic acid accumulation and a lowering of the pH. In order to try to restore the pH balance, myocytes utilise the Na⁺/H⁺ exchanger to remove excess protons, however this has the ancillary effect of increasing the intracellular Na⁺ concentration (Wang et al., 2000). Normally excess Na⁺ is pumped out of the cell using the Na⁺/K⁺-ATPase, however since ATP levels are depleted in ischaemic cells, the Na⁺/K⁺-ATPase cannot work at full capacity. This causes the sarcolemmal Na⁺/⁺ exchanger to operate in the reverse mode, pumping out high levels of ⁺ into the cytosol, eventually resulting in calcium overload (Allen and Xiao, 2003). In addition to this ⁺ overloaded state, the contractile machinery of the myocyte is directly compromised due to the low ATP levels and the myocyte will appear in a state of contracture which causes a shortening and stiffening of the myocardium (Hohl et al., 1982). Once ATP production has been resumed upon reperfusion, the contractile machinery is reactivated, however this often occurs faster than restoration of normal cytosolic Ca⁺ levels and can cause uncontrolled ⁺ dependent contraction, rapid oscillations in ⁺ transport from the sarcoplasmic reticulum and eventually hypercontracture (Gustafsson and Gottlieb, 2008). In this hypercontracted state, myocytes are prone to mechanical damage which can contribute to the spread of necrosis.

1.3 The JAK/STAT Pathway

1.3.1 JAK/STAT Family Members

While research into the underlying molecular mechanisms of MI remains challenging, there is great potential to uncover candidate targets for novel therapeutic intervention through elucidation of the precise signalling cascades that control cell fate following cardiac damage. One of the pathways which has recently come to the fore as instrumental in determining cell fate is the JAK-STAT pathway. This pathway may represent a significant emerging target for therapeutic intervention in cardiac disease and thus it is of great interest to uncover the regulatory mechanisms involved in JAK/STAT signalling during I/R injury.

The JAK/STAT pathway is an evolutionary conserved signalling network involved in a wide range of distinct cellular process, including inflammation, apoptosis, cell cycle control and development. JAKs are cytosolic tyrosine kinases which are associated with the intracellular domain of membrane bound receptors, whose function is to transduce signals from extracellular ligands such as cytokines, growth factors and hormones to the nucleus in order to orchestrate the appropriate cellular response (O'Shea et al., 2002). There are four family members; JAK1, 2, 3 and Tyk2, all of which show different receptor affinities, they all however transduce their signal through recruitment of STAT transcription factors (Levy and Darnell, 2002). The STAT family consists of seven members; STAT1, 2, 3, 4, 5a, 5b and 6, and although they are structurally similar proteins, they are functionally heterogeneous (Levy and Daenell, 2002). STATs possess a series of conserved structural domains; the N-terminal domain (NTD) is involved in reciprocal STAT interactions and is loosely tethered to the rest of the STAT protein, the coiled coil (CC) domain contains consensus sites for nuclear transport, the DNA binding domain (DBD) binds to conserved regulatory sequences in the promoters of target genes, the src homology 2 (SH2) domain controls receptor binding and the C-terminal domain (CTD) contains the phosphorylation sites necessary for STAT activation (Fig 1.3). The work presented here focuses on STAT1 and STAT3, as there is currently little data to suggest a prominent role for any other members of the STAT family in I/R injury and therefore they will not be discussed further.



Fig 1.3 Model of STAT protein structure (for reference STAT3 is shown) consisting of an N-terminal domain (NTD), a coiled coil domain (CC), a DNA binding domain (DBD), a linker domain, a Src homology 2 domain (SH2) and a C-terminal transactivation domain (CTD). STATs can be phosphorylated at distinct residues which control their activation and DNA binding, shown here are the tyrosine 705 and serine 727 phosphorylation sites in STAT3.

1.3.2 STAT Activation

A large array of cytokines and growth factors utilize the JAK/STAT network to transduce their cognate signal to the nucleus, for example IL-6, IL-10, cardiotrophin 1 (CT-1) and G-CSF induce STAT3 activity, while interferons (IFN) utilize predominantly STAT1 and STAT2. Ligand binding to the extracellular domain of JAK associated cytokine receptors induces receptor dimerisation and JAK autophosphorylation. JAKs then transphosphorylate the cytoplasmic domain of the cytokine receptor and create a docking site for the SH2 domain of STATs (Levy and Darnell, 2002). Once STATs bind to the intracellular receptor chain, they are phosphorylated by JAKs at distinct tyrosine residues, causing the bound STATs to be released from the receptor and translocate to the nucleus where they bind specific sequences such as the IFN- γ activated sequence (GAS) in the promoters of target genes (Fig 1.4) (Levy and Darnell, 2002). Once bound to DNA, the NTD is responsible for recruiting RNA Pol II and co-factors such as the histone acetyl transferase p300 (Hou et al., 2008).

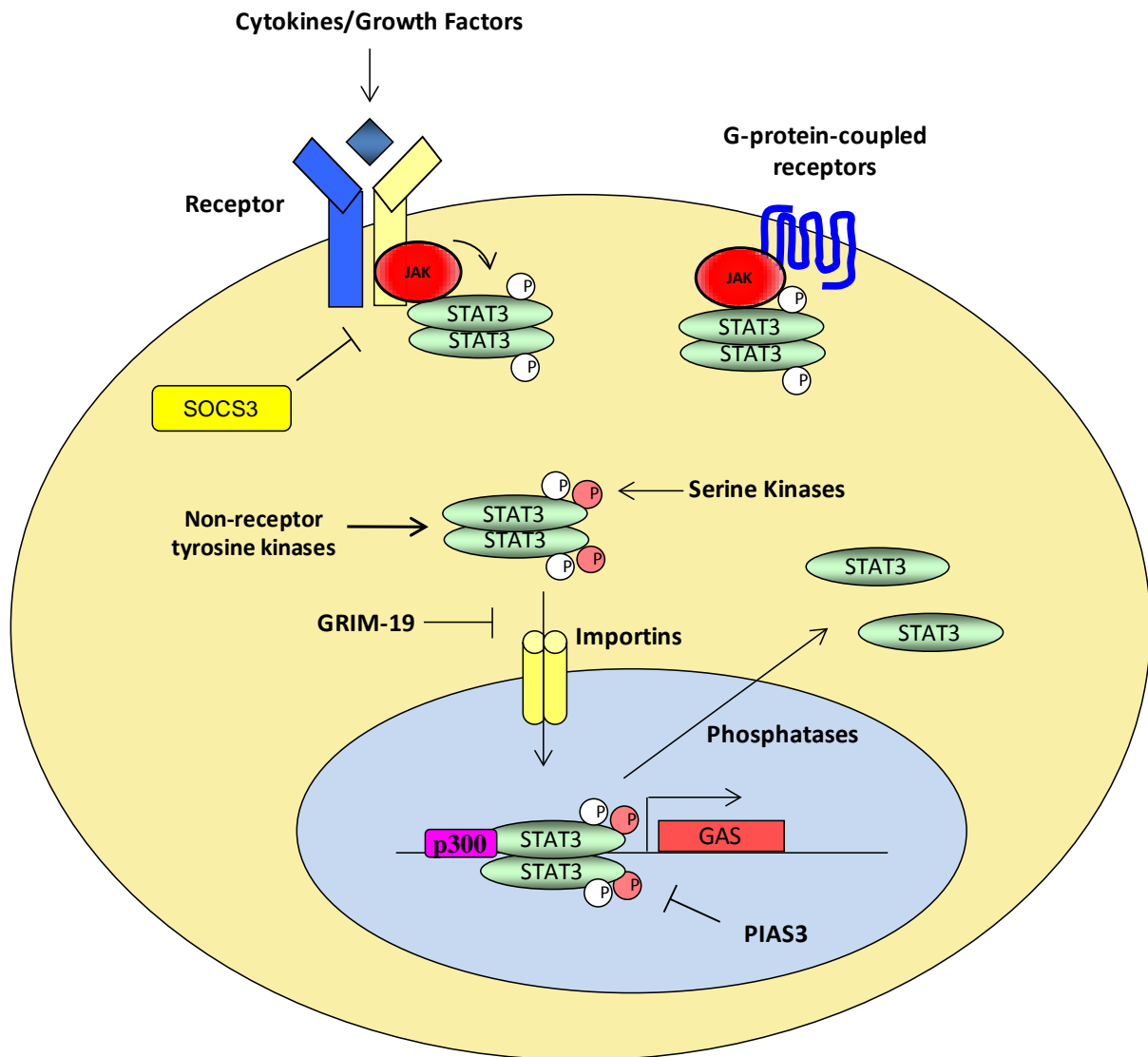


Fig 1.4. Outline of the JAK/STAT3 Pathway. Members of the JAK tyrosine kinases are recruited to cytokine receptors, growth factor receptors or G-protein coupled receptors. They induce tyrosine phosphorylation of STAT3 which causes it to translocate to the nucleus. In addition, STAT3 can be phosphorylated by non-receptor tyrosine kinases and serine kinases. Transport into the nucleus is controlled by importins and once in the nucleus, active STAT3 binds to target sequences such as the IFN- α activated sequence (GAS), this is aided by histone acetyl transferases such as p300. Dephosphorylation allows STAT3 to dissociate from DNA and return to the cytosol. Activation of STAT3 is antagonised SOCS3 and nuclear translocation is blocked by GRIM-19. In the nucleus PIAS blocks STAT3 binding to DNA.

There are currently around 36 known cytokine receptor combinations that respond to 38 cytokines which utilize distinct combinations of JAKs and STATs (Murray, 2007). The selective use of receptor combinations outlined in Fig 1.5 allow a certain specificity for signaling but it is currently unknown precisely how cytokines exert differing responses utilizing the same JAK and STAT combinations. The JAK/STAT pathway can also be stimulated by G-protein coupled receptors such as the angiotensin II receptor and this may be mediated through Rho family GTPases (Marrero et al., 1995, Pelletier et al., 2003). Another mode of JAK/STAT activation is via non-receptor tyrosine kinases such as Src, Fer, Abl, Etk and Lck which all induce STAT3 activity (Yu et al., 1995, 1997, Nelson et al., 1998, Lund et al., 1999, Wen et al., 1999, Priel-Halachami et al., 2000). The IL-6 family of cytokines comprises IL-6, IL-11, leukaemia inhibitory factor (LIF), oncostatin M (OSM), ciliary neurotrophic factor (CNTF), cardiotrophin-1 (CT-1) and cardiotrophin-like cytokine (CLC). IL-6 cytokine receptors are comprised of the signal transducer gp130 in combination with IL-6R, IL-11R, LIF-R or OSM-R. All IL-6 cytokines potently activate STAT3 and this is followed by internalization and degradation of gp130 (Fischer and Hilfiker-Kleiner, 2007). Serum levels of IL-6, soluble gp130, LIF and CT-1 have all been shown to be elevated in patients suffering from heart failure and these levels correlate with the severity of left ventricular dysfunction, suggesting that the IL-6/STAT3 axis may have a role to play in myocardial cell death (Roig et al., 1998, Hirota et al., 2004, Toree-Aminone et al., 1996, Khan et al., 2006).

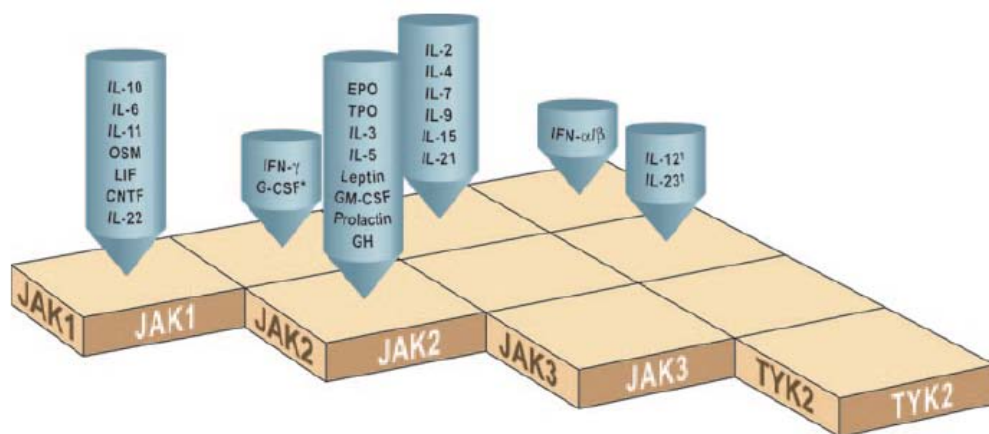


Fig 1.5. JAK usage by cytokines. Shown are cytokines and the JAK combinations which they utilize. Taken from Murray, 2007.

Dimerization of STATs appears to be essential for DNA binding and retention in the nucleus. Traditionally it was thought that inactive STATs were present as monomers and only undergo dimerization after phosphorylation, however accumulating evidence suggests that unphosphorylated STATs are present in the cytosol as dimers or higher order multimers (Ndubuisi et al., 1999). Unphosphorylated STAT1 dimers are formed by reciprocal interactions of their N-terminal domains, coiled-coil and DNA binding domains in an anti-parallel conformation (Fig 1.6) (Zhong et al., 2005). Phosphorylation promotes dimerization through the SH2 domains in a parallel confirmation which is essential for DNA binding and nuclear retention and these parallel and anti-parallel conformations appear to be mutually exclusive (Fig 1.6) (Mao et al., 2005, Wenta et al., 2008). Recently it has been shown that tyrosine phosphorylation of STAT1 is dispensable for DNA binding *per se*, however phosphorylation promotes the parallel conformation which increases DNA binding activity by more than 200 fold (Wenta et al., 2008).

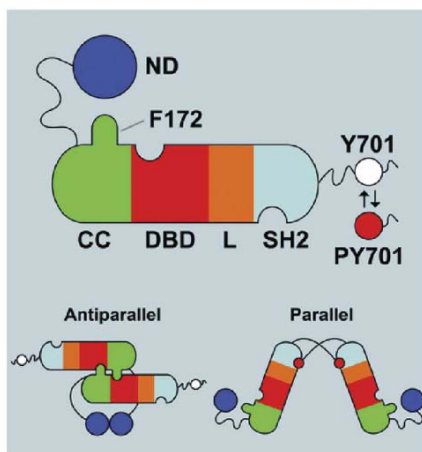


Fig 1.6. STAT1 conformations. The domains are N-terminal domain (ND), coiled:coil domain (CC), DNA-binding domain (DBD), linker domain (L), and SH2 domain (SH2). The ND is shown tied to the CC through a flexible tether (not to scale), and the residues C-terminal to the –SH2 include the Y701, which is phosphorylated (red dot) when the molecule is activated. The C-terminal region is also flexible as indicated by the wavy black line. At the *bottom* of the figure are diagrams of the parallel and antiparallel structures supported by crystallographic results (Chen et al. 1998; Mao et al. 2005). Notable is the F172 residue that is important in the antiparallel structure. Taken from Martens et al., 2006.

1.3.3 STAT Nuclear Import

In the last few years we have gained a much more detailed understanding as to how the phosphorylated STATs are transported to the nucleus. Work from Uwe Vinkemer's group and others has shown that once phosphorylated, STAT dimers are transported to the nucleus in both an energy-dependent and an energy independent manner (Meyer et al., 2004). Importins such as importin •5 bind to phosphorylated STAT dimers and transport them through nuclear pore complexes with a conserved sequence in the coiled-coil domain essential for nuclear import (Ma et al., 2003). Conversion of RanGTP to RanGDP in the nucleus allows STATs to re-enter the cytosol, utilizing exportins such as chromosomal region

maintenance 1 (CRM1) (McBride et al., 2000). The CRM1 binding site in STAT1 is located within the DNA binding domain, suggesting that CRM1 is prohibited from binding when STAT1 is bound to chromatin (McBride et al., 2000). Using protein microinjection techniques, Marg et al. demonstrated that unphosphorylated STAT1 could move freely between the cytoplasm and the nucleus (Marg et al., 2004). This occurred in the absence of cytokine stimulation and even when the RanGTPase active transport system was disrupted by depleting the cells of energy. It seems therefore that two modes of STAT nuclear transport exist, an energy-independent method involving unphosphorylated STATs in which direct interaction with nucleoporins allows constant shuffling between the cytoplasm and nucleus and an energy-dependent system where phosphorylated STATs need to be actively transported into the nucleus (Meyer and Vinkemeier, 2004). Since nuclear translocation of STATs is a relatively fast process (5-10 minutes), a mechanism exists to replenish the cytosolic pool of STATs to allow further ligand induced activation and prolong target gene transcription.

1.3.4 STAT Nuclear Export

Nuclear export is controlled by STAT dephosphorylation and inhibition of tyrosine phosphatases prolongs STAT1 retention in the nucleus. The kinetics of nuclear retention correlate with the level of STAT-DNA binding, suggesting that STATs are protected from dephosphorylation while bound to DNA (Meyer et al., 2003). How then do nuclear phosphatases gain access to STATs? In the case of STAT1, Darnell and colleagues have proposed an elegant model whereby following dissociation from DNA, the N-terminal domains of both proteins in the dimer interact and undergo rearrangement (Zhong et al., 2005). This forms an anti parallel structure allowing the coiled coil domain of one monomer to bind to the DNA binding domain of the other, thus exposing the phosphate residues to nuclear phosphatases (Zhong et al., 2005, Mao et al., 2005). This antiparallel configuration allows the two molecules to remain in association following nuclear export. Thus it seems that a nuclear pool of activated STATs is maintained by constant export and re-import which is controlled by a tightly regulated tyrosine phosphorylation-dephosphorylation cycle (Meyer et al., 2003). The schematic of the import/export cycle of STATs is depicted in Fig 1.7.

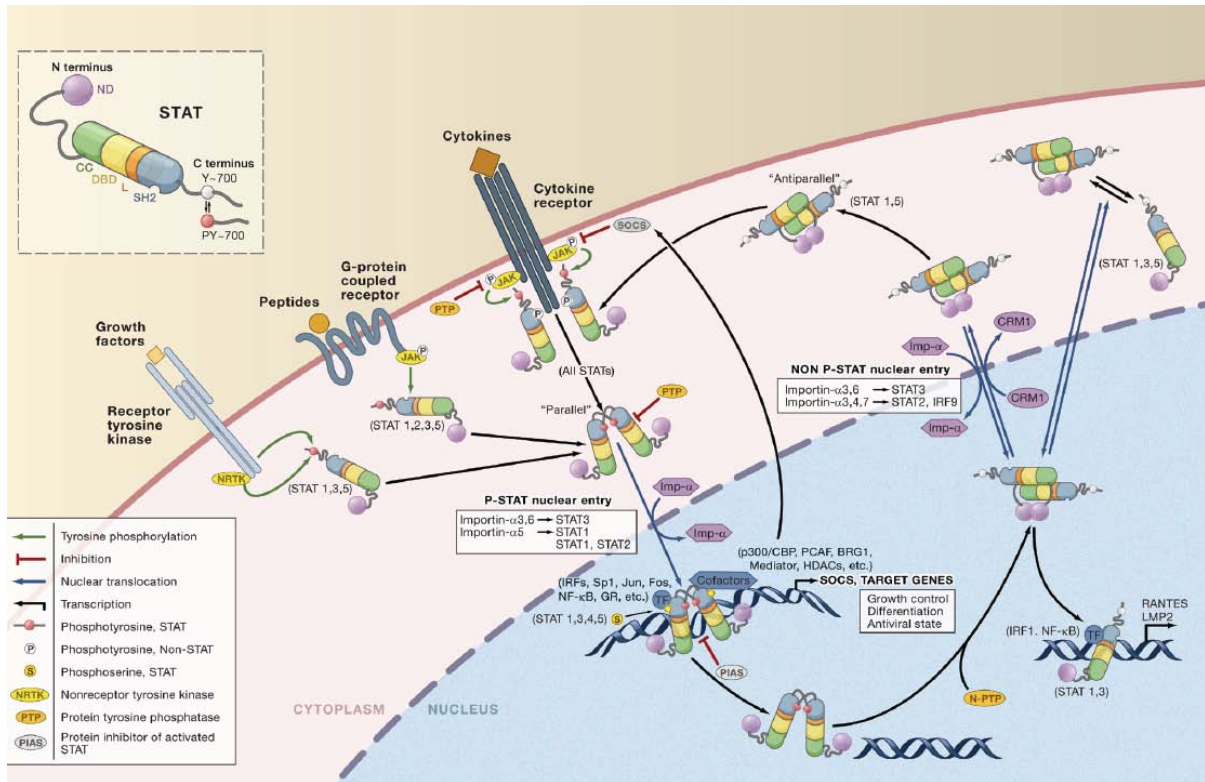


Fig 1.7. STAT import/export cycle. STAT tyrosine phosphorylation by cytokine, growth factor or G-protein coupled receptors induces a STAT parallel conformation and nuclear import through importin- α , the anti-parallel confirmation allows access to nuclear phosphatases and subsequent nuclear export via CRM1. Unphosphorylated STATs can also shuttle freely between the cytosol and nucleus.

1.3.5 STAT Serine Phosphorylation

As well as tyrosine phosphorylation, STAT1 and 3 can both undergo serine phosphorylation at position 727. While serine phosphorylation is cell and stimulus specific, it appears to be necessary for full transcriptional activity of STATs in many instances, for example mutating STAT3 at serine 727 to alanine (S727A) reduces transactivation of STAT3 responsive promoters (Shen et al., 2004). The transcriptional outcome of STAT serine phosphorylation may be determined by the target promoter itself, with different STAT target genes displaying varying transcriptional responses to a STAT1 serine mutant (Kovarik et al., 2001). Several serine kinases have been shown to be capable of phosphorylating STATs under different conditions. STAT3 serine kinases include ERK and PKC \bullet (see table 1.1 for full list of STAT3 serine kinases), while STAT1 serine kinase include p38 MAPK, Ca(2+)/calmodulin-dependent kinase (CaMK) II and PKC \bullet (Nair et al., 2002, Uddin et al., 2002, Ramsauer et al., 2002). Serine phosphorylation may serve to prime STATs for an altered transcriptional

response once a second signal for tyrosine phosphorylation is received (Decker and Kovarik, 2000). Furthermore, serine phosphorylation may augment transcriptional responsiveness through altered co-factor recruitment, for example, serine phosphorylation of STAT3 has been shown to influence recruitment of the co-factor p300/CBP, a histone acetyl transferase (HAT) which facilitates chromatin unwinding and transcription factor access to target DNA (Schuringa et al., 2001). Evidence for the important role for STAT serine phosphorylation *in vivo* comes from studies of mutant mice where the serine residue at position 727 is mutated to an alanine (S727A). STAT1 S727A mice displayed increased mortality upon *Listeria monocytogenes* infection and have increased resistance to LPS-induced endotoxic shock, however this mutation only affects a subset of STAT1 target genes (Varinou et al., 2003). In contrast, STAT3 S727A mice exhibited 75% perinatal lethality and are more sensitive to LPS-induced endotoxic shock (Shen et al., 2004, Shen et al, 2005).

By having two modes of activation, tyrosine and serine phosphorylation allow tight regulation of STAT activity so that signals from several pathways can converge to modulate STAT induced gene activation. Recently Kovarik's group demonstrated that STAT1 Y701 phosphorylation and nuclear translocation were a prerequisite for serine phosphorylation by interferons (Sadzak et al., 2008). Moreover, STAT1 mutants which were unable to associate with chromatin were refractory for S727 phosphorylation, suggesting that STAT1 needs to be assembled into chromatin-associated transcriptional complexes to become S727-phosphorylated and fully biologically active in response to IFNs.

Kinase	Stimulus	Cell Type	Reference
ERK	EGF	3T3	Chung et al., 1997
JNK	UV	COS-1	Lim and Cao, 1999
mTOR	CNFT	Neuroblastoma	Yokogami et al., 2000
PKC•	IL-6	HepG2	Schuringa et al., 2001
ERK	Leptin	macrophages	O'Rourke and Shepherd, 2002
RSK	UV	lymphoblasts	Zhang et al., 2003
Cdk5	Neuregulin	myotubes	Fu et al., 2004
MSK1	Erythropoietin	erythroid cells	Wierenga et al., 2003
p38 MAPK	IL-13	monocytes	Xu et al., 2003
NLK	IL-6	HepG2	Kojima et al., 2005
Cdk1	Nocadazole	Hela	Shi et al., 2006

Table 1.1. List of kinases which have been shown to phosphorylate STAT3 at ser727, the stimulus and the cell type are also listed.

1.3.6 STAT Dephosphorylation

While there are a multitude of studies concerning the initial phosphorylation and activation of STATs, there are relatively few studies concerning STAT dephosphorylation. The first STAT1 phosphatase identified was T cell protein tyrosine phosphatase 45 (TC45) which was shown to be responsible for Y701 dephosphorylation in response to IFN-• (ten Hoeve et al., 2002). •-arrestin-1, which interacts with STAT1 serves as a platform for dephosphorylation by recruiting TC45 (Mo et al., 2008). •-arrestin-1-deficient mouse embryonic fibroblasts underwent Y701 phosphorylation as normal in response to IFN-•. However, while phosphorylation in wild type cells began to decline by 90 min, STAT1 remained phosphorylated at Y701 for up to 3 hr in the absence of •-arrestin-1 (Mo et al., 2008). Functionally this was manifested by an enhanced IFN-• mediated antiviral response to vesicular stomatitis virus when •-arrestin-1 was inhibited (Mo et al., 2008).

Another mode of STAT1 dephosphorylation is via Src homology region 2 domain-containing phosphatase 2 (SHP2) which was shown to bind to the SH2 domain of STAT1 in response to

IFN- α and EGF and repress both tyrosine and serine phosphorylation in the nucleus (Wu et al., 2002). This association is exploited by the human cytomegalovirus which increases SHP2 binding to STAT1, reducing STAT1 phosphorylation and thereby dampening the antiviral response (Davon and Barignon, 2008).

Less is known about phosphatases which target STAT3, but recently a tyrosine phosphopeptide screen of cells overexpressing the receptor protein tyrosine phosphatase T (PTPRT) identified STAT3 as a substrate (Zhang et al., 2007). RNAi mediated inhibition of PTPRT in MCF-7 cells significantly increased STAT3 Y705 phosphorylation and overexpression of PTPRT dramatically reduced IL-6 mediated STAT3 tyrosine phosphorylation and nuclear translocation as well as reducing STAT3 target gene expression. T cell protein tyrosine phosphatase TC-PTP has also shown to be capable of dephosphorylating STAT3 following IL-6 treatment in 293 cells (Yammamoto et al., 2002).

These studies show that in addition to the regulatory mechanisms involved in STAT activation there are signaling pathways which limit the duration of STAT phosphorylation. This is necessary to avoid any unwanted side effects of prolonged STAT activation. For example, dysregulated phosphorylation of STAT1 might lead to an excessive inflammatory response or increased levels of apoptosis. It is also necessary in allowing repeated rounds of STAT activation; STAT dephosphorylation allows STATs to be returned to the cytosol where they can once again be phosphorylated. In the future, more detailed understanding of STAT dephosphorylation will add to our knowledge of the regulation of the JAK/STAT pathway.

1.3.7 Negative Regulation of STATs by SOCS

The suppressor of cytokine signaling (SOCS) proteins control the negative regulation of cytokine responses. There are seven members of the SOCS family (SOCS1-7) which are all induced by cytokines and therefore they form part of a negative feedback loop of cytokine control, in addition SOCS proteins can be induced by other agonists such as LPS, statins and cAMP. SOCS1 and SOCS3 are potent inhibitors of the JAK/STAT pathway, The SH2 domain of SOCS1 and SOCS3 is necessary to facilitate binding to a site in active JAK1, JAK2 and Tyk2 while the SOCS kinase inhibitory region (KIR) is responsible for suppressing JAK kinase activity (Narazaki et al., 1998, Sasaki et al., 1999). The SOCS SH2

domain determines other target selectivity, for example the SH2 domain of SOCS3 binds to phosphorylated tyrosine residues on cytokine receptors such as Tyr757 of gp130 and Tyr800 of IL-12, SOCS1 can bind to both the IFN- α and IFN- γ receptors and both the SOCS1 and SOCS3 SH2 domain can bind to the Y1007 residue in the activation loop of JAK2 (Yasukawa et al., 1999, Yohimura et al., 1997)

In addition, SOCS proteins function as E3 ubiquitin ligases and therefore target proteins for proteasomal degradation (Yoshimura et al., 2007). This is mediated through a region in the C terminus known as the SOCS box which binds a complex containing elongin B/C, cullin-5 and RING-box-2 (RBX2) which recruit E2 ubiquitin transferase, resulting in 20S mediated proteasomal destruction of SOCS-bound proteins (Kamura et al., 1998, Zhang et al., 1999, Vuong et al., 2004). Deletion of the SOCS box in SOCS1 led to enhanced levels of phosphorylated STAT1 and increased IFN- α responses, showing that this region is necessary for the full activity of SOCS1 (Zhang et al., 2001). Initial phosphorylation of JAKs appears to be necessary for SOCS-mediated degradation. In unstimulated cells, JAK2 was found to be mono-ubiquitinated whereas stimulation with IL-3 or IFN- α led to phosphorylation at Y7001, recruitment of SOCS1 and subsequent polyubiquitination and degradation (Ungureanu et al., 2002).

The need for correct control of JAK/STAT signaling is highlighted in studies of SOCS1-deficient mice, these mice develop an excessive fatal IFN- α response which could be rescued by the administration of anti-IFN- α antibodies (Alexander et al., 1999). Lymphocytes from these mice exhibit accelerated apoptosis with age and SOCS1^{-/-} MEFs are far more sensitive to TNF- α mediated apoptosis than their wild type counterparts, showing that tempering of the IFN- α /STAT1 axis is necessary to restrain exuberant STAT1-mediated apoptosis (Naka et al., 1998, Morita et al., 2000).

The SOCS proteins provide a level of specificity for cytokine signaling through the JAK/STAT pathway. For example, STAT3 is essential for the biological effects of both IL-6 and IL-10, however IL-6 is a pro-inflammatory cytokine whereas IL-10 is anti-inflammatory. The differing responses appear to be controlled at the level of SOCS3; IL-6 and IL-10 both upregulate SOCS3, however SOCS3 selectively dampens IL-6 signalling by binding to the IL-6R subunit gp130 without having any effect on IL-10 signalling. IL-6 therefore induces transient STAT3 activation while IL-10 promotes prolonged STAT3 activity; this is

evidenced by the prolonged STAT3 phosphorylation seen in SOCS3 deficient cells following IL-6 treatment (Lang et al., 2003). Prolonged STAT3 activation is therefore instrumental in the anti-inflammatory response and leads to suppression of pro-inflammatory cytokine production by toll-like receptors (Fig 1.8). Moreover, IL-6 treatment of macrophages deficient in SOCS3 or harboring mutation of the SOCS3 binding site on gp130 produces an anti-inflammatory response, clearly showing that the duration of STAT3 activity determines the differing biological responses to IL-6 and IL-10 (Yasukawa et al., 2003). This was confirmed by studies demonstrating an anti-inflammatory response using modified leptin and erythropoietin receptors which could activate STAT3 but not bind SOCS3 (El Kasmi et al., 2006) and by using a constitutively active STAT3 which also mediates an anti-inflammatory response (Williams et al., 2007). Thus it seems that regulation of the duration of STAT3 phosphorylation by SOCS3 determines the outcome of anti-inflammatory cytokine signaling.

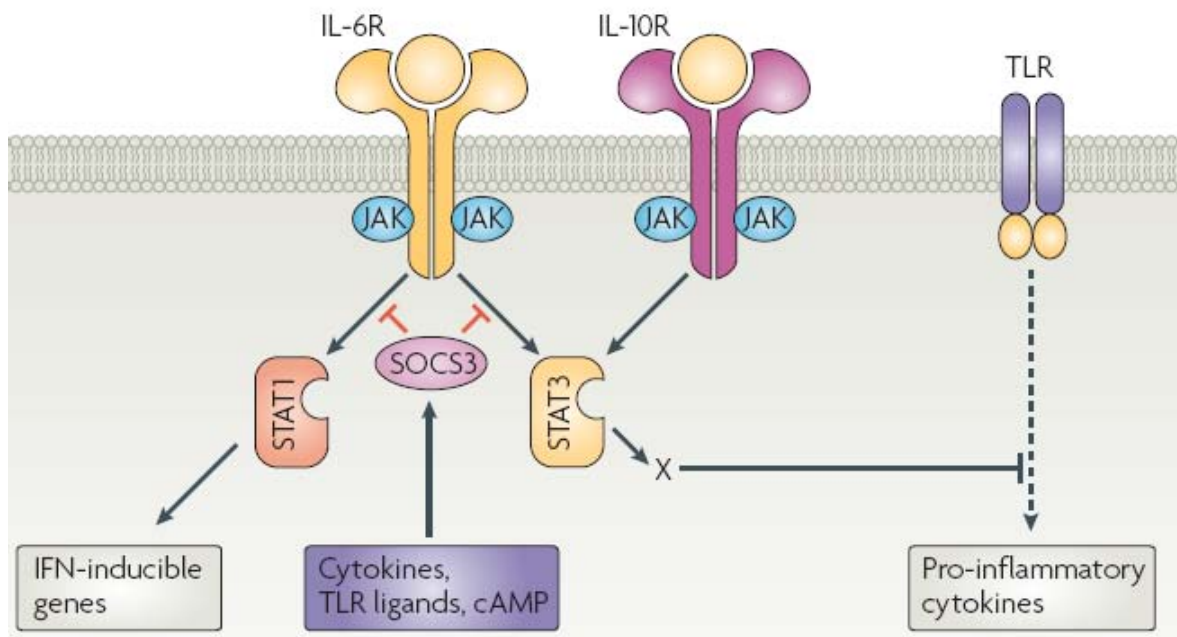


Fig 1.8. Inhibition of STAT signaling by SOCS3. SOCS3 expression is induced by cytokines TLR ligands and cAMP. SOCS3 blocks STAT3 and STAT1 activation by the IL-6 pathway but does not affect IL-10 signalling. SOCS3 therefore inhibits pro-inflammatory IL-6 activity while allowing anti-inflammatory IL-10 signalling through prolonged STAT3 activation. An unknown protein or proteins (x) is thought to be responsible for STAT3 mediated inhibition of pro-inflammatory responses induced from TLRs. Taken from Yoshimura et al., 2007.

1.3.8 Inhibition of STAT DNA Binding by PIAS

Another group of STAT regulators are the protein inhibitor of activated STAT (PIAS) family. PIAS3 was originally found to block STAT3 mediated DNA binding and repress STAT3 mediated gene transcription without affecting STAT1 and likewise PIAS1 was shown to specifically bind to and inhibit STAT1 DNA binding (Chung et al., 1997, Liu et al, 1998). In a similar manner to SOCS1 deficient mice, deletion of PIAS1 also led to enhanced IFN antiviral responses *in vivo* (Liu et al., 2004). Proteins which interfere with this PIAS-STAT interaction can in turn enhance STAT mediated transcription, for example the proto-oncogene Gf1-1 (growth factor independence-1) was found to antagonize the STAT3-PIAS3 interaction and overcome PIAS3 mediated repression of STAT3 target genes (Rodel et al., 2000). Interestingly, PIAS1 binding to STAT1 was shown to be inhibited when STAT1 was methylated by protein arginine methyl-transferase PRMT1, demonstrating post-translational control of STATs in addition to phosphorylation (Mowen et al., 2000).

PIAS proteins have been shown to function as E3-type small ubiquitin-like modifier (SUMO) ligases and STAT1 was found to be SUMOylated at Lys703 by PIAS1 and PIAS3 (Ungureanu et al., 2003). Lys703 SUMOylation appears to be dependent upon prior ser727 phosphorylation by p38 MAPK and ERK and mutation of the SUMO site was shown to enhance IFN- α responsiveness (Vanhatupa et al., 2008, Ungureanu et al., 2003). However a separate study found no effect on STAT1 activity following Lys703 mutation (Rogers et al., 2003). Therefore, in addition to inhibition of JAK/STAT signaling at the receptor site, STATs can also be prohibited from binding DNA, demonstrating the multiple levels of control that are employed to regulate JAK/STAT responses.

1.3.9 Inhibition of STAT3 Nuclear Translocation by GRIM-19

GRIM-19 was originally isolated from an anti-sense mRNA screen of genes involved in promoting cell death in response to IFN- α plus retinoic acid and was later found to be a component of mitochondrial NADH:ubiquinone oxidoreductase (complex I) (Angell et al., 2000, Fearnley et al., 2001, Murray et al, 2003). Yeast-two-hybrid screens identified STAT3 as a GRIM-19 binding protein; this interaction does not affect the initial activation of STAT3 nor its ability to bind DNA but appears to inhibit STAT3 nuclear translocation, forming aggregates with STAT3 at the peri-nuclear region (Lufei et al., 2003, Zhang et al., 2003).

GRIM-19 represses STAT3 transcriptional activity but has no effect on other STAT proteins and is therefore a specific negative regulator of STAT3. GRIM-19 was shown to suppress growth in Src transformed cells which have constitutive STAT3 activity, inhibit cellular transformation induced by constitutively active STAT3 and substantially reduce tumor volume in xenografts from STAT3 overexpressing cells (Lufei et al., 2003, Kalakonda et al., 2007). Therefore GRIM-19 represents a novel inhibitor of STAT3 activity and may have important roles in limiting the oncogenic potential of STAT3 in cancer.

1.3.10 Non-Transcriptional Regulation of Gene Expression by STATs

Recently RNAi screens in *Drosophila* have found interactions between the JAK/STAT pathway and chromatin regulators. Shi et al. conducted a genetic screen for modifiers of the oncogenic allele of the *Drosophila* JAK homolog Hop known as tumorous lethal (⁻¹). They identified several chromatin modifying genes such as the non-histone chromosomal protein heterochromatin 1 (HP-1), the histone methyl transferase Su(var)3-9 and the histone deacetylase Rpd3 and found that crossing flies deficient in either of these genes with ⁻¹ flies resulted in increased numbers of melanoic tumors (Shi et al., 2006). Moreover, these genes are essential components of heterochromatin and over-activity of Hop/JAK was found to block heterochromatin-mediated silencing of genes which are not normally regulated by the JAK/STAT pathway (Shi et al., 2006). Increasing heterochromatic gene silence via a HP-1 transgenic completely abolished ⁻¹ tumorigenicity, suggesting that heterochromatic gene silencing is necessary for constitutive JAK mediated tumorigenesis. The *Drosophila* STAT homolog STAT92E was found to bind to HP-1 only when STAT92E was unphosphorylated, this association was present in the nucleus where it was responsible for stabilised HP-1 localisation and histone H3 methylation (Shi et al., 2008). STAT92E phosphorylation led to reduced heterochromatin localization, dissociation of HP-1 and heterochromatin destabilization suggesting that STAT phosphorylation may therefore regulate access to chromatin.

Chromatin remodeling through the JAK/STAT pathway has also been shown in human cells. Phosphorylation of STAT1 was found to be essential for remodeling of the major histocompatibility complex (MHC) locus, where following IFN- γ stimulation the chromatin carrying the entire locus loops out from chromosome 6 (Christova et al., 2007). Binding of STAT1 to the MHC gene engaged recruitment of the chromatin remodeling enzyme BRG1

(BRM/SWI2-related gene 1) the ATPase component of the SWI/SNF chromatin remodeling complex, followed by binding of RNA polymerase II. A separate study showed that STAT1 deficient cells expressing a STAT1 S727A mutant had reduced recruitment of the co-factor CBP, reduced histone H4 hyperacetylation and decreased RNA polymerase II recruitment to the gbp2 promoter following IFN- α stimulation (Ramsauer et al., 2007). STAT3 has likewise been shown to be capable of remodeling chromatin at the p21 promoter through its association with BRG1 and cdk9 (Giraud et al., 2004). Taken together these studies highlight the emerging role of the JAK/STAT pathway in epigenetic control and demonstrate that STATs modulate transcriptional responses on multiple levels.

Unphosphorylated STAT1 has been shown to have other direct effects on gene expression; using a Y701F STAT1 mutant, Stark's group showed that STAT1 could still mediate low molecular mass polypeptide (LMP2) expression in the absence of tyrosine phosphorylation (Chatterjee-kishore et al., 2000). This was found to be due to unphosphorylated STAT1 complexing with interferon regulatory factor 1 (IRF1) to induce LMP2 transcription. A micro-array study found that cells overexpressing a STAT3 Y705F mutant could up-regulate over a thousand transcripts when compared to STAT3 deficient cells (Yang et al., 2005). The mechanism of regulation appears to be distinct, since unphosphorylated STAT3 complexes with unphosphorylated NF- κ B to drive expression of genes that do not respond directly to phosphorylated STAT3 (Yang et al., 2007). These studies did not examine epigenetic regulation which might be partially responsible for some of the effects, neither was the level of serine phosphorylation addressed in these studies. Another question is whether gene expression through non-phosphorylated STATs is driven by anti-parallel dimers. These questions notwithstanding, it is intriguing that STAT1 and STAT3 when not tyrosine phosphorylated are still capable of mediating gene expression and greatly adds to the complexity of JAK/STAT signalling.

1.4 The JAK/STAT Pathway and Cardiac Injury

1.4.1 JAK/STAT Signalling– A Key Player in Apoptosis

Both STAT1 and 3 have been shown to play direct roles in controlling cell fate. Darnell's group initially demonstrated that STAT3 could function as an oncogene, was responsible for v-Src mediated cellular transformation and could induce tumors in nude mice (Bromberg et al., 1998 1999). When STAT3 was deleted specifically from T cells, IL-6 could no longer induce proliferation nor protect these cells from apoptosis (Takeda et al., 1998). Clear evidence for the anti-apoptotic activity of STAT3 came from a host of studies demonstrating that constitutive activation of STAT3 was responsible for apoptotic resistance in tumor cells from myeloma, melanoma, mycosis fungoides, head and neck, prostate, ovarian and breast cancers. (Catlett-Falcone et al., 1999, Niu et al., 1999, Nielsen et al., 1999, Grandis et al., 2000, Gao et al., 2001, Garcia et al., 2001, Burke et al., 2001). There has been a lot of recent interest in the development of novel inhibitors of STAT3 as possible cancer therapeutics, which have been shown to induce apoptosis in cancer cells and slow cancer growth *in vivo* (Leong et al., 2003, Nam et al., 2005, Turkson et al., 2005). Fibroblasts transformed with a constitutively active form of STAT3 were resistant to serum withdrawal and UV-induced apoptosis and showed cell cycle dysregulation (Shen et al., 2001). These studies clearly established STAT3 as an anti-apoptotic transcription factor and identified several STAT3 target genes responsible for this effect, including Bcl-2, Bcl-, FLIP, Mcl-1 and survivin as well as inhibition of caspase expression (Shen et al., 2001, Epling-Burnette et al., 2001). Recently STAT3 has also been shown to inhibit p53 expression, providing another means whereby STAT3 controls growth arrest and apoptosis (Niu et al., 2005).

Although STAT3 is generally thought to be an anti-apoptotic transcription factor, it has been shown to be pro-apoptotic under certain circumstances. One notable example of pro-apoptotic STAT3 activity is in the involuting mammary gland. STAT3 is highly activated during normal mammary gland involution and specific deletion of STAT3 in mammary tissue was found to delay involution due to reduced apoptosis (Chapman et al., 1999). One mechanism of STAT3-mediated apoptosis during involution is through upregulated IGFBP-5 (Insulin growth factor [IGF] binding protein-5) which sequesters the pro-survival factor IGF-1 to casein micelles (Chapman et al., 1999). During involution, activity of the anti-apoptotic kinase Akt is normally downregulated, however Akt downregulation fails to occur in STAT3-

deficient mammary glands (Abell et al., 2005). This was accompanied by reduced expression of the phosphoinositide-3-OH- kinase (PI(3)K) subunits p50• and p55• but with no change in the p85 subunits, therefore STAT3 promotes a switch in PI(3)K subunit usage which results in inhibition of Akt activity and instigation of apoptosis (Abell et al., 2005). This phenomenon has also been demonstrated in SOCS3-deficient MEFs, where STAT3 activity is greatly prolonged. LIF treatment of SOCS3^{-/-} MEFs resulted in STAT3 dependent apoptosis which was accompanied by increased p50• and p55• PI(3)K subunit expression and reduced Akt activity (Lu et al., 2006). Likewise, SOCS3-deficient mammary glands undergo elevated levels of apoptosis during involution, accompanied by elevated STAT3 activity (Sutherland et al., 2006, Robinson et al., 2007). Leptin has also been shown to induce apoptosis in mammary cells in a STAT3 dependent manner (Motta et al., 2007). The STAT3 target gene CCAAT/enhancer binding protein delta (C/EBP•) has been shown to be important in transducing a pro-apoptotic STAT3 signal; deletion of C/EBP• in the mammary gland delayed involution due to failed induction of several pro-apoptotic mediators, including BAX, IGFBP-5 and clusterin (Thangaraju et al., 2005). Apoptosis and involution does eventually occur in the STAT3 deficient mice, possibly through a p53 dependent mechanism (Matthews and Clarke, 2005). These studies show that STAT3 is capable of promoting apoptosis in certain settings and therefore adds to the complexity of STAT signaling during apoptosis.

Early studies on STAT1 mediated apoptosis revealed that STAT1 could induce cell death through upregulation of caspase 1 (Chin et al., 1997). STAT1 null cells are resistant to TNF induced apoptosis due to defective constitutive expression of caspases 1, 2 and 3, while other pro-apoptotic target genes include Fas, FasL, p21 and p53 (Levy and Darnell, 2002). Furthermore, following DNA damage, STAT1 acts as a cofactor for p53 and modulates the cell-cycle checkpoint response through an ATM-Chk2 pathway (Townsend et al., 2004, 2005). STAT1 can also induce apoptosis through inhibition of the antiapoptotic NF-•B pathway. TNF promotes STAT1 binding to the TRADD/TNF receptor complex, this inhibits TRADD binding to TRAF2 and RIP and subsequent NF-•B activation (Wang et al., 2000). Recently, acetylated STAT1 has been shown to bind to the p65 subunit of NF-•B and inhibit NF-•B dependent transcription of anti-apoptotic genes (Kramer et al., 2006). Interestingly in fibroblasts, increased expression of STAT3 inhibited the proapoptotic effects of STAT1, suggesting that STAT1 and 3 can act antagonistically to one another to control cell fate (Shen et al., 2001).

1.4.2 STATs as Mediators of Myocardial Cell Death

STAT1 activity is upregulated in cardiac myocytes following simulated I/R and exacerbates cardiac damage through induction of pro-apoptotic STAT1 effectors, such as caspase1, Fas and FasL (Stephanou et al., 2000). Support for the role of STAT1 as a pro-apoptotic factor in the myocardium comes from studies which show that inhibition of STAT1 activity during I/R results in significant cardioprotection. For example, both infusion and oral administration of the green tea polyphenol extract epigallocatechin-3-gallate reduced infarct size and caspase activity following I/R in a STAT1 dependent manner (Townsend et al., 2004). A pro-apoptotic role has also been ascribed to STAT1 in neuronal ischaemia, STAT1 deficient mice show reduced neurological damage following ischaemia and this was associated with reduced caspase 3 activity and reduced neuronal cell death (Takagi et al., 2002). Many of the proapoptotic effects of STAT1 are attributable to the C-terminal domain, with phosphorylation at serine 727 being indispensable for I/R induced apoptosis and Fas/FasL expression (Stephanou et al., 2002). Interestingly, S727 phosphorylation of STAT1 is necessary for PKC• induced apoptosis following DNA damage (DeVries et al., 2004). The proapoptotic effects of STAT1 can be blocked by p38 MAPK inhibition, suggesting cross-talk between the JAK-STAT pathway and the MAP kinase pathway during I/R injury (Stephanou et al., 2001). There is far less data concerning the role of STAT3 in I/R injury in the myocardium but some studies have suggested that STAT3 may have cytoprotective roles in the heart. STAT3 overexpression protected mice from doxorubicin induced cardiomyopathy and transfection of STAT3 into cardiac myocytes abrogated the proapoptotic effects of STAT1 following I/R injury (Negoro et al., 2000, Stephanou et al., 2004).

1.4.3 JAK/STAT Pathway in Ischaemic Preconditioning

Preconditioning (PC) refers to the administration of transient sublethal episodes of ischaemia before a prolonged I/R injury, which renders the heart less susceptible to the deleterious effects of I/R mediated damage. PC can reduce infarct size by up to 80%, providing a very efficacious adjunctive therapy where reperfusion injury is unavoidable (Xuan et al., 2003). PC can be divided into two separate phases, an early phase which occurs immediately after reperfusion and lasts for up to 2 hr and a late phase which is sustained for up to 72 hr. Several studies from Roberto Bolli's group and others have recently uncovered the obligatory role of the JAK/STAT pathway in mediating the cardioprotective effects of late PC through iNOS

and COX-2 induction. Adenoviral mediated gene transfer of iNOS confers a protective effect equivalent to that of PC and inhibition of COX-2 abrogates iNOS dependent cardioprotection (Xuan et al., 2003, Li et al., 2003). In a mouse model of late PC, JAK1, JAK2, STAT1 and STAT3 but not any other members of the JAK/STAT pathway were phosphorylated (Xuan et al., 2001). PC induces STAT1 and STAT3 tyrosine phosphorylation through JAK1/2 and serine phosphorylation by a PKC α -Raf-MEK-ERK pathway, both of which appear to be necessary for full transcriptional activation of PC associated genes (Xuan et al., 2003, 2005). Upregulation of COX-2 by PC was abrogated by the JAK2 inhibitor AG490 and PC-mediated cardioprotection is completely abolished in cardiac specific STAT3^{-/-} mice, providing clear evidence for a fundamental role for STAT3 in control of cell survival by PC (Xuan et al., 2001, Smith et al., 2004). Interestingly, IL-6 may be a major cytokine involved in this process, since late PC affords no cardioprotection in IL-6 deficient mice (Dawn et al., 2004). NF- κ B activity is also necessary for late PC and may act synergistically with the JAK/STAT pathway to upregulate iNOS (Yuan et al., 1990).

STAT3 also seems to serve as a focal point for TNF- α mediated preconditioning, since STAT3 inhibition abolishes TNF- α induced cardioprotection, data which is suggestive of a crosstalk between the TNF- α -NF- κ B-STAT pathways (Lecour et al., 2005, Smith, 2002). STAT3 also plays a role in early PC, inhibition of STAT3 activity with the JAK2 inhibitor AG490 was found to abrogate the infarct sparing effects of PC through increased apoptosis associated with reduced expression of Bcl-2 and increased expression of Bax (Hattori et al., 2001). These studies therefore place the JAK/STAT pathway at the centre of this exciting cardioprotective intervention and further research into its precise molecular control may serve to refine the process and contribute to its development as an established therapy for I/R injury.

1.4.4 Role of STAT1 and 3 in Hypertrophy and Angiogenesis

Since cardiac myocytes are a terminally differentiated cell type, myocyte death can have a severe effect on cardiac output, as these cells cannot be efficiently replaced. As a result of this imbalance, the heart seeks to compensate for the reduced cardiac output through a process called hypertrophy, in which cardiac myocytes enlarge and increase metabolic output to compensate for the increased workload now required from a fewer number of cells (Frey et al., 2004). Hypertrophy is initially compensatory and reduces wall stress and oxygen

consumption, which serves to maintain normal cardiac output, however if biomechanical stress remains chronic due to hypertension or myocardial infarction, over time chamber dilation and remodelling ensues and cardiac function declines which may ultimately lead to heart failure (Frey et al., 2004). Progression to heart failure is determined by a fine balance between compensatory hypertrophy and cardiac myocyte apoptosis.

Acute pressure overload and mechanical stress have been shown to activate JAK1, JAK2, TYK2, STAT1, 2 and 3, while members of the IL-6 family of cytokines (including CT-1, LIF and IL-6 itself) which utilize the JAK/STAT pathway have come to the fore as potent mediators of hypertrophy (Pan et al., 1999). IL-6 family cytokine receptors consist of a ligand binding receptor and a common non ligand binding transducer, gp130. Binding of IL-6 family cytokines induces homo or heterodimerisation of gp130 which subsequently activates JAK/STAT and Ras-ERK1/2 pathways. Constitutive activation of gp130 in a transgenic line overexpressing IL-6 and the IL-6R potently induced hypertrophy and gp130 has also been shown to promote hypertrophy in human cardiac cells (Horota et al., 1995, Ancey et al., 2003). Mice where gp130 has been knocked out in the myocardium have normal cardiac structure and function. However these mice fail to develop compensatory hypertrophy following acute pressure overload and instead develop dilated cardiomyopathy (Hirota et al., 1999). After seven days of pressure overload, 90% of the gp130^{-/-} mice died due to extensive myocyte apoptosis, suggesting that gp130 is critical in the transition from compensatory hypertrophy to heart failure. gp130 transduces its signal mainly through induction of STAT3, indeed gp130 deficient mice failed to induce STAT3 in response to pressure overload which may account for the increased levels of apoptosis. Inhibition of STAT3 abolishes gp130 mediated hypertrophy and inhibits LIF dependent induction of the hypertrophic genes c-fos and atrial natriuretic factor (ANF) (Kunisada et al., 1998).

Transgenic mice which overexpress STAT3 in the myocardium show signs of hypertrophy by 12 weeks of age, their hearts display enlarged left ventricles, increased cardiac myocyte cell width and expression of the hypertrophic genes • myosin heavy chain (•-MHC) and ANF (Kunisada et al., 2000). gp130-induced hypertrophy is tightly controlled by a negative feedback loop where STAT3 activity induced by hypertrophy is temporally limited through upregulation of SOCS3, a potent negative regulator of JAKs which allows tight regulation of hypertrophy programme (Yasukawa et al., 2001). These studies show that IL-6 family cytokines may prevent heart failure through inhibition of apoptosis and induction of

compensatory hypertrophy, mediated through gp130 and STAT3. Interestingly, it has been reported that patients with end stage dilated cardiomyopathy have enhanced STAT3 protein expression and tyrosine phosphorylation (Podewski et al., 2003). A schematic of the known roles of STAT1 and STAT3 in cardiac pathology is outline in Fig 1.9.

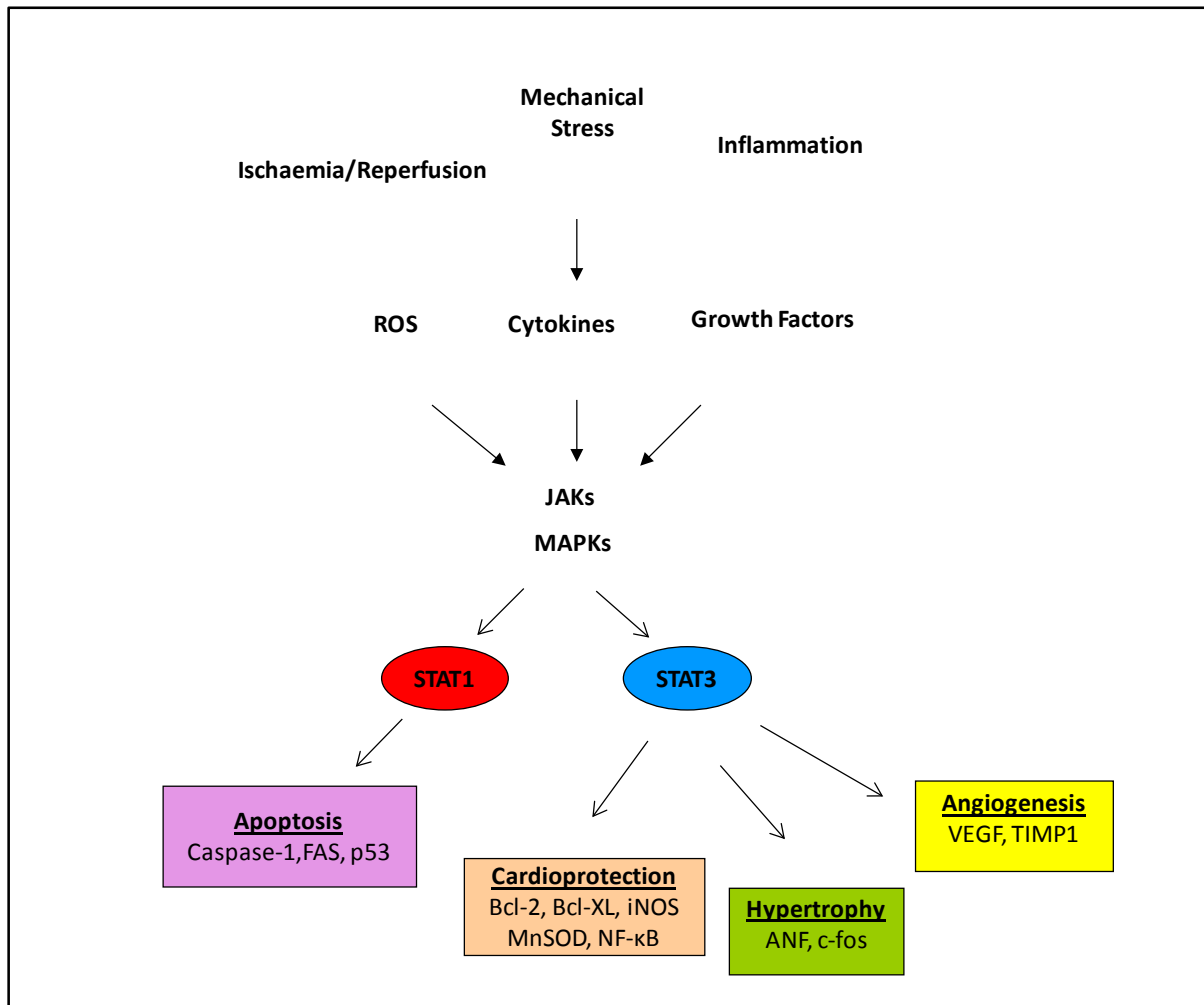


Fig 1.9. Outlined roles of the JAK/STAT pathway in cardiac pathology. In the heart, I/R injury, mechanical stress and inflammation lead to the activation of JAKs and MAPKs which mediate tyrosine and serine phosphorylation of STAT1 and STAT3. STAT1 upregulates genes involved in apoptosis such as caspase-1, FAS and p53. STAT3 transactivates cardioprotective genes, hypertrophic genes and genes involved in angiogenesis.

1.5 Urocortins

1.5.1 The Urocortin Family

Urocortins are 40 amino acid peptide members of the corticotrophin-releasing factor (CRF) family. Urocortins are widely expressed in the heart, CNS, gut, skeletal muscle, skin and immune system and have roles in inflammation, gut motility, appetite, neuronal activity and the cardiovascular system (Latchman, 2002). There are three members; urocortin I (Ucn1), urocortin 2 (stresscopin related peptide, SRP) and urocortin 3 (stresscopin, SCP). The actions of urocortins are mediated through two G-protein coupled receptors, CRF-R1 and CRF-R2; Ucn1 binds both receptors while Ucn2 and Ucn3 only bind to CRF-R2 (Boonprasert et al., 2008).

1.5.2 Urocortins and Heart Failure

Cardiac expression of Ucn1 is increased during hypoxia and hypertrophy and circulating Ucn1 levels are elevated in patients suffering from heart failure (Ng et al., 2004). Ucn1 infusion in humans leads to elevated ACHT and cortisol levels and the effects of Ucn1 on the cardiovascular system include vasodilatation, increased blood flow, elevated heart rate and positive chronotropic and ionotropic effects (Parkes et al., 1997). Ucn1 administration has beneficial effects in experimental heart failure, including increased cardiac output, reduced peripheral resistance and decreased circulating levels of the vasoconstricting hormones angiotensin II, vasopressin and endothelin-1 (Rademaker et al., 2002). Ucn1 also lowers mean arterial pressure and circulating levels of ANP and BNP and continuous infusion significantly delays the onset of heart failure (Rademaker et al., 2005, 2007). Ucn2 and Ucn3 also have beneficial cardiovascular activity. Ucn2 increases contractility in rabbit ventricular myocytes and reduces diastolic pressure and increases left ventricular ejection fraction and cardiac output in a mouse heart failure model, effects which were absent in CRF-R1 deficient mice (Bale et al., 2004). Likewise, Ucn3 increases cardiac output and peripheral resistance in ovine heart failure (Yang et al., 2006, Rademaker et al., 2005). Blocking CRF-R2 in an ovine heart failure model lead to increased arterial blood pressure and peripheral resistance as well as increased rennin and aldosterone levels, suggesting that endogenous urocortins serve a beneficial purpose during heart failure (Rademaker et al., 2005).

1.5.3 Urocortins and Ischaemia

As well as having roles in heart failure, urocortins have been shown to be beneficial in I/R injury. Our group has previously shown that Ucn1 could protect cultured cardiac myocytes from I/R injury *in vitro* and reduce infarct size and enhance cardiac function *ex vivo* (Brar et al., 2000, Scarabelli et al., 2002). Importantly, Ucn1 can protect the heart when added just prior to reperfusion, making it attractive as a possible therapeutic (Schulman et al., 2002). Ucn1 reduced CPK release, decreased the numbers of cleaved caspase-3 positive cells and helped maintain the reserves of high energy phosphates during I/R injury *ex vivo* (Scarabelli et al., 2002). Ucn1 is hypotensive *in vivo*, however, administering urocortin during experimental I/R *in vivo* reduces infarction size, lowers MAP and reduces incidences of ventricular tachycardia and fibrillation (Schulman et al., 2002, Liu et al., 2005). In agreement with a protective role for urocortins in the myocardium, deletion of the urocortin receptor CRF-R2 leads to increased susceptibility to I/R injury (Brar et al., 2004). Treatment of cardiac myocytes with urocortins leads to activation of the MEK1/2-ERK1/2 and PI(3)K-Akt pathways, both of which appear to be necessary for fully fledged cardioprotection by urocortins (Chanalaris et al., 2003, Brar et al., 2002). Interestingly, protein synthesis is required for cardioprotection by urocortins, suggesting that proteins downstream of ERK1/2 and Akt mediate cardioprotection (Lawrence et al., 2002.) Several of these downstream mediators have recently been identified. Ucn1 upregulates the expression of the Kir 6.1 potassium channel subunit and inhibition of K(ATP) channels abrogates urocortin's protective effect, urocortin also downregulates the calcium-insensitive phospholipase A2 enzyme (Lawrence et al., 2002, 2003). Mitochondrial translocation of PKC• also appears to be necessary for Ucn-I mediated cardioprotection, co-administration of a PKC• translocation inhibitor abrogated the ability of urocortin to maintain mitochondrial membrane integrity and protect from apoptosis during I/R (Lawrence et al., 2004, 2005).

1.6 Mitochondrial Transport

1.6.1 Import into the Mitochondria

In the heart, mitochondria account for almost 40% of total cardiac myocyte volume and are responsible for generating over 90% of the cell's energy (McLeod et al., 2003). Almost 99% of all mitochondrial proteins are synthesised in the cytosol and need to be transported to the mitochondria to maintain mitochondrial biogenesis. Up to 10-15% of all nuclear genes in eukaryotes code for mitochondrial proteins and these proteins must be translocated into the mitochondria and inserted into one of four compartments; the outer membrane, intermembrane space (IMS), inner membrane or matrix (Neupert and Herrmann., 2007, Yamano et al., 2007). The majority of mitochondrial proteins contain an N-terminal presequence which is recognised by components of the mitochondrial import machinery (Yamano et al., 2007). The presequence is recognised by the translocase of outer mitochondrial membrane (TOM) complex which inserts proteins into the intermembrane space or passes the polypeptides to the translocase of inner mitochondrial membrane (TIM) complex for insertion into the matrix (Wiedemann et al., 2007). Once mitochondrial precursor polypeptides have been correctly imported, the pre-sequence is cleaved by mitochondrial processing peptidase (MPP), generating the mature protein that is subsequently folded into its correct confirmation.

1.6.2 The TOM Complex

The TOM complex is responsible for transport of almost all mitochondrial proteins and consists of seven separate subunits. The receptor component of the TOM complex is comprised of Tom70, Tom20 and Tom22 (Fig 1.10). Tom70 and Tom20 can bind separate motifs but also have certain overlapping functions (Endo and Kohda, 2002). The N-terminal of Tom20 is anchored to the outer membrane, allowing the cytosolic C-terminal domain of the receptor to bind to pre-sequence containing proteins (Yamano et al., 2007). Tom70 on the other hand recognises proteins containing an internal targeting sequence which are destined for the inner membrane. Tom22 connects Tom20 to the translocation pore and cooperates with Tom20 in pre-sequence binding (Neupert and Herrmann, 2007). The main pore forming subunit of the TOM complex is Tom40 and is associated with the stabilising proteins Tom5, Tom6 and Tom7 (Fig 1.10) (Kato and Mihara, 2008).

Ott et al. recently showed that the TOM complex is obligatory for Bax insertion into the mitochondrial outer membrane (Ott et al., 2007). By using a temperature sensitive Tom40 mutant yeast strain or by pre-incubating isolated mitochondria with antibodies against Tom20 or Tom22 they showed decreased release of cytochrome c into the cytosol in response to tBid/Bax treatment. Moreover, they were able to demonstrate using immunoprecipitation that Tom40 interacts directly with Bax in a transitory manner. Bellot et. al demonstrated that Tom22 also interacts with Bax in a transient manner and confirmed that inhibition of Tom22 leads to a reduction in Bax dependent apoptosis (Bellot et al., 2007). Thus it seems that the TOM complex is essential for Bax mediated apoptosis and therefore the TOM complex may play an important role in controlling cell fate.

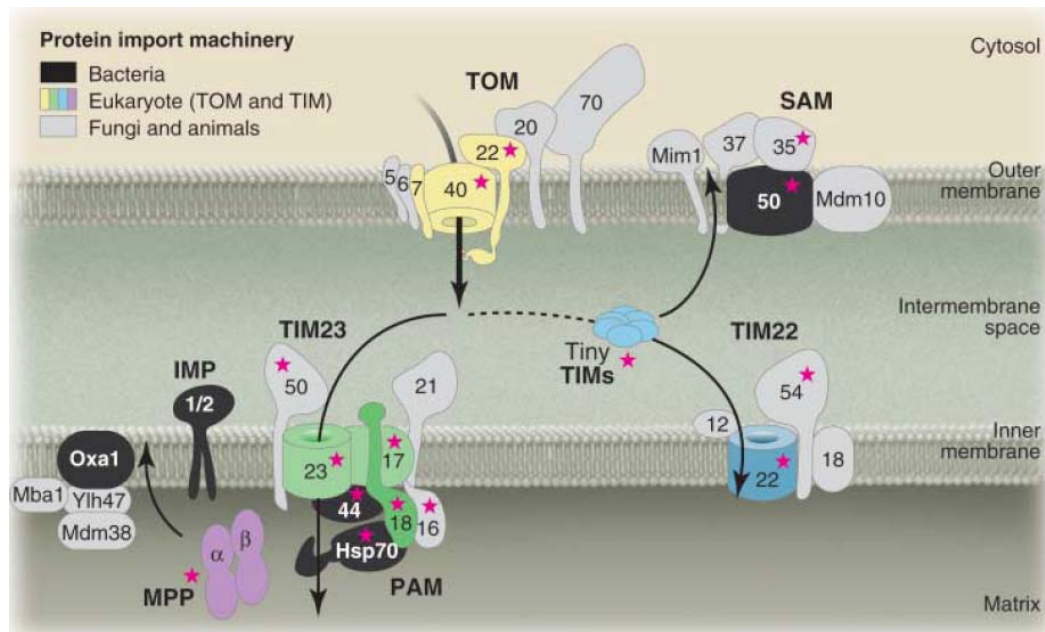


Fig 1.10 .The mitochondrial import Machinery. Components of the TOM, TIM and SAM complexes are shown. Arrows indicate the directional flow of proteins to their designated mitochondrial compartments. Stars indicate proteins that have been show to be essential for yeast viability. PAM – protein import motor, MPP - mitochondrial processing peptidase, IMP - inner membrane peptidase. Taken from Dolezal et al., 2006.

1.6.3 The TIM22/TIM23 Complex

Once proteins have passed through the TOM complex they are passed to one of two inner membrane transport machines known as the TIM22 and TIM23 complexes. Proteins destined for the matrix, and many which are destined for the IMS are transported by the TIM23 translocase, while proteins destined for the inner membrane are routed by the TIM22 complex (Fig 1.10) (Koechler, 2004). The TIM23 complex is composed of the pore forming Tim23 channel, the Tim17 regulatory subunit and Tim50. Mitochondrial polypeptides first bind to Tim50 which in turn passes them to Tim23; Tim50 regulates the opening and closing of the channel and Tim17 helps to determine whether the substrates are inserted into the inner membrane or transported to the matrix (Meinecke et al., 2006, Chakinska et al., 2005). Tim44 on the inner membrane binds to mitochondrial HSP70 (mtHSP70) and recruits it to the TIM23 complex where it binds to the incoming unfolded proteins (Moro et al., 2002). The energy needed to transport proteins is provided by ATP hydrolysis which causes mtHSP70 to dissociate from Tim44 and bind to the incoming protein; successive rounds of mtHSP70 binding enable complete translocation of the precursor protein (Liu et al., 2003).

The TIM22 complex is composed of the inner membrane proteins Tim22, Tim54 and Tim18 and is responsible for import of members of the solute carrier family and a number of small Tim proteins destined for integration into the inner membrane (Jensen and Dunn, 2002). Unlike the TIM23 complex, the TIM22 machinery does not require ATP, instead the motor energy is provided solely by inner membrane electrical potential (Dolezal et al., 2006). Transport through the TIM22 complex is aided by a family of so-called tiny-Tim proteins which guide hydrophobic precursors across the intermembrane space and include Tim8, Tim9, Tim10, Tim12 (Koechler, 2004). The tiny-Tims have varying substrate specificities; for example, transport of Tim23 through the TIM22 complex requires Tim8 and Tim13, while transport of carrier proteins requires Tim9 and Tim10 (Paschen et al., 2000). The importance of this import pathway is underscored by the finding that mutations in Tim8 (also known as deafness-dystonia polypeptide 1 - DDP1) causes deafness dystonia syndrome (also known as Mohr-Tranebjaerg Syndrome) with symptoms including deafness, blindness and mental retardation (Jin et al., 1996). The mutation in Tim8 prohibits its binding to Tim13 and thus biogenesis of Tim23 is compromised which leads to the neurodegeneration seen in this condition (Paschen et al., 2000).

1.6.4 The SAM Complex

The outer membrane of the mitochondria contains many α -barrel proteins such as the voltage-dependent anion channel (VDAC), Tom40 and Mdm10 (mitochondrial disruption and morphology 10). These α -barrel proteins require a different sorting route to other mitochondrial proteins and this is provided by the sorting and assembly machinery (SAM) complex (also known as the translocase of outer membrane α -barrel proteins - TOB). The SAM complex is functionally coupled to the TOM complex and consists of the channel forming Sam50 (Tob55), the α -barrel receptor Sam35 (Tob38) and Sam37 (Tob37) (Fig 1.10) (Kutik et al., 2008). Along with Tom40, Sam50 and Sam35 are the only mitochondrial outer membrane proteins essential for cellular viability (Milenkovich et al., 2004, Dolezal et al., 2006). The mammalian homologs of Sam35 and Sam37 have been identified as metaxin 1 and metaxin 2 respectively (Armstrong et al., 1999).

1.7 The DNA Damage Response

1.7.1 Double Strand Breaks

DSBs occur naturally as a facet of normal cellular function, for example through meiosis mediated genome rearrangements, through physical stress during mitosis, during V(D)J recombination in lymphocytes and through endogenous ROS damage (Shrivastav et al., 2008). DSBs are also generated by external DNA damaging agents such as UV, ionizing radiation (IR) and cancer chemotherapeutics such as topoisomerase inhibitors. Failure to correctly repair DSBs can lead to chromosomal instability and cancer, therefore cells have developed sophisticated systems to detect DSBs and repair the damaged DNA. Once a DNA lesion has been induced, the DNA damage response (DDR) machinery is activated, resulting in cell cycle arrest via a series of DNA damage checkpoints. This allows the cell time to repair the lesion or alternatively when there are too many lesions to repair, initiate the apoptotic cascade (d'Addia di Fagagna, 2008).

1.7.2 Initiation of the DNA Damage Response: ATM and H2AX

Following the generation of DNA double strand breaks (DSBs) the MRN complex is recruited to the site of damage. The MRN complex is composed of Nbs1 (Nijmegen breakage

syndrome 1), Mre11 (meiotic recombination 11) and Rad50 and is essential in sensing damaged DNA (Hopfner et al., 2002). Mre11 possesses both exo- and endonuclease activities which participate in unwinding the DNA, in addition Mre11 binds both Rad50 and Nbs1 and holds them together in a complex (Rupnik et al., 2008). Rad50 is responsible for holding the broken ends of the chromosome together and Nbs1 regulates binding of several downstream DNA repair proteins (Rupnik et al., 2008). While the broken DNA ends are being held in place, a signalling cascade is initiated to recruit other members of the DDR to the required area. (Fig 1.11). Once the MRN complex is attached to the broken DNA, Nbs1 binds the PI3K-related serine/threonine kinase ataxia-telangiectasia mutated (ATM) (Uziel et al., 2003). This has recently been shown to be achieved through the generation of ssDNA oligos by the exonuclease activity of Mre11 which act as a signal for ATM recruitment and activation (Jazayeri et al., 2008). ATM is inactive in normal cells, residing as a dimer in a multimeric complex and upon recruitment by Nbs1, ATM undergoes auto-phosphorylation on serine 1981, leading to dimer dissociation and ATM activation (Bakkenist and Kastan, 2003). ATM phosphorylates a plethora of targets which participate in the DDR including H2AX, Chk2, p53, BRCA1, SMC1, Artemis and Nbs1, ATM activation therefore causes cell cycle arrest at the G1/S, intra-S and G2/M checkpoints and facilitates DNA repair (Lee and Paull, 2007). Mutations in the ATM gene cause the inherited disorder Ataxia-telangiectasia (A-T) which is characterized by cerebellar ataxia, immunodeficiency and increased risk of cancer (Savitsky et al., 1995).

The key step in the ATM signal transduction cascade appears to be phosphorylation of the histone protein H2AX at serine 139. •H2AX (the phosphorylated form of H2AX) recruits additional ATM monomers, resulting in a positive feedback loop and this amplification leads to a spread of •H2AX over a several hundred kilobase region around the site of the double stranded DNA break (Burma et al., 2001). This event generates a molecular beacon which recruits the entire downstream apparatus of the DDR (Fig 1.11). Cells from H2AX deficient mice show genomic instability and radiation-induced chromosomal aberrations, underscoring the central role of H2AX in the signalling and repair of DSBs (Celeste et al., 2002). Recently, H2AX has been shown to be regulated by post-translational modifications other than phosphorylation. Ikura et al. showed that ionizing radiation lead to H2AX acetylation by the histone acetyl transferase Tip60, this was followed by ubiquitination of H2AX by Ubc13 and subsequent release of H2AX from damaged chromatin (Ikura et al, 2007). H2AX phosphorylation may also influence chemoresistance; radiosensitive tumors were shown to

retain \bullet H2AX activity for longer than radioresistant tumors and a peptide mimicking the carboxy terminal tail of H2AX increased cell death in irradiated radioresistant tumor cells (Tanega et al., 2004). In addition to its role in the DDR, H2AX is also involved in apoptosis. UVA irradiation leads to phosphorylation of H2AX by JNK and this was found to be essential for DNA fragmentation mediated by caspase-activated DNase (CAD) (Lu et al., 2006). H2AX deficient cells have also been shown to have a greater sensitivity to the topoisomerase II inhibitor etoposide (Dona et al., 2008)

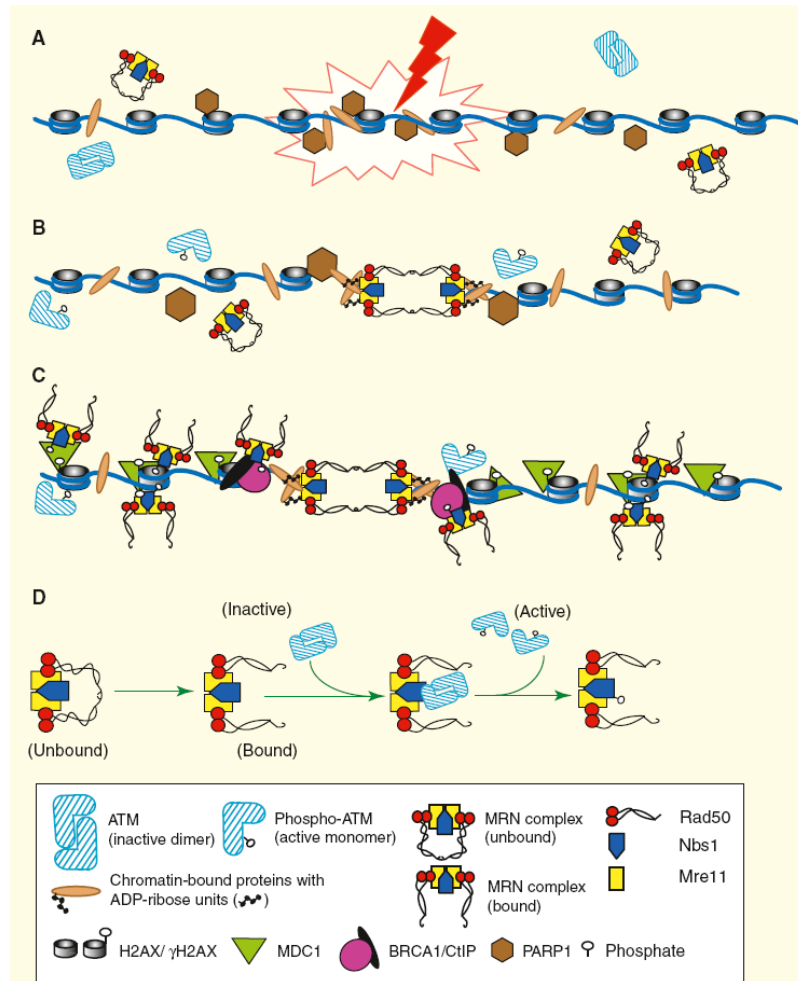


Fig 1.11. Schematic of the DNA damage response. (A) Following DNA damage, the MRN complex is recruited to the site of the DSB, PARP1 attaches ADP-ribose units to chromatin-bound proteins. (B) The MRN complex binds to the broken DNA and holds the ends together, NBS1 interacts with \bullet H2AX and Mre11 which signals further recruitment of the MRN complex. Autophosphorylation of ATM leads to activation of downstream components of the DDR pathway. (C) MDC1 is recruited by \bullet H2AX, MDC1 then recruits repair proteins such as BRCA1 and its binding partner CtIP are recruited to the broken ends and begin the repair process. (D) Model of the role of the MRN complex in activation of ATM. Taken from Rupnik et al., 2008.

DNA is repaired in two ways; non homologous end joining (NHEJ) and homologous recombination (HR). Breaks produced by collapsed replication forks are primarily repaired by HR whereas NHEJ repairs breaks when the homologous sister chromatid cannot be located due to condensed chromatin (Shrivastav et al., 2008). NHEJ proceeds in a stepwise manner, the broken DNA end is processed by the MRN complex followed by binding of Ku70 and Ku80. Next the DNA-dependent protein kinase catalytic subunit (DNA-PKcs) is recruited to the DSB and undergoes autophosphorylation and in turn phosphorylates DNA Ligase IV which completes the repair (Adachi et al., 2001). H2AX has been shown to modulate both the HR and nonhomologous end joining NHEJ pathways of DSB repair (Bassing et al., 2002).

Single stranded breaks are formed by replicative stress and UV radiation and result in a distinct signaling cascade; single-stranded DNA-binding protein replication protein (RPA) binds the area around the ssDNA break and recruits ATM and Rad3-related protein (ATR) (Abraham, 2001). ATR in turn activates a separate signal transduction pathway from ATM, however this will not be discussed in detail here since the results presented all deal with double stranded breaks.

1.7.3 Amplification of the DNA Damage Response: MDC1

Once the DNA damage signal is initiated it needs to be amplified; this is achieved through the mediator of DNA damage checkpoint protein 1 (MDC1). Within minutes of DNA damage MDC1 is recruited by •H2AX and becomes phosphorylated in an ATM/Chk2 dependent manner (Goldberg et al., 2003). MDC1 is central in recruiting the DNA repair factors 53BP1 and BRCA1 as well as further recruitment of the MRN complex to the DSB site (Stewart et al., 2003). Reduced expression of MDC1 is associated with decreased apoptosis and defective intra-S phase and G2/M checkpoints due to reduced Chk1 phosphorylation (Lou Z et al., 2003, Stewart et al., 2003). Silencing of MDC1 had no effect on •IR mediated activation of ATM or •H2AX, however reduced MDC1 levels lead to a more rapid decline in phosphorylation of H2AX (Stucki et al., 2005). Thus MDC1 is dispensable for the initial phosphorylation of ATM and H2AX immediately following formation of a DSB, however MDC1 is necessary for subsequent amplification of the DDR by further recruiting ATM,

resulting in an ATM-MDC1-H2AX positive feedback loop (Lou et al., 2006). Therefore MDC1-mediated ATM accumulation at DSBs induces continual phosphorylation of γ -H2AX and maintains the DDR (Stucki et al., 2005). MDC1^{-/-} mice exhibit deficiencies in checkpoint activation and DNA repair, ATM signalling in these mice was found to be defective, leading to reduced phosphorylation of Nbs1, Chk1 and Chk2 and insufficient activation of the DDR (Lou et al., 2006). MDC1 therefore plays a central role in the DNA damage response pathway by amplifying the ATM signal and orchestrating recruitment of repair factors to DSBs. Once MDC1 recruits a sufficient amount of ATM, Chk1 and Chk2 become phosphorylated in an ATM dependent manner and diffuse throughout the nucleus spreading the DDR from the site of the break. If the DNA lesion is damaging enough, it thus leads to activation of the checkpoint response involving p53 and cell-division cycle 25 (CDC25) phosphatases. Ultimately lesions that are difficult to repair or persistent will result in cellular senescence or apoptosis.

1.8 The Innate Immune System

1.8.1 Inflammation

The innate immune system is the body's first line of defense when challenged with a foreign object or invading pathogen. Activation of the innate immune system leads to localised inflammation at the site of initial contact with the invading microorganism and is characterised by dilation of blood vessels, cell trafficking to infected tissue and release of inflammatory mediators and chemoattractants. Once they cross the epithelial barrier, invading pathogens are recognised by resident tissue macrophages. Activated macrophages release a host of cytokines and chemokines which promote the recruitment of neutrophils to the site of infection and initially kill invading microorganisms through the release of various reactive oxygen and nitrogen species. This is gradually followed by further recruitment of macrophages which ingest invading pathogens and secrete more inflammatory mediators, all of which contribute to overcoming the initial infection. Mediators of the innate immune system also induce upregulation of co-stimulatory molecules on dendritic cells (DCs), resulting in recruitment of cells of the adaptive immune system, necessary when the innate immune system cannot overcome the pathogenic challenge.

1.8.2 Toll-Like Receptors (TLR)

Detection and response to microbial infection is mediated by a limited number of pattern recognition receptors (PRRs) expressed on DCs or macrophages which recognise conserved molecular products from bacteria, viruses, fungi and protzoa. This recognition by the innate immune system stimulates production of cytokines, type I interferons and chemokines as well as promoting DC maturation and ultimately recruitment of the machinery of the adaptive immune response (Kawai and Akira, 2005). Mammalian PRRs include a family of receptors termed the Toll-like receptors (TLR), so called because of their homology to the *Drosophila* Toll protein, and it is now widely accepted that TLRs are the main architects in controlling the innate immune response following infection. Do date, 11 mammalian TLRs have been characterised, all of which recognise distinct microbial PAMPs (Fig 1.12). Some TLRs are expressed as cell surface receptors and recognise structures present on the bacterial cell surface, for example TLR4 is a receptor for LPS, TLR2 recognises peptidoglycan and TLR5 binds flagellin (O'Neill, 2006). Alternatively, TLRs can be expressed in the cytosol in endosomal vesicles; these include TLR3 which recognises double-stranded viral RNA, TLR7 and TLR8 recognise single-stranded viral RNA and TLR9 binds to unmethylated CpG DNA motifs of bacteria and viruses (O'Neill, 2004). The diversity of structures to which TLRs can bind allows the innate immune system to mount a rapid first line of defense without the need to recognise species-specific antigens.

TLR 1	Triacylated lipoproteins
TLR 2	Peptidoglycan/zymosan
TLR 3	dsRNA (Poly I:C)
TLR 4	Lipopolysaccharide
TLR 5	Flagellin
TLR 6	Diacylated bacterial lipopeptide
TLR 7	ssRNA
TLR 8	ssRNA
TLR 9	CpG DNA

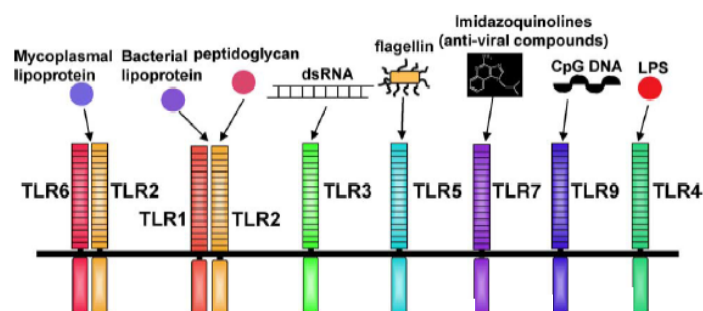


Fig 1.12. TLRs and their cognate ligands. Table outlining TLRs and their known ligands. On the right; a schematic of TLRs recognising molecular patterns associated with pathogens. Adapted from Yamamoto et al., 2006.

1.8.3 TLR Adaptors

TLR signalling is propagated through a series of protein-protein interactions between adaptor proteins (Fig 1.3). All TLRs apart from TLR3 recruit MyD88 (myeloid differentiation primary response gene 88) via MAL/TIRAP (myelin and lymphocyte protein/ TIR domain-containing adaptor protein) through TIR (translocated intimin receptor) domain interactions, binding of MyD88 triggers recruitment and sequential phosphorylation IRAK4 (interleukin 1 receptor-associated kinase 4) and IRAK1, causing them to dissociate from the receptor complex and bind to TNF receptor-associated factor 6 (TRAF6) (Dunne and O'Neill, 2005). TRAF6 induces TAK1 (TGF- β activated kinase 1) activity and ultimately activation of the NF- κ B and MAPK pathways, which are the main mediators of cytokine production (Fig 1.13). A second MyD88 independent pathway is employed by TLR3 and TLR4 which makes use of the adaptor protein TRIF (TIR domain containing adaptor inducing IFN- α), TRIF induces TBK1 (TANK binding kinase 1) and IKK α which phosphorylate the transcription factor IRF3, leading to its nuclear translocation and subsequent upregulation of IFN- α (Hoebe et al., 2003, Sato et al., 2003). NF- κ B and MAPK are also induced via the MyD88 independent pathway, however activation is delayed, due to the requirement of secondary cytokine production via IRF3 (Kawai and Akira, 2005, Yammamoto et al., 2003). The picture has now emerged where various pathogens rapidly induce appropriate host responses through a limited number of receptors and adaptor molecules, promoting initial pathogenic clearance or activation of the adaptive immune response.

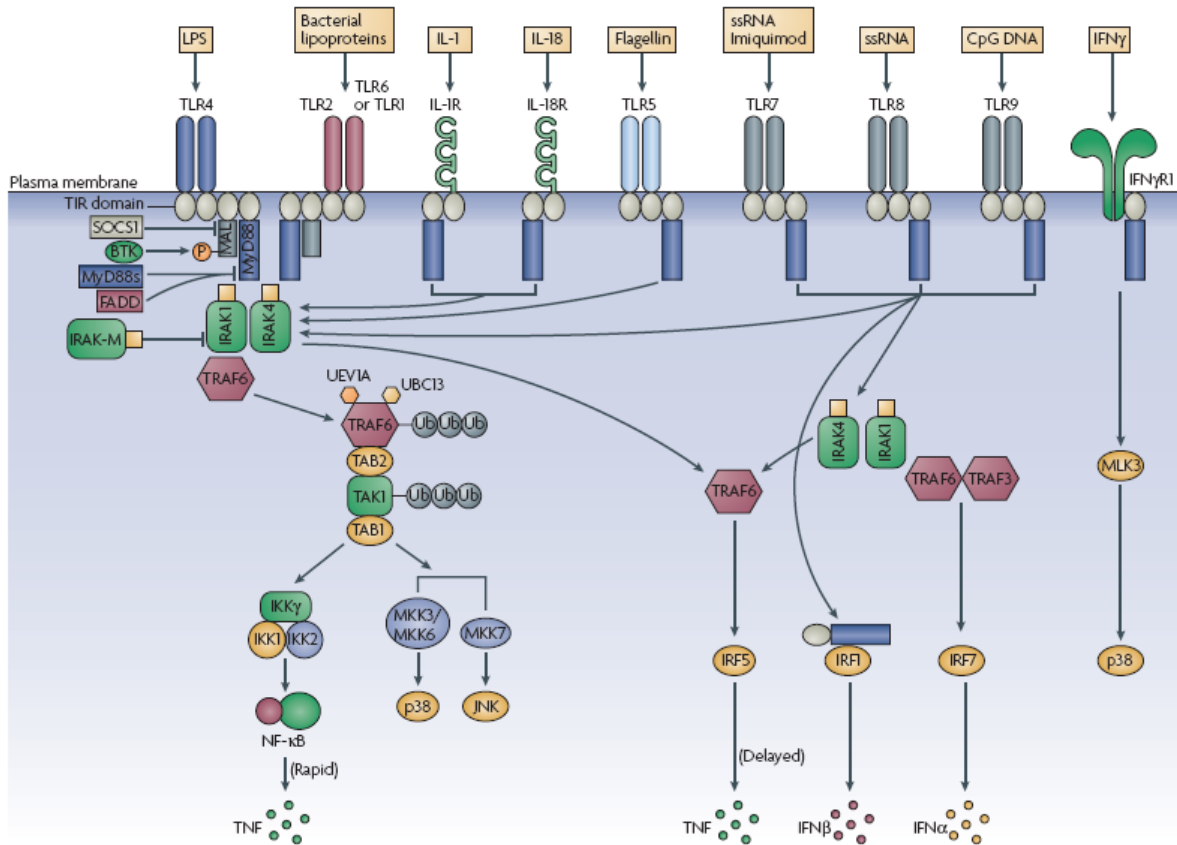


Fig 1.13. Signalling pathways initiated by TLR stimulation. All TLRs recruit either MyD88 and/or TRIF and these in turn recruit IRAK4. A series of protein-protein binding events lead to a complex of IRAK4, IRAK1, TRAF6, TAK1, the TAK1 binding proteins TAB1 and TAB2 and the ubiquitinating factors UEV1A and UBC13 which modify and activate TRAF6 and TAK1. TAK1 is a mitogen-activated protein kinase kinase kinase and phosphorylates and MKK3, MKK6 and MKK7 leading to subsequent p38 and JNK activity. TAK1 also activates the IKK complex responsible for NF- κ B activation and pro-inflammatory cytokine production such as TNF- α . In the case of TLR7, TLR8 and TLR9, IRAK4 recruitment also leads to TRAF3/6 mediated interferon regulatory factor (IRF) activation and upregulation of TNF- α , IFN- β and IFN- α . In addition MyD88 recruitment to the IFN- γ receptor can activate p38 through mixed lineage kinase-3 (MLK3). The bridging factor MAL (MyD88-adaptor protein like) is responsible for MyD88 recruitment and is regulated by BTK (Burton's tyrosine kinase) and SOCS1. (Taken from O'Neill & Bowie, 2007)

1.9 The Adaptive Immune System

1.9.1 Antigen Presentation

In contrast to the innate immune system, the antigen-specific adaptive immune system has developed to recognise and destroy specific pathogens and develop a lasting immunity to individual organisms. A particular microbial antigen must first be recognised by antigen presenting cells (APC) such as dendritic cells, macrophages or B cells, loaded on MHC (major histocompatibility complex) molecules and presented to T cells. APCs such as dendritic cells reside in the peripheral tissues where they constantly scan their surroundings for foreign antigens. Once they come in contact with antigen, they migrate to draining lymph nodes where they prime naïve T cells which bear the corresponding antigen-specific TCR (T cell receptor) (Randolph et al., 2005). Additional obligatory co-stimulatory signals are provided by the interaction of CD28 on the T cell with CD80 or CD86 on APCs (Randolph et al. 2005).

1.9.2 CD8 Cells

Activated T cells form two distinct classes, CD8⁺ and CD4⁺. CD8⁺ T cells recognise antigen loaded on MHC class I molecules and attack predominantly virally infected cells or cells harboring intracellular bacteria. Activated CD8⁺ T cells are also known as cytotoxic T cells, once they recognise antigen on an infected cell they can directly induce apoptosis by secreting cytotoxic granules such as perforin and granzyme or through FASL-FAS interactions (Bevan, 2004). Triggering the apoptotic programme has a select advantage in that it does not damage neighboring non-infected cells.

1.9.3 CD4 Cells and Th1/Th2/Th17 Differentiation

CD4⁺ helper T cells (Th) recognise specific MHC class II – peptide complexes on APCs. Once the antigen is recognised by the naïve Th cells and the Th cell receives co-stimulation from APCs, they begin produce IL-2, undergo proliferation and differentiate into three main classes of armed effector Th cells with distinct gene expression patterns. These three Th cell subsets known as Th1, Th2 and Th17 perform distinct functions in the immune system.

Th1 cells promote cell-mediated immunity and produce cytokines such as IL-2, IFN- γ and lymphotoxin- β (LT- β) (Murphy and Reiner, 2002). These cytokines promote CD8 T cell proliferation and differentiation, activate macrophages, neutrophils and natural killer (NK) cells and stimulate the production of opsonizing and complement-activating antibodies for enhanced attachment during phagocytosis (Szabo et al., 2003). IFN- γ stimulation of macrophages increases their production of toxic oxygen radicals, nitric oxide, and hydrolytic lysosomal enzymes, enabling the killing of microbes within their phagolysosomes, it also stimulates production of TNF- α , IL-1 β and IL-12 (Angello et al., 2003).

Th2 cells produce IL-4, IL-5, IL-9, IL-10 and IL-13, collectively these cytokines induce B cell differentiation into antibody secreting plasma cells (Mowen and Glimcher, 2004). They also promote antibody class switching which induces mast cell degranulation, this is critical in parasite killing since the majority of extracellular parasites are too large to be ingested by phagocytes (Mowen and Glimcher, 2004). Moreover, Th2 cells are central players in allergy and promote eosinophilic responses, Th2 cells can also counteract a strong Th1 response via production of the anti-inflammatory cytokine IL-10 (Fiorentino et al., 1991).

Th17 cells are a pro-inflammatory subset associated with host defence against infectious agents and auto-immune disease (Dong, 2008). Production of IL-23 stimulates the proliferation of Th17 cells which secrete IL-17A, IL-17F and IL-21; these cytokines then promote further recruitment of macrophages and neutrophils to areas of infected tissue (Dong, 2008). IL-17 has been shown to have roles in several inflammatory diseases such as arthritis, colitis and multiple sclerosis (Rohn et al., 2006, Komiyama et al. 2006).

The class of effector cell generated depends on the nature of the invading pathogen, for example, intracellular bacteria and viruses promote development of a Th1 dominated response, whereas allergens and extracellular parasites are strong inducers of Th2 responses. Differentiation into Th1, Th2 or Th17 is established during the priming phase of an immune reaction and depends on the cytokine profile produced by cells of the innate immune system; IL-12, IL-18 and IFN- γ promote Th1 cell production, IL-4 and IL-25 induce a Th2 phenotype and TGF- β , IL-6 and IL-21 prime Th17 cells (Fig 1.14). TLR ligands can also influence generation of effector T cell lineages; TLR2 ligands favour Th2 responses and IL-10 production, whereas TLR4, 5 and 9 promote Th1 differentiation (Schnare, 2001).

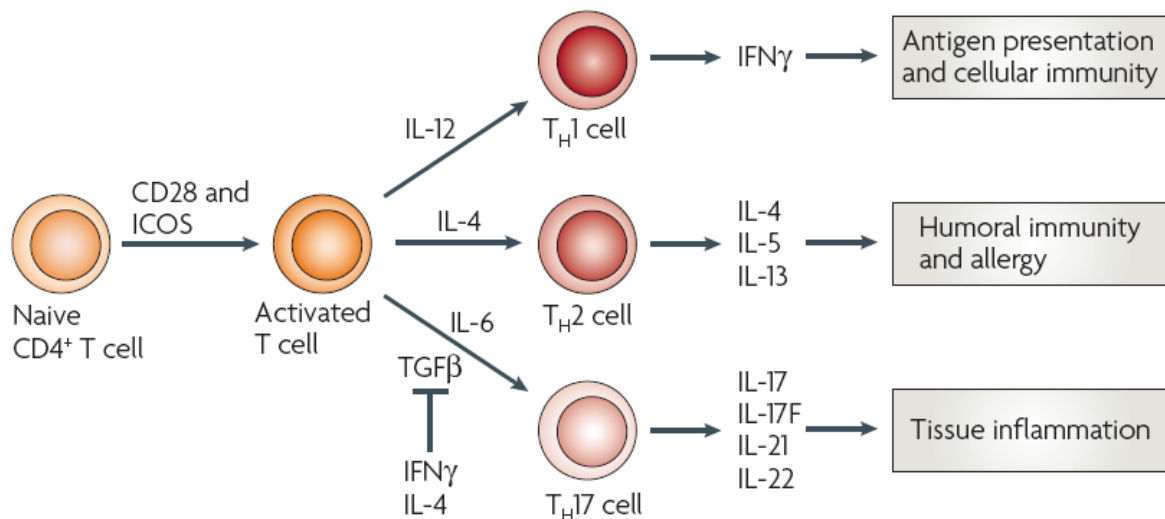


Fig 1.14. Outline of T-helper cell differentiation. Naïve CD4⁺ T cells are activated by co-stimulatory molecules such as CD28 and inducible T-cell co-stimulator (ICOS). Activated T cells differentiate down three lineages; Th1, Th2 or Th17. IL-12 stimulates Th1 cells which produce IFN- γ , secretion of IFN- γ is important in antigen presentation and cellular immunity. Th2 cells are stimulated by IL-4 and produce IL-4, IL-5, IL-10, and IL-13 which have roles in B cell production and allergic responses. TGF- β and IL-6 stimulate the production of Th17 cells which produce IL-17, IL-17F, IL-21 and IL-22 - cytokines important in pro-inflammatory responses. Taken from Dong C, 2008.

1.10 Cytokines

1.10.1 TNF

TNF is a potent pro-inflammatory cytokine which has many pleiotropic effects including leukocyte and lymphocyte activation and migration, activation of endothelial cells with upregulation of adhesion molecules and chemokines, recruitment of neutrophils through extravasation from the blood stream to the site of infection, fever the acute phase response and apoptosis (Bradley, 2008). TNF- α is a potent inducer of AP-1 and NF- κ B transcription factors, which are important in cytokine, chemokine and adhesion molecule upregulation.

1.10.2 IL-10

The immune system has evolved multiple ways to limit the duration of the inflammatory response; one of the main ways this is achieved is through production of anti-inflammatory cytokines such as IL-10. IL-10 is produced from macrophages, DCs, B cells and CD4⁺ Th2

cells. IL-10 inhibits macrophage activation, resulting in reduced levels of TNF- α , IL-1, IL-6, IL-12, COX-2, iNOS and several chemokines (Couper et al., 2008). IL-10 has been shown to reduce antigen presentation by macrophages and DCs by abrogating MHC class II, CD80 and CD86 expression (Couper et al., 2008). Furthermore, IL-10 suppresses Th1 function through inhibition of IL-12, this in turn reduces IFN- γ and LT- α secretion from Th1 cells (Haddad et al., 2003). The importance of IL-10 as a modifier of immune function is underscored by the fact that many tumors acquire an IL-10 secreting phenotype which allows them to circumvent cell-mediated immunity (Williams et al., 2004). Moreover, IL-10^{-/-} mice develop spontaneous intestinal inflammation when housed under specific pathogen free conditions, these mice remain healthy when housed under gnotobiotic conditions, suggesting that IL-10 is involved in regulating host responses to the intestinal flora (Sellon et al., 1998, Berg et al., 1998). IL-10 has been shown to limit pathological inflammation in several disease models, including inflammatory bowel disease (IBD), septic shock, experimental autoimmune encephalomyelitis (EAE) and collagen-induced arthritis (Williams, 2004).

STAT3 has been shown to be essential for IL-10 mediated anti-inflammatory effects in macrophages. Removal of STAT3 binding sites in the IL-10 receptor abrogated the ability of IL-10 to suppress LPS-mediated TNF- α production (Riley et al., 1999). The anti-inflammatory effects of STAT3 are abrogated by cyclohexamide, suggesting that either STAT3 dependent target genes are required or that STAT3 titrates away cofactors from inflammatory gene promoters (Murray, 2005). Macrophage or endothelial cell-specific STAT3 knockout mice develop colitis similar to that seen in IL-10^{-/-} mice (Welte et al., 2003). One candidate that has emerged as a potential mediator of IL-10 signalling is the STAT3 target protein Bcl-3, a member of the I κ B family. Lentiviral mediated overexpression of Bcl-3 inhibited TNF- α production from LPS stimulated macrophages, while IL-10 could not suppress TNF- α production from macrophages deficient in Bcl-3 (Kuwata et al., 2003). Bcl-3 was shown to bind to the p50 and p52 subunits of NF- κ B and enhance p50 mediated inhibition of TNF- α by binding to the TNF- α promoter (Kuwata et al., 2003). As discussed earlier, SOCS3 serves as a main regulator of STAT3 signaling and determines whether STAT3 induces a pro- or anti-inflammatory signal.

1.10.3 IL-12

IL-12 is a potent pro-inflammatory cytokine secreted by several cell types. It consists of two subunits; p35 and p40, encoded by two unrelated genes on separate chromosomes which form a functional p70 heterodimer (Kang et al., 2005). IL-12 is secreted by macrophages, DCs, neutrophils and mast cells among others and promotes production of IFN- γ , TNF- α , IL-2, IL-8 and GM-CSF from T cells and NK cells. It increases cell mediated cytotoxicity in CD8⁺ T cells and NK cells by increasing the formation of cytotoxic granules and upregulates adhesion molecule expression (Kang et al., 2005). IL-12 is the main stimulator of Th1 polarisation and along with IFN- γ antagonises Th2 differentiation.

When IL-12 is present early during clonal expansion, it irreversibly primes CD4⁺ and CD8⁺ T cells to produce high levels of IFN- γ upon restimulation (Trinchieri et al., 2003). T cells enhance IL-12 not only through IFN- γ and IL-4 production but also through direct cell contact, priming DCs with a bacterial stimulus upregulates CD40 and makes them responsive to CD40L expressed on T cells, allowing optimal IL-12 production (Trinchieri et al., 2005). IL-12 is negatively regulated by several cytokines; including IL-10 and TGF- β , indeed IL-12 may limit its own synthesis by inducing T cells to secrete IL-10 (Meyaard et al., 1996). IL-10 has been shown to inhibit IL-12p40 transcription by inhibiting cRel recruitment to the IL-12p40 promoter in a STAT3 dependent manner (Hoentjen et al., 2005). Overproduction of IL-12 can have detrimental consequences as evidenced in IL-10 deficient mice which develop an IL-12 mediated intestinal inflammation (Davidson et al., 1998).

1.11 MAPK Signalling in the Innate Immune System

1.11.1 Upstream Signals

Innate immune signals received through TLRs result in the activation of two main pathways, the NF- κ B pathway and the MAPK pathway. The MAPKs are an evolutionary conserved family of Thr/Tyr kinases with vast numbers of substrates and as such are involved in a wide range of biological processes. They are activated in response to a large variety of signals; including inflammatory cytokines, ischaemia, DNA damage, oxidative stress, heat shock and growth factors. Their function is to transduce signals from the extracellular environment to regulatory elements within the cell. There are three major groups of MAPKs, the c-Jun NH2-

terminal kinases (JNK), the p38 MAPKs and the extracellular signal-regulated kinases (ERK). MAPKs are proline-directed serine/threonine kinases and are activated by dual phosphorylation at a Thr-X-Tyr motif. MAPK activation is controlled by a three-tier protein kinase cascade, where MAPK are phosphorylated by a MAP kinase kinase (MEK/MKK/MAP2K), these in turn are activated by MKK kinases (MKKK/MEKK/MAP3K) (Fig 1.15) (Chang and Karin, 2001). The choice of proteins involved in each signalling module confers a level of adaptability and complexity to the control of MAPK signalling cascades. The diverse cellular stresses which produce a varied number of cellular responses, controlled by just a few MAPKs illustrates an underlying level of specificity to each signalling module.

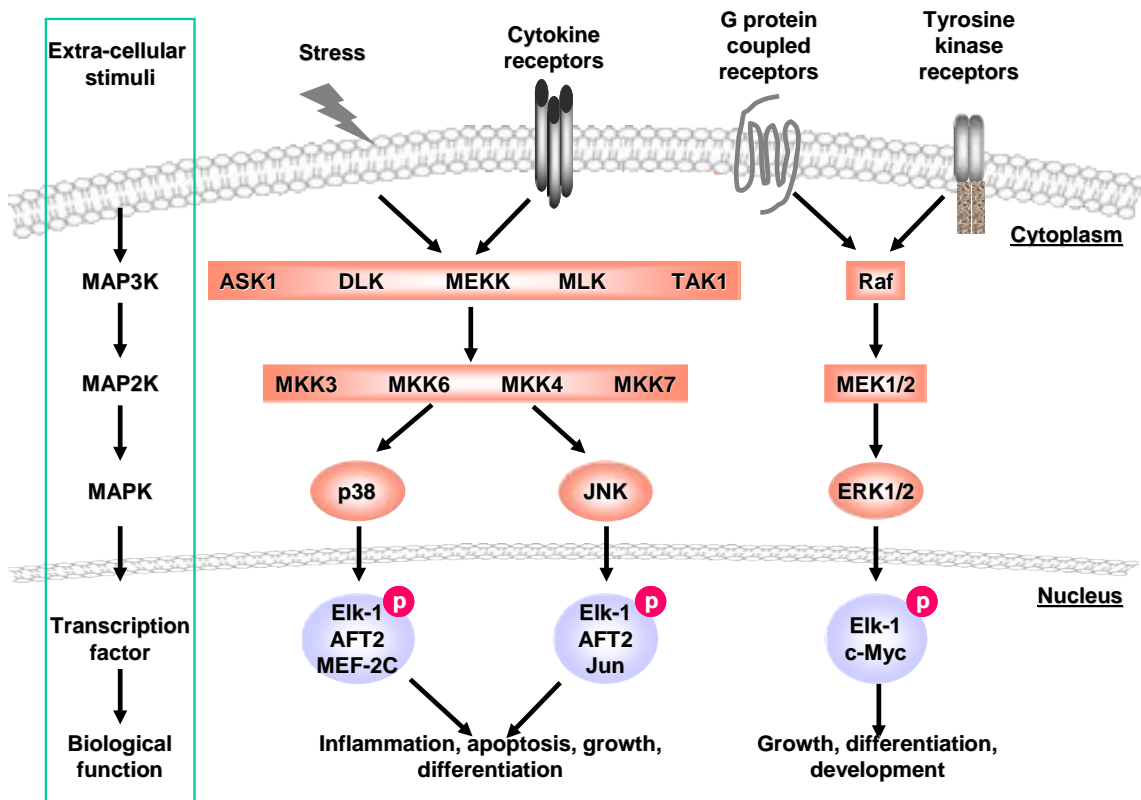


Fig 1.15. The MAPK signaling cascade. MAPK signaling is controlled by a cascade from MAP3Ks>MAP2K> MAPK. Stress, Cytokines, G-proteins, and tyrosine kinases receptors all activate MAP3Ks, leading to activation of the main MAPKs p38, JNK and ERK. Downstream transcription factors include Elk-1, AFT2, MEF2, Jun and c-Myc. Adapted from Cellsignaling.com

1.11.2 p38 MAPK

p38 is induced by a variety of cellular stress including LPS, heat shock, osmotic shock, oxidative stress and pro-inflammatory cytokines such as TNF- α and IL-1 α . p38 has 4 isoforms; p38 α and p38 β which share 75% homology and the more distantly related proteins p38 δ and p38 γ . p38 α and β are ubiquitously expressed, whereas p38 δ and γ have limited tissue specificity (Saklavata, 2004). Although they share a high degree of homology, individual p38 isoforms have differing affinities for substrates (Ashwell, 2006). p38 is activated by MKK 3, 4 and 6 and upstream MAP3Ks include TAK1, ASK1, MLK1 and MEKK4 (Zarubin and Han, 2005). Several targets of p38 are directly involved in the inflammatory response; including MAPK activated protein kinase (MK2), MNK1, ATF, ELK1 and NFAT (Ashwell, 2006).

The use of the p38 MAPK inhibitor SB203580 has shown that p38 MAPK is necessary for induction of several pro-inflammatory factors, such as TNF- α , IL-1 α , IL-6, iNOS and COX-2 and that p38 can upregulate cytokine production through direct phosphorylation of transcription factors or through transcript stabilisation (Ashwell, 2006). Many inflammatory cytokines contain an AUUUA motif in a U rich region of their 3' untranslated region known as AU-rich element (ARE). AREs inhibit mRNA expression at the transcriptional and posttranscriptional level by targeting mRNA for deadenylation and promoting 3'-5' exonuclease decay (Dean et al., 2003). Indeed insertion of AREs into otherwise stable mRNAs results in their destabilisation and reduced protein expression (Neininger et al., 2002, Dean et al., 2004). Activation of p38 stabilises many mRNA transcripts containing AREs, including TNF- α , IL-3 IL-6, IL-8 and COX-2 (Kaminska, 2005). The p38 target protein MK2 has a prominent role in transcript stabilisation as evidenced in MK2^{-/-} mice, which are unable to produce TNF- α in response to LPS, this renders them resistant to endotoxic shock (Kotlyarov et al., 1999). MK2 controls TNF- α expression through its ARE, since deletion of the ARE allows LPS induced TNF- α production in the absence of p38 and MK-2 (Kontoyiannis et al., 1999). Tristetrapolin (TTP), a member of the zinc finger family of RNA binding proteins destabilises TNF- α mRNA by binding to its ARE, MK2 appears to phosphorylate 14-3-3 binding sites on TTP, causing it to be sequestered away from mRNA, thereby stabilising the TNF- α mRNA transcript (Carballo et al., 1998).

Using pharmacological inhibition and deletion of MKKs, several studies have demonstrated a prominent role for p38 in the production of IL-10 and IL-12 in both leukocytes and lymphocytes (Yi et al., 2002, Foey et al., 1998, Lu et al., 1999). p38 activity can also effect cytokine translation. Poly-adenylated mRNAs form circular structures due to the 5'-cap binding complex binding to poly-A-binding protein and this circularisation process promotes translation (Saklavata, 2004). Phosphorylation of eIF-4e by the p38 inducible kinase MNK1, increases the interaction between the cap-binding complex and capped mRNAs, enhancing cytokine polysome assembly (Chang and Karin, 2001).

The important role of p38 in inducing cytokine expression is borne out in animal studies where p38 activity has been blocked. Inhibition of p38 activity has been shown to be effective in reducing mortality from toxic shock in mice, improving mucosal healing in Crohn's disease and ameliorating the symptoms of rheumatoid arthritis (Badger et al., 1996, Hommes et al., 2002). Inhibition of p38 reduced cytokine secretion from ex vivo peripheral blood mononuclear cells (PBMCs) and improved clinical outcome to human endotoxemia (Branger et al., 2002). Preliminary studies have also shown p38 inhibitors to be clinically beneficial in human patients with inflammatory conditions, for example p38 inhibitors are currently in phase II trial for rheumatoid arthritis (Pargellis and Regan, 2003).

1.11.3 c-Jun N-terminal Kinase (JNK)

JNK exists as three isoforms, JNK1, 2 and 3; JNK1 and JNK2 are widely expressed whereas JNK3 expression is limited to the brain, heart and testis (Weston and Davis, 2002). JNKs are activated by MKK4 and 7, which transduce signals from the MAP3Ks ASK1, MLK-3, TAK1 and MEKK1-4 (Chang and Karin, 2001). Downstream targets of JNK include c-Jun, ATF2, AP-1, Elk1, p53 and Bcl-2 and active JNK is a potent inducer of apoptosis in response to several cellular insults such as UV irradiation, I/R injury, heat shock and inflammatory cytokines such as TNF-• (Wada and Penninger, 2004). The promoters of several cytokines and chemokines contain binding sites for the inflammatory transcription factor AP-1. AP-1 is a heterogeneous collection of dimeric transcription factors, comprising fos, jun and ATF subunits. JNK has been shown to phosphorylate and upregulate each of these three subunits, thereby enhancing AP-1 activity and cytokine production (Derijard et al., 1994). Similarly to p38, JNK is also involved in TNF-• translational control, overexpression of dominant

negative JNK overcomes LPS induced depression of the translational blockade associated with the ARE (Swanek et al., 1997).

1.11.4 Extracellular Regulated Kinase (ERK)

ERK consists of two isoforms ERK1 (p44) and ERK2 (p42) and is activated primarily in response to mitogens and growth factors. These act through G-protein coupled receptors, which activate the small G-protein Ras, this in turn activates Raf which phosphorylates the MAP2Ks MEK1 and MEK2 (Shaul and Seger, 2007). ERK targets include MK1, ribosomal S6 kinase (RSK), c-myc, cytoplasmic phospholipase () and the transcription factor Elk1. Activation of ERK promotes entry to the cell cycle, differentiation, cell migration and actin skeleton reorganization, and inhibition of apoptosis (Xia et al., 1995, Wada and Penninger, 2004). ERK also has a role in mediating cytokine expression. Inhibition of ERK activity through deletion of its upstream activator, Tpl2 (tumor progression locus 2), showed that ERK is indispensable for LPS induced TNF- α production, this is achieved through enhanced nucleo-cytoplasmic shuffling of the TNF- α transcript, which involves targeting of the ARE (Dumitru et al., 2000). Pharmacological inhibition of ERK also blocks IL-10 production in macrophages and ERK activation promotes phosphorylation of histone H3 at the IL-10 locus making it more accessible to SP1 and STAT3 transcription factors (Yi et al., 2002).

1.11.5 MAPK Phosphatase -1 (MKP-1)

Pro-inflammatory cytokine release must be tightly controlled since dysregulated cytokine production can lead to severe pathologies, including inflammatory, allergic and autoimmune diseases such as septic shock, asthma, Crohn's disease, rheumatoid arthritis and multiple sclerosis. Since MAPKs are so vital to the production of pro-inflammatory cytokines, it is not surprising that the body has evolved effective regulatory systems to limit the extent of MAPK activation following inflammatory stimuli. One way in which this is achieved is through a family of dual specificity phosphatases known as DUSPs or MAPK phosphatases (MKP) which dephosphorylate members of the MAPK family. The MKP family consists of 10 members, all of which have different affinities to each of the 3 MAPKs. MKP-1 has been shown to dephosphorylate all three MAPKs with different affinities, with the order of preference being p38>JNK>ERK, MKP-3 is specific for ERK while MKP-5 inhibits JNK

(Lang et al., 2006, Ashworth et al., 1996, Zhang et al., 2004). MKP-1 is a nuclear enzyme encoded by an immediate early gene and its transcription is induced by most stimuli which activate MAPKs, such as mitogens and stress signals (Sun et al., 1993). In contrast, MKP-3 resides in the cytosol and is not induced by mitogens or stress but is induced during neuronal differentiation (Muda et al., 1996).

MKP-1 upregulation in response to various stresses is dependent on p38 MAPK and MKP-1 has been shown to bind to the C-terminal domain of p38 MAPK resulting in enhanced phosphatase activity, suggesting the existence of a negative feedback loop (Hutter et al., 2002, Li et al., 2001). MKP-1 has also been shown to be both transcriptionally upregulated and phosphorylated by ERK, although the precise role of ERK mediated phosphorylation has not been resolved. Brondello et al. reported that ERK mediated phosphorylation of MKP-1 at two serine residues in its carboxy terminus stabilised MKP-1 and reduced its ubiquitin mediated degradation by the proteasome (Brondello et al., 1999). Lin et al. recently demonstrated however, that ERK mediated phosphorylation at S296 and S323 promotes binding of the E3 ubiquitin ligase skp2, which promotes MKP-1 ubiquitination and degradation (Lin and Yang et al., 2006). The use of pharmacological inhibitors of ERK has also produced similar conflicting data with some studies showing LPS induced MKP-1 expression being ERK dependent while others finding no dependency whatsoever; thus the precise role of ERK in MKP-1 induction is still unclear (Valledor et al., 2000).

MKP-1 is induced in response to peptidoglycan stimulation in RAW264.7 cells and primary peritoneal macrophages (Shepherd et al., 2004). The time course of induction of MKP-1 correlated with inhibition of p38 and JNK activation. Furthermore, knockdown of MKP-1 prolonged p38 phosphorylation and resulted in an increase in peptidoglycan induced TNF- α secretion while overexpression had the opposite effect. Inhibition of MKP-1 in alveolar macrophages enhanced LPS mediated TNF- α production associated with prolonged activation of p38 MAPK (Zhao et al., 2005). Transfection of MKP-1 cDNA into RAW264.7 macrophages reduced LPS induced p38, ERK and JNK phosphorylation in response to LPS as well as reducing production of TNF- α and IL-6 (Chen et al., 2002). These studies suggest that MKP-1 may have a fundamental role in control of the innate immune response.

1.12 Inflammatory Diseases

1.12.1 Multiple Sclerosis

Multiple sclerosis (MS) is an inflammatory disease of the central nervous system, characterised by demyelination and axonal loss, resulting in chronic multifocal sclerotic plaques (Compston and Coles, 2002). Myelin is secreted by oligodendrocytes and forms an insulating sheath around axons, facilitating axonal conductance. Loss of myelin can result in impaired motor, sensory and autonomic functions, all seen to varying degrees in patients suffering from MS (Compston and Coles, 2002). Autoreactive anti-myelin specific T cells are found in the normal population but these are usually suppressed by regulatory T cells (Ellerman et al, 1988). In MS patients however there is a breakdown in tolerance and autoreactive T cells proliferate and enter the CNS where they re-encounter the myelin antigen and induce activation of resident microglia (Raivich and Banati, 2004). Activated microglia then represent the antigen to the T cells, resulting in sustained inflammation and autoimmunity

Experimental autoimmune encephalomyelitis (EAE) is a demyelinating autoimmune pathology that has many of the characteristics of MS and thus has been commonly used as an animal model for this disease. EAE is induced experimentally by immunizing with autoantigens derived from the myelin sheath, such as myelin oligodendrocyte glycoprotein (MOG) or myelin basic protein (MBP). T cells become primed with these peptides in the periphery and migrate to the CNS where they become autoreactive, leading to autoimmune inflammation (El Behi et al., 2005). EAE, like MS, is characterised by distinct phases of pathology; preclinical stage, onset of neurological symptoms, paralysis and remission (Raivich et al., 2004).

The CNS has evolved multiple ways to deal with autoreactive T cells, including the dearth of DCs in the CNS microenvironment and production of FAS ligand to induce T cell apoptosis (Sabelko-Downes et al., 1999). It seems that in the inflammatory setting promoted by autoreactive T cells these control mechanisms are overcome leading to neuronal destruction. Progression of EAE is associated with infiltration of CD4⁺ T cells, CD8⁺ T cells and B cells, although the issue as to whether these cells are primed in the periphery or in situ in the CNS has not been fully resolved (El Behi et al., 2005). While T cell infiltration into the CNS

parenchyma is necessary for development of EAE, infiltrating macrophages or resident microglia are the main effectors of pathology by causing demyelination and oligodendrocyte death which results in axonal deterioration (McGeachy et al., 2005).

Several studies have demonstrated a role for macrophage and DC derived IL-12, TNF- α , IFN- γ and IL-1 β in promoting EAE (Leonard et al., 1995, Korner et al., 1997, Jacobs et al., 1991, McGeachy et al., 2005). IL-12 is a potent inducer of Th1 polarisation and was originally thought to be critical for EAE induction. The use of an anti-IL-12 antibody prevented disease while IL-12 p40^{-/-} mice were resistant to EAE (Leonard et al., 1995, Segal et al., 1998). However, it has now been realised that these results may have been misinterpreted. IL-23 is heterodimer comprised of the p40 subunit common to IL-12 and a unique p19 subunit and it seems that it is IL-23 rather than IL-12 which is indispensable for development of EAE (Cua et al., 2003). This is borne out by the fact that unlike IL-12 p40^{-/-}, IL-12p35^{-/-} mice are not resistant to EAE, while in IL-23^{-/-} mice Th1 primed cells entered the CNS parenchyma but this did not lead to EAE (Cua et al., 2003, Gran et al., 2002). IL-10 has been demonstrated to be effective in reducing the severity of EAE, this has been shown by treating mice with recombinant IL-10 and intracranial injection of an IL-10 producing adenovirus (Bettelli et al., 2003). As would be expected on the basis of these experiments, IL-10 deficient mice are more susceptible to EAE, whereas IL-10 T cell transgenic mice are resistant (Samoilova et al., 1998, Bettelli et al., 1998). Thus, inflammatory cytokine production in the periphery and in the CNS are instrumental in MS pathology and new targets which alter the cytokine profile and clinically influence MS progression have become of great interest, scientifically and medically.

1.12.2 Inflammatory Bowel Disease (IBD)

IBDs are chronic inflammatory diseases of the gut that present clinically as two associated pathologies; Crohn's disease and ulcerative colitis. For as yet unknown reasons, the intestinal mucosa elicits an inflammatory response to the normally non-immunogenic intestinal flora. The resulting influx of neutrophils, macrophages and T cells drives intestinal inflammation, leading to the clinical symptoms of weight loss, diarrhea and abdominal pain (Stokkers and Hommes et al., 2004). TNF appears to be a main mediator in driving intestinal inflammation in Crohn's disease and currently the most successful therapy in Crohn's disease is the anti-TNF monoclonal antibody infliximab (Stokkers and Hommes et al., 2004). A functional IL-

IL-10 producing Th2 response appears to be necessary to suppress the effects of IBD. IL-10^{-/-} mice develop spontaneous chronic colitis and deletion of STAT3 in macrophages and neutrophils leads to exacerbated Th1 mediated response to bacterial antigens, resulting in intestinal colitis (Takeda et al., 1999). Furthermore, recombinant IL-10 has been shown to inhibit IBD induced by T cell transfer into RAG2^{-/-} hosts, while intragastric administration of IL-10 secreting *Lactococcus lactis* ameliorated the clinical symptoms of colitis (Steedler et al., 2000).

Chapter 2: Materials and Methods

2.1 Reagents

The following TLR ligands were used: LPS from *E. coli* serotype O111:B4 (Sigma), peptidoglycan (PGN) from *Staphylococcus aureus* (Fluka), Poly (I-C) (Amersham Pharmacia Biotech), phosphorothioate-modified CpG oligonucleotide DNA (TCCATGACGTTCTGACGTT, synthesized by the Keck Facility at Yale University), synthetic lipoprotein, flagellin and loxoribine (all from Invivogen). ELISA antibodies for IL-6, TNF- α , IL-12 and IL-10, the neutralizing antibody for IL-10 (JES5-2A5), and recombinant cytokines were from BD-Pharmingen. Inhibitors for MAPKs (SP600125, SB203580, U0126) and Ro106-9920 were from Calbiochem. Hydrogen peroxide and tempol were from Sigma. A complete list of cell lines used is presented in Appendix 1C.

2.2 Animals

MKP-1^{-/-} mice were re-derived from cryopreserved embryos obtained from Bristol-Myers Squibb [153] and were backcrossed onto C57/Black6 for at least 8 generations. Mice deficient in myeloid differentiation factor 88 (MyD88) were kindly provided by Shizuo Akira, Osaka University, Japan [154]. Mice with a frameshift mutation in the TIR domain-containing adaptor inducing IFN- γ (TRIF) gene (mice) were kindly provided by Bruce Beutler, Scripps Research Institute, La Jolla, U.S [155]. TIGER (Transgenic IL-10 GFP Expressing Reporter) mice were kindly provided by Dr. Sean Kim, Yale University, CT, U.S. All mice were used between 8 and 10 weeks of age. Sprague Dawley rats were obtained from UCL biological services unit at ICH. All experiments were conducted in accordance with the guidelines of Institutional Animal Care and Usage Committee of Yale University or in adherence with the Home Office Guidance on the Operation of the Animals (Scientific Procedures) Act 1986, published by HMSO, London. Mouse genotyping was carried out by digesting tail tips in digestion buffer (10mM Tris-Cl, 50mM KCl, 20mM DTT, 2% proteinase K, 0.1% Triton X-100, pH 9.0) at overnight followed by heating to for 5 min. PCR was carried out with 35 cycles of /45 sec, /45 sec, / 1 min. MKP-1 genotyping was performed using a triple primer set consisting of 5'-CCAGGTAAGTGTGTCGGTGGTGC-3' and 5'-CAGCGCATCGCC TTCTATCGCC-3' and 5'-GTCTAGGAGGATTGTGCCAGG-3'.

2.3 In Vivo Procedures

2.3.1 Myocardial Ischaemia and Reperfusion in the Rat

Myocardial I/R was carried out in collaboration with Dr. Ahila Sivarajah at the Center for Experimental Medicine, The William Harvey Research Institute, Queen Mary, University of London. Male Wistar rats (255-285g) were anaesthetised with thiopentone sodium (Intraval[®] 120 mg/kg i.p.). Anesthesia was maintained by supplementary injections of thiopentone sodium as required. The trachea was cannulated and the animals were ventilated with a Harvard ventilator (inspiratory oxygen concentration: 30%; 70 strokes/min, tidal volume: 8-10 ml/kg). Body temperature was maintained at 37 ± 1 and the right carotid artery was cannulated and connected to a pressure transducer (Senso-Nor 840, Senso-Nor, Horten, Norway) in order to monitor mean arterial pressure (MAP) and heart rate (HR), which was displayed on a data acquisition system (MacLab 8e, ADI Instruments, Hastings, UK). The right jugular vein was then cannulated for the administration of drugs. A para-sternal thoracotomy was then performed, using an electrosurgery device to cauterize the intercostal arteries before cutting through three ribs. The chest was retracted and pericardium dissected from the heart. The left anterior descending (LAD) coronary artery was isolated and a snare occluder was placed around the LAD. The retractor was then removed and the animal allowed to stabilize for 15 min. The occluder was tightened at time 0. After 25 min of LAD-occlusion, the occluder was released to allow reperfusion for the indicated times. At the end of the reperfusion period, the LAD was re-occluded and 1 ml of Evans Blue dye (2% w/v) was injected into the animal, via the jugular vein. Evans Blue dye binds albumin and stains the tissue through which it is able to circulate, so that the non-perfused vascular (occluded) tissue remains un-colored. Each animal was killed with an over-dose of anesthetic, the heart excised, and excess dye washed off. The heart was then sectioned into slices of 3-4 mm, the right ventricle wall was removed, and the risk area (the non-perfused and, hence, non-stained myocardium) was separated from the non-ischemic (blue) tissue and immediately snap-frozen in liquid nitrogen. For ROS inhibition experiments, animals were subjected to (i) Sham operation, (ii) LAD coronary artery occlusion (25 min) and reperfusion (30 min) treated with saline 5 min prior to the onset of reperfusion, or (iii) LAD coronary artery occlusion (25 min) and reperfusion (30 min) treated with 100 mg/kg tempol 5 min prior to the onset of reperfusion (n=4 in all cases). Tissue was either snap frozen in liquid nitrogen for subsequent protein extraction or fixed in 10% formalin.

2.3.2 Endotoxic shock

Toxic shock occurs as a result of bacterial overload and is a useful model to examine *in vivo* responses to pro-inflammatory insult. Age and sex-matched wild-type (WT) and MKP-1^{-/-} mice were challenged with 10 mg/kg or 2.5 mg/kg of LPS by intraperitoneal (i.p.) injection and survival of mice was monitored up to 50 hr. The incidence of mouse lethality was compared and analyzed using the log rank test, performed by GraphPad Prism version 3.0.

2.3.3 Listeria Infection

L. monocytogenes (strain 43251) was inoculated into trypticase soy broth (Becton Dickinson, MD) and incubated overnight with shaking at 37°C. Following this, the bacteria were harvested by centrifugation, resuspended in trypticase soy broth containing 20% glycerol, and stored at -70°C as 1-ml aliquots. Before each experiment, an aliquot was thawed, inoculated into 50 ml of trypticase soy broth, and incubated at 37°C with shaking until mid-log-phase growth was reached. The optical density of the bacterial suspension was read with a spectrophotometer, and the numbers of CFU of *L. monocytogenes* were extrapolated from a standard growth curve. To prepare the inoculum for the mice, appropriate dilutions were made in sterile endotoxin-free phosphate-buffered saline to achieve the desired bacterial concentration. The actual number of CFU in the inoculum was verified by plating on agar plates of tyrsicated casein. MKP-1^{+/+} and MKP-1^{-/-} mice were injected *i.v* with 1.0 x cfu of *L. monocytogenes*, 72 hr later, spleens and livers were harvested into 0.1% Triton in PBS and homogenized. The number of viable *L. monocytogenes* in the spleen and liver was assessed by plating serial 10-fold dilutions of tissue homogenates onto agar plates of tyrsicated casein. Plates were cultured at and colony number was counted after 24 hr. Bacterial load data is expressed as colony forming units (cfu) per organ.

2.3.4 Experimental Autoimmune Encephalomyelitis (EAE)

EAE is a mouse model of the human inflammatory disease multiple sclerosis and is used to test immune defects *in vivo*. EAE was induced by s.c. flank injections of 50 µg of myelin oligodendrocyte glycoprotein (MOG)₃₅₋₅₅ peptide (synthesized in the Keck Facility at Yale University) emulsified in complete Freund's adjuvant (CFA; Difco) supplemented with heat-killed *Mycobacterium tuberculosis* (500 µg per mouse; Difco). Mice received i.p. injections of 200 ng of *B. pertussis* toxin (List Biological, Campbell, California, USA) immediately after the first immunization and again 72 hr later. The mice were observed daily for clinical

signs and scored on a scale of 0–5: 0, no clinical signs; 1, flaccid tail; 2, wobbly gait; 3, partial hindlimb paralysis; 4, complete hindlimb paralysis; 5, complete hindlimb paralysis and forelimb weakness or paralysis.

2.3.5 Dextran Sulphate Sodium (DSS) Induced Colitis

In patients, colitis is comprised of two related disorders; Crohn's disease and ulcerative colitis. To model these conditions *in vivo*, DSS administration is used. DSS induces colitis by damaging the epithelial lining of the digestive tract, thus allowing access of the commensal flora to the gut which initiates an immune response. MKP-1^{+/+} and MKP-1^{-/-} mice were given 2.5% DSS *ad libitum* in drinking water for 7 days followed by replacement with regular drinking water. Body weight was measured daily over a 3 week period.

2.3.6 Middle Cerebral Artery Occlusion (MCAO)

MCAO is an *in vivo* rat model of human stroke. MCAO and magnetic resonance imaging (MRI) was carried out in collaboration with Dr. Romina Badin at the biophysics unit, ICH, University College London. Rats were anesthetized with 3% isoflurane in 100% and maintained at 2% isoflurane in a 70:30 : mix delivered by a nose cone. The common, internal, and external carotid arteries were exposed by a cervical midline incision. A 290 µm monofilament suture was introduced into the lumen of the common carotid artery and advanced approximately 17 mm to occlude the MCA. After 30 mins, the suture was removed and rats were reperfused for the indicated times. Rectal temperature was maintained at 37°C ±1°C via a heating blanket controlled by a thermocouple and physiological monitoring included electrocardiography (ECG) recordings and rectal temperature recordings. MRI scans were performed using a 2.35-T horizontal bore magnet (Oxford Instruments, Oxford, UK) interfaced to a SMIS console (Guildford, UK). Images were acquired using a volume transmitter coil and a separate decoupled surface receiver coil. A multislice T2-weighted spin echo (SE) sequence (TR=1500 ms, TE=120 ms, 8 averages, 9 slices) with a 1-mm-slice thickness was also run to determine the lesion volume. Total scan time was 35 mins. All images were reconstructed with IDL Software Version 5.2.

2.4 Cell Culture

2.4.1 Freezing and Recovery of Cell Lines

1 x cells were centrifuged at 300 x g for 5 min and resuspended in FBS containing 10% DMSO and placed in cotton wool overnight at -, the following day cells were placed in liquid nitrogen for long term storage. Cells were recovered by thawing liquid nitrogen stocks rapidly at and transferring to a 25 flask. The medium was changed and cells were passaged as required using 2.5% trypsin (Gibco). All cell lines were grown in dulbeccos modified eagles medium (DMEM) containing 10% foetal bovine serum (FBS, Hyclone) with 40 units/ml penicillin (Gibco) and 40µg/ml streptomycin (Gibco). All cell culture plastics were from Nunc.

2.4.2 Preparation of Neonatal Rat Ventricular Cardiac Myocytes

Neonatal rat ventricular cardiac myocytes (NRVM) were isolated from the hearts of 1-3 day old Sprague Dawley rats. Hearts were removed and placed in oxygenated ADS buffer (116 mM NaCl, 5.4 mM KCl, 20 mM HEPES, 0.8 mM , 405.7 µM , 5.5 mM glucose, pH 7.35). Heart tissue was digested in 10 ml oxygenated ADS buffer supplemented with 0.1% collagenase and 0.025% pancreatin for 15 min, liberated cells were pelleted at 300g for 5 min and resuspended in FBS. This digestion procedure was repeated 7 times after which cells were plated at for 1 hr to allow adherence of fibroblasts. Myocytes were plated at a density of 2.5 x /ml in DMEM with penicillin, streptomycin and 15% FBS on plates pre-coated for 1 hr with 1% gelatin. Cells were allowed to attach overnight and the media was replaced with DMEM 1% FBS. This yielded typical cultures of >95% cardiac myocytes as assessed by desmin staining.

2.4.3 Hypoxia/Reoxygenation of NRVM

To model myocardial infarction *in vitro*, cardiac myocytes were subjected to hypoxia/reoxygenation injury. Cells were incubated for 4 hours in ischaemic buffer (137mM NaCl, 12mM KCL, 0.49mM , 0.9 mM , 4 mM HEPES, 20mM sodium lactate, 10 mM deoxyglucose, pH 6.2) in a hypoxic chamber with 5% , 95% argon. Following hypoxia, medium was replaced with DMEM 1% FBS and cells were reoxygenated in 5% in a incubator. For experimental controls, cells were incubated for four hours in Esumi control

buffer (137 mM NaCl, 3.8 mM KCl, 0.49 mM , 0.9 mM , 4 mM HEPES, 10 mM glucose, pH 7.4) then in DMEM 1% FBS.

2.4.4 Isolation of Bone Marrow Derived Macrophages

The femur and tibia of 6-10 week old mice were removed and the bone marrow was extracted into 10% DMEM by flushing with a 25 gauge needle. Cells were spun at 300 x g and resuspended in ACK buffer (150 mM , 10 mM , 0.1 mM EDTA, pH 7.2) for 5 min to remove red blood cells. Cells were filtered through a cell strainer and washed twice in 50 ml 10% DMEM and resuspended in DMEM with 20% FBS and 30% L929 supernatant (source of M-CSF). Bone marrow cells were cultured at an initial density of approximately cells/ml for 5-6 days and fresh medium was added at day 3. Cells were harvested in cold 0.2% EDTA (Invitrogen) and plated at a density of 2-4 x cells/ml in DMEM with 10% FBS. Macrophages were cultured for at least 12 hr before stimulation.

2.4.5 Isolation of Bone Marrow Derived Dendritic Cells

The femur and tibia were removed from 6-10 week old mice and the bone marrow was extracted into RPMI 1640 supplemented with 5% FBS, 50 units/ml penicillin, 50 units/ml streptomycin and 50µM beta mercaptoethanol by flushing with a 25 gauge needle. Cells were spun at 300 x g and resuspended in ACK buffer for 5 min to remove red blood cells. Cells were filtered through a cell strainer and washed twice in RPMI 1640. Lymphocytes were killed with a cocktail of 50 µg/ml mAbs and rabbit complement for 60 min at . The antibodies used were B220 (anti CD145), GK1.5 (anti-CD4), TIB120 (anti- Ia), TIB 211 (anti – Iy2) and were obtained from Pharmingen or as hybridomas from American Type Tissue Culture Collection (ATCC), Manassas Virginia. Cells were then washed twice and resuspended at a final concentration of 1 x 10⁶/ml in RPMI supplemented with 5% FBS, 50 units/ml penicillin, 50 units/ml streptomycin, 50µM beta mercaptoethanol and 1% GM-CSF, fresh media was added every two days and cells were treated on day 6.

2.4.6 T Cell Isolation from Mouse Spleen and Lymph Node

Superficial cervical, mediastinal, axillary, mesenteric and inguinal lymph nodes as well as spleen were removed from 6–10-week-old mice, ground and placed through a cell strainer. Cells were washed in 50 ml 10% DMEM and then resuspended in ACK buffer for 5 min to

remove red blood cells. CD4 and CD8 T cells were enriched by immunomagnetic selection using antibodies against CD4 and CD8 and magnetic beads conjugated with goat anti-mouse and anti-rat Ig (Miltenyi Biotec). Cells were cultured in Bruff's medium (10% FCS, penicillin, streptomycin and L-glutamine).

2.4.7 T cell Differentiation

CD4 T cells form distinct effector subsets *in vivo* following antigenic stimulation, these subsets can be recapitulated *in vitro* using distinct combinations of cytokines. For T cell differentiation, the purified CD4 T cells were stimulated with 5 µg/ml anti-CD3 (145-2C11), 2 µg/ml anti-CD28 (37.5.1), 10 U/ml recombinant mouse IL-2, 30 U/ml, irradiated splenocytes (2000 Gray, 5 fold APC per T cell) and for Th1 cell; 2 ng/ml rIL-12 (a gift from Wyeth Research), and 10 µg/ml anti-IL-4 (clone 11B11) or Th2 cells; 500 U/ml rIL-4 and 10 µg/ml anti-IFN (clone XMG2.1), antibodies were from ATCC, Manassas, Virginia. After 5 days of T cell differentiation, live effector cells were obtained by Ficoll centrifugation (LSMOL Lymphocyte Separation Medium, Cappel) and restimulated at 1×10^5 cells per well (96 well flat bottom plate, Falcon) with plate bound anti-CD3 or with 1 µg/ml PMA and 1 µM ionomycin.

2.4.8 Preparation of High Titre Adenoviral Stocks

In order to maximise gene expression in cardiac myocytes adenovirus was used. Adenoviral stocks of Ad-GFP and Ad-DN ST3 (dominant negative STAT3) were kind gifts from Prof. Brian Foxwell, Imperial College London and the Ad-STAT3C (constitutively active STAT3) was a kind gift from Michitaka Ozaki, Okayama University. The adenovirus vector is a type five adenovirus with deletion of the E1A region necessary for viral replication. High titre adenoviral stocks were prepared by infecting one well of a 6 well plate of 293 cells at 80% confluency for 2 days or until full cytopathic effect (CPE) was seen. Cells and lysate were removed, freeze-thawed three times and added to a T75 flask of 80% confluent 293 cells until full CPE was reached. This procedure was repeated and 10 large flasks (T175) of 80% confluent 293 cells were infected for 32 hr. Cells were harvested, pelleted at 300 x g for 5 min and then resuspended in 10 ml of 0.1M Tris pH 8.0. Cells were freeze-thawed three times and passed through a blunt needle four times to shear chromatin. Cellular debris was pelleted by centrifugation at 600 x g for 5 min. The supernatant was removed and made up to 11.4 ml with 0.1M Tris pH 8.0, 6.6 ml of saturated CsCl solution was added to a final volume

of 18 ml. The suspension was centrifuged at 180,000 x g for 16 hr. The virus band was removed by piercing with a needle and cleaned using a PD10 column. The virus was eluted from the column in PBS, filter sterilized and stored at -. Adenoviral titre was determined by plaque assay on 293 cells. For experimental infections, cells were infected at the indicated multiplicity of infection (MOI) for 24 hr, after which time the medium was changed and cells were left for a further 24 hr before treatment.

2.5 Analysis of Protein Levels

2.5.1 Western Blotting

Western blotting was used to detect the expression levels of total proteins or their phosphorylated forms in cell lysates. Cardiac tissue was snap frozen in liquid nitrogen and ground to a fine powder using a pestle and mortar and lysed in RIPA buffer (0.75 M NaCl, 5% (v/v) NP40, 2.5% (w/v) deoxycholate, 0.5% (w/v) SDS, 0.25 M Tris-HCl pH 8.0, containing protease inhibitor cocktail) or cells were lysed directly in RIPA. After lysis, the lysates were centrifuged at 13,000 x g to pellet cell debris. Protein concentration from the supernatant was determined using the BCA protein assay kit (Pierce, Rockford, USA). Laemmli loading buffer (50 mM Tris-Cl, pH 6.8, 2% SDS, 10% glycerol 0.1% bromophenol blue) and dithiothreitol to a final concentration of 10 mM were added to protein lysate and the solution was boiled for 5 min. 20 µg of protein was electrophoresed on polyacrylamide gels, transferred to Hybond-C nitrocellulose membranes (Amersham Biosciences, Bucks, UK) and blocked for 30 minutes in 4% non-fat dry milk in TBS. Membranes were incubated with primary antibody (1:1000 dilution, see Appendix 1) at overnight in 4% non-fat dry milk. Horse radish peroxidase (HRP) conjugated secondary antibodies (DAKO, Glostrup, Denmark) were applied at 1:2000 dilution and incubated at room temperature for one hour. Membranes were washed in tris buffered saline (TBS) containing 0.05% Tween 20 and proteins visualised by enhanced chemiluminescence (ECL, Amersham Biosciences, Bucks, UK) and exposed to light sensitive film (Kodak, New Haven, USA).

2.5.2 ELISA

ELISA was used as a method to measure cytokine secretion from macrophages in culture. 96 well plates were coated overnight at with 1 µg/µl of appropriate capture antibody diluted in PBS. Plates were washed 3 times with PBST then incubated with blocking buffer (1% BSA, 5% sucrose, 0.05% sodium azide in PBS) for 1 hr at room temperature. Plates were then washed 3 times with PBST and 50 µl of cytokine standard or culture supernatant at the appropriate dilution was added and incubated at room temperature for 2 hr. Plates were washed 5 times with PBST and incubated with 1µg/µl of biotin-conjugated detection antibody for 2 hr, followed by incubation with avidin-HRP for 30min. The HRP substrate 3,3',5,5'-tetramethylbenzidine (TMB) was used for chromogenic detection at 450 nm in a spectrophotometer. Serum levels of cytokines were also measured using Beadlyte (Upstate) mouse multi-cytokine detection system which utilises beads conjugated to monoclonal antibodies specific for a target cytokine. Antibody-coupled beads were incubated with plasma samples for 30 min followed by washing and 30 min incubation with biotin-conjugated detection antibody. Samples were washed and incubated with streptavidin-PE for 10 min and finally analysed on a Bio-plex Instrument (Biorad) per manufacturer's protocols.

2.5.3 Immunohistochemistry

Immunohistochemistry was used to detect protein expression in tissue sections. Following indicated treatments; the myocardial risk area was separated, cut transversely into 4 slices, fixed in 10% formalin and embedded in paraffin. 4 µm sections were deparaphinised in xylene followed by serial rehydration, antigen retrieval was carried out by microwaving in 10 mM sodium citrate buffer pH 6.0 for 5 min. Sections were incubated in 1% to quench endogenous peroxidase activity and non-specific binding was blocked using 5% normal goat serum. Individual sections were incubated overnight with 1:50 dilution of anti-phospho STAT Y701(Zymed) or anti-phospho STAT3 Y705 (Cell Signalling Technology). In control sections, the corresponding serum was used in place of primary antibody. After washing in PSB the sections were incubated for 1 hr with 1:100 dilution of biotin-conjugated secondary antibody (Vector Laboratories) followed by streptavidin-biotin peroxidase complex solution (DAKO) for 30min. After a further PBS wash, the colour reaction was developed by incubating sections with 3'3-diaminobenzidine (Sigma) for 5 min. The sections were rehydrated through an ethanol series into xylene and mounted using DPX mounting media. Images were captured on a Zeiss Axioscop 2 plus microscope.

2.5.4 Intracellular staining

Intracellular staining was used to measure cytokine expression *in vitro* using fluorescently conjugated cytokine antibodies. Monensin (GolgiStop from Pharmingen) was added in the final 4 hr of T cell activation. Cells were harvested and washed twice in staining buffer (1% FBS in PBS). Cells were fixed in 4% paraformaldehyde on ice for 10 min, washed twice and permeabilised by 0.1% saponin. Cells were stained with appropriate fluorophore-conjugated antibodies for 30 min and then analysed by flow cytometry.

2.5.6 Determination of tissue malondialdehyde concentration

Levels of malondialdehyde (MDA) serve as a marker for oxidative stress. MDA in heart tissue was measured by high-performance liquid chromatography (HPLC). Tissue was homogenized using an Ultra-Turrax homogeniser in 2 ml 50 mM potassium phosphate buffer (pH 6.0) containing 0.5% (w/v) hexadecyltrimethylammonium bromide. 25 μ l of homogenate were incubated with 2.5 μ l 0.2% (w/v) butylated hydroxytoluene in ethanol and 375 μ l 1% (v/v) phosphoric acid, and then derivatised with 345 μ l 15 mM 2-thiobarbituric acid at 100°C for 60 min. 200 μ l of the derivatised solution were collected and mixed with 200 μ l methanol. After addition of 15 μ l 1 M and 4 μ l 2M KOH/2.4 M samples were centrifuged (13000rpm for 10 min at 4°C). HPLC was performed on a Hypersil 5 μ m ODS column at a flow rate of 1 ml/min, isocratically with an eluant of 65% 50 mM (pH 7.0)/35% methanol. Fluorescence was monitored by a Jasco FP-1520 detector (excitation wavelength 515 nm; emission wavelength 553 nm) and values of molar concentration were calculated by comparison with reference solutions of MDA-tetrabutylammonium salt (Sigma-Aldrich, Poole Dorset, UK) derivatised and analysed in parallel. Protein concentration in the homogenate was measured by the method of Peterson (Peterson, 1977), and MDA was expressed as nmol/mg protein.

2.5.7 Nuclear Extract

To measure the levels of transcription factor binding by ELISA, nuclear proteins were first extracted from cells. Cells were removed into ice-cold PBS and pelleted at 300 x g for 15 min. 400 μ l of buffer A (10 mM HEPES pH 7.9, 10 mM KCl, 0.1 mM EDTA, 0.1 mM EGTA and protease/phosphatase inhibitors; 100 mM DTT, 100 mM PMSF, 50 mM NaVO₄, 0.5 M NaF, 5 mg/ml leupeptin, 10 mg/ml aprotinin, 1 mg/ml pepstatin) was added and cells were allowed to swell on ice for 15 min. 25 μ l of 5% NP40 was added, followed by vortexing and centrifugation at 13000 x g for 30 seconds. 50 μ l buffer C (20 mM HEPES pH 7.9, 400

mM NaCl, 1 mM EDTA, 1 mM EGTA and protease/phosphatase inhibitors as per buffer A) was added to the pellet and was incubated at for 15 min with shaking. The extract was spun at 13000 x g for 5 min and the supernatant was stored at -.

2.5.8 Electromobility Shift Assay (EMSA)

EMSA is a method of measuring transcription factor binding in nuclear lysates using radiolabelled oligonucleotide probes corresponding to the consensus binding site of the transcription factor of interest. Complimentary oligonucleotides were annealed in STE buffer (10 mM Tris, 50 mM NaCl, 1 mM EDTA) by heating to for 5 min, then allowing to cool to room temperature. 100 ng of annealed oligo were labeled with 30 μ Ci dCTP using 200 U MMLV reverse transcriptase. 10 μ g nuclear extract was added to 500 pg probe, 1 μ g polyIdC and diluted in binding buffer (10 mM HEPES, 50 mM KCL, 50 mM NaCl, 25 mM KPO₄, 5 mM , 2 mM DTT, 1 mM EDTA and 10% glycerol) followed by incubation at rt for 15 min. Samples were electrophoresed on polyacrylamide gels, dried for 1hr at and exposed to autorad film at -.

2.6 Gene Expression Analysis

2.6.1 RNA Extraction

For RNA extraction from cells, 0.5-1 ml Trizol (Invitrogen) was added directly to the tissue culture dish, tissue was ground to a fine powder under liquid nitrogen and homogenized in 1 ml Trizol using a dounce homogenizer. Samples were incubated at rt for 5 min and 200 μ l chloroform was added per 1 ml Trizol, samples were mixed vigorously and incubated at rt for 3 min. Samples were centrifuged at 12,000 x g for 15 min at . The upper aqueous phase was transferred to a new tube and RNA was precipitated with 0.5 ml propan-2-ol for 15 min at rt. Samples were centrifuged at 12,000 x g for 20 min at and the pellet was washed in 1ml 70% ethanol. RNA was centrifuged at 7,500 x g for 5 min at , residual ethanol was removed and the pellet was allowed to air dry for 15 min. The pellet was resuspended in 25 μ l of diethylpyrocarbonate (DEPC) treated water and concentration was measured spectrophotometrically at . A / of ~ 1.8 was considered free of protein contaminants and an / of ~ 2.0 was considered free of phenol contamination. For qPCR and gene array applications, RNA purity was examined using the Bioanalyser 2100 (Agilent Technologies, Palo Alto, CA).

2.6.2 cDNA Synthesis

1 µg total RNA was DNase treated at rt for 15 min, the reaction was stopped by heating to for 10 min with 25 mM EDTA. 200 ng random hexamer primer and 1 µl of 10 mM dNTP was added, heated to for 5 min and cooled on ice. 4 µl first strand buffer (Invitrogen), 2 µl of 0.1 M DTT and 1 µl superscript II reverse transcriptase (Invitrogen) were added to the sample, followed by thermal cycling of for 10 min, for 50 min and for 15 min. cDNA was diluted to 100 µl final volume.

2.6.3 Quantitative Real Time PCR (qPCR)

qPCR was used to accurately measure the mRNA levels of genes using Sybr Green which binds to the minor groove of DNA causing it to fluoresce. Following each round of PCR the total fluorescence in the sample is measured which corresponds to the amount of DNA present after each cycle. In chapters 3-5, qPCR was carried out using Platinum SYBR Green (Invitrogen, Paisley, U.K.) on the DNA Engine Opticon system (MJ Research, Waltham, MA). For PCR reactions, 5 µl SYBR Green was added to 5 µl cDNA with 500 nM primers in a 20 µl reaction and the PCR conditions were for 3 min followed by 45 cycles of for 30 sec, for 30 sec, for 30 sec. A melt-curve was performed from to , reading every 0. with a 1 sec hold between reads. Specific primers were designed with the aid of CloneWorks and the Ensembl database and are listed in Appendix 2, where possible primers were intron-spanning. For single-exon genes, a control cDNA reaction without reverse transcriptase was included to confirm the absence of genomic DNA. qPCR data presented in chapter 6 was performed on the applied biosystems ABI 7500 Real-time PCR system using TaqMan® TAMRA™ primer/probe sets purchased from ABI. 5 µl cDNA was used with 200 nM primer and GeneAmp® Fast PCR 2x master mix with ROX passive reference. Thermal cycling was carried out as follows: for 2 min, for 10 min and 40 cycles of for 15 sec and for 1 min. All PCR reactions were visualised on agarose gels to ensure the presence of a single product. HPRT, •-Actin and •2-microglobulin were used together as normalizing genes and for each experiment both target and normalizing gene PCR efficiency was firstly determined to ensure normalizing genes were acceptable. Expression changes were calculated using the $2^{-\Delta\Delta C_t}$ method and expressed as fold change over control.

2.6.4 Luciferase Promoter Assay

To measure gene promoter regulation *in vitro*, promoter sequences are cloned into a plasmid vector upstream of the luciferase gene. Promoter activity therefore results in luciferase expression which can be measured by luminometry. Cells were seeded in 24 or 96 well plates at the indicated densities. After 24 hr fresh media was added and transfections were carried out using the fugene-6 liposomal reagent according to the manufacturers instructions. 50 ng luciferase reporter and 50 ng CMV-renilla plasmid were used for each transfection. Fresh media was added 24 hr after transfection. After indicated treatments cells were washed with PBS and lysed in 100 µl of promega passive lysis buffer. Luciferase activity was measured using a Teaconic luminometer, 25 µl luciferase reagent was added to 50 µl cell lysate and luciferase activity was measured for 10 seconds, 25 µl of stop and glow reagent was then added and renilla activity was measured for a further 10 sec. Relative luciferase activity was calculated as luciferase activity/renilla activity and normalised to untreated controls.

2.7 Affymetrix Microarray Analysis

Microarray analysis allows one to measure the expression of thousands of transcripts simultaneously. Target RNAs from cells or tissue samples are converted into double stranded biotinylated RNA probes. These probes are hybridized to target oligonucleotides deposited on the surface of the microarray chip surface. After washing away unbound targets, the microarray is stained with phycoerythrin labeled streptavidin and read with a scanner. The levels of expression of each individual gene can then be compared against control samples to get a measurement of differential expression.

2.7.1 cDNA Preparation

1µl of 100 ng/µl T7 Oligo(dT) primer was added to 1 µg RNA in 11 µl of nuclease-free water and incubated at 37°C for 10 min. This was added to 1 µl of 10 mM dNTP, 4 µl first strand buffer, 1 µl RNase inhibitor, 2 µl of 0.1 M DTT and 1 µl Superscript II (all from Invitrogen) and heated to 65°C for 10 min, 42°C for 50 min and 70°C for 10 min. Second strand synthesis was performed in a final volume of 150 µl with 30 µl reaction buffer (100 mM Tris-Cl pH 6.9, 23 mM MgCl₂, 450 mM KCl, 0.75 mM •-NAD⁺, 50 mM DTT), 3µl of 10 mM dNTP, 4 µl *E. coli* DNA polymerase I (10 units/µl), 1 µl *E. coli* DNA Ligase (10 units/µl), 1 µl *E. coli* RNase H (2 units/µl) and incubated at 37°C for 2 hr. To fill in the 3' overhangs of the first strand, 2 µl of T4 DNA polymerase (5 units/µl) was then added and incubated for 5 min at 37°C, followed by addition of

10 µl of 0.5M EDTA to stop the reaction. The second strand DNA synthesis reaction was cleaned by adding equal volume of (25:24:1) phenol:chloroform:isoamylalcohol and centrifuging at 12,000 x g for 2 min. The aqueous layer was transferred to a new tube and DNA was precipitated with 0.5 volumes of 7.5 M ammonium acetate and 2.5 volumes of pre-cooled ethanol. Samples were centrifuged at 12,000 x g for 15 min and DNA pellets were washed twice with 500 µl of 80% ethanol and resuspended in a final volume of 12 µl in RNase free water.

2.7.2 Preparation of Biotinylated cRNA Target by In Vitro Transcription

12 µl of phenol/chloroform precipitated double stranded cDNA was used per 40 µl reaction with 4µl biotin labeled ribonucleotides, 2 µl T7 RNA polymerase, 4 µl 10X DTT, 4 µl 10X RNase inhibitor and 4 µl 10X IVT reaction buffer (Enzo Life Sciences, Farmingdale, NY). Reaction was incubated at 37°C for 16 hr. Contaminants were removed using RNeasy clean-up kit (Quiagen, USA) according to the manufacturer's instructions. cRNA was made up to 100 µl with RNase-free water and added to 350 µl of buffer RLT. 250 µl ethanol was added and the sample was added to the RNeasy spin column. Samples were centrifuged at 13,000 x g for 15 sec, 500 µl of RPE buffer was then added followed by centrifugation at 13,000 x g for 15 sec. Next, 500 µl of 80% ethanol was added and samples were centrifuged at 13,000 x g for 5 min and eluted in 30µl RNase-free water by centrifugation at 13,000 x g for 1 min. The quality of biotinylated aRNA was assessed using a Bioanalyser 2100.

2.7.3 Target cRNA Fragmentation and Hybridisation

Probe arrays were from Affymetrix (Rat expression 230) and contain 25-mer probe sets interrogating 15,000 mRNA transcripts and EST clusters from the UniGene database. These arrays contain maintenance genes (GAPDH, beta-Actin, hexokinase 1), which facilitate expression normalization between each sample. They also contain hybridization controls of eukaryotic origin (bioB, bioC, bioD, Cre), to provide alignment signals for the image analysis software as well as 100 probe sets for normalization controls to allow for fluorescence differences between chips due to the procedure alone. 15 µg biotinylated aRNA was hydrolysed into 60-200 nt fragments in a 30 µl reaction with 6 µl cRNA fragmentation buffer (200 mM Tris-acetate, pH 8.1, 500 mM KOAc, 150 mM MgOAc), heated to 94°C for 35 min then placed on ice. 15 µg fragmented cRNA was added to 3 nM control oligonucleotide, 15 µl hybridization controls, 30 µg herring sperm DNA, 150 µg BSA, 150 µl 2X hybridization

buffer (200 mM MES buffer, 2 M NaCl, 40 mM EDTA, 0.02% Tween-20), 30 µl DMSO in 300 µl and heated to for 5 min, for 5 min and centrifuged at 13,000 x g to remove any insoluble material. The probe array was filled with 1X hybridization buffer and incubated at for 10 min, this solution was then removed, replaced with 200 µl hybridization solution (10 µg RNA probe) and rotated at 60 rpm for 16 hr at .

2.7.4 Fluidics Protocol for Microarray Staining

Microarray signals are generated by binding of phycoerythrin labeled streptavidin (SAPE) to the biotinylated cRNA targets which are hybridized to the RNA probes on the chip. An amplification step is also included in which an anti-streptavidin goat antibody binds to SAPE, this is followed by a biotinylated anti-goat antibody and then a further SAPE binding. Microarrays were washed with buffer A (900 mM NaCl, 60 mM , 6 mM EDTA, 0.01% Tween-20) with 10 cycles of 2 mixes/cycle at followed by 4 cycles of 15 mixes/cycle with buffer B (90 mM NaCl, 6 mM , 0.6 mM EDTA, 0.01% Tween-20) at . The probe array was stained for 10 min in a solution containing 10 µg/ml SAPE in stain buffer (900 mM NaCl, 60 mM , 6 mM EDTA, 0.01% Tween-20, 0.2 µg/ml BSA, 0.2 µg/ml Ficoll, 0.2 µg/ml polyvinylpyrrolidone) at and washed with buffer A for 10 cycles, 4 mixes/cycle at . The probe was then stained for 10 min in antibody solution (5 µg/ml biotinylated antibody in stain buffer) at , then stained for a further 10 min with SAPE solution at . The final wash consisted of 15 cycles, 4 mixes/cycle with buffer A at and the array was kept at in holding buffer (100 mM MES, 1 M NaCl, 0.01% Tween-20). Microarrays were scanned using an Affymetrix GeneChip scanner.

2.7.5 Microarray Data Analysis

Quality control was carried out using Affymetrix GCOS software. Downstream analysis was conducted with Bioconductor and Genespring 7.3.1. The R 2.8 programmes affyImGUI and OneChannelGUI were downloaded from the Bioconductor resource in conjunction with the required BioC 2.3 software packages and used to read CEL files and prepare intensity box-plots and RNA degradation plots. Background correction, normalization and summarization of the probe-level data into probe-set expression values were carried out using Robust Multi-array Analysis (RMA) and GC-RMA. Differential expression was calculated using limma and outputs included the log₂-fold change, the moderated t-statistic, P-value and the posterior log-odds of differential expression with Benjamini and Hochberg false discovery rate (FDR).

Using Genespring 7.3.1, signal values were calculated using MAS 5.0, scaled to 100 and normalised to the median. Statistical analysis was carried out using a two-tailed students t-test with Welsh correction and Benjamini and Hochberg FDR. Genes were considered to be differentially expressed where there was a fold change with a P value <0.05. Gene ontology analysis was carried out using a combination of Affymetrix GO terms and manual Pubmed searches and with the Ingenuity package.

2.7.6 Ingenuity Pathway Analysis

To uncover function groupings and putative interaction networks, lists of differentially expressed genes were analysed using Ingenuity Pathway Analysis (IPA) software (Ingenuity Systems, Redwood City, CA). Datasets containing gene identifiers and expression values were mapped to the corresponding identifier in the Ingenuity Pathway Knowledge Base (IPKB) which ascribes functional groupings and known interactions from the published literature. The Fischer's test is used to calculate a p-value which determines whether the biological function assigned to the gene signature is due to chance alone. Therefore functional analysis describes biological functions that are most significant to the genes in each list. The IPA algorithm applies a score to rank networks based on the number of focus genes and the network size. Networks are related graphically where each gene is represented as a node, links between nodes denote biological relationships between genes and are supported by at least one peer reviewed publication. Colour intensity signifies levels of differential regulation and uncoloured nodes are integrated by the IPA algorithm being relevant to the network but not differentially regulated in the input gene signature.

2.8 Propagation and Purification of Plasmid DNA

2.8.1 Preparation of Competent JM109

The E.Coli strain JM109 was used for the propagation of plasmid DNA. E.Coli was streaked on a Luria Bertani (LB) agar plate (1% NaCl, 1% tryptone, 0.5% yeast extract, 2% agar) for 16 hr, a single colony was picked and bacteria were grown overnight in 10 ml LB medium in an orbital shaker at . 1 ml of overnight culture was inoculated into 99 ml LB and grown at in an orbital shaker until an optical density of 0.3-0.4 at 600 nm had been reached. Cells were centrifuged at 3000 x g for 5 min at and resuspended in 10 ml of MR buffer (10 mM RbCl, 10 mM MOPS, pH 7). Cells were centrifuged at 3000 x g for 5 min at and 8 ml MRC buffer

was added (10 mM RbCl, 50 mM , 100 mM MOPS, pH 6.5), cells were incubated on ice for 30 min. Bacteria were then centrifuged at 3000 x g for 5 min at , resuspended in 5 ml MRC buffer containing 15% glycerol, snap frozen in liquid nitrogen and stored at -.

2.8.2 Transformation of JM109

500 ng plasmid was added to 50 µl competent *JM109* E.Coli and left on ice for 30 min. Cells were then heat shocked to for 45 seconds and placed in ice for 2 min. The E.Coli were then added to 1ml LB medium in a 1.5 ml ependorff tube and incubated in an orbital shaker at for 90 min. 500 µl of transformed E.Coli was then added to an LB agar plate containing 0.1 mg/ml ampicillin or 0.05mg/ml kanamycin, incubated at overnight and stored at .

2.8.3 Large Scale plasmid DNA Extraction from E.Coli

A single colony of transformed E.Coli was inoculated into 500 ml LB medium with the appropriate selection antibiotic and incubated overnight in an orbital shaker at . The following day, cells were centrifuged at 6000 x g for 15 min at and resuspended in 10 ml P1 buffer (10 mM EDTA, 50 mM Tris-HCl, pH 8.0, 100 µg/ml RNase A). 10 ml P2 buffer was added (0.2 M NaOH, 1%SDS) and cells were incubated at rt for 5 min. 10 ml chilled P3 buffer was added (3 M potassium acetate, pH 5.5) and incubated on ice for 20 min followed by centrifugation at 20,000 x g for 30 min at . The supernatant was added to an equilibrated anion exchange Quiagen-tip and the resin was washed twice with QC buffer (1.0M NaCl, 50 mM MOPS, pH 7.0, 15% isopropanol). The plasmid DNA was eluted in buffer QF (1.25 M NaCl, 50 mM Tris-Cl pH 8.5, 15% isopropanol) and precipitated in 0.7 volumes of isopropanol. DNA was centrifuged at 15,000 x g for 30 min at and the DNA pellet was washed with 70% ethanol. After centrifuging for 10 min at 15,000 x g, the DNA pellet was allowed to air dry for 10 min and was resuspended in TE buffer (10mM Tris-Cl, 1 mM EDTA, pH 8.0). DNA concentration was determined by reading absorbance at 260 nm in a spectrophotometer, where an OD of 1 is equal to 50 µg/ml of double stranded DNA. / readings indicate levels of protein contamination, only plasmid preparations with an / of <1.8 were used. Typical yields from 500 ml culture were 0.5-1 mg plasmid DNA.

2.8.4 DNA Restriction Digest and Agarose Gel Electrophoresis

All plasmid DNA preparations were examined by restriction endonuclease digestion to ensure that the insert was correct. 0.3 µg plasmid DNA was incubated with 10 U recombinant

DNA endonucleases from NEB in the appropriate buffer as recommended by NEB and incubated for 16 hr at . Agarose gel electrophoresis was used to determine the size of digested products. 1% agarose was dissolved in TAE (0.04 M Tris-HCl, 0.02 M sodium acetate, 1 mM EDTA), for small DNA products of ~ <300 base pairs TBE buffer was used (45 mM Tris base, 45 mM boric acid, 1 mM EDTA pH 8.0) as it has a better resolving capacity for small DNA fragments. 0.5 µg/µl ethidium bromide was added to the gel to allow visualization of DNA under UV light. DNA loading dye was added from a 6 x stock (0.25% bromophenol blue, 0.25% xylene cyanol, 30% glycerol) and DNA was electrophoresed for 1 hr at 100V.

2.8.5 DNA Transfection

A complete list of the constructs used in these studies presented in Appendix 1B. NRVM were transfected using the calcium phosphate method. was added dropwise to a solution containing plasmid DNA with 50% HBS (280 mM NaCl, 50 mM HEPES) and 70 mM to give a final concentration of 0.125 M. The DNA/ mix was incubated at room temperature for 20 min and then added to cells. Fresh DMEM 1% FBS was added after 16 hr. Typical transfection efficiencies were of the order of 5-15%. Cell lines were transfected using the liposomal reagent fugene-6, which was added to DNA at a ratio of 2:1 or 3:1 (µl fugene-6: µg DNA), incubated for 20 min then added to cells. Fresh DMEM 10% FBS was added after 16 hr. Typical transfection efficiencies were of the order of 50-90%.

2.9 Cell Death Measurements

2.9.1 TdT mediated dUTP nick end labeling (TUNEL)

TUNEL allows fluorescent labelling of new 3'-OH DNA ends generated by DNA fragmentation, in this way terminal transferase (TdT) is used to catalyze binding of rhodamine labelled dUTP to the end of DNA strand breaks produced during apoptosis (Gavrieli et al., 1992). It must be noted however, that as well as the double strand breaks generated during apoptosis, TUNEL may also label single strand breaks generated by necrosis (Charriaut-Marlangue et al., 1995). TUNEL was carried out using commercial kits purchased from Roche. Cells grown on coverslips in 24 well plates were washed in PBS and fixed in 4% paraformaldehyde for 10 min at rt. Cells were then washed twice with PBS and permeabilised using 0.5% Triton-X 100 for 10 min at rt, followed by two washes with PBS. 250 μ M dUTP, 10U dTdT and 250 μ M CoCl₂ in TdT reaction buffer (1 M potassium cacodylate, 125 mM Tris-HCl, 1.25 mg/ml BSA, pH 6.6) were added to cells in for 1 hr at . The reaction was stopped by incubating cells in 1 mM EDTA for 5 min. Hoecht reagent was added to stain nuclei and cells were washed 6 times in PBS. TUNEL positive cells were visualised by fluorescence microscopy using a rhodamine filter (550-580nm) and appeared as bright red nuclei.

2.9.2 Exclusion of Trypan Blue

Trypan blue is a stain which enters dead cells with disrupted outer membranes and thus the level of cell death can be assessed by counting the number of blue cells compared against cells which exclude the dye. Cells were added to 0.4% trypan blue solution (Sigma) at appropriate dilutions and incubated for 5 min at room temperature. Dead cells appear blue under light microscopy and the number of dead cells was counted using a haemocytometer.

2.9.3 Annexin V Staining

Measurement of apoptosis using annexin V is based on the fact that once cells begin to undergo apoptosis, phosphatidylserine (PS) flips from the inner to the outer leaflet of the cell membrane. Annexin V is a ⁺-dependent phospholipid binding protein with a high affinity for PS (Meers et al., 1991). Fluorescently labelled annexin V can thus be used to quantify levels of exposed PS by flow cytometry and is therefore a sensitive marker of apoptosis (Kooperman et al., 1994). Cells were washed once in PBS, trypsinised for three minutes and

removed to polypropylene FACS tubes. Cells were centrifuged for 5min at 300 x g , washed once in PBS and resuspended in 300 µl of AnnexinV binding buffer (0.1 M HEPES pH 7.4, 1.4 M NaCl, 25 mM) with 3 µl of AnnexinV-PE (BD biosciences) and 5 µl 7AAD (1 mg/ml Sigma). Annexin V and 7AAD fluorescence was measured after 30 min in the FL2 and FL4 channels respectively of a Becton Dickinson flow cytometer.

2.9.4 Quantification of Infarct Size in the Heart

Following 25 min ischaemia and 2 hr reperfusion, the heart was removed, the left ventricle separated and the risk area was removed (assessed by Evans Blue staining, section 2.3.1). The tissue from the risk area was cut into small pieces and incubated with 0.5 mg/ml *p*-nitroblue tetrazolium for 30 min at 37°C. Dehydrogenase enzymes present in viable tissue catalyse conversion *p*-nitroblue tetrazolium to a formazan derivative and therefore infarcted tissue (nonviable) will exclude the stain. The stained tissue was separated from the infarcted tissue, weighed, and the infarct size expressed as a percentage of the risk area.

2.9.5 Statistical analysis

All values are presented as mean ± standard error mean (SEM) of *n* observations. Where two values are being compared a student's *t* test was used. Where groups of values were compared a Two-way analysis of variance (ANOVA) was used followed by either a Dunnett's or Bonferroni post test. Microarray data was analysed using the modified Bayesian method linear models statistics (Limma) followed by Benjamini-Hochberg false discovery rate for multiple testing. Differences among groups were considered significant at $p < 0.05$.

**Chapter 3: Investigating the
Role of STAT3 in
Ischaemia/Reperfusion
Injury**

3.1 Aims

Molecular control of I/R injury is a highly organised and complex process. However, while our understanding of intracellular signalling pathways activated during reperfusion has grown considerably during the last decade, uncovering the precise signalling cascades which control cell death in the myocardium is highly desirable if we are to develop novel clinical interventions for I/R injury. Knowledge of transcription factors which regulate the expression of proteins involved in apoptosis should greatly improve our understanding of how cell death is orchestrated in cardiac cells following I/R damage. Thus transcription factors constitute appealing targets for therapy. It is now well appreciated that STAT1 serves as a pro-apoptotic transcription factor following I/R injury in the heart (Stephanou et al., 2000, 2002). Less is known however about the role of STAT3 in the myocardium during I/R injury. STAT3 has been shown to function as an anti-apoptotic transcription factor in certain cell types and a pro-apoptotic factor in others (Bromberg et al., 1999, Chapman et al., 1999, Shen et al 2001). With this in mind, the aims of this chapter were as follows.

- In general, to ascertain whether STAT3 has a role in I/R mediated cell death in cardiac cells
- Characterise the expression and transcriptional activity of STAT3 in cardiac myocytes during I/R injury
- Identify the kinases responsible for STAT3 phosphorylation in cardiac myocytes
- Characterise the activity of STAT3 during I/R injury *in vivo*
- Dissect the role of ROS in mediating STAT1 and STAT3 activity

3.2 Overexpression of STAT3 Protects Cardiac Myocytes from Ischaemia/Reperfusion Induced Cell Death

In order to ascertain if STAT3 has a role in cardiac myocyte cell death, transient transfection experiments were carried out using neonatal rat ventricular cardiac myocytes (NRVM). Since murine STAT3 expression constructs were more readily available, their activity in rat cardiac myocytes was initially tested by dual-luciferase promoter assays since murine and rat STAT3 are 99% identical at the protein level. Two well characterised STAT3 target promoters were used, p21 and Ly-6E. STAT3 has been shown to bind to the p21 promoter directly by ChIP assay and the Ly-6E promoter contains an upstream GAS element responsive to STAT3 (Khan et al., 1993, Giraud et al., 2004). Cells were transfected for 48 hr with reporter constructs and with either STAT3 or pcDNA3. Luciferase activity normalised to renilla demonstrated that STAT3 increased promoter activity of p21 by 3.1 ± 0.8 fold and Ly-6E by 3.1 ± 0.2 fold (Fig 3.1). This demonstrates that the murine STAT3 construct is indeed transcriptionally active in NRVMs.

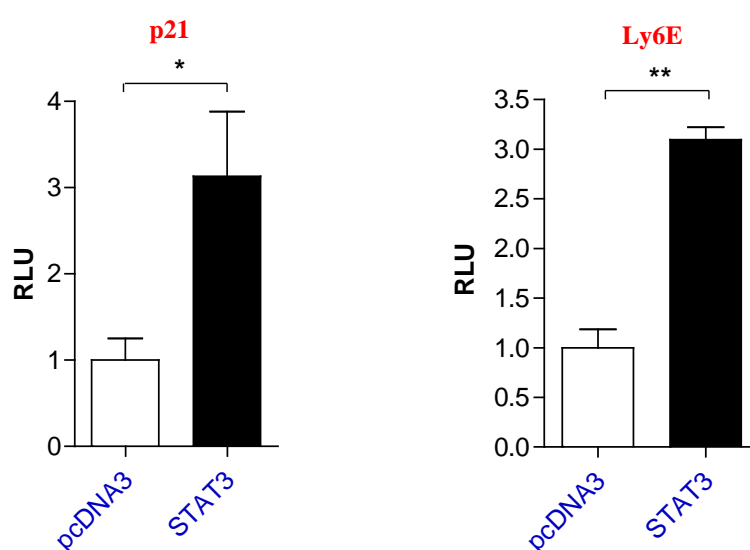


Fig 3.1. Murine STAT3 is transcriptionally active in neonatal rat ventricular myocytes. 0.5 μ g of the p21 or Ly6E promoter construct and 100 ng CMV-renilla construct were transfected into cardiac myocytes in 6 well plates with 0.5 μ g STAT3-pcDNA3 vector or pcDNA3 alone. Luciferase activity was measured after 48 hr and expressed as relative luciferase units (RLU) normalised to 1. * $p < 0.05$, ** $p < 0.01$, students t-test, $n=3$, experiment repeated in triplicate.

An *in vitro* I/R system was used to measure I/R induced cell death in NRVMs using the method of Esumi (Esumi et al., 1991). In this system glycolysis is inhibited with 2-deoxyglucose, while the addition of 12 mM potassium and 20 mM lactate at pH 6.5 leads to membrane depolarisation and increased hydrogen ion and $^{+}$ concentration. Furthermore, the cells are deprived of oxygen by placing them in an ischaemic chamber (5% , 95% Argon); this *in vitro* system therefore mimics most of the conditions experienced by cardiac myocytes during ischaemic damage *in vivo*. Since true I/R injury can only be experienced in an *in vivo* context, this *in vitro* system is more correctly termed *simulated* I/R injury but for clarity's sake it will herein be referred to simply as I/R injury. For control experiments, cells were placed in a buffer similar to the Esumi buffer but which importantly was at pH 7.4 and contained 3.8 mM KCL without 2-deoxyglucose or sodium lactate. The control cells were incubated in a standard 5% chamber for the duration of the ischaemic episode. Following ischaemia, cells were reoxygenated by washing away the ischaemic buffer and replacing it with DMEM with 1% foetal calf serum (FCS); fresh buffer was also added to control cells.

After the indicated times of reperfusion, the myocytes were fixed in 4% paraformaldehyde and levels of cell death were measured using the terminal transferase dUTP nick-end labeling (TUNEL) technique. Cell death is assessed by counting TUNEL positive cells (red) using fluorescent microscopy and expressed as the percentage of TUNEL positive cells per number of transfected cells (GFP positive cells). A representative example of a GFP and a TUNEL positive cell is shown in Fig 3.2a and the average increase in TUNEL positive cells following I/R injury is shown in Fig 3.2b. It should be noted that there is a level of 20% cell death in the control cells and there are several possible reasons for this; (1) a significant number of cells which die during the myocyte isolation can remain attached in culture and give a low level of false positives, (2) myocytes are maintained in 1% FCS and thus there is natural cell death over time in each culture and (3) there is also a low level of background staining inherent in the TUNEL technique. Notwithstanding these technical limitations, it is clear that *in vitro* I/R injury increases cell death in a time- dependent manner (Fig 3.2b).

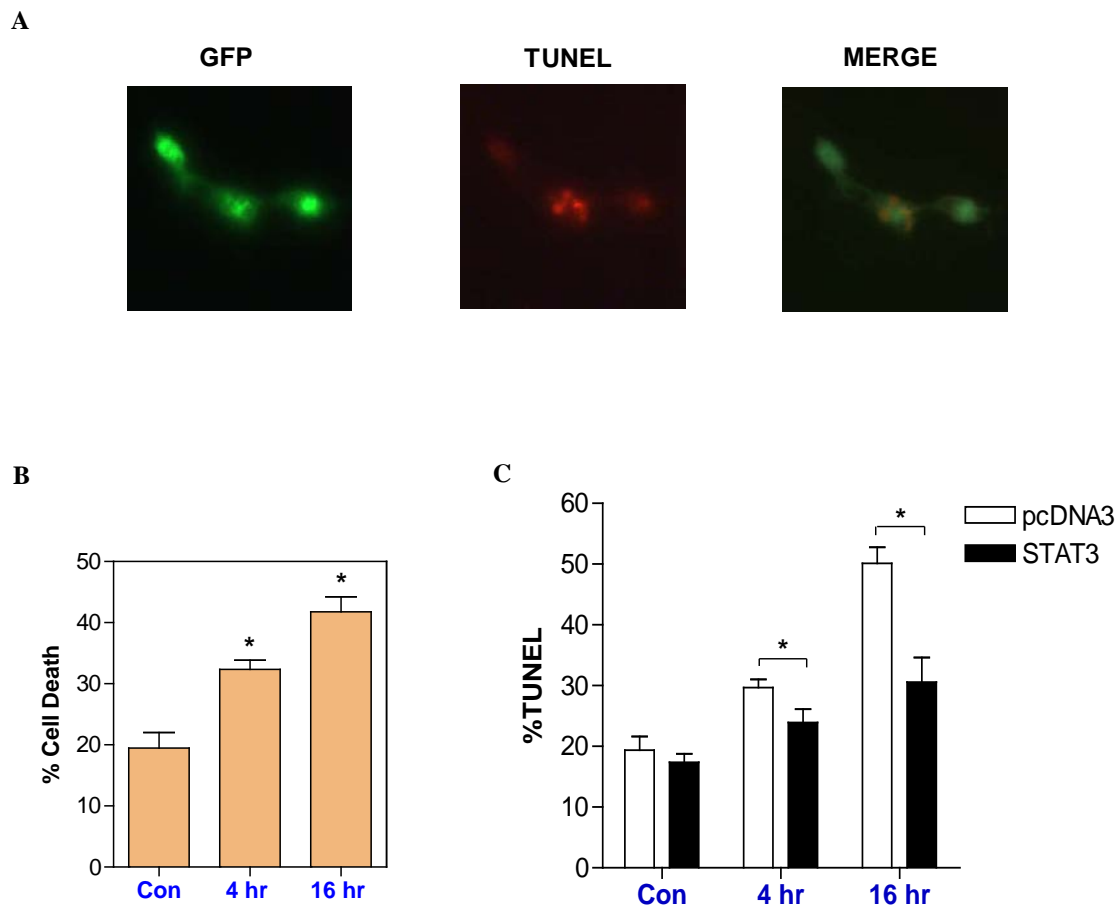


Fig 3.2. Transfection of STAT3 into cardiac myocytes confers protection from ischaemia/reperfusion injury. (A). GFP (460-480nm) and TUNEL (550-580nm) double positive cells were assessed by fluorescent microscopy. (B) Typical cell death observed following I/R injury by counting the number of TUNEL positive cells per total population of GFP positive. Statistical analysis was carried out with a one way ANOVA with Dunnett's post test, * $p < 0.05$ compared to con (C) Cardiac myocytes were transfected in 6 well plates with 0.5 μ g GFP construct and 0.25 μ g STAT3-pcDNA3 or pcDNA3 for 48 hr and subjected to I/R injury for the indicated times. Cell death was measured using TUNEL, a minimum of 200 GFP positive cells were counted per experiment. Experiments repeated in triplicate, statistical analysis was carried out using a 2-way ANOVA with a Bonferroni post test, * $p < 0.05$.

To assess the effect of STAT3 overexpression on cell viability, NRVMs were co-transfected with GFP and either STAT3 or pcDNA3 empty vector. 48 hr after transfection, cells were exposed to 4 hours ischaemia, followed by either 4 hr or 16h reperfusion (I/R). As expected, I/R resulted in significant cell death, most notably after 16 hr reperfusion when $50.0 \pm 4.5\%$ of cells were TUNEL positive (Fig 3.2c). Importantly, transient expression of STAT3 conferred significant protection from I/R mediated cell death after 16 hr reperfusion, reducing the number of TUNEL positive cells by $39.0 \pm 8.1\%$ (Fig 3.2c). This suggested that STAT3 may function as an anti-apoptotic factor during I/R injury.

3.3 Adenoviral Delivery of Dominant Negative STAT3 Increases I/R mediated Cell Death in Cardiac Myocytes

To further clarify the role of STAT3 in myocardial apoptosis, a dominant-negative STAT3 adenovirus (Ad ST3-DN) was employed. The Y705 phosphorylation site in the C-terminal domain of STAT3 is essential for STAT3 activation and a tyrosine-phenylalanine mutant (Y705F) functions in a dominant-negative manner (Kunisada et al., 1998, Williams et al., 2004). To measure cell death in these experiments, annexin V/7-AAD staining was used as an alternative to TUNEL. 7-amino-actinomycin D (7-AAD) is a fluorescent dye (630-660nm) which interchelates DNA and can only enter cells which have disrupted cell membranes and as such can be used as a marker of necrosis. Using annexin V in combination with 7-AAD allows the distinction of apoptotic and necrotic cell populations, cell populations positive for both annexin V and 7-AAD are undergoing secondary necrosis, which occurs when apoptosis has reached an advanced stage in the absence of phagocytosis. For all experiments using this method, cell death is given as the total population of apoptotic and necrotic cells.

Cardiac myocytes were initially transduced with a GFP control adenovirus (Ad GFP) or Ad ST3-DN for 48 hr at a multiplicity of infection (moi) of 10, 100 and 300. GFP expression was visualised by fluorescent microscopy and revealed that an moi of 100 was sufficient to give >90% transfection efficiency (Fig 3.3a). Cell lysates from transduced cardiac myocytes were examined for STAT3 expression and showed very high levels of overexpressed STAT3-DN, especially at an moi of 100 and 300 (Fig 3.3b). Next, cardiac myocytes were transduced with Ad GFP or Ad ST3-DN at moi=100 for 48 hr, cells were then subjected to I/R and levels of

cell death were examined. Using this approach, adenoviral delivery of dominant negative STAT3 was found to increase I/R mediated cell death from 46.0 ± 3.1 % in the GFP control group to 81.2 ± 6.9 % in the STAT3 D/N group (Fig 3.4a), representative flow cytometry plots are shown in Fig 3.4b. Since dominant negative STAT3 blocks STAT3 mediated transcriptional activity (Williams et al., 2004), this data demonstrates that a fully transcriptionally active STAT3 is necessary to protect cardiac myocytes from I/R induced cell death, further verifying the cytoprotective role of STAT3 in cardiac myocytes.

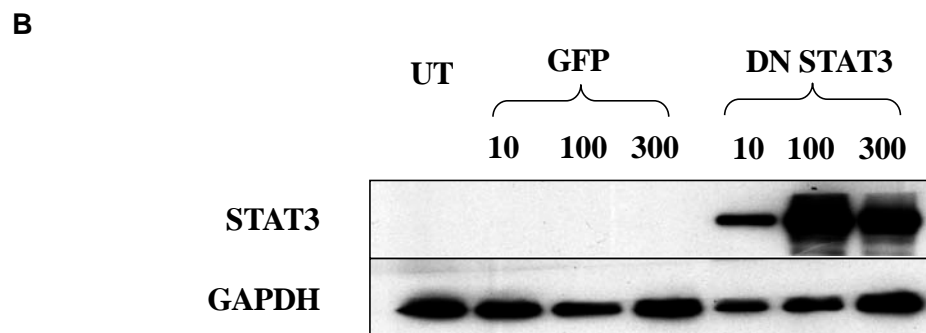
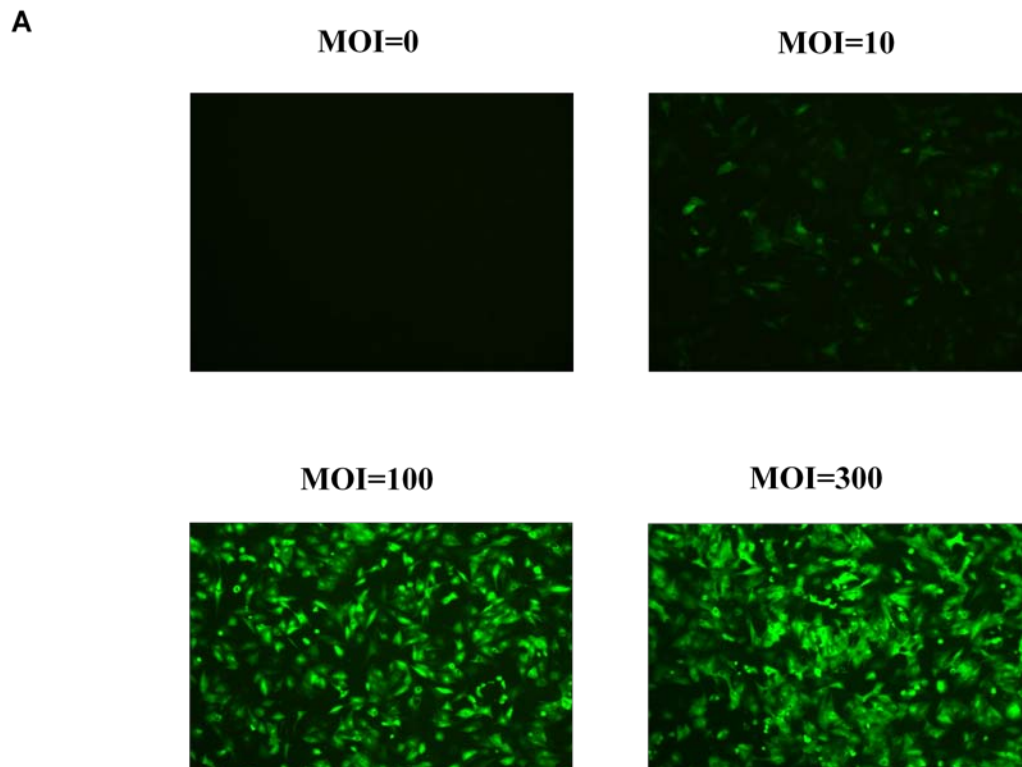
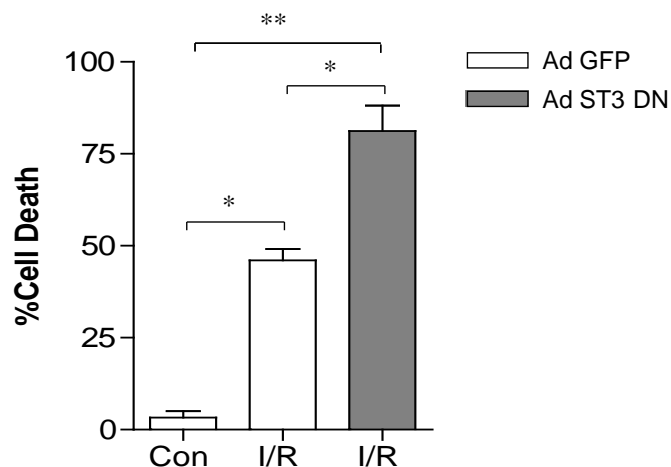


Fig 3.3 Adenoviral transduction of cardiac myocytes. Cardiac myocytes were seeded in 12 well plates at a density of 6×10^5 /cm². Ad GFP or Ad ST3-DN with viral titres of 5×10^6 ifu/ml and 10×10^6 ifu/ml respectively were added at moi of 10, 100, 300. **(A)** 48 hr post transduction, GFP expression was visualised by fluorescent microscopy. **(B)** Lysates from transduced cells were examined for STAT3 expression by western blot, GAPDH was used as a loading control.

A



B

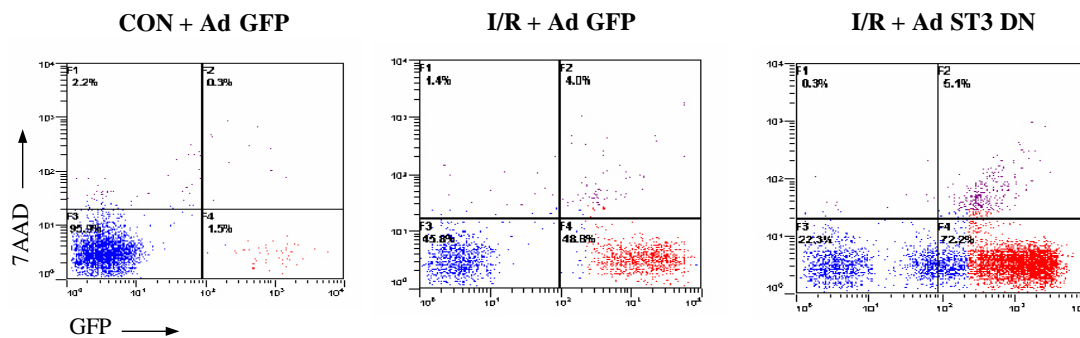


Fig 3.4. Dominant negative STAT3 increases I/R induced cell death in cardiac myocytes. Cardiac myocytes were transduced in 6 well plates for 48 hr with control Ad GFP or Ad STAT3-DN at moi=100. Cells were then subjected to 4 ischaemia and 16 hr reperfusion and cell death was ascertained by annexin V and 7AAD staining measured by flow cytometry. (A) % annexin V / 7AAD positive cells, * p<0.05, ** p<0.01, one way ANOVA with Bonfferoni post test, n=3 per group, average of two experiments. (B) Representative flow cytometry plots for each group.

The preceding experiments addressed the question as to whether STAT3 protects myocytes from I/R injury. A significant amount of the cellular damage induced during I/R injury is due to oxidative stress and the production of toxic free radicals during both the ischaemic and reperfusion phases. To extend these findings the question was therefore asked whether STAT3 can also protect myocytes from oxidative stress. STAT3 or pcDNA3 were transfected into NRVMs for 48 hr at which time myocytes were treated with 0.1 mM H_2O_2 for a further 16 hr and assessed for cell death using Annexin V with 7AAD (Fig 3.5). STAT3 overexpression led to a $20.2 \pm 5.4\%$ reduction in TUNEL positive cells, showing that like its protective activity during I/R, STAT3 can also protect against oxidative stress.

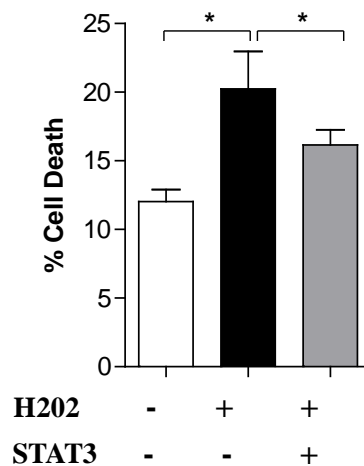


Fig 3.5. STAT3 Protects Cardiac Myocytes From Oxidative Stress. Cardiac Myocytes were transfected in 6 well plates with GFP together with pcDNA3 control or with STAT3 expression construct. After 48 hr, myocytes were treated for 16 hr with 0.1 mM H_2O_2 and levels of cell death were measured by Annexin V/7AAD staining. Statistical analysis was carried out using a one way ANOVA with Bonferroni post test, * $p < 0.05$, $n = 3$ per group, representative experiment shown.

3.4 Deletion of STAT3 Sensitises Cells to Oxidative Stress and I/R Injury

While overexpression is a very useful tool to examine the effects of increased transcription factor activity, it may lead to spurious results due to the non-physiological levels of expression. Mice with a floxed STAT3 allele do exist, however our lab was unable to attain them. However, mouse embryonic fibroblasts (MEFs) deficient in STAT3 were available and were used to further validate the protective role of STAT3 and to ascertain the cellular response to I/R and oxidative damage in the context of STAT3 deficiency. The MEFs used for these studies were obtained from Valeria Poli's group and have been immortalised by transformation with SV40 large T antigen (Alzoni et al., 2001). STAT3 deletion was carried out by Cre mediated deletion of a floxed STAT3 allele, which removes exons 12-14, the ^{fl} MEFs used in these studies are thus herein referred to here as wild type (Costa-Pereira et al., 2002). Western blotting confirmed total deletion of STAT3 (Fig 3.6a). It should be noted here that MEFs are more sensitive to I/R injury than neonatal cardiac myocytes. Subjecting MEFs to 2 hr ischaemia and 16 hr reperfusion revealed that STAT3^{-/-} MEFs were highly susceptible to I/R injury, indeed few STAT3^{-/-} cells remained attached to the culture dish following this stress (Fig 3.6b). To quantify the difference in cell death, STAT3^{+/+} and STAT3^{-/-} MEFs were challenged with a less lethal dose of reperfusion injury of 2 hr. This resulted in a 2.8 ± 0.7 fold increase in cell death in the STAT3^{-/-} MEFs compared to STAT3^{+/+} MEFs when quantified by both annexin V/7-AAD staining and a 2.8 ± 0.4 fold increase when quantified by trypan blue uptake (3.6 c,d).

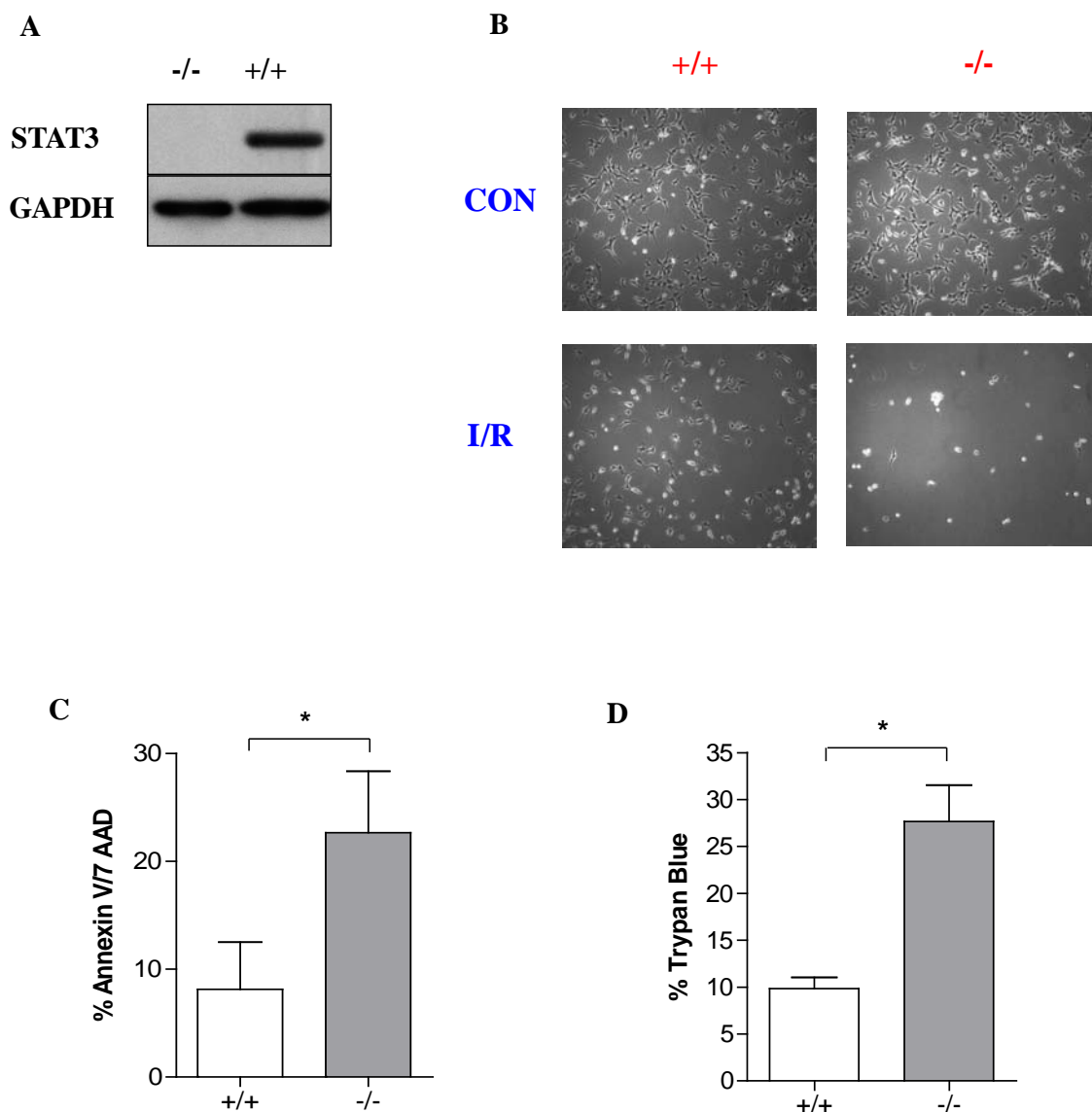


Fig 3.6. STAT3^{-/-} MEFs are highly sensitive to I/R damage. (A) Western blot demonstrates that STAT3^{-/-} MEFs are completely deficient in STAT3 protein. (B) STAT3^{+/+} and STAT3^{-/-} MEFs were subjected to 2 hr ischaemia and 16 hr reperfusion and visualised under light microscopy. (C) MEFs were subjected to 2 hr ischaemia followed by 2 hr reperfusion and cell death was quantified by annexin V and 7AAD staining (D) Cells were treated as in C and cell death was quantified by trypan blue uptake * p<0.05, student's t-test, n=3 per group, average of three experiments

Next, wild type and STAT3 knockout MEFs were treated with three separate doses of for 24 hr and cell death was measured by flow cytometry (Fig 3.7a). At doses of 0.5, 1 and 5 mM , STAT3 deficient cells were significantly more susceptible to oxidative stress; 0.5 mM induced a 1.5 ± 0.1 fold increase in cell death in STAT3^{-/-} cells, 1 mM induced a 1.7 ± 0.2 fold increase and 5 mM a 1.8 ± 0.1 fold increase (Fig 3.7a). A kinetic analysis, this time using trypan blue uptake, showed that at 8 hr of 0.5 mM there was a 2.5 ± 0.6 fold increase in cell death in STAT3^{-/-} MEFs and at 24 hr of 0.5 mM treatment there was a 1.7 ± 0.6 fold increase (Fig 3.7b). This demonstrates that there is both a time and dose dependent increase in cell death in STAT3 deficient MEFs.

Taken together, both the I/R and experiments clearly show that the absence of STAT3 renders fibroblasts susceptible to the toxic effects of I/R injury and mediated oxidative stress. Furthermore, these experiments are consistent with the previous data showing that in cardiac cells, overexpression of STAT3 confers protection from, and inhibition of STAT3 increases susceptibility to I/R injury.

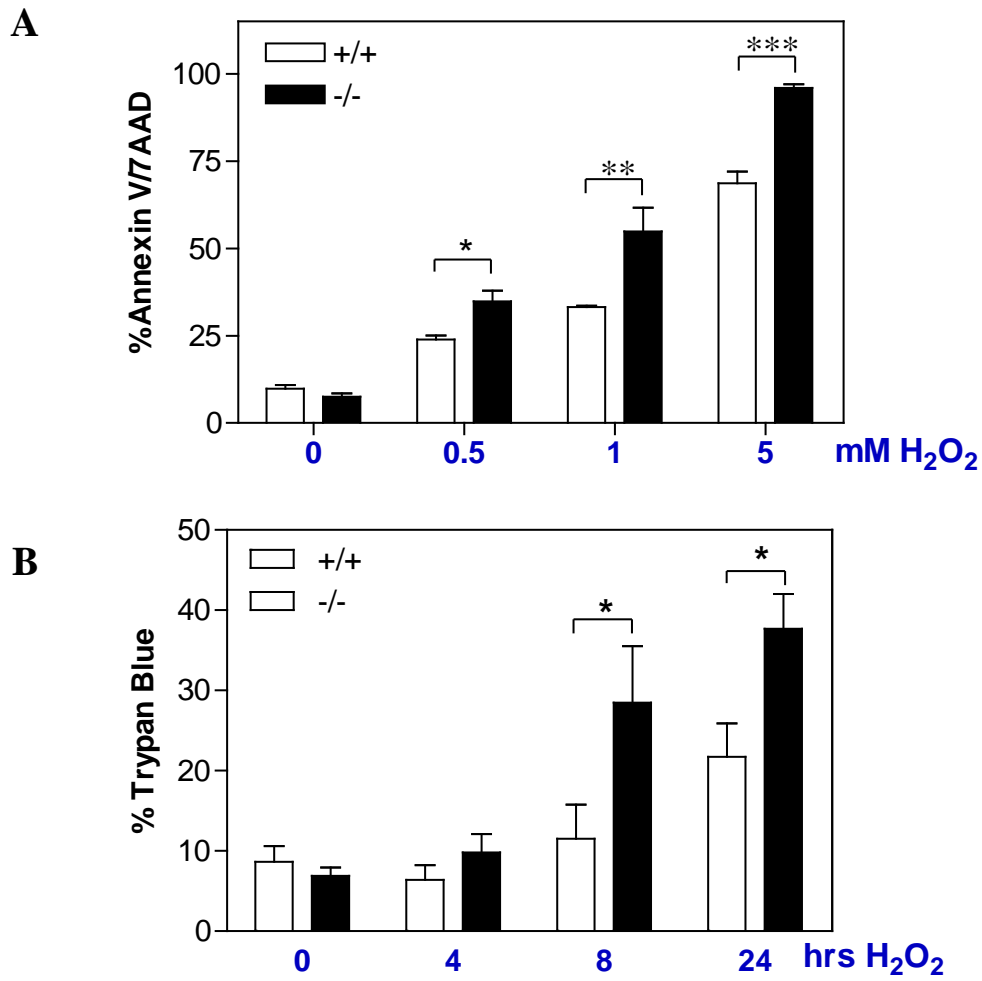


Fig 3.7 STAT3^{-/-} MEFs undergo enhanced cell death following oxidative stress. (A) STAT3^{+/+} and STAT3^{-/-} MEFs were treated with indicated concentrations of H_2O_2 for 24 hr and cell death was assessed by annexin V and 7AAD staining. (B) MEFs were treated with 0.5 mM H_2O_2 for the indicated times and cell death was measured by trypan blue uptake. Statistical analysis was carried out using a 2-way ANOVA with Bonferroni post test, * $p < 0.05$, ** $p < 0.01$, *** $p < 0.001$

3.5 STAT3 becomes Phosphorylated and Transcriptionally Active Following Ischaemia/Reperfusion in vitro

While the previous experiments demonstrate that exogenous STAT3 can protect myocytes from I/R damage, it is unclear whether endogenous STAT3 becomes activated during I/R injury. In resting conditions, the majority of STAT3 in cells is inactive and only becomes active once it is phosphorylated at either Y705 or S727 (Levy and Darnell, 2002). To assess the STAT3 phosphorylation status, myocytes were subjected to either 4 hr ischaemia or ischaemia plus 4 hr or 16 hr reperfusion, followed by western blotting with phospho-specific antibodies. Fig 3.8a shows that both STAT3 tyrosine and serine phosphorylation were induced during ischaemia, and stayed active up to 16 hr (Fig 3.8a). The levels of total STAT3 remained constant, showing that this was specifically due to increased phosphorylation rather than an increase in total protein. This demonstrates that during I/R injury, myocytes increase the activity of STAT3 which may be important in initiating a cardioprotective programme.

The levels of pro-apoptotic STAT1 phosphorylation was examined in order to compare with that of STAT3. STAT1 was phosphorylated at both Y701 and S727 during ischaemia, remained constant up to 16 hr reperfusion whereas the levels were reduced over time in agreement with previous studies (Fig 3.8b) (Stephanou et al., 2000, 2002). Again, total protein levels remained unchanged. Caspase-9 cleavage was also examined as a positive control for I/R induced apoptosis. Fig 3.8b shows that in this system, ischaemia induced partial caspase-9 cleavage, whereas reperfusion led to significant cleavage after 16 hr; this is consistent with previously published results (Stephanou et al., 2001).

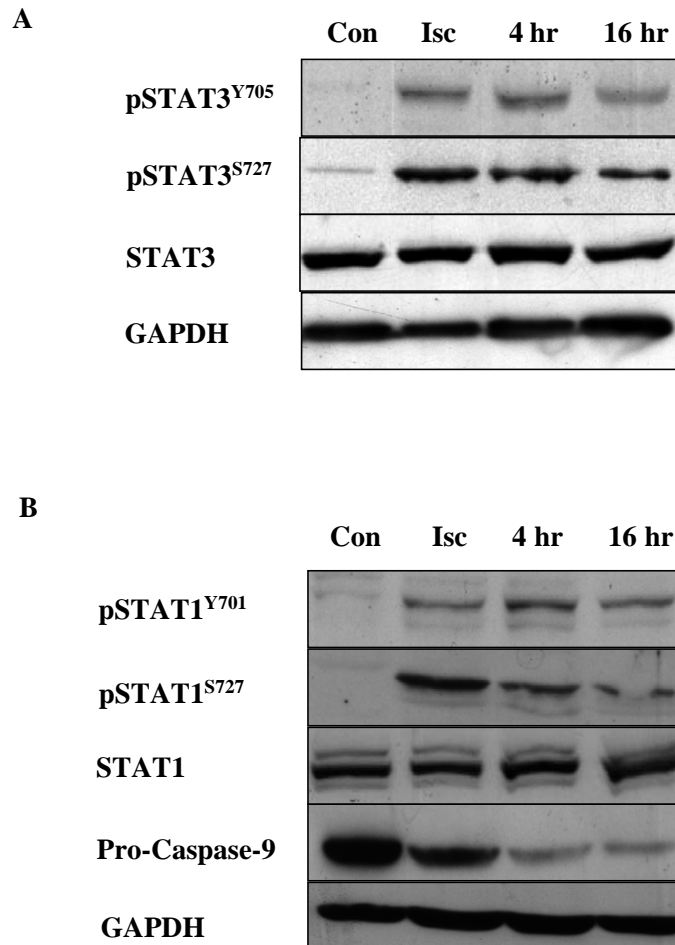


Fig 3.8. Activation of STAT3 and STAT1 following I/R Injury. NRVMs were subjected to 4 hr ischaemia or ischaemia plus the indicated times of reperfusion and lysates were subjected to western blots using antibodies for (A) Tyrosine and serine phosphorylated STAT3 or (B) Tyrosine and serine phosphorylated STAT1 and caspase-9. GAPDH was used as a loading control.

While STAT3 is phosphorylated at both sites, this does not prove *per se* that STAT3 dependent transcriptional activity is increased during I/R. STAT3 transcriptional activity was therefore assessed by examining the expression of STAT3 target genes using qPCR. qPCR reactions were carried out with Sybr Green and PCR quantification was determined using the $2^{-\Delta\Delta C_t}$ method (Livak and Schmittgen, 2001). Although the Livak and Schmittgen method is one of the most highly cited methods for normalising qPCR, it only suggests using a single normalising gene. There has been subsequent debate in the literature as to the merits and possible pitfalls of normalising to a single control gene, thus for these studies it was chosen to normalise to three separate genes, namely *hprt*, *actin* and *•2-microglobulin*. This minimises the chance of spurious results due to differences in concentration of input RNA, differing RNA quality and unequal reverse transcription efficiency. All three normalising genes were used in qPCRs unless otherwise stated.

When using the $2^{-\Delta\Delta C_t}$ method, it is necessary to first ensure that the PCR efficiency of the target is the same as that for the normalising genes. An example is given of two tested genes (STAT3 and c-Fos) and two normalizing genes (Actin and HPRT) (Fig 3.9). An example qPCR amplification plot for these 4 genes is shown in Fig 3.9a and the melt curves are shown in Fig 3.9b, there were 4 distinct peaks in the melt curves showing the presence of a single product for each primer pair. qPCR was carried out on a 2-fold dilution series from a pooled set of cDNA and the threshold Ct value was plotted (y axis) versus log cDNA dilution (x axis) (Fig 3.9c). The PCR efficiency was calculated using the equation $m = (-1/\log E)$, where m is the slope of the line and E is the efficiency (Schmittgen and Livak, 2008). Schmittgen and Livak recommend that the PCR efficiency of the normalizing and control genes should be within 10% of each other and this approach was adopted for all qPCR studies (Schmittgen and Livak, 2008). Fig 3.9c shows the dilution series for HPRT, actin, STAT3 and c-fos and demonstrates that their efficiencies were within 10% of each other and thus HPRT and actin were acceptable as normalizing genes. This standard approach was adopted herein for all qPCR experiments.

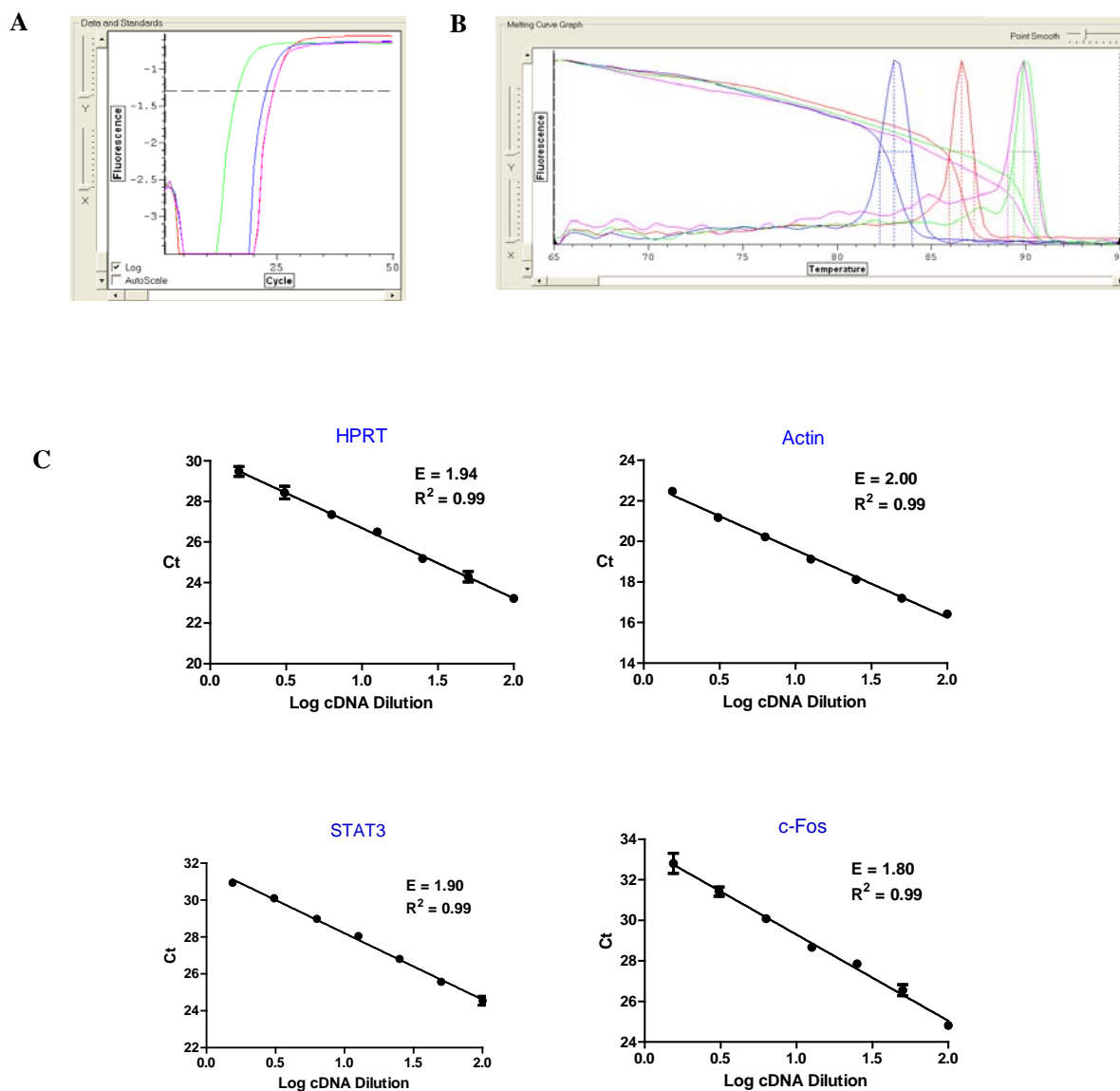


Fig 3.9. Testing qPCR efficiency. (A) Standard amplification plots for actin, HPRT, STAT3 and c-fos. (B) Standard melt curves for actin, HPRT, STAT3 and c-fos. (C) qPCR of a 2-fold series dilution of pooled cDNA samples was carried out using primer pairs for the indicated genes and the Ct values were plotted against the log DNA dilution $n=3$. Linear regression was carried out to give the values and the slope (m). The efficiency (E) was calculated from the equation $m = (-1/\log E)$ and at 100% efficiency should be equal to 2.

Two STAT3 target genes, SOCS3 and c-Fos, were chosen as they have previously been shown to be targets of STAT3 in other cell types (Hou et al., 2008, Yang et al., 2003). However, since it has not been shown that they are induced by STAT3 in cardiac myocytes, it was necessary to first confirm this before measuring their expression during I/R injury. Therefore, NRVMs were transduced for 24 hr with a constitutively active STAT3 adenovirus (STAT3C) and the levels of SOCS3 and c-Fos were measured by qPCR. Initially STAT3C was transduced at a moi of 10, 100 and 300 and moi=100 was found to give significant STAT3 protein expression (Fig 3.10a). Both SOCS3 and c-Fos were significantly upregulated by 24 hr STAT3C transduction at moi=100, whereas the levels of a non-STAT3 target gene HSP70 remained constant, demonstrating that both SOCS3 and c-Fos are true STAT3 targets in cardiac myocytes (Fig 3.10b).

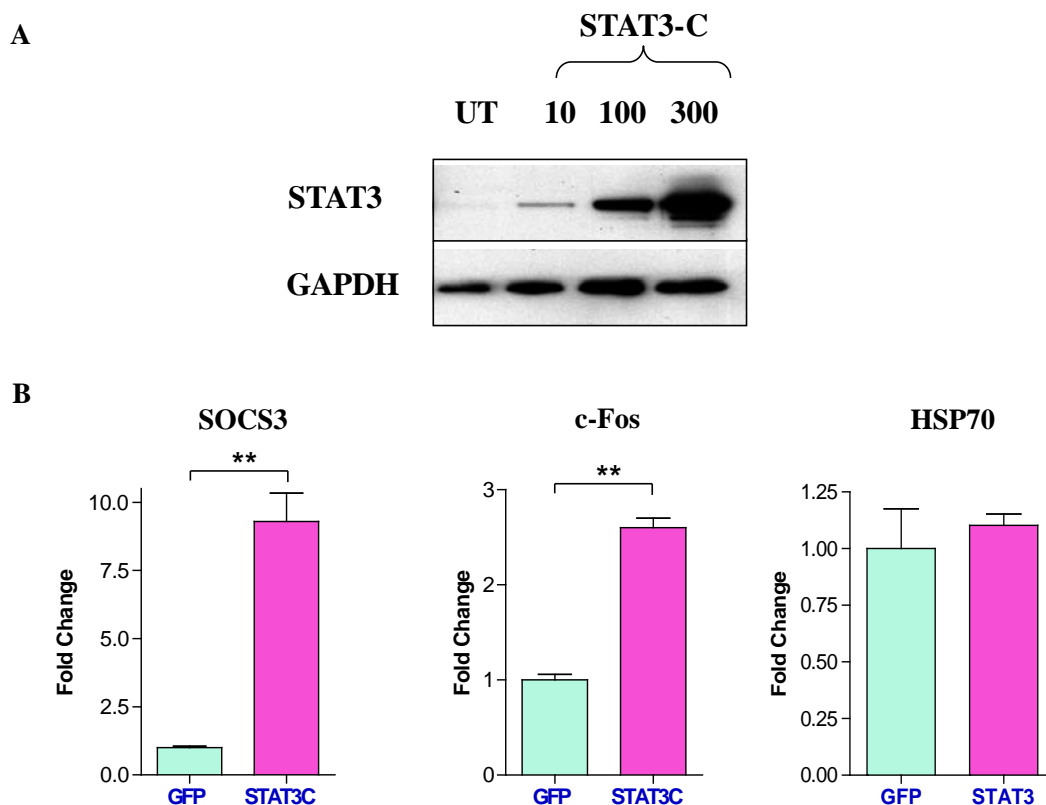


Fig 3.10 Characterisation of STAT3 dependent gene expression in cardiac myocytes. (A) NRVMs were transduced with STAT3C at moi of 10, 30 and 100 and STAT3 expression was assessed by western blot, GAPDH was used as a loading control. **(B)** NRMVs were transduced with STAT3C adenovirus at moi=100. After 24 hr, the expression of SOCS3, c-fos and HSP70 was examined by qPCR. ** $p < 0.01$, students t-test, $n = 3$ per group, repeated in duplicate.

Next, a time course of I/R injury was carried out in neonatal myocytes and the levels of STAT3 and the STAT3 target genes SOCS3 and c-fos were measured by qPCR. The fold changes for each time point of reperfusion were divided by the average of the corresponding time points for samples which had been incubated in Esumi control buffer without I/R and subsequently normalized to the control time point (4 hrs in Esumi control buffer) (Fig 3.11). Analysing in this way takes into account any background fluctuations which occur over time in culture.

STAT3 mRNA expression was found to be reduced by $39.8 \pm 10.3\%$ by 4 hr and remained reduced up to 24 hr (Fig 3.11a). The mechanism of reduced STAT3 mRNA expression by I/R is unknown but possibilities include decreased transcript stability or induction of STAT3 specific miRNAs during I/R. It is interesting that this reduced mRNA expression was not paralleled by a decrease in protein expression (see Fig 3.8), although more detailed kinetic analysis of STAT3 protein turnover would be necessary to verify this. Expression of both STAT3 target genes however was increased by I/R injury; after 4 hr reperfusion SOCS3 expression was increased 5.5 ± 1.3 fold and c-fos expression increased 38.9 ± 12.7 fold (Fig 3.11b,c). Expression of both genes was still elevated after 24 hr reperfusion but returned to baseline after 48 hr reperfusion. This data in conjunction with the phosphorylation data in Fig 3.8 suggests that STAT3 transcriptional activity is at its highest in the first few hours after reperfusion.

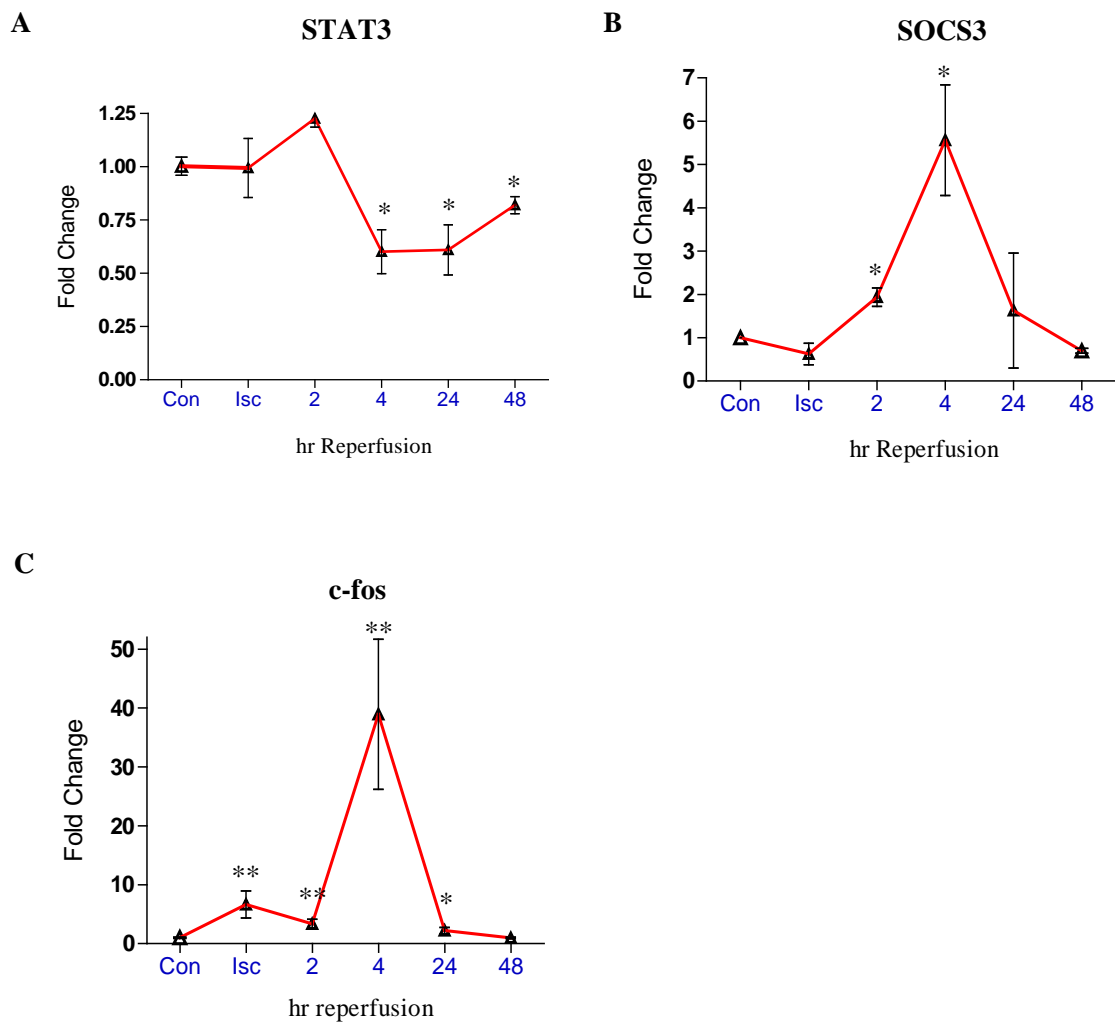


Fig 3.11. STAT3 mRNA expression is decreased and STAT3-dependent gene expression is increased by I/R injury. NRVMs were subjected to a time course of I/R injury and the levels of STAT3, SOCS3 and c-Fos were measured by qPCR and normalized to control (con) levels. Statistical analysis was carried out using a one-way ANOVA with Dunnett's post test, n=3 samples, experiments repeated in triplicate, * p<0.05, ** p<0.01 compared to con.

As an alternative to qPCR, the Ly6E reporter system was again employed, since Ly-6E was earlier shown to be a STAT3 target gene in cardiac myocytes (Fig 3.1). I/R injury (24 hr reperfusion) was found to induce a 46.5 ± 7.7 fold increase in Ly6E luciferase activity, confirming that I/R does indeed increase STAT3 mediated transcriptional activity (Fig 3.12). Taken together, these data suggest that STAT3 becomes active during reperfusion and instigates a transcriptional programme which attempts to rescue the cell from reperfusion mediated cell death.

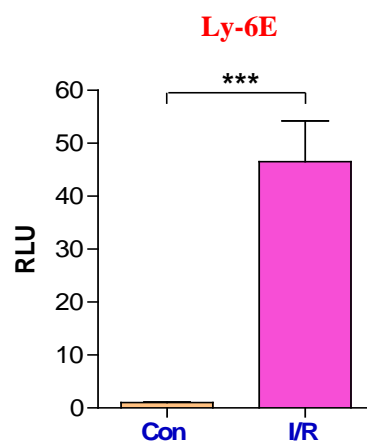


Fig 3.12. STAT3 dependent luciferase reporter activity is enhanced by I/R injury. 1 μ g of Ly-6E luciferase reporter and 0.1 μ g CMV-renilla were transfected into NRVMs in 6-well plates for 24 hr. Cells were then subjected to 4 hr ischaemia and 24 hr reperfusion (I/R) or control and luciferase activity was measured, the RLU of the control was set to 1. *** $p < 0.001$, $n = 3$, experiment repeated in duplicate.

3.6 Oxidative stress induces STAT3 serine phosphorylation through an ERK-dependent pathway

It is well appreciated that phosphorylation of STAT3 at Y705 is mediated by JAK kinases, most notably JAK1 and JAK2, indeed inhibition of JAK2 with AG490 abrogates tyrosine phosphorylation of STAT3 in cardiac myocytes (Mascareno et al., 2005). It is unclear however what kinase is responsible for phosphorylating STAT3 at serine 727 in cardiac myocytes. Several reports have identified putative STAT3 serine kinases (see table 1.1), including MAP kinases, PKC and cyclin dependent kinases, however on careful analysis of the literature it is clear that STAT3 S727 phosphorylation is both cell - type and - stimulus dependent.

In an effort to identify the serine kinase responsible for STAT3 phosphorylation in cardiac myocytes, a time course was first carried out by treating NRVMs with 100 μM . Basal phosphorylation of STAT3 S727 could be detected in resting cells but this was increased significantly by 15 min treatment and remained elevated up to 4 hr while treatment had no effect on total STAT3 protein levels (Fig 3.13a). Next, myocytes were treated with 100 μM for 30 min in the presence of the MEK1/2 inhibitor U0126, the p38 MAPK inhibitor sb203580, the JNK inhibitor sp600125, or DMSO control and STAT3 phosphorylation was examined (Fig 3.13b). Inhibition of JNK or p38 MAPK had no effect on STAT3 serine phosphorylation, however U0126 treatment almost completely abolished STAT3 S727 phosphorylation to a level below that of baseline, densitometric analysis showed a reduction of almost 90% in the U0126 treated cells compared to DMSO control (Fig 3.13c). As expected, inhibition of MEK1/2 reduced the levels of phosphorylated ERK1/2. To verify that inhibition of the MEK1/2-ERK1/2 pathway abrogated STAT3 S727 phosphorylation, a second unrelated MEK1/2 inhibitor, PD98059, was used. This likewise reduced the levels of phosphorylation, confirming that the reduction is not due to a non-specific effect of U0126 (Fig 3.13d). This data clearly shows that STAT3 is phosphorylated at serine 727 in cardiac myocytes by oxidative stress and that the kinase responsible is likely to be either ERK itself or possibly a downstream ERK target. Crosstalk between the MEK1/2 – ERK 1/2 pathway and the STAT3 pathway may therefore represent an important point in cell fate decisions in cardiac myocytes.

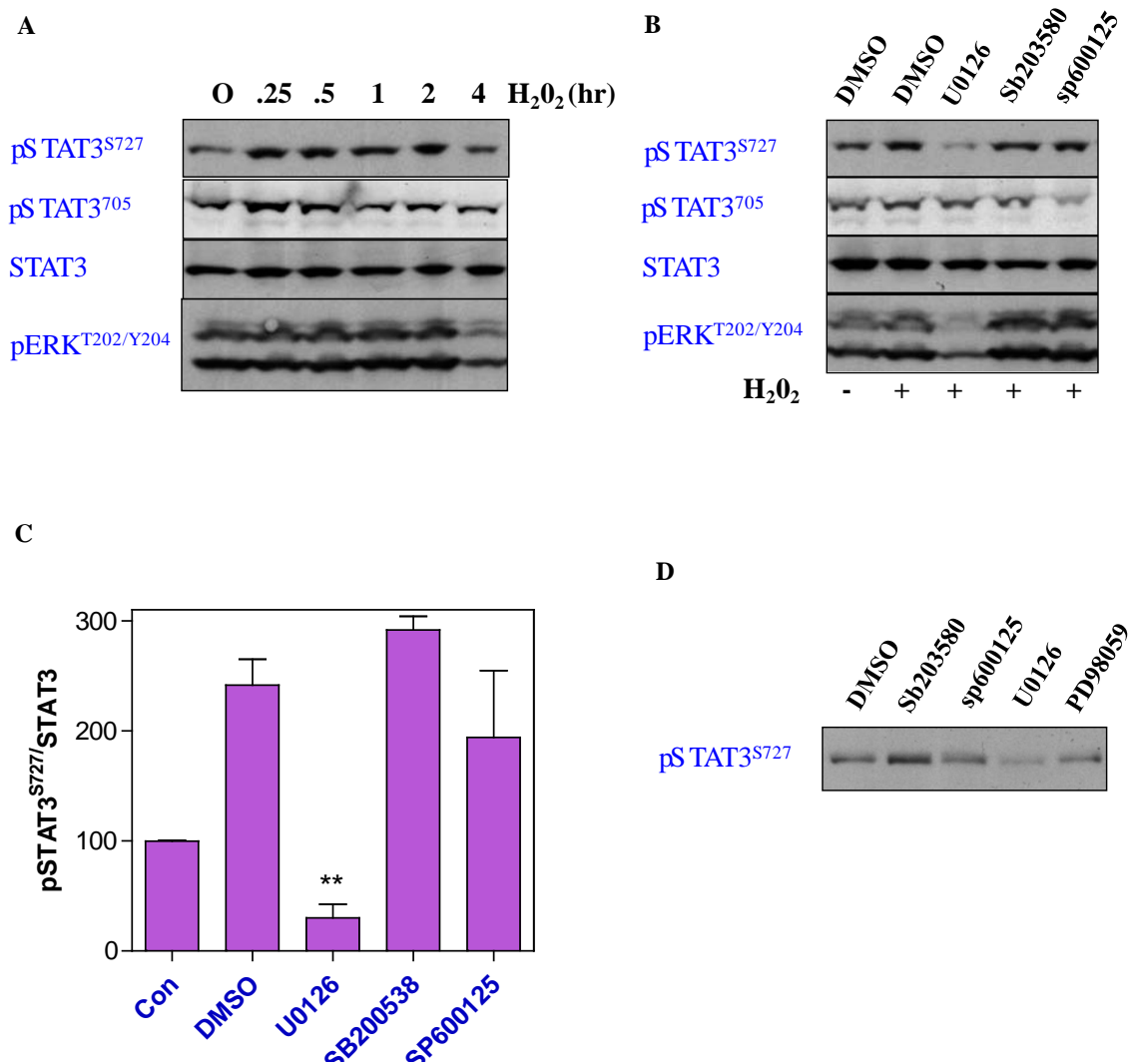


Fig 3.13. STAT3 serine 727 phosphorylation is ERK1/2 dependent. (A) NRVMs were treated with 100 μ M for up to 4 hr and western blots were carried out using the indicated antibodies. (B) NRVMs were treated with 100 μ M for 30 min in the presence of the MEK1/2 inhibitor U0126, the p38 MAPK inhibitor SB200538, the JNK inhibitor SP600125 or DMSO control and western blots were carried out using the indicated antibodies (C) The levels of total and serine 727 phosphorylated STAT3 from B were quantified by densitometry and the ratio of /STAT3 was calculated, the samples which were not treated with (con) were set at 100% with all other samples expressed relative to this, repeated in triplicate. (D) NRVMs were treated as in B with the addition of the MEK1/2 inhibitor PD98059.

3. 7 Activation of STAT1 and STAT3 following *in vivo* ischaemia/reperfusion injury

Since STAT3 was shown to act as an anti-apoptotic factor during I/R injury *in vitro* (see above), and STAT1 has been demonstrated to increase cardiac myocyte apoptosis *in vitro* (Stephanou et al., 2000), the *in vivo* activation of STAT1 and 3 was examined. The left coronary artery is responsible for supplying the left ventricle with blood and has two main branches; the anterior descending (LAD) and the circum-flex. In this *in vivo* model of I/R injury, the anterior descending left coronary artery is constricted as this artery is the one most commonly obstructed in human pathology. This model was carried out in conjunction with Dr. Ahila Sivarajah at St. Bartholomew's and The Royal London School of Medicine and Dentistry.

A time course of 25min LAD occlusion followed by up to 2 hr of reperfusion was carried out in male wistar rats. In order to assure consistency between animals, mean arterial blood pressure (MAP) and heart rate were measured throughout the experiment (Fig 3.14a). MAP fell during ischaemia but remained constant throughout reperfusion, while heart rate remained constant during both ischaemia and reperfusion. At the end of reperfusion, Evans blue dye was infused to separate the risk from non-risk area of the left ventricle (Fig 3.14b), the risk area denotes the area of the heart most deprived of oxygen (causing it to exclude Evans dye) and therefore the area at risk of becoming infarcted. To ensure that the model was working consistently, the infarct size was measured in 8 animals. The infarct size is expressed as a percentage of the area at risk; 2 hr of reperfusion injury increased the infarct size from $8 \pm 1\%$ in the sham group to $56 \pm 2\%$ in the I/R group (Fig 3.14c).

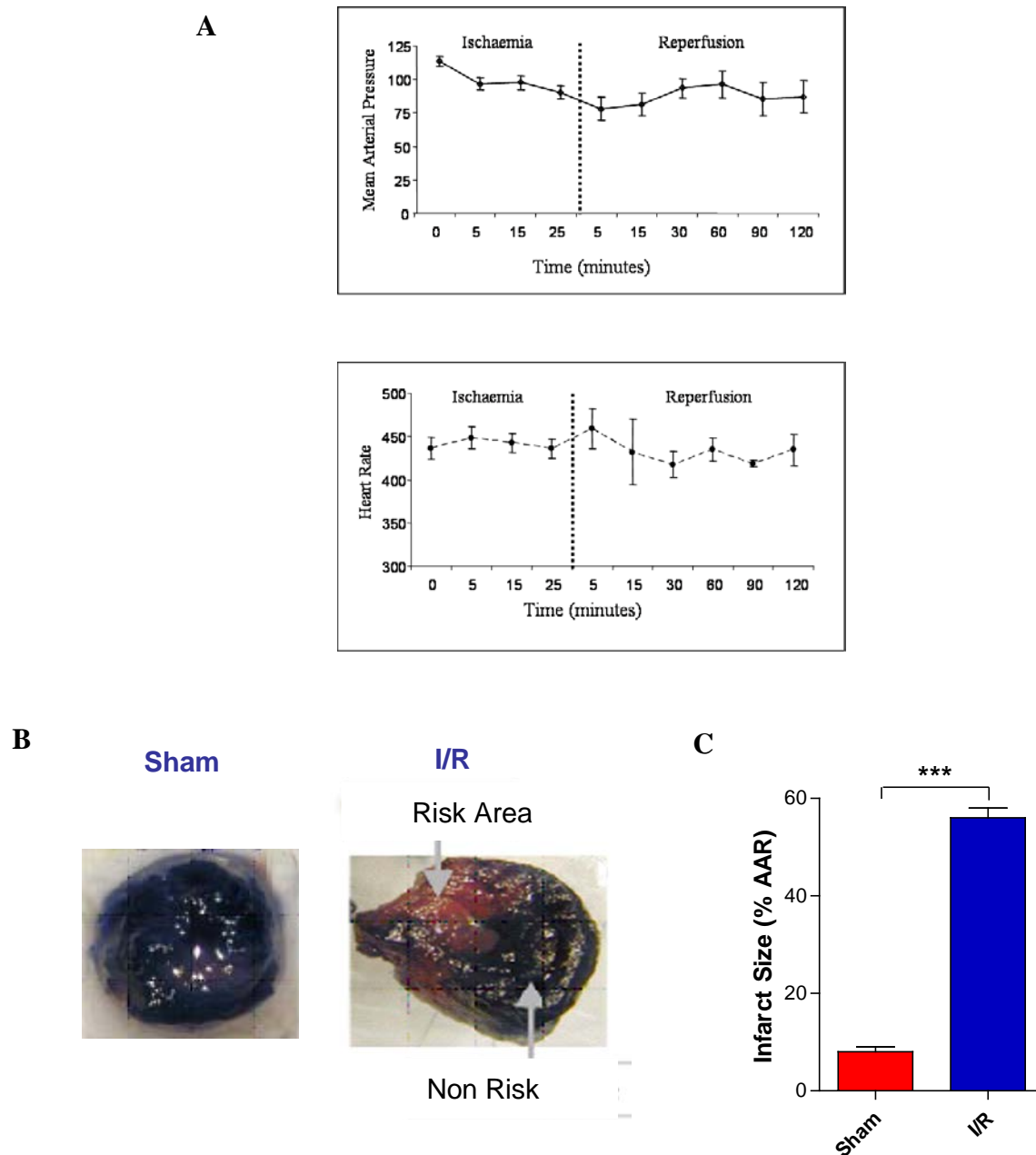


Fig 3.14. Parameters of the *in vivo* ischaemia/reperfusion model. (A) Measurement of mean arterial pressure and heart rate. The right carotid artery was cannulated and connected to a pressure transducer in order to monitor mean arterial pressure and heart rate throughout ischaemia and reperfusion (n=8 animals). (B) Separation of left ventricle into risk and non-risk. Following reperfusion, the coronary artery was re-occluded and Evans Blue dye was injected into the left ventricle which allows separation of the ventricle into risk and non-risk. (C) Infarct measurement; the area at risk (AAR) was separated, and incubated with 0.5 mg/ml *p*-nitroblue tetrazolium for 30 min at C, the non-stained tissue was weighed and expressed as a percentage of the total weight of the AAR. n=8 animals, *** p <0.001.

Next, the extent of DNA damage and apoptosis was examined. DNA damage results in rapid phosphorylation of histone 2AX on serine 139 (known as γ -H2AX) which is a standard molecular marker for the induction of DNA damage (Rogakou et al., 1998). γ -H2AX was rapidly induced by reperfusion with maximum activity at 30 min, demonstrating that reperfusion is a potent inducer of DNA damage (Fig 3.15). Similarly, cleavage of caspase-9 occurred in a reperfusion dependent manner, showing that the apoptotic pathway is rapidly activated in this model of reperfusion injury (Fig 3.15).

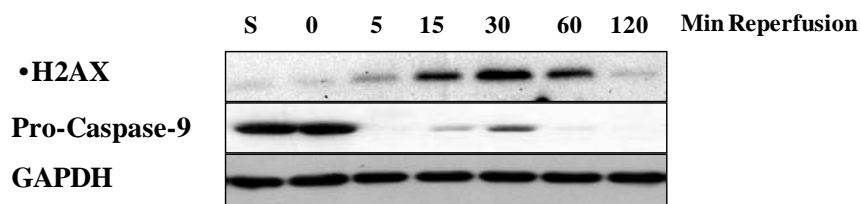


Fig 3.15. Reperfusion activates the DNA damage and apoptotic pathways. A time course of reperfusion was carried out *in vivo*, tissue was isolated from the risk area and cell lysates were immunoblotted for γ -H2AX (S139), pro-caspase 9 and GAPDH, S = sham operated.

Western blot analysis revealed activation of both STAT1 and 3 with distinct patterns of tyrosine and serine phosphorylation (Fig 3.16a). Importantly, only minimal activation of both STATs was seen in the non-risk area, demonstrating that STATs are only activated in areas of myocardial damage. STAT3 was phosphorylated at tyrosine 705 during ischaemia and reperfusion injury increased activity, reaching a maximum at 30 min, followed by a decline thereafter. The kinetic pattern of serine phosphorylation in STAT3 differed in that although it was induced by ischaemia it did not increase during reperfusion, however similarly to Y705, serine phosphorylation declined after 1 hr. No consistent difference in total STAT3 levels was seen throughout the time course of reperfusion. In contrast to STAT3, was not activated during ischaemia but similarly to STAT3, STAT1 tyrosine phosphorylation reached a maximum by 30 minutes of reperfusion (Fig 3.16b). Fig 3.16c illustrates the kinetics of STAT1 and STAT3 tyrosine phosphorylation using densitometric analysis. It is clear that tyrosine phosphorylation of both proteins followed a very similar pattern, peaking at 30 min and then rapidly declining by 1 hr. Indeed this profile suggests that proteins which control the

negative regulation of STAT1 and STAT3 activity may be concomitantly activated during reperfusion injury which might account for this rapid dephosphorylation.

Interestingly, STAT1 was phosphorylated at serine 727 during ischaemia but no serine phosphorylation was detected during reperfusion. This suggests that co-ordinate distinct pathways lead to STAT phosphorylation following I/R injury. Since STATs are intimately involved in apoptotic control (STAT3 can protect cardiac myocytes from I/R injury, while STAT1 promotes cardiac myocyte apoptosis) this *in vivo* phosphorylation of both tyrosine and serine residues may be important for cardiac myocyte survival during myocardial infarction.

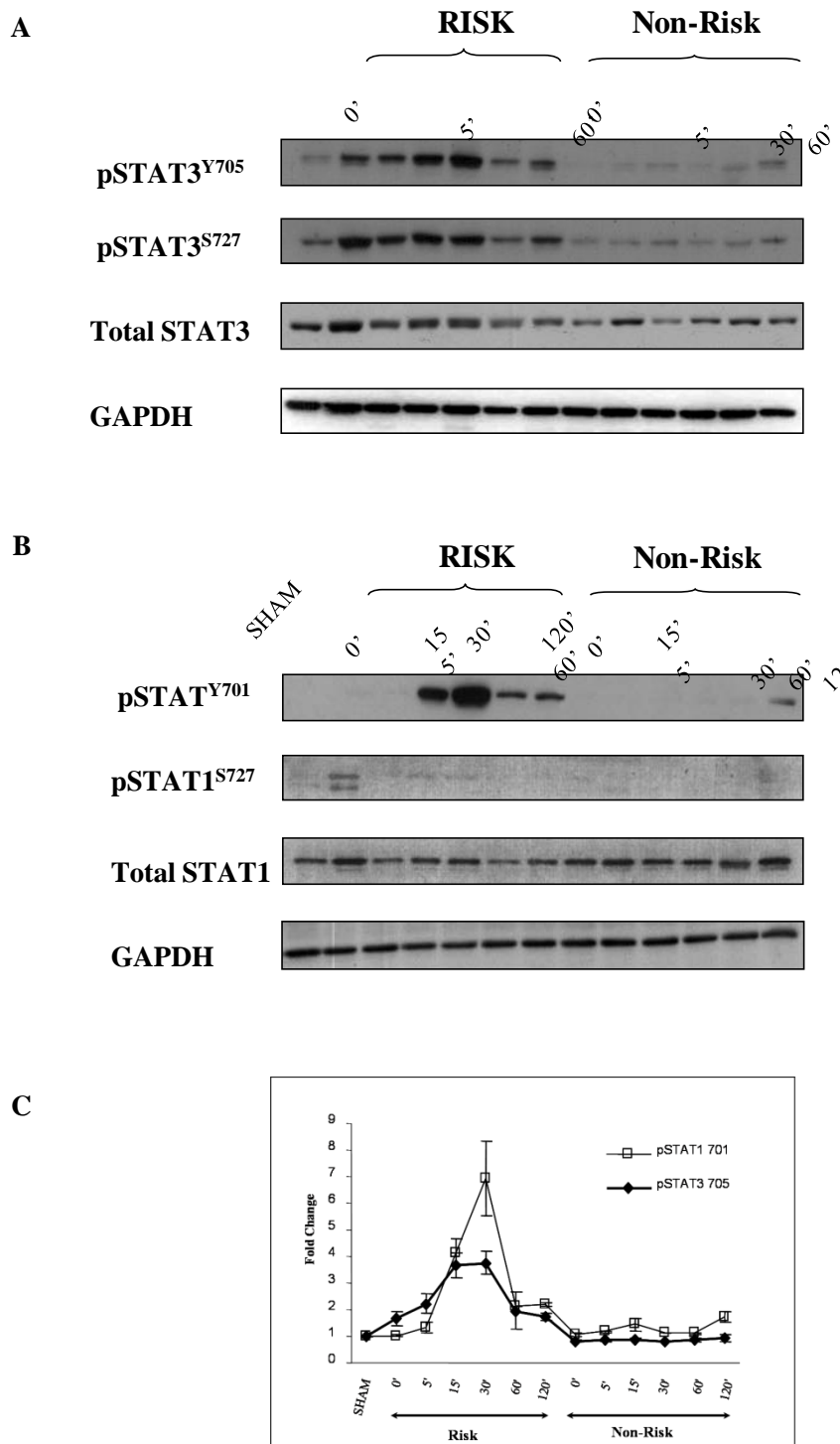


Fig 3.16. Time course of STAT1 and STAT3 activation following I/R injury. Tissue from the risk and non-risk areas was analysed by western blot for (A) tyrosine phosphorylated, serine phosphorylated and total STAT1 and (B) tyrosine phosphorylated, serine phosphorylated and total STAT3. Equal loading was confirmed using GAPDH (C) Densitometric analysis was performed using a Biorad GS-800 detection system. Values are normalised to sham levels, n=3 animals.

3.8. Increased Expression of STAT3 Target Genes Following *in vivo* I/R injury

STAT3 was found to be phosphorylated at both residues following I/R injury and this would suggest that I/R is a potent inducer of STAT3 transcriptional activity. To address this question, qPCR analysis was carried out on STAT3 target genes. The expression of SOCS3 (8.8 ± 0.7 fold), c-Fos (64.1 ± 20.7 fold) and Bcl-2 (3.3 ± 0.1 fold) were all significantly upregulated after 2 hr of reperfusion (Fig 3.17). This fits well with the phosphorylation data where STAT3 reached maximal activity by 30 min, gene expression initiated at that time would be expected to peak 1-2 hr later. Importantly there was no increase in STAT3 mRNA expression which suggests that the increased expression of the STAT3 targets is more likely to be due to the increased phosphorylation per STAT3 molecule and not an overall increase in total STAT3 content.

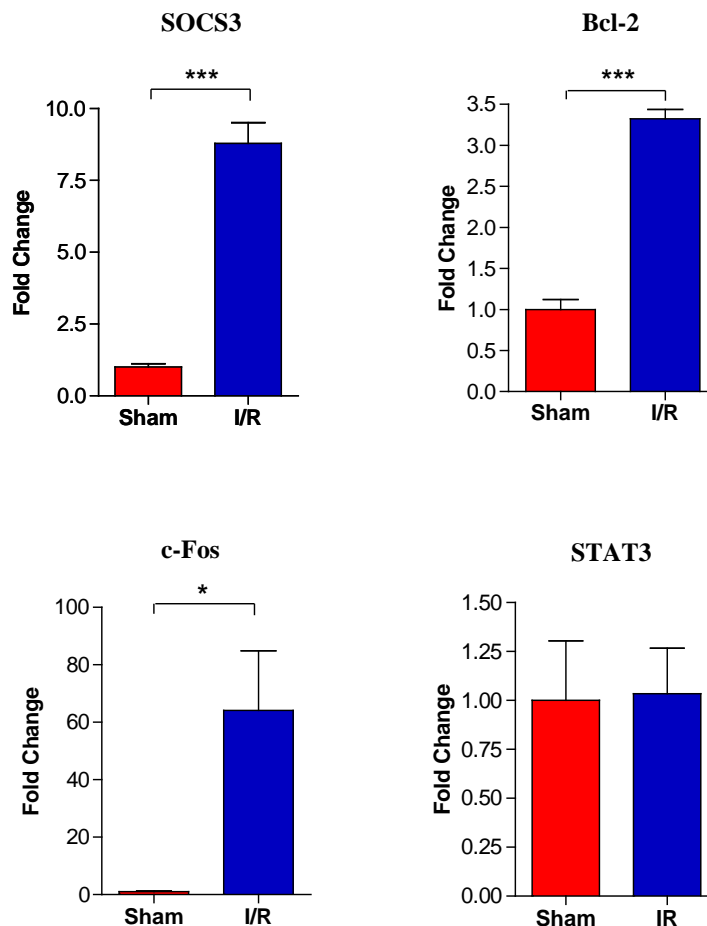


Fig 3.17. Expression of STAT3 target genes are increased following I/R injury *in vivo*. RNA was extracted from the left ventricles of rats subjected to I/R injury (2 hr reperfusion) or sham surgery and the levels of SOCS3, Bcl-2, c-Fos and STAT3 were measured by qPCR and normalized to sham. n=4 animals, *p<0.05, ***p<0.001, students t-test.

3.9 I/R injury in the brain induces distinct kinetics of STAT activity

In order to ascertain if the rapid activation of STAT1 and STAT3 in the heart is a general phenomenon of reperfusion injury or if it is specific to the myocardium, a time course of I/R injury in the brain was carried out. Technical aspects of this study were carried out in conjunction with Dr. Romina Badin of the Biophysics unit at the Institute of Child Health. This cerebral ischaemia/stroke model involves transient focal cerebral ischaemia via middle cerebral artery occlusion (MCAO) by insertion of suture 17 mm from carotid bifurcation for 30 min followed by removal of the suture and reperfusion (Fig 3.18a). The MRI images in Fig 3.18b show T2-weighted proton density scans from 6 hr and 24 hr reperfusion; by 6 hr early infarction can be delineated while 24 hr after reperfusion the infarct lesion can clearly be seen.

Following 30 min of ischaemia, the brain was reperfused for 10, 30, 60, 120 and 360 min. The basal ganglia and cortex were dissected out and separated into ipsilateral and contralateral areas. While no STAT activation was seen in the cortex in this model (not shown), both STAT1 and STAT3 became tyrosine phosphorylated at 6 hr post-reperfusion in the basal ganglia, on the ipsilateral but not contralateral side (Fig 3.18 C and D). Surprisingly, this is in contrast to the relatively quick effect of reperfusion on STAT activation in the myocardium. This suggests that the rapid (~15 min) reperfusion induced tyrosine phosphorylation of STAT1 and STAT3 in the myocardium may occur through a mechanism distinct from that of I/R induced activation in the brain.

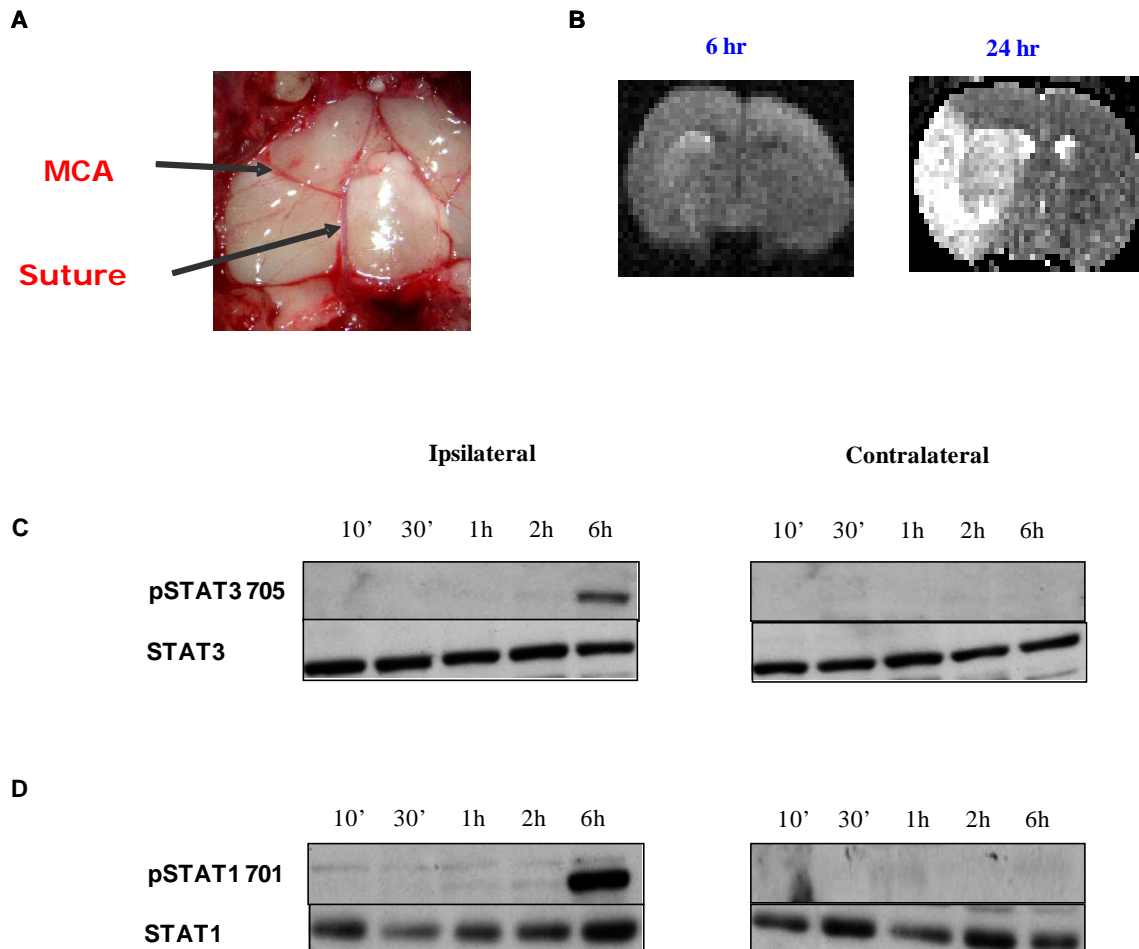


Fig 3.18. STAT activation following cerebral I/R injury. Middle cerebral artery occlusion (MCAO) was carried out in adult male Spague-Dawley rats for 30 min, followed by the indicated times of reperfusion. **(A)** Occlusion of MCA with suture. **(B)** Representative centre slice T2-weighted images of animals reperused for 6 hr or 24 hr, infarct lesion appears as bright signal. **(C and D)** Representative western blots of tyrosine phosphorylated STAT1 and 3 from ipsilateral and contralateral basal ganglia, total STAT1 and 3 are shown as loading controls. n=3 animals.

3.10 Reperfusion Induced Myocardial STAT Tyrosine Phosphorylation is Mediated by ROS

It is well appreciated that ROS are rapidly generated by reperfusion injury and indeed ROS have been shown to be capable of inducing both STAT Y705F activity *in vitro* (Simon et al., 1998) and S727 activity *in vitro* (Fig 3.13). Therefore, the possibility that ROS production is a trigger of STAT phosphorylation during *in vivo* I/R injury was examined. For these experiments, 30 min of reperfusion was chosen, as maximal STAT activation occurs at this time (Fig 3.16). Rats underwent 25 min ischaemia and were then infused with 100 mg/kg of the antioxidant tempol, followed by 30 min reperfusion. ROS inhibition was assessed by measuring tissue malondialdehyde (MDA) levels, a marker of lipid peroxidation (Hogberg et al, 1975). Tempol infusion lowered MDA levels to the levels of sham operated or non-risk tissue, suggesting that tempol is effective at abolishing the majority of ROS production by reperfusion (Fig 3.19a). Tempol infusion also reduced infarct size by 57.1 ± 5.0 %, demonstrating that a large majority of tissue damage following reperfusion can be attributed to ROS production (Fig 3.19b)

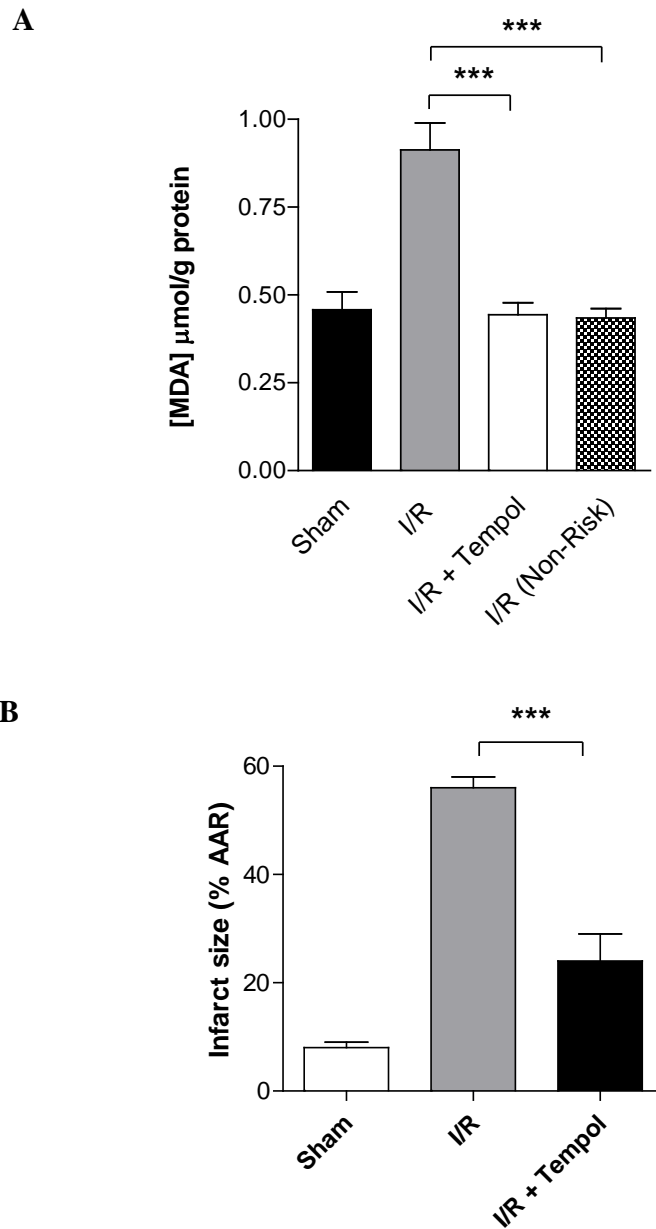


Fig 3.19 Infusion of tempol inhibits ROS production and lowers infarct size. Rats underwent sham operation, 25 min ischaemia and either 30 min (A) or 2 hr (B) reperfusion with infusion of saline or 100 mg/kg tempol. (A) Tissue MDA levels were measured by HPLC from each of the indicated groups (B) Infarct size was measured using NBT staining. Statistical analysis was carried out using a one way ANOVA with Bonferoni post correction, *** $p < 0.0001$, $n=6$ animals

Tempol infusion before the onset of reperfusion led to a reduction in the levels of tyrosine phosphorylated STAT1 by $71 \pm 5\%$ and of STAT3 by $45 \pm 15\%$ (assessed by densitometry), there was also a reduction in S727 phosphorylation of STAT3 (41.4 ± 20.7) but this was not statistically significant over three animals (Fig 3.20a,b). This suggests that following reperfusion injury, the rapid generation of ROS is a major contributor to STAT1 and STAT3 activation. The levels of the STAT1/3 kinase JAK2 paralleled the tyrosine phosphorylation by I/R injury and reduction by tempol. Fig 3.20c Shows a 2-fold increase in pJAK2 levels during I/R, which were reduced back to sham levels by tempol infusion. This suggests that JAK2 is also activated by ROS and it is likely that this kinase lies upstream of STAT1/3 in ROS mediated STAT1 and STAT3 tyrosine phosphorylation.

While JAK2 may be a major regulator of STAT phosphorylation status during I/R, it is likely to be one of many JAK/STAT regulating proteins active during I/R injury. With this in mind, the expression of the recently characterised STAT3 inhibitor GRIM-19 was measured (Lufe C et al., 2003). GRIM-19 levels were reduced by $68 \pm 11.3\%$ during I/R injury and were increased back to almost 80% of sham levels by tempol infusion (Fig 3.20c). This is the first time that GRIM-19 has been shown to be regulated by I/R injury and the rapid reduction in protein levels (i.e. 30 min) is suggestive of protein degradation and thus may represent a novel mechanism of STAT3 regulation during I/R injury.

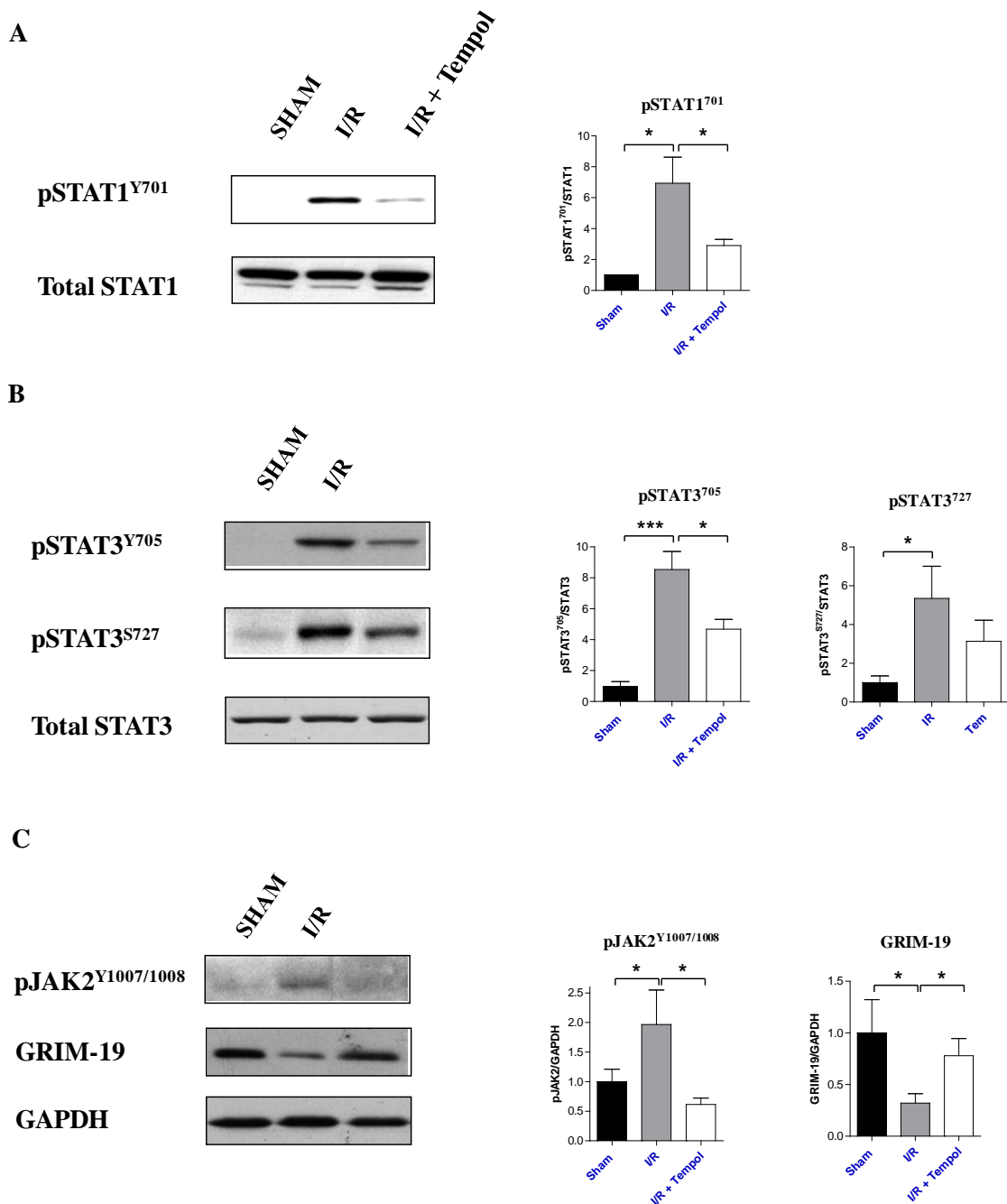


Fig 3.20. Tempol infusion reduces JAK/STAT activation and increases GRIM-19 expression. 100 mg/kg tempol was infused prior to 30 min reperfusion, the risk area was separated, snap frozen in liquid nitrogen and lysed in RIPA buffer. Western blot analysis was carried out for (A) and total STAT1 (B), and (C) ¹⁰⁰⁸ and GRIM-19, equal loading was confirmed with GAPDH. For each western the corresponding densitometric analysis is shown, raw numbers were normalised by initially setting I/R to 100% and re-normalised to express as fold change over sham. n=4 for each group * p<0.05, *** p<0.001 analysed by one way ANOVA with Bonferroni post test.

In order to examine the tissue distribution of STAT1/3 tyrosine phosphorylation, immunohistochemistry was carried out. Intense STAT1 and STAT3 phospho-tyrosine staining was noted in myocardial cross-sections after 30 min of reperfusion and this was found to be mainly localised to the nucleus (Fig 3.21). STAT1 and STAT3 tyrosine phosphorylation also appeared to be evident in endothelial cells surrounding vessels but endothelial cell-specific co-staining would need to be carried out to confirm this. Tempol infusion was found to dramatically lower STAT1 and STAT3 phospho-tyrosine staining, thus confirming the results seen with western blot. Moreover, this staining pattern suggests that STAT1/3 tyrosine phosphorylation is not solely confined to the cardiac myocyte population of the heart and may also play a prominent role in endothelial cell apoptosis.

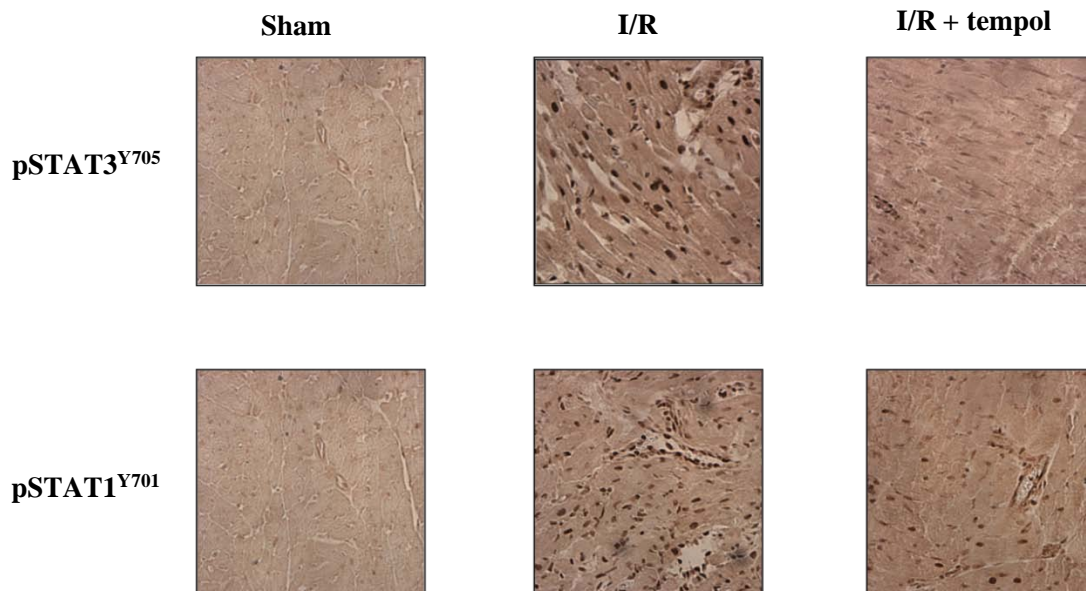


Fig 3.21. Immunohistochemical staining of STAT phosphorylation following tempol infusion. Rats underwent sham operation, I/R (30 min reperfusion) or I/R with infusion of 100 mg/kg tempol. The risk area was separated from each sample and fixed in 10% formalin, 5µm tissue sections were stained with the indicated antibodies.

3.11 Increased Phosphorylation Following IFN-• Treatment Increases Infarct Size and Reduces the Protective Effect of Tempol

The previous results showed that infusion of antioxidants during reperfusion lowered the levels of STAT1 and STAT3 phosphorylation. However, since STAT1 is pro-apoptotic in the myocardium and STAT3 is anti-apoptotic, it is unclear what the effects are of lowering both. Indeed the possibility exists that inhibition of both STAT1 and STAT3 might have no overall effect. Since tempol is clearly cardioprotective, the most likely scenario is that reducing pro-apoptotic STAT1 activity may play a major role in anti-oxidant protection. To address this, rats underwent ischaemia with 2 hr reperfusion and were infused with the potent STAT1 agonist IFN-•, tempol or tempol and IFN-• in combination prior to reperfusion. This two hour time-point was chosen as previous experiments have shown this to be the optimal time-point for conducting infarct measurements (McDonald et al., 1999). The mean arterial pressure (MAP) and pressure rate index (PRI) fell during ischaemia, while heart rate was slightly increased, these indices returned to near baseline levels during reperfusion (Fig 3.22). Importantly, none of the drug treatments significantly altered any of the heart function readouts, showing that any effect was not due to global changes in blood pressure (Fig 3.22).

When compared to sham-operated animals, 2 hr of reperfusion caused a significant increase in infarct size to 56 ± 2 % (Fig 3.23a). Administration of IFN- γ (25 $\mu\text{g}/\text{kg}$) 5 min prior to reperfusion upregulated STAT1 activity and caused a 30 ± 1 % increase in myocardial infarct size when compared with I/R alone, indicating that increased STAT1 activity is associated with increased myocardial damage *in vivo* (Fig 3.23). Importantly, IFN-• reduced the cardioprotective effect of tempol. Tempol infusion alone reduced the infarct size by 57.1%, whereas tempol + IFN-• together lead to a reduction in infarct size by 21.9% compared to IFN-• treatment alone. This is mirrored in the western blot which shows that the decrease in phosphorylation caused by tempol was completely blocked by IFN-• (Fig 3.23b). This strongly implicates STAT1 activation as a main target in tempol-mediated cardioprotection and together with previous work (Townsend et al., 2004) suggests that the inhibition of proapoptotic STAT1 activity may be a general mechanism of antioxidant protection during I/R injury.

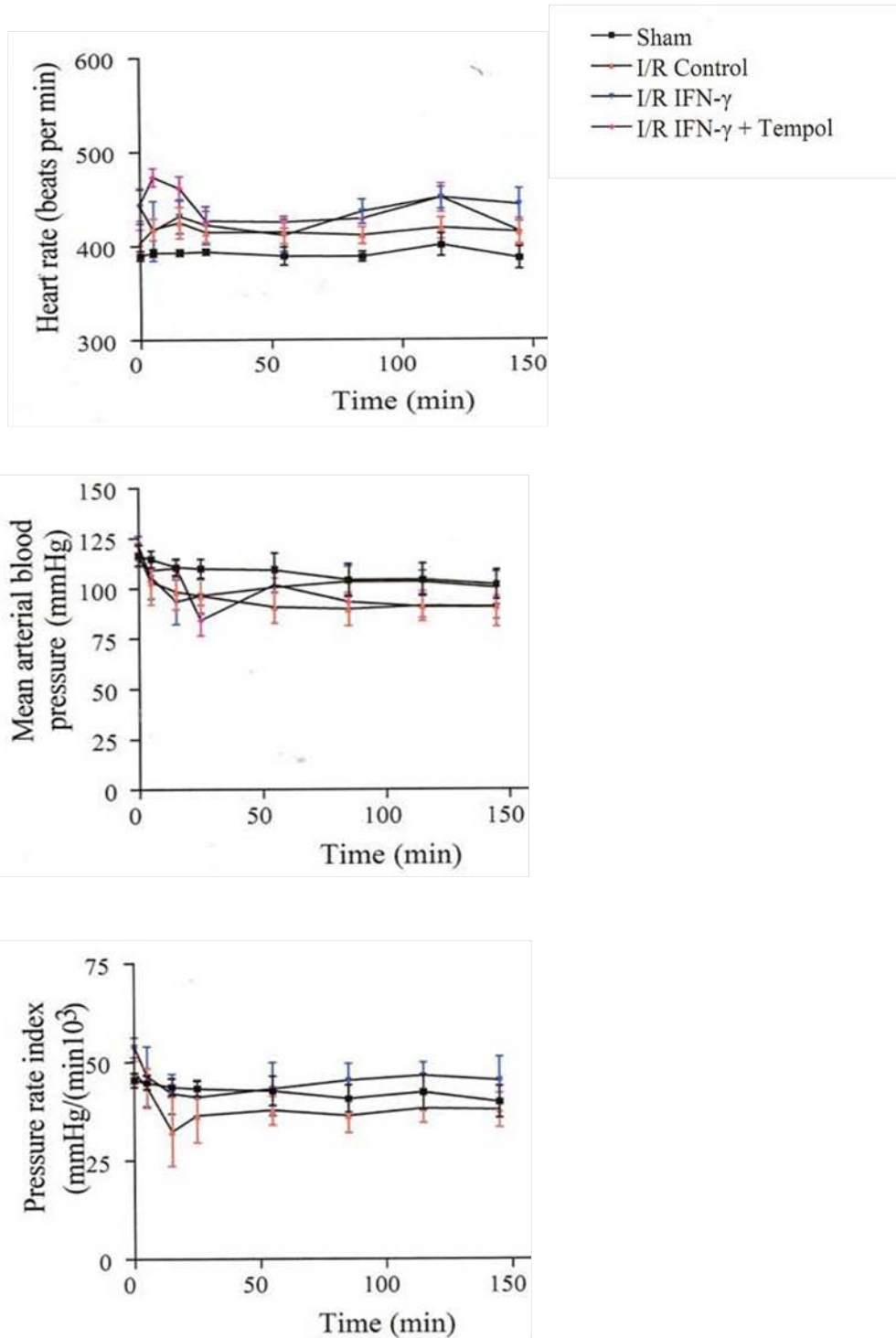


Fig 3.22. Effect of I/R and drug infusion on blood pressure, heart rate and pressure rate index. The rat carotid artery was cannulated and connected to a pressure transducer to measure MAP and heart rate, the pressure rate index was calculated as the product of MAP and HR. Animals (n=4) were monitored throughout the 30 min ischaemia and 120 min reperfusion in each of the indicated groups.

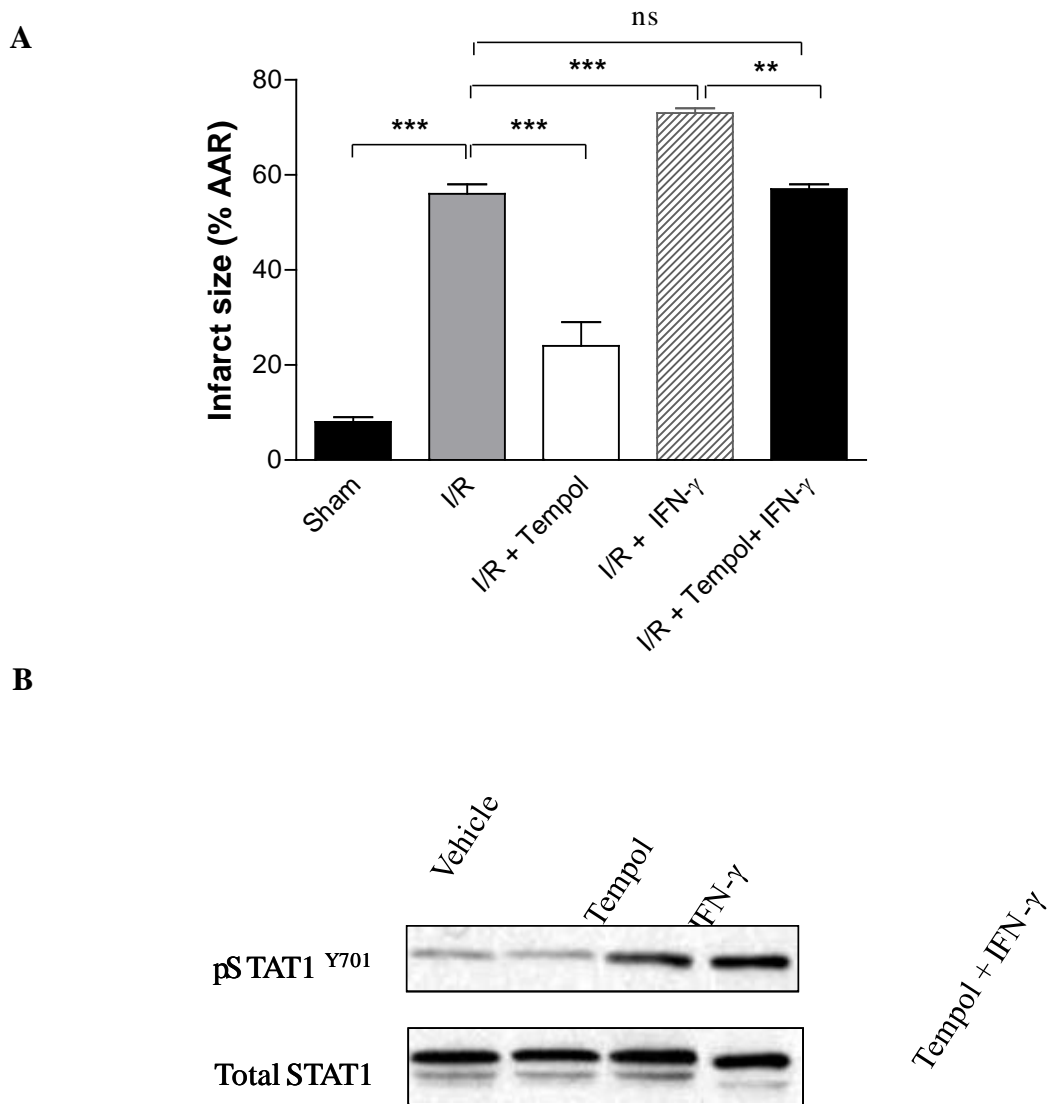


Fig 3.23. IFN- \bullet induced STAT1 increases infarct size and abrogates the protective effect of tempol. (A) Infarct size was measured in rats subjected to sham operation or 25 min LAD occlusion and 2 hr reperfusion with infusion (5 min prior to reperfusion) of either saline (I/R n=7), 100 mg/kg tempol (n=7), 25 μ g/kg IFN- \bullet (n=6) or both tempol and IFN- \bullet together (n=6), statistics were carried out with a one-way ANOVA with a Bonferoni post test, *** p<0.001, ** p<0.01. (B) Western blot analysis of STAT1 phosphorylation from heart tissue from the indicated treatment groups, n=3.

3.12 Discussion

STAT transcription factors have been shown to play a prominent role in cell fate following various stresses. The work presented here demonstrates that STAT3 plays an important role in protection from I/R injury in cardiac myocytes. Transient overexpression of STAT3 and transduction with a dominant negative STAT3 virus both revealed that STAT3 functions as an anti-apoptotic transcription factor in cardiac myocytes. Likewise, experiments in STAT3-deficient cells revealed that in the absence of STAT3 signalling, oxidative stress mediated cell death is greatly exacerbated. In support of this, transient overexpression of STAT3 also increased survival in NRVMs exposed to .

Both STAT1 and STAT3 were phosphorylated at tyrosine 701/705 and serine 727 following I/R injury *in vitro*. Both tyrosine and serine phosphorylation peaked at 1 hr, levels stayed elevated up to 20 hr while levels tapered off. The differential effects of phosphorylation on individual tyrosine or serine residues are unknown. The current dogma posits that Y705 phosphorylation is obligatory for DNA binding and nuclear retention but that S727 phosphorylation is necessary for a fully fledged transcriptional response (Levy and Darnell, 2002). It is likely that S727 phosphorylation serves as a rheostat for STAT3 activity and may influence promoter choice, chromatin on/off rates as well as the duration and level of transcript production. STAT1 phosphorylation *in vitro* displayed a broadly similar pattern, the exception being that phosphorylation is more pronounced during ischaemia. In support of these phosphorylation studies, qPCR analysis of STAT3 target genes confirmed the increased transcriptional activity of STAT3 during I/R. Both SOCS3 and c-Fos were maximally expressed between 2 and 4 hr of reperfusion which follows closely after the time of maximal STAT3 phosphorylation. Taken together, the *in vitro* studies show that STAT3 is rapidly induced during I/R injury and oxidative stress and show that this activity is important in allowing cardiac myocytes to minimise the deleterious effects of I/R injury.

It is interesting to observe that the MEK-ERK pathway feeds into the STAT3 pathway during oxidative stress. treatment led to STAT3 Y705 and S727 phosphorylation within 15 min and S727 phosphorylation was shown to be ERK1/2 dependent, while the MAPKs appeared to have no affect on Y705 phosphorylation. ERK1/2 has previously been shown to confer protection from oxidative stress and I/R injury (Yue et al., 2000, Adderlay and Fitzgerald, 1999), therefore this ERK1/2-STAT3 crosstalk may represent a novel cardioprotective

pathway whereby oxidative stress promotes ERK mediated STAT3 serine phosphorylation and subsequent cardioprotection. It would be interesting to examine if increased ERK activity can still confer cardioprotection in mice where the STAT3 S727 residue has been mutated to an alanine.

As with the evidence from NRVMs *in vitro*, phosphorylation of and were induced during ischaemia *in vivo*. phosphorylation was enhanced during reperfusion, while phosphorylation did not increase over the levels observed in ischaemia as seen *in vitro*. STAT1 was also activated by I/R but showed distinct kinetics to STAT3. Interestingly both STAT1 and STAT3 tyrosine phosphorylation peak after 30 min of reperfusion and are then dephosphorylated, demonstrating that rapid activation of both STATs is an important feature of I/R injury. In support of this, the STAT3 target genes SOCS3, Bcl-2 and c-Fos were all upregulated by I/R *in vivo*. Analysis of STAT activity in a regional model of I/R injury in the brain suggest that a different STAT signalling pathway may exist in the cerebellum. Temporal analysis revealed that STAT1 and STAT3 tyrosine phosphorylation was delayed with respect to myocardial I/R. No STAT phosphorylation was seen until 6 hr of reperfusion. Although these are distinct models of I/R, it nonetheless highlights that reperfusion may not activate the same set of signalling pathways in all tissues damaged by I/R and cautions against generalisations made about I/R injury in different contexts.

Importantly, very little STAT phosphorylation was observed in the non-risk area of the heart following I/R which suggests that the activation of STAT1 and STAT3 is confined largely to the area of most cellular damage. By measuring MDA levels it was shown ROS are generated solely in the risk area, which is supported by the finding that phosphorylation of histone 2AX, a marker for DNA damage occurs rapidly in the risk area following I/R injury. Inhibition of ROS with the free radical scavenger tempol, reduced infarct size following I/R injury *in vivo*. Furthermore, inhibition of ROS reduced both STAT1 and STAT3 tyrosine phosphorylation, suggesting that ROS production following I/R injury is one of the main instigators of STAT activation during I/R injury.

Precisely which kinases are responsible for ROS-induced STAT activity are currently unknown but the finding that pJAK2 levels were also reduced by tempol suggests that JAK2

may be involved. JAK2 activity has been shown to be induced within 5 min of treatment and indeed ROS production *in vivo* has been shown to occur within minutes after restoration of blood flow following ischaemia (Abe and Berk, 1999, Zhao, 2004). The activity of non-receptor tyrosine kinases was not examined in this study but Src, Fyn, Lck and Abl have all been shown to be activated by oxidative stress and therefore may also play a role in STAT phosphorylation during I/R injury (Harwick and Sefton, 1995, Aikawa et al., 1997, Abe et al., 2000, Sun et al., 2000)

Expression of the STAT3 inhibitor GRIM-19 was also found to be reduced during I/R and its levels were restored by tempol treatment. GRIM-19 has been shown to bind to STAT3 following IL-6 or IFN- γ treatment and STAT3 S727 phosphorylation was shown to be obligatory for this interaction (Zhang et al., 2003). Overexpression of GRIM-19 inhibited STAT3 dependent transcriptional activity (Zhang et al., 2003, Lufei et al., 2003), and it is noteworthy therefore that levels of GRIM-19 and active STAT3 were inversely related during I/R. Free radical mediated transcriptional inhibition or protein degradation of GRIM-19 levels may constitute one pathway in which STAT3 transcriptional activity is elevated during I/R.

It seems therefore that JAK/STAT activation following cardiac stress may be modular in nature. In the first instance, intracellular ROS generation following the restoration of ATP synthesis may directly activates STAT1 and STAT3, possibly through activation of JAK1/2, non-receptor tyrosine kinases or reduction of GRIM-19 as well as through STAT serine kinases such as ERK1/2. This early response may set the stage for early upregulation of pro- and anti-apoptotic genes which are instrumental in the early decision to commit to apoptosis and the formation of infarct. This is borne out by the finding that mice deficient in cardiac STAT3 have reduced infarct sizes, whereas hearts overexpressing a constitutively active form of STAT1 suffer more severe infarction following I/R (Stephanou et al., 2002, Hilfiker-Kleiner et al., 2004). A second temporal level of JAK/STAT control might come from the later release of a variety of cytokines, hormones and growth factors which leads to the upregulation of genes involved in maintenance of cardiac integrity, the release of angiogenic factors, development of compensatory hypertrophy and control of the remodelling programme.

Tempol was found to dramatically lower STAT1 tyrosine phosphorylation, suggesting that some of the protective effects of tempol might be attributable to inhibition of this proapoptotic transcription factor. In the presence of IFN- γ , tempol no longer showed a STAT1 inhibitory effect and this was associated with a reduction in tempol's infarct sparing activity. Taken together these data suggests that inhibition of STAT1 activity may play a prominent role in the cardioprotective action of tempol, although of course it must be noted that IFN- γ promotes many effects other than STAT1 activation. Previously it has been shown that the green tea polyphenol epigallocatechin-3-gallate (EGCG), could reduce infarct size following I/R injury in rats (Townsend et al., 2004). This was associated with a reduction in STAT1 activity and suggests that other antioxidants may also function through inhibition of the proapoptotic activity of STAT1.

In the course of this work several studies have been published which support the aforementioned data. Oshima and colleagues demonstrated that mice engineered to express cardiac-specific constitutively active STAT3 showed a 60% reduction in infarct size following I/R injury (Oshima et al., 2005). This infarct sparing effect was attributed to STAT3 mediated induction of the antioxidant proteins metallothionein 1 and 2, as crossing the STAT3 overexpressing mice onto a metallothionein negative background abolished the cardioprotective effect of STAT3. Although total deletion of STAT3 is embryonically lethal (Takeda et al., 1997), further evidence for the role of STAT3 as a cardioprotective transcription factor is highlighted in studies using cardiac myocyte-specific STAT3 knockout mice (Hilfiker-Kleiner et al., 2004). These mice suffer from decreased left ventricular capillary density and show symptoms of heart failure after 12 months, including cardiac fibrosis, impaired contractile function and a decrease in systolic function over time. Cardiac-specific STAT3 deficient mice are also more susceptible to I/R- induced cardiac injury, displaying larger infarct sizes and a greater number of caspase-3 and TUNEL positive cells following reperfusion when compared with wild type controls (Hilfiker-Kleiner et al., 2004).

Granulocyte-colony stimulating factor (G-CSF) has recently been shown to confer protection from myocardial and cerebral ischaemia through STAT3 upregulation, with G-CSF failing to illicit protection in mice overexpressing dominant negative STAT3 (Harada et al., 2005, Komine-kobayashi et al., 2006). STAT3 has also been shown to play a role in endothelial cell apoptosis in response to I/R by inhibiting FAS and caspase-3 expression (Zhang et al., 2005). While this is the first study to show STAT3 serine phosphorylation by I/R injury, some recent

studies have begun to address the role of STAT3 serine phosphorylation in the myocardium. Mice in which serine 727 has been mutated to an alanine show enhanced susceptibility to doxorubicin-induced heart failure (Shen et al., 2004). Upregulation of ICAM has been shown to increase neutrophil recruitment during I/R injury while its expression is associated with cardiac pathology (Palazzo et al., 1998). Following I/R in endothelial cells, serine phosphorylated STAT3 was shown to bind to the GAS element in the ICAM-1 promoter in association with Sp1 and enhance ICAM-1 expression following reperfusion (Yang et al., 2005). These studies are all in agreement with the data presented in this thesis and reaffirm the central finding that STAT3 activity is enhanced during I/R injury and is part of an anti-apoptotic programme which rescues myocytes from I/R damage.

Chapter 4: Investigating Gene Expression changes in Myocardial Infarction using Microarray Analysis

4.1 Aims

In the previous chapter, the STAT3 dependent genes *c-fos* and *socs3* were shown to be induced during I/R injury in the *in vivo* rat heart, an effect which could be blocked by free radical scavenging with tempol. In order to ascertain if other STAT3 target genes are upregulated during I/R injury, global gene expression analysis was carried out on rat hearts using Affymetrix gene arrays. These arrays allow examination of 15,866 individual transcripts simultaneously and thus give an indication of total transcriptional changes brought about by I/R *in vivo* when compared to the hearts of sham operated rats. In addition to the effect on STAT3 target genes, the transcriptional profile of I/R injured hearts can be used to identify changes in the expression of genes which may not have been previously documented as having a role in I/R injury and thus potentially identify novel physiological changes. To extend these studies, the effects of free radical inhibition on global gene expression was also examined by infusing with the anti-oxidant tempol before reperfusion.

In addition to the first aim, a second set of experiments was carried out to examine the transcriptional effects of two other novel cardioprotective peptides. Both the CRF family members urocortin1 and urocortin2 (stresscopin-related peptide) have been shown to be beneficial in experimental MI (Rademaker et al., 2005, 2008). Urocortins work through binding G-protein coupled receptors; Ucn1 binds to both the corticotropin-releasing factor (CRF) receptors CRFR1 and CRF2, whereas Ucn2 binds specifically to CRFR2 (Kuperman et al. 2008). Although Ucn1 is clearly beneficial in preventing ischaemic damage, its effect on CRF1 may limit its usefulness as a therapeutic peptide since it stimulates the hypothalamic pituitary axis (HPA) (Tsatsanis et al., 2007). Moreover, administration of Ucn1 to healthy adults led to increases in plasma levels of corticotrophin (ACTH), cortisol and atrial natriuretic peptide (ANP) and decreases ghrelin levels (Davis et al., 2004). For this reason, long term Ucn1 treatment in patients may have significant drawbacks.

Ucn2 may avoid some of the potential side effects of Ucn1 as it is specific for the CRF2 receptor. Intravenous infusion of Ucn2 in patients with heart failure increased cardiac output and decreased blood pressure but had no effect on hormone responses (David et al., 2007). It is currently unknown how the responses to Ucn1 and Ucn2 differ at the transcriptional level and to address this question rats were infused with Ucn1 or Ucn2 before reperfusion and the effect on global gene expression was examined. The rationale for these experiments is to better understand the similarities and differences in the transcriptional effects of Ucn1 and

Ucn2 in experimental MI and to compare them to anti-oxidant treatment. Analysis of downstream transcriptional effects might reveal a common subset of targets between the two peptides which could potentially be exploited as targets for therapeutic intervention through the rational design of more selective peptides.

4.2 Drug Infusion, Gene Array Procedure and Quality Control

These experiments were carried out in conjunction with Dr. Ahila Sivarajah at St. Bartholomew's and The Royal London School of Medicine and Dentistry. Rats were randomly separated into 5 groups with 3 rats in each group; group 1: sham surgery, group 2: I/R with saline infusion, group 3: I/R with infusion of 100 mg/kg tempol, group 4: I/R with infusion of 15 µg/kg urocortin and group 5: I/R with infusion of 15 µg/kg urocortin 2. The hearts were removed and the right atrium and ventricle were separated and discarded. RNA was extracted from the left ventricular tissue, quality assessed on an Agilent 2100 array and processed into cRNA as outlined in the materials and methods. The cRNA was also run on an Agilent 2100 to ensure that the RNA from each sample had a similar size distribution. cRNA was hybridised overnight to Affymetrix RAE230A gene arrays and scanned on an Affymetrix scanner 3000. After scanning, each microarray image was manually inspected to look for any misalignment features.

Microarrays were subjected to quality control to test the data set for differences in chip quality, variance in sample hybridisation and quality of RNA. Quality control was initially carried out using Affymetrix GCOS software. An important control with microarray experiments is to ensure that the fluorescence is similar across all the arrays used in the study. The RawQ value, which is a measure of total fluorescence of each array, had a mean value of 2.54 ± 0.51 which is within accepted normal range of 1.5-3.0 (Heber and Sick, 2006) (Table 4.1a). Background fluorescence values for Affymetrix arrays normally range between 10 and 100, average background fluorescence across the 15 tested arrays was 68.86 ± 11.25 which was within accepted limits (Heber and Sick, 2006)(Table 4.1a). The scaling factor is used to set the same median intensity across all arrays i.e. more intensely stained arrays have a low scaling factor while weakly stained arrays have a larger scaling factor. Affymetrix sets a maximum threshold of 3 standard deviations away from the mean for a sample to be included in the data set. The scaling factor standard deviation across the 15 arrays was 0.90, allowing

all 15 arrays to be included in downstream analysis (Table 4.1a). The percentage present is a measure of the total number of possible transcripts expressed. The average percent present call was $50.5\% \pm 6.3$ (Table 4.1b) which fits well with published rat myocardial data sets (<http://www.affymetrix.com/support/technotes/expression>).

A

	RawQ	Background	SF
SH1	2.46	71	0.79
SH2	2.91	73.7	0.39
SH3	2.37	65.9	0.60
IR1	2.13	63.4	3.32
IR2	1.9	59.3	2.07
IR3	2.11	63.3	1.99
Tem1	2.17	60.3	0.66
Tem2	2.5	72.6	0.72
Tem3	2.05	56	0.67
Ucn1	3.52	93.3	0.73
Ucn2	3.1	81.4	0.54
Ucn3	3.34	81.5	0.51
UcnII1	2.73	82	0.75
UcnII2	2.02	53	0.95
UcnII3	2.85	71.2	0.43

B

	Present	Absent	Marginal
SH1	50.1	47.9	2.0
SH2	58.3	40.1	1.6
SH3	56.6	41.7	1.7
IR1	38.2	59.9	1.8
IR2	42.6	55.5	1.9
IR3	41.0	57.0	2.0
Tem1	57.1	41.4	1.5
Tem2	48.9	49.0	2.1
Tem3	58.6	39.8	1.6
Ucn1	47.7	50.3	2.0
Ucn2	52.4	45.8	1.8
Ucn3	53.2	45.2	1.6
UcnII1	47.6	50.5	1.9
UcnII2	51.2	46.8	1.9
UcnII3	54.6	43.6	1.8

C

	GAPDH	Beta-Actin
SH1	1.14	0.96
SH2	1.42	1.29
SH3	1.36	0.95
IR1	2.57	2.37
IR2	1.9	3.3
IR3	1.27	0.99
Tem1	1.53	1.46
Tem2	1.52	1.22
Tem3	2.04	1.92
Ucn1	1.19	1.19
Ucn2	1.3	1.23
Ucn3	1.3	1.43
UcnII1	1.31	1.19
UcnII2	1.21	1.44
UcnII3	1.33	1.15

Table 4.1. Quality control statistics for microarrays. Quality control statistics were obtained using Affymetrix GCOS software for all 15 microarrays used in the study. **(A)** RawQ score, background fluorescence and scaling factor (SF). **(B)** % calls for all probe sets. **(C)** 3'/5' scores for GAPDH and •-Actin probes

RNA target quality was examined in each array to ensure that any differential expression was not simply due to RNA degradation in some of the arrays. Since RNA becomes degraded in a

5'-3' manner, examination of the number of probes hybridising to the 3' end compared to the 5' end of the transcript gives an indicator of potential RNA degradation and 3'-5' ratios of greater than 3 are regarded to be indicative of poor target quality (Archer et al., 2006). The average 3'/5' ratios over the 15 arrays was 1.49 ± 0.39 for GAPDH and 1.47 ± 0.63 for β -Actin, allowing them all to be included in further analysis (Table 4.1c). Since rRNA does not contain polyadenylated 3' ends, the oligo(dT) primer should not produce any rRNA product unless the rRNA has been degraded, thus exposing polyadenylated sequences within the rRNA primary structure (Archer et al., 2006). Therefore, a positive signal for 5S rRNA represents another indicator of poor RNA quality, the 5S rRNA signal was absent from all 15 arrays.

Further analysis was carried out in Bioconductor using linear models statistics (Limma); two software packages, AffyImGui and OneChannelGui, were used for this analysis (Wettenhall et al., 2006, Sanges et al., 2007). Expression values were normalised using GCRMA (GC-Robust Multichip Average) (Qin et al., 2006) and box-plots of the raw and normalised data were generated showing the median and inter-quartile range (Fig 4.1a,b). The intensity varied within the groups with the I/R group being the lowest, however GCRMA normalisation was sufficient to normalise across all groups (Fig 4.1b). Similarly a perfect patch (PM) intensity distribution showed that the I/R group displayed less intensity (Fig 4.1c). This is also reflected in the fact that the scaling factor was higher in this group (Table 4.1a). While taking this into account, it is still clear that the GCRMA method gives a similar profile after normalisation (Fig 4.1b) and thus all arrays were included for further analysis.

To ensure that all the arrays had similar quality of hybridised RNA and similar second strand synthesis efficiencies, RNA degradation plots were produced in which the probe number on the x-axis is plotted against the mean intensity on the y-axis. It is important to note that since RNA degradation occurs in a 5' to 3' and an oligo d(T) primer is used during amplification, Affymetrix chips have a greater number of probes designed to the 3' end of transcripts and thus one would expect a positive slope in the degradation plot. Fig 4.1d shows that all the arrays produced a similar profile with the average slope being 2.36 ± 0.55 . Importantly the I/R group did not have significantly different slope values from the other groups which suggests that the reduced probe intensity seen in Fig 4.1c was not due to poor RNA target quality.

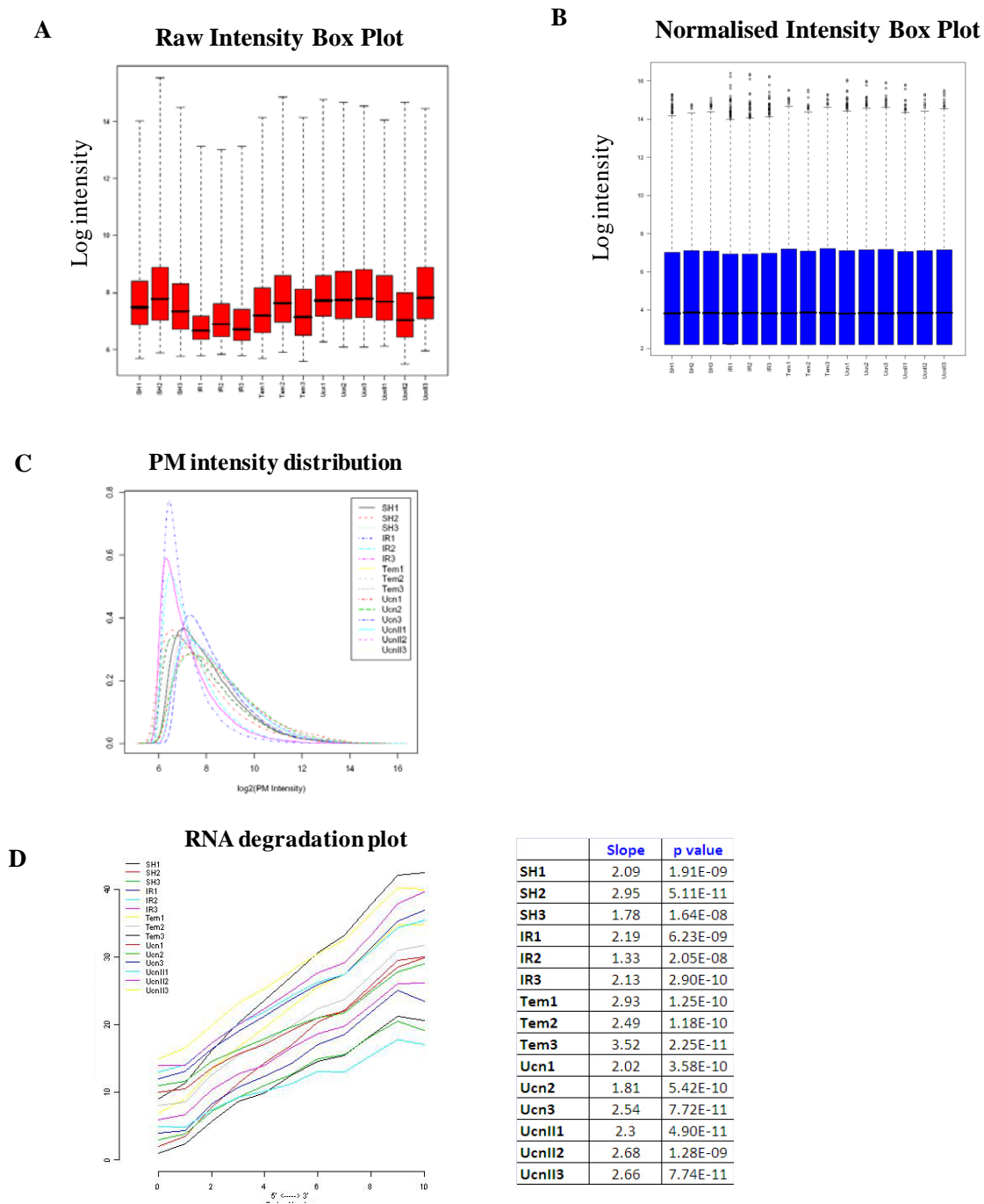


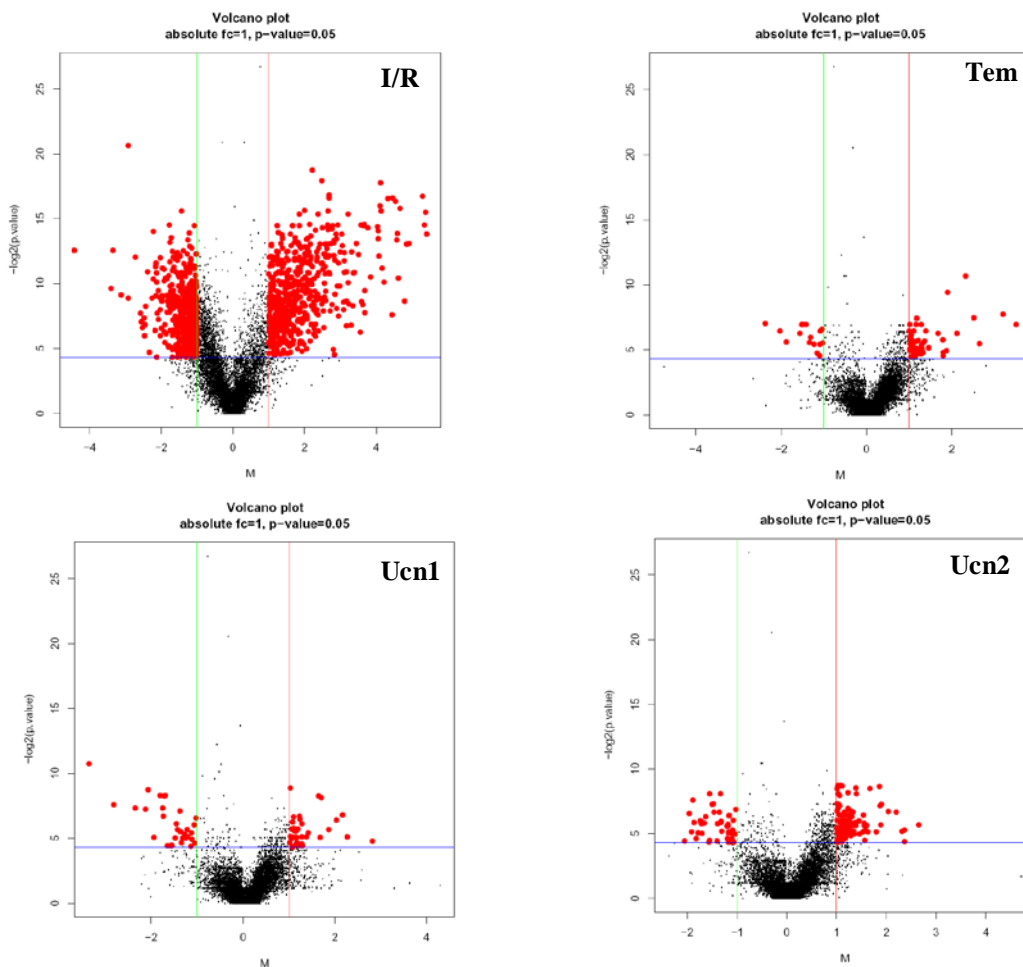
Fig 4.1. GCRMA normalisation, probe intensity and RNA degradation plots. (A) Intensity Box Plot of the fluorescence from the 15 microarrays. (B) Box Plot following GCRMA normalisation. (C) Perfect matched (PM) probe intensity distribution from the 15 microarrays. (D) RNA degradation plot with slopes and corresponding p values.

4.3 Parameters for Differential Expression

Since the 15 arrays passed all quality control checks, differential expression between the groups was examined. Genes were considered differentially expressed between two groups if there was a fold change greater than 2 with a t-test p value of <0.05. In addition, the false discovery rate (FDR) cut-off was set to 0.05 using the Benjamini and Hochberg equation (Benjamini and Hochberg, 1995). The Volcano plots in Fig 4.2a graphically highlight in red those genes fulfilling these selection criteria, log fold change is shown on the *x* axis and the p value is shown on the *y* axis. As well as assigning p values, Limma also assigns a log odds (LOD) score for each differentially expressed gene known as the B value, which is based on Bayes log posterior odds (Smyth, 2004). For each B value the % chance of differential expression is given as $[\exp(B)/(1 + \exp(B))] \times 100$ and a positive B value is a good indicator of differential expression (Lönstedt and Speed, 2002).

The breakdown of differential expression is indicated in Fig 4.2b. In total, I/R was found to upregulate 480 genes and downregulate 553 genes when compared to the sham group. Each of the drug treatment groups was compared to the I/R group in order to assess the effect of the drugs on I/R dependent gene expression. Tempol was found to upregulate 52 genes and down regulated 14 genes, the Ucn1 group had 38 upregulated genes and 27 downregulated genes and Ucn2 upregulated 104 genes and downregulated 37. The entire set of differentially regulated genes is shown in Appendix 3. Not all differential expression induced by the three drug treatments were reversal of expression changes during I/R. Fig 4.2c lists the numbers of genes changed which by tempol, Ucn1 and Ucn2 which were not affected by I/R.

A



B

	Probe Sets	Annotated Genes	Upregulated	Downregulated
IR Vs Sham	1109	798	480	553
Tem Vs IR	67	38	52	14
Ucn1 Vs IR	67	47	38	27
Ucn2 Vs IR	142	90	104	37

C

	Regulated by I/R	Not Regulated by I/R
Tem	31	16
Ucn1	27	22
Ucn2	65	39

Fig 4.2. Volcano plots and numbers of differentially expressed genes. (A) Volcano plots for I/R vs. Sham and tempol, Ucn1 and Ucn2 vs. I/R, fold change and p value cut-off lines are shown, differentially expressed genes are highlighted in red. (B) Numbers of probe sets and annotated genes upregulated or downregulated in each group. (C) Numbers of annotated genes changed by drug treatments which were also regulated by I/R.

4.4 Gene Ontology Analysis of Genes Differentially Expressed by I/R Injury

The top 20 most differentially expressed genes following I/R are shown in table 4.2 and include chaperones, transcription factors and immune regulators. Since there are over 1000 differentially expressed transcripts, functional classification was carried out to group the transcripts into distinct biological processes using gene ontology (GO) terms. This was done in two ways; firstly GO terms were assigned manually using literature searches to define the most common function for each gene. With this method, each gene is assigned to a single group and thus avoids the drawback of having several GO terms designated to a single gene. Using this approach it was clear that the majority of changes were either transcripts without an assigned identity or annotated genes of unknown function (Fig 4.3). The next major grouping comprised genes involved in metabolic regulation, which is not surprising since perturbed metabolic function is a hallmark of I/R injury (Lopaschuk et al., 2000). Along with the genes involved in metabolism, there are changes in expression of large numbers of genes involved in mitochondrial regulation and ion transport. Interestingly, the next two major categories were genes involved in transcriptional control and genes involved in the regulation of RNA and DNA. Thus it seems that the expression of almost 200 genes involved in the maintenance of DNA stability and transcription/translation of mRNA are altered and suggests that a large transcriptional regulatory network is activated by reperfusion injury. A cursory examination of transcriptional regulators showed that several transcription factors were among the most highly differentially expressed genes, for example all the components of heterodimeric transcription factor AP-1 were induced; Fos (40.8 ± 1.5 fold), Fos11 (30.2 ± 1.6 fold) c-Jun (4.8 ± 0.4 fold) and JunB (4.0 ± 0.7 fold), other highly differentially regulated transcription factors include Atf3 (23.9 ± 2.8 fold), Klf15 (-21.6 ± 1.9 fold), Erg1 (17.2 ± 1.3 fold), Erg2 (16.6 ± 0.6 fold) and Klf6 (9.3 ± 0.6 fold).

Table 4.2. The 20 genes with the highest rate of differential expression between the sham and I/R groups.

Symbol	Gene Title	FC	P value	B value
Hspa1a/Hspa1b	heat shock 70kD protein 1A/1B (mapped)	41.5	2.2E-05	9.6
Fos	FBJ osteosarcoma oncogene	40.8	4.3E-05	8.7
Hspa1b	heat shock 70kD protein 1B (mapped)	39.3	9.1E-06	11.2
Fosl1	fos-like antigen 1	30.2	1.1E-04	6.7
Npy	neuropeptide Y	28.9	1.2E-04	6.6
Cxcl2	chemokine (C-X-C motif) ligand 2	27.7	2.5E-03	1.6
Plaur	plasminogen activator, urokinase receptor	25.5	1.7E-05	10.1
Il1r2	interleukin 1 receptor, type II	24.7	7.3E-04	3.6
Atf3	activating transcription factor 3	23.9	9.6E-05	7.0
Nr4a3	nuclear receptor subfamily 4, group A, member 3	23.2	1.2E-05	10.6
Klf15	Kruppel-like factor 15	-21.6	1.6E-04	6.1
Dnajb1_predicted	DnaJ (Hsp40) homolog, subfamily B, member 1	20.9	4.4E-05	8.7
Srxn1	sulfiredoxin 1 homolog (S. cerevisiae)	20.2	1.0E-05	10.8
Pf4	platelet factor 4	18.6	9.1E-04	3.3
Pglyrp1	peptidoglycan recognition protein 1	17.9	4.3E-04	4.4
Sphk1	sphingosine kinase 1	17.3	4.5E-06	12.0
Egr1	early growth response 1	17.2	1.6E-05	10.2
Homer1	homer homolog 1 (Drosophila)	16.9	3.9E-03	1.0
Serpine1	serine (or cysteine) peptidase inhibitor, member 1	16.9	2.3E-04	5.5
Egr2	early growth response 2	16.6	9.1E-05	7.1

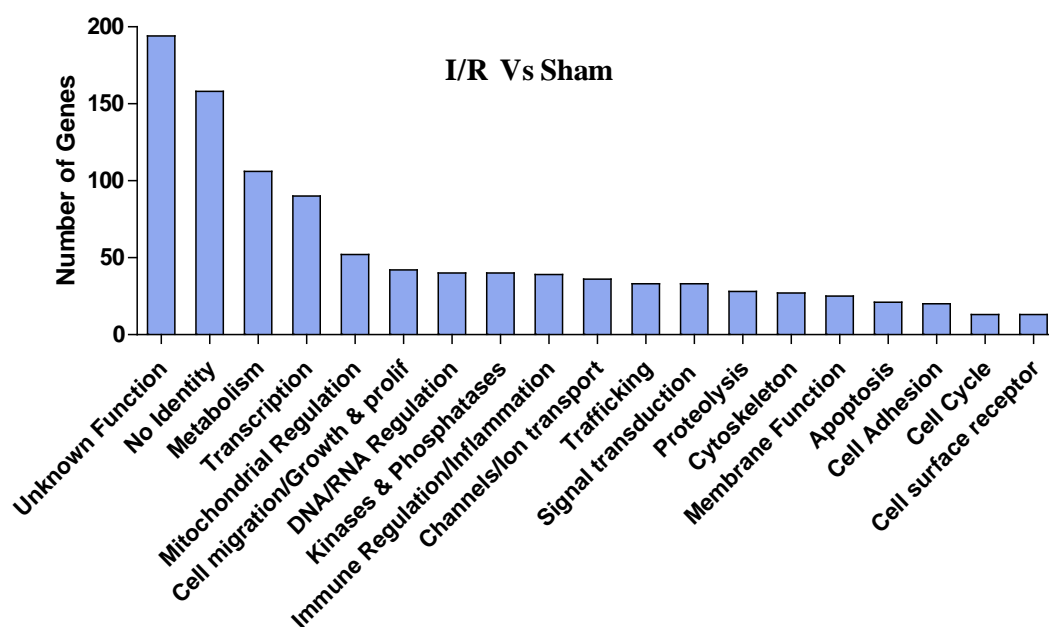


Fig 4.3. Manual Gene Ontology analysis of genes differentially expressed by I/R compared to sham. GO terms were assigned to the 1109 probe sets based on manual searching of the literature to define the most common function of each gene.

Since manual designation of GO terms may be subject to bias, a second alternative method was used. The list of differentially regulated genes was functionally annotated using the Ingenuity package. Genes were firstly assigned into groups based on significant p values using a right tailed Fischer Exact Test. This takes into account the number of genes associated with a pathway in the input list compared to the total number of genes associated with that pathway in the Ingenuity database. It is therefore a measure of functional groups which are over represented in the data set. This analysis revealed that the most significant functional groups were cell death, growth and proliferation and similarly to the manually assigned list, metabolism and DNA regulation were highly overrepresented (Fig 4.4a).

The Ingenuity package also provides delineation of genes into separate pathways and Fig 4.4b shows the most significant pathways from the I/R data set. The left y-axis represents the proportion of genes in the data set divided by the total number of genes known to be involved in a particular pathway; the right y-axis denotes the negative log of the p value. Surprisingly, the highest scoring pathway was ketone body metabolism with 20% of genes involved in this pathway differentially expressed during I/R, all of the genes in this list were downregulated. Ketone bodies are known to provide protection from oxidative stress, possibly by acting as anti-oxidants (Hacles., 2008) and administration of the ketone body acetoacetate was shown to increase cardiac contractile performance and restore GSH/GSSG levels in the stunned myocardium (Squires., 2003, Mallet., 2003). Downregulation of genes involved in ketone body metabolism may therefore be damaging to the heart. Unsurprisingly 15% of genes involved in cardiovascular hypoxic signaling were differentially regulated. Cytokine responses were also prevalent, including IL-6, IL-10, TGF- β and acute phase signaling, highlighting the important role of inflammation in I/R injury.

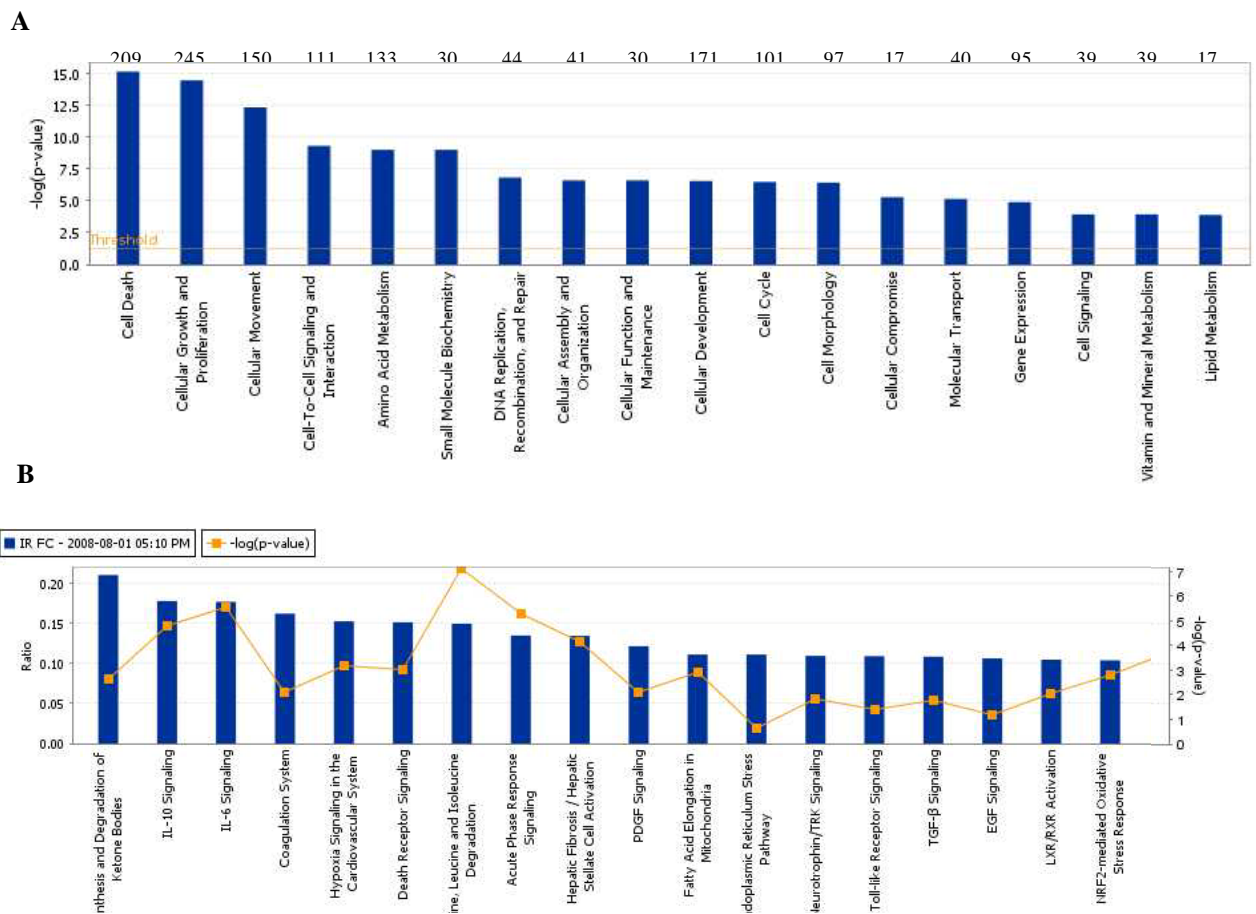


Fig 4.4. Ingenuity analysis of genes differentially expressed by I/R. (A) Functional annotation of 1109 probe sets identified as being differentially expressed by I/R. Groups are ranked according to p value significance, the $p < 0.05$ threshold is shown, on top are the number of genes in each grouping. (B) Pathway analysis; pathways are ranked by ratio (x axis) which represents the number of molecules in a given pathway that meet cutoff criteria (fold change > 2 , $p < 0.05$) divided by total number of molecules that make up that pathway. The orange line denotes the p value as given on the y axis.

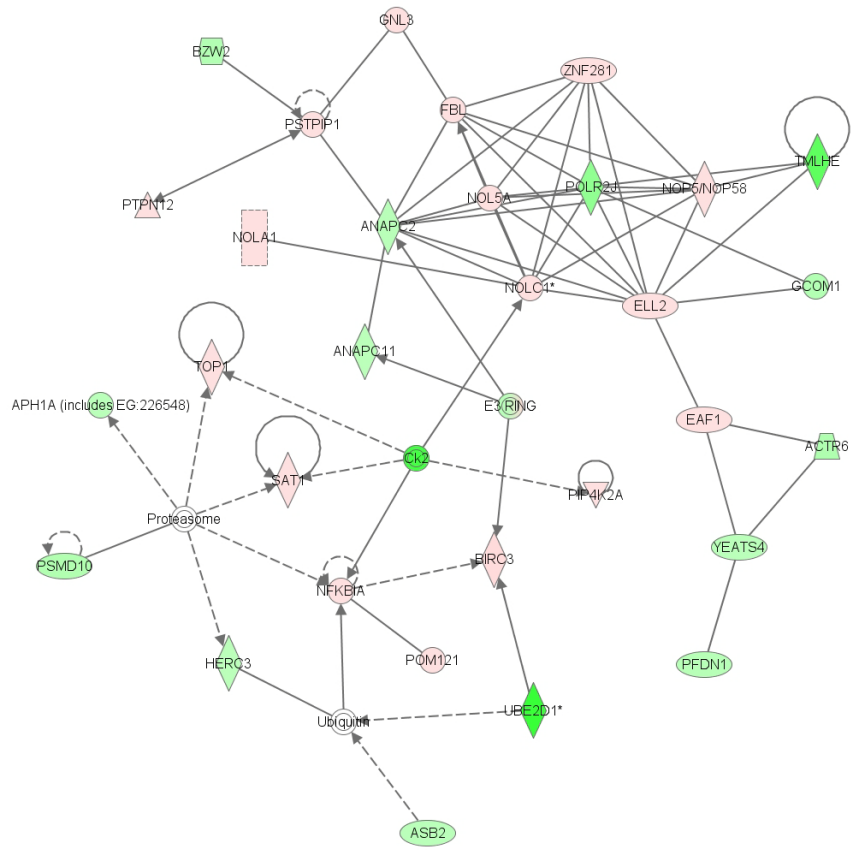
Next, network analysis was carried out using the Ingenuity package, this uses a right-tailed Fisher's Exact Test and takes into account the number of molecules in the input list (which have a fold change > 2 and $p < 0.05$) and the total number of molecules eligible to be included in the network. Upregulated genes are colored red and downregulated genes are colored green. Network interactions are generated from published associations and include protein binding and transcriptional regulation between two molecules. There were 5 networks identified, all of which had a p value of less than 10^{-36} . The first network (Fig 4.5a) is split into two main nodes consisting of Casein Kinase 2 with ubiquitin/proteasome related genes and a transcriptional network centered around RNA Polymerase II, subunit J (PolR2J).

The second network (Fig 4.5b) is a transcriptional regulatory network with the transcription factor Myc (c-Myc) at its centre which was upregulated 6.5 ± 0.1 fold by I/R. c-Myc is a highly pleiotropic transcriptional regulator and exerts its effects through recruitment of histone acetylase, basal transcription machinery, DNA methyltransferases and chromatin modifiers (Dang et al., 2006). Indeed c-Myc is thought to regulate as much as 15% of the genome, predominantly genes involved in cell cycle regulation, ribosome biogenesis, metabolism and cell adhesion (Dang et al., 2006). Therefore the c-Myc regulatory network depicted in Fig 4.5b may represent only a fraction of the total number of genes which are differentially regulated during I/R as a result of increased c-Myc expression.

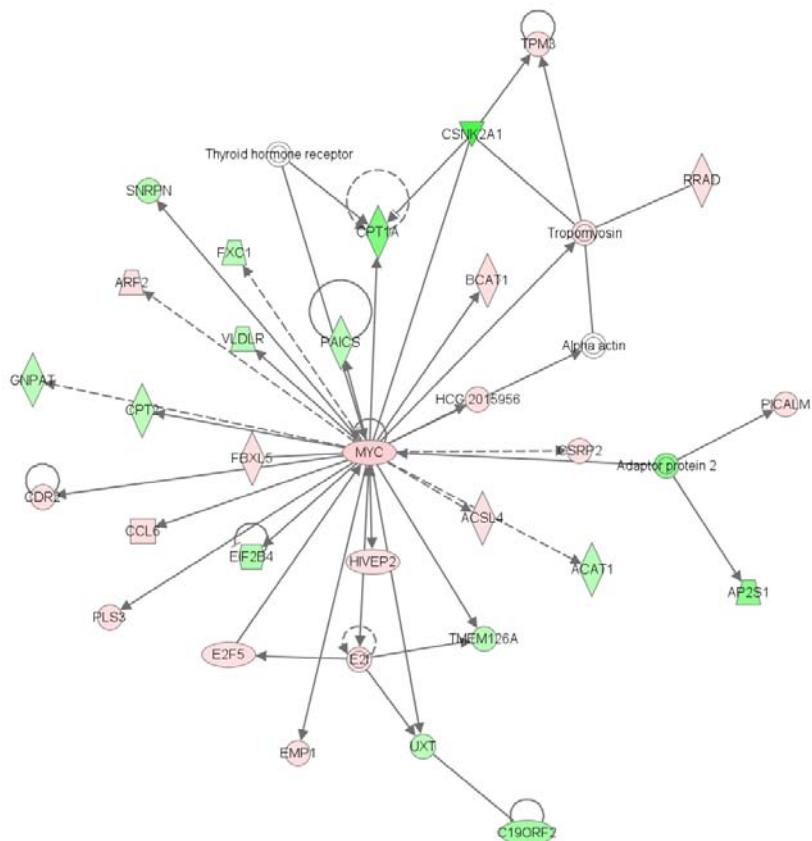
The third network involves AP-1 regulation (Fig 4.5c); all the proteins which constitute the AP-1 complex are present (Fos, FosL1, cJun and JunB) and include other upregulated transcription factors such as Atf3, Erg1, and Ets2. The fourth network comprises several heat shock proteins including, HSP70 (HSPA1), HSP90 and HSP27 (HSPB1) as well as other chaperones including several members of the DNAJ family of chaperones which modulate HSP70 function (Fig 4.5d). HSPs and chaperones have well documented roles in protection from I/R injury (Robison et al., 1995, Li G et al., 2008).

The final network found was composed of the members of the IL-1 family and several CC and CXC chemokines which are induced by IL-1 (Fig 4.5e). An IL-1• inflammatory cascade has recently been observed in a model of renal I/R injury and indeed blockade of IL-1• secretion has been proposed as a therapeutic strategy in myocardial I/R injury (Furuichi et al., 2006, Wanderer, 2008)

A



B



E

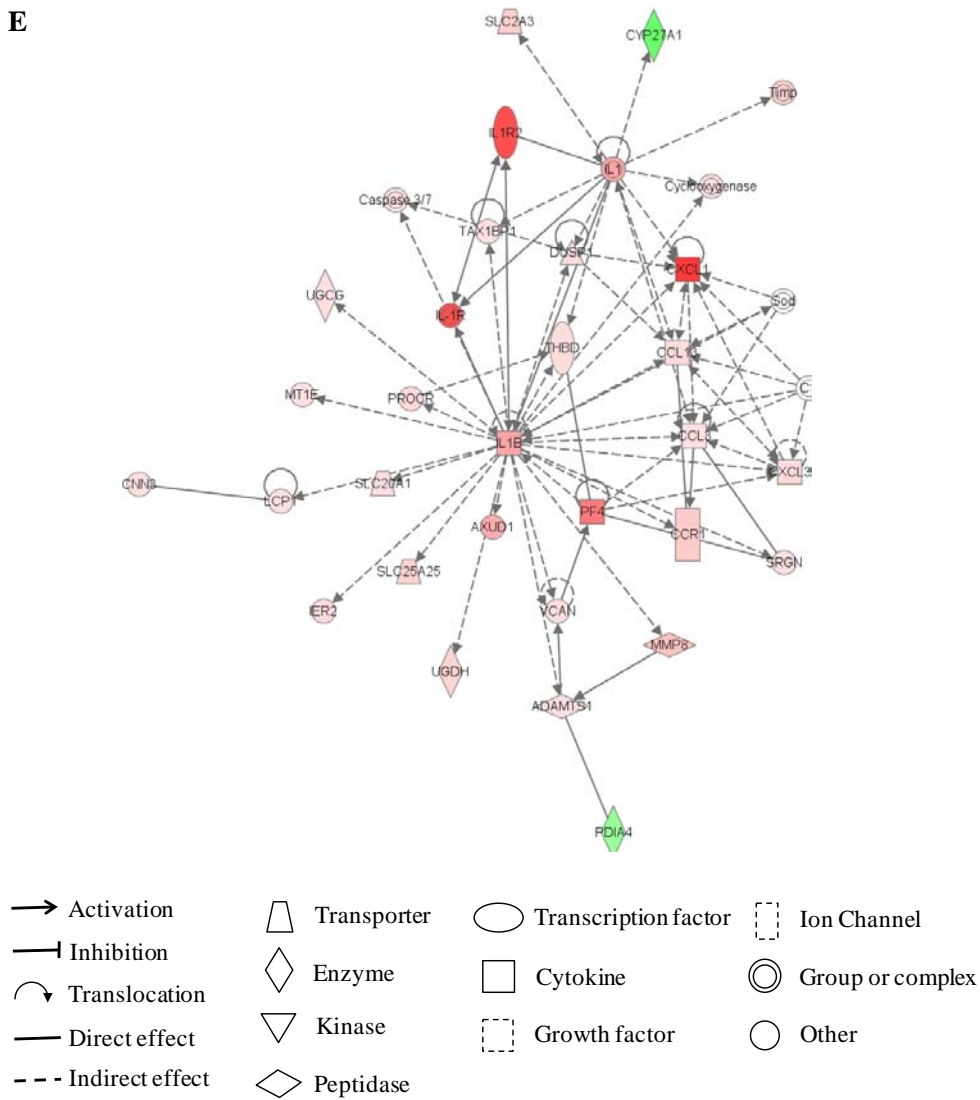


Fig 4.5. Ingenuity network analysis of genes differentially expressed during I/R. Five significant regulatory networks were identified from the 1109 probe sets identified as being differentially expressed by I/R (A-E). Interactions are defined from the curated Ingenuity database and comprise referenced published protein-protein interactions and transcriptional regulation. Upregulated genes are shown in red and downregulated genes are shown in green.

4.5 Differential Expression mediated by Tempol Infusion During I/R

Gene ontology analysis of the tempol group, i.e. differential expression between tempol and saline infusion during I/R, demonstrated that like the I/R group, the majority of differentially expressed genes in the tempol group were either unidentified transcripts or genes with no known function (Fig 4.6). Similarly to the I/R dataset, genes involved in transcription and translation were the most prominent grouping. The list of the 20 most differentially expressed genes is shown in Table 4.3. Of the most highly expressed genes, several are involved in cytoskeletal control and myocardial contraction. For example, radixin (2.74 ± 0.1 fold increase) and vinculin ($59.6 \pm 1.6\%$ decrease) both anchor actin to the cell membrane (Humphries et. al, 2007), tropomyosin ($60.2 \pm 0.1\%$ decrease) forms part of the thin filament of the sarcomere and controls actin-myosin interaction and ATP2a2 (2.5 ± 0.2 fold increase) and the ryanodine receptor (3.5 ± 0.4 fold increase) control myocardial contraction by regulating the release of Ca^{2+} from the sarcoplasmic reticulum. This suggests that restoration of calcium homeostasis and myocyte contractility may be central to tempol mediated cardioprotection. Ingenuity functional group analysis is shown in Fig 4.7a and placed genes in several distinct groups including cell signalling, molecular transport and cell death. Ingenuity pathway analysis was not informative due to the low numbers of genes in each pathway. One significant network was found and is shown in Fig 4.7b. This network centres around two main nodes, the sarcomeric proteins Ryr/ATP2a2 and the apoptosis regulating transcription factor p53. Although p53 itself did not pass the significance test, p53 expression was found to be reduced $37.8 \pm 6.8\%$ by tempol with a p value of 0.06, suggesting the possibility that p53 regulation may play a role in tempol mediated cardioprotection. This also highlights the usefulness of the network analysis approach in uncovering potential regulatory interactions.

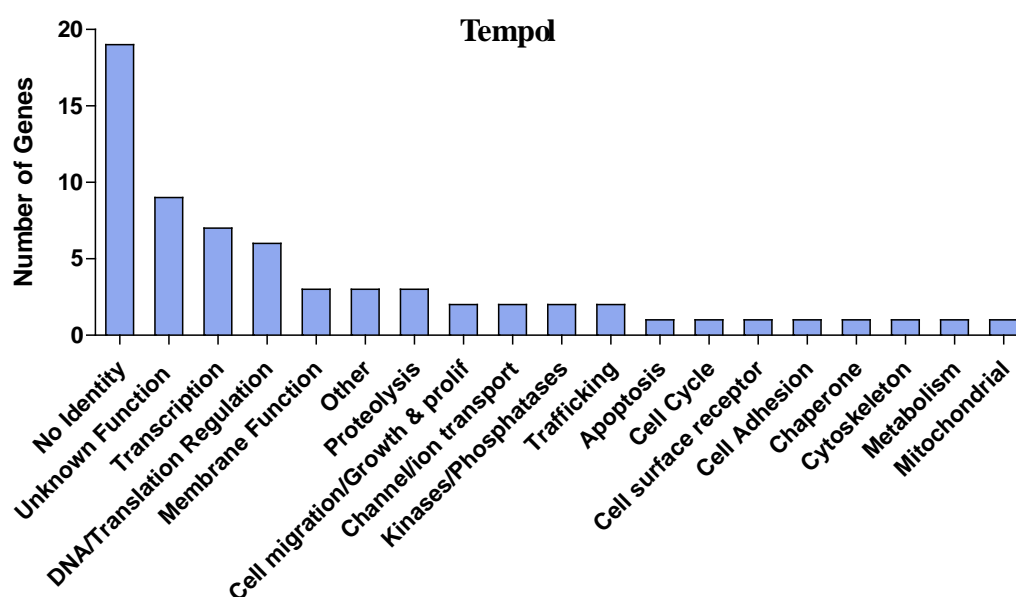


Fig 4.6. Manual GO analysis differentially expressed genes between tempd and I/R. GO terms were assigned to the 67 probe sets based on manual searching of the literature to define the most common function of each gene.

Table 4.3. Top 20 differentially expressed genes between tempd and I/R

Symbol	Gene Title	FC	Pvalue	B value
Nfe2l1_predicted	nuclear factor, erythroid derived 2,-like 1 (predicted)	6.2	0.02	1.1
Rpl7	Ribosomal protein L7	-5.2	0.01	4.3
Gbas	glioblastoma amplified sequence	4.3	0.01	2.3
Dut	deoxyuridine triphosphatase	3.7	0.00	6.3
Ryr2	ryanodine receptor 2, cardiac	3.5	0.04	0.2
Tm9sf1	transmembrane 9 superfamily member 1	3.5	0.02	1.7
Orc4	origin recognition complex, subunit 4	3.2	0.01	2.4
Rdx	Radixin	2.7	0.03	0.8
Qk /// Qki	quaking homolog, KH domain RNA binding / quaking	2.6	0.01	2.7
Tpm3	tropomyosin 3, gamma	-2.5	0.02	1.3
Atp2a2	ATPase, Ca++ transporting, cardiac muscle, slow twitch 2	2.5	0.04	0.2
Vcl_predicted	Vinculin (predicted)	-2.5	0.02	1.9
Abcc1	ATP-binding cassette, sub-family C (CFTR/MRP), member 1	2.5	0.03	0.7
Hspa4	heat shock protein 4	2.4	0.02	1.0
Pja2	praja 2, RING-H2 motif containing	2.4	0.01	3.5
Ppp3ca	protein phosphatase 3, catalytic subunit, alpha isoform	2.4	0.03	0.8
Pdia4	protein disulfide isomerase associated 4	2.4	0.04	0.1
Tmem98	transmembrane protein 98	2.4	0.04	0.1
Gramd3	GRAM domain containing 3	2.3	0.04	0.2
Hmgb1	high mobility group box 1	2.3	0.02	1.6

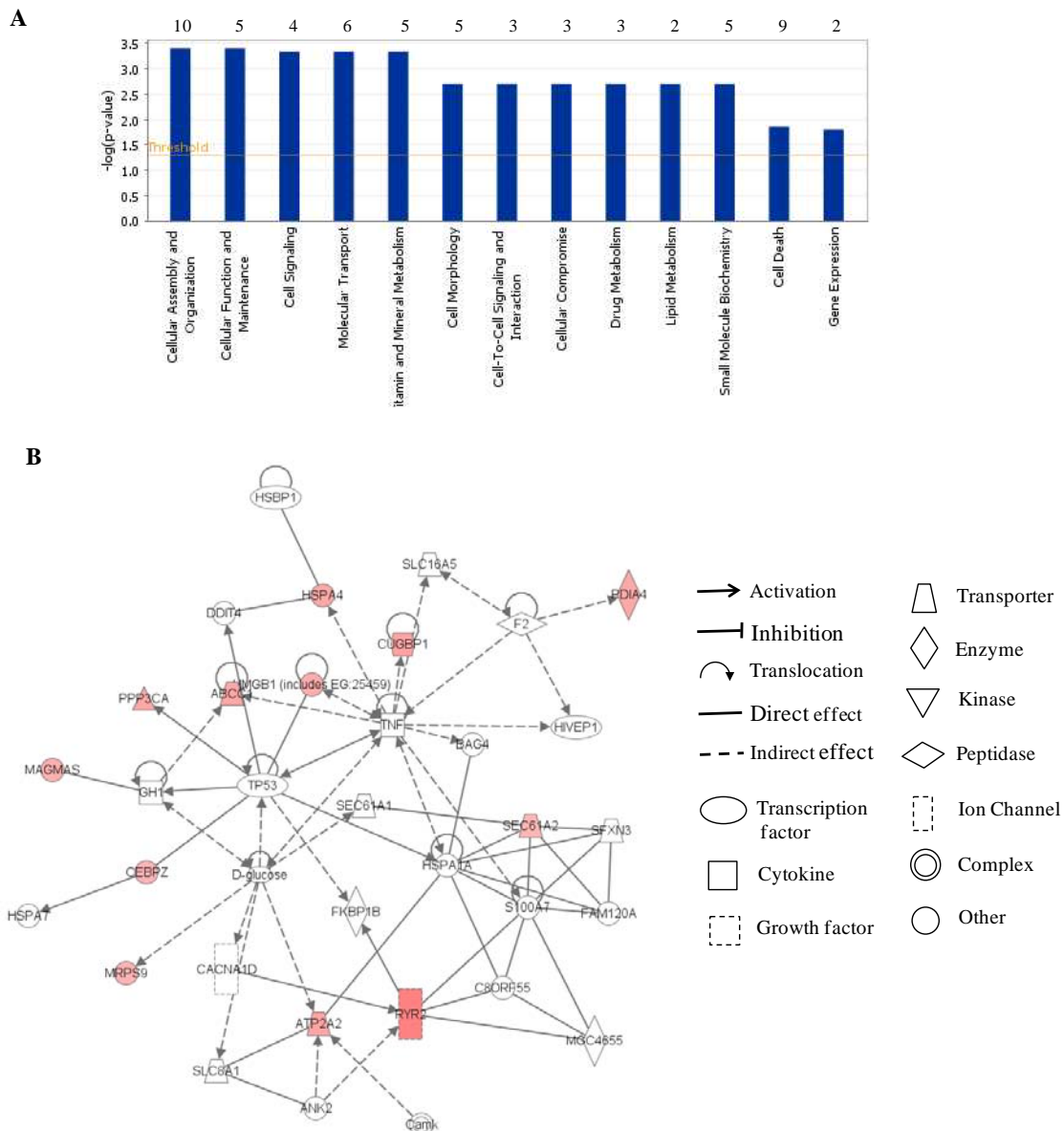


Fig 4.7. Ingenuity analysis of differential expression between tempol and I/R. (A) Functional analysis of 67 probe sets identified as being differentially regulated by tempol. Groups are ranked according to p value significance, the $p < 0.05$ threshold is shown, on top are the number of genes in each grouping. (B) Network analysis, a single network was identified from the 67 probe sets. Interactions are defined from the curated Ingenuity database and comprise referenced published protein-protein interactions and transcriptional regulation. Upregulated genes are shown in red and downregulated genes are shown in green.

4.6 Differential Expression mediated by Ucn1 and Ucn2 Infusion During I/R

Ucn2 infusion during I/R injury resulted in twice as many (142) significantly differentially expressed genes as Ucn1 (67). This may not be biologically relevant however since an examination of the number of genes passing the 2-fold cut-off without applying a significant p value filter revealed that there were 234 genes differentially expressed in the Ucn1 group and 241 in the Ucn2. Therefore the lower number of significantly differentially expressed genes in the Ucn1 group is due to greater heterogeneity between the three urocortin microarrays resulting in fewer genes passing the significance filter. The top 20 most differentially expressed genes between Ucn1, Ucn2 and saline treatment during I/R is shown in Table 4.4. Of the 67 and 142 genes differentially expressed by Ucn1 and Ucn2 respectively, 30 of them were common to both. This suggests that although both hormones signal through CRF receptors, they have distinct effects on gene expression patterns. Manual gene ontology analysis showed that transcription, translation and proteolysis were prominent subgroups in both the Ucn1 and Ucn2 dataset (Fig 4.8). Ingenuity functional group analysis of both hormones showed that all the groups assigned to Ucn2 were present in Ucn1, with genes involved in cell death or cell growth being the largest set (Fig 4.9). Therefore, although Ucn1 and Ucn2 regulate distinct genes, gene ontology analysis suggests that their transcriptional programmes may exert similar biological effects.

Network analysis identified one significant network for each hormone (Fig 4.10). Most of the genes shown in the Ucn1 network are on the periphery of the network, the central molecules are p53, CREB, IFN- γ and glucose. There was no signal for CREB1 or IFN- γ found on the microarray so differential expression could not be calculated but qPCR analysis showed that Ucn1 did indeed lower the expression of IFN- γ (Fig 4.13b). In addition, Ucn1 has previously been shown to regulate glucose utilization (Keperman et al., 2008) and p53 and CREB might well be regulated at the level of phosphorylation. The Ucn2 network is centred on the kinases ERK, JNK and Akt, although Ucn2 has no effect on the expression of these kinases, Ucn2 has previously been shown to phosphorylate ERK and Akt in cardiac myocytes and phosphorylate JNK in intestinal cells (Chanalaris, 2003, 2005). This network suggests that likewise, Ucn2 may alter gene expression through MAPK or Akt pathways in I/R injury.

Ucn1

Symbol	Gene Title	FC	P value	B value
Rpl7	Ribosomal protein L7	-10.3	0.00	7.4
Slc34a1	solute carrier family 34 (sodium phosphate), member 1	-7.0	0.01	4.2
Birc4	baculoviral IAP repeat-containing 4	4.8	0.03	1.0
Cap2	CAP, adenylate cyclase-associated protein, 2 (yeast)	4.6	0.04	0.2
Clu	clusterin	-4.4	0.01	3.7
Ccdc58_predicted	coiled-coil domain containing 58 (predicted)	-4.2	0.00	5.6
Nrarp	Notch-regulated ankyrin repeat protein	4.1	0.01	2.8
Nfe2l1_predicted	nuclear factor, erythroid derived 2,-like 1 (predicted)	4.0	0.05	0.0
Lsm12	LSM12 homolog (<i>S. cerevisiae</i>)	3.6	0.02	1.8
Gnb1	guanine nucleotide binding protein, beta 1	-3.3	0.00	5.0
Dut	deoxyuridine triphosphatase	3.1	0.00	5.0
Napsa	napsin A aspartic peptidase	-2.9	0.05	-0.2
Igf1	insulin-like growth factor 1	-2.8	0.03	0.7
Arf2	ADP-ribosylation factor 2	2.7	0.02	1.3
Tmem98	transmembrane protein 98	2.6	0.03	1.0
Rac2	RAS-related C3 botulinum substrate 2	-2.6	0.02	1.4
Kcnj8	potassium inwardly-rectifying channel, subfamily J8	-2.5	0.04	0.2
Cdh2	cadherin 2	2.4	0.05	-0.2
Mccc2	methylcrotonoyl-Coenzyme A carboxylase 2 (beta)	2.4	0.01	2.4
Ppp6c	protein phosphatase 6, catalytic subunit	2.4	0.04	0.0

Ucn1

Symbol	Gene Title	FC	P value	B value
Ssr3	signal sequence receptor, gamma	6.3	0.02	1.0
Cap2	CAP, adenylate cyclase-associated protein, 2 (yeast)	5.2	0.05	-1.0
Nfe2l1_predicted	nuclear factor, erythroid derived 2,-like 1 (predicted)	5.2	0.03	0.3
Gbas	glioblastoma amplified sequence	4.6	0.01	2.7
C1qr1	complement component 1, q subcomponent, receptor 1	-4.1	0.05	-0.9
Rabgap1	RAB GTPase activating protein 1	-3.8	0.03	0.1
Orc4	origin recognition complex, subunit 4	3.7	0.01	3.5
Pdia4	protein disulfide isomerase associated 4	3.7	0.01	3.3
Ralgds	ral guanine nucleotide dissociation stimulator	-3.5	0.04	-0.6
Mt1a	metallothionein 1a	-3.4	0.03	-0.1
Rpl7	Ribosomal protein L7	-3.3	0.02	1.5
Limd1_predicted	LIM domains containing 1 (predicted)	-3.3	0.02	1.2
Timp3	tissue inhibitor of metalloproteinase 3	-3.3	0.03	-0.2
Dut	deoxyuridine triphosphatase	3.2	0.00	5.2
Srp72	signal recognition particle 72	-3.2	0.02	1.3
Them4	thioesterase superfamily member 4	3.1	0.03	0.0
Tm9sf1	transmembrane 9 superfamily member 1	3.1	0.02	0.8
Eif2c2	eukaryotic translation initiation factor 2C, 2	3.0	0.05	-0.9
Ap2s1	adaptor-related protein complex 2, sigma 1 subunit	3.0	0.03	0.2
Sparc	secreted acidic cysteine rich glycoprotein	-2.9	0.05	-1.0

Table 4.4. Top 20 differentially expressed genes between Ucn1, Ucn2 and I/R.

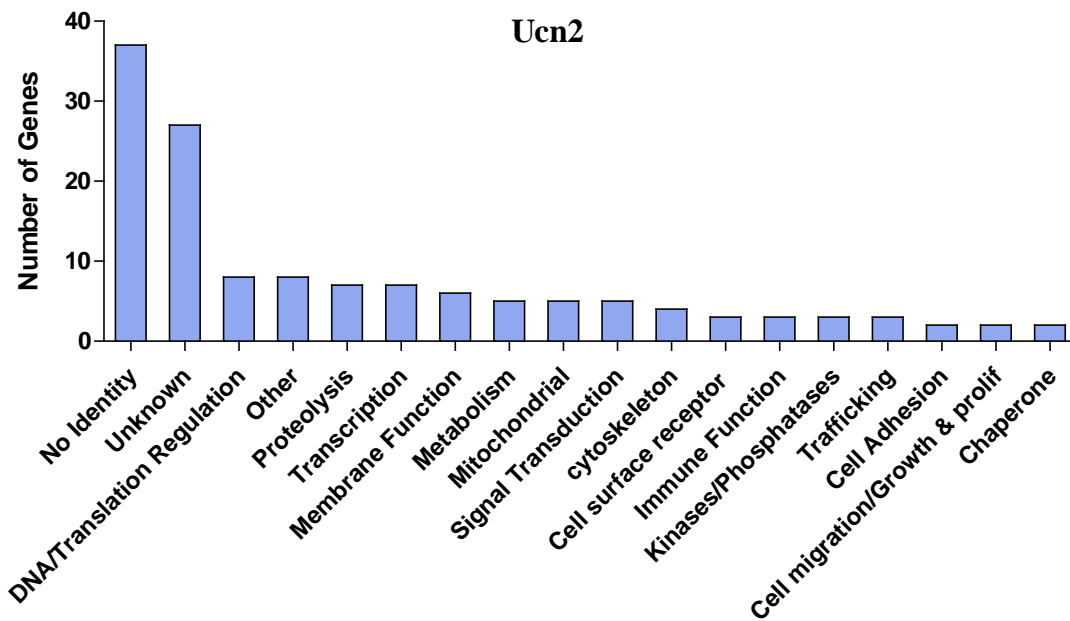
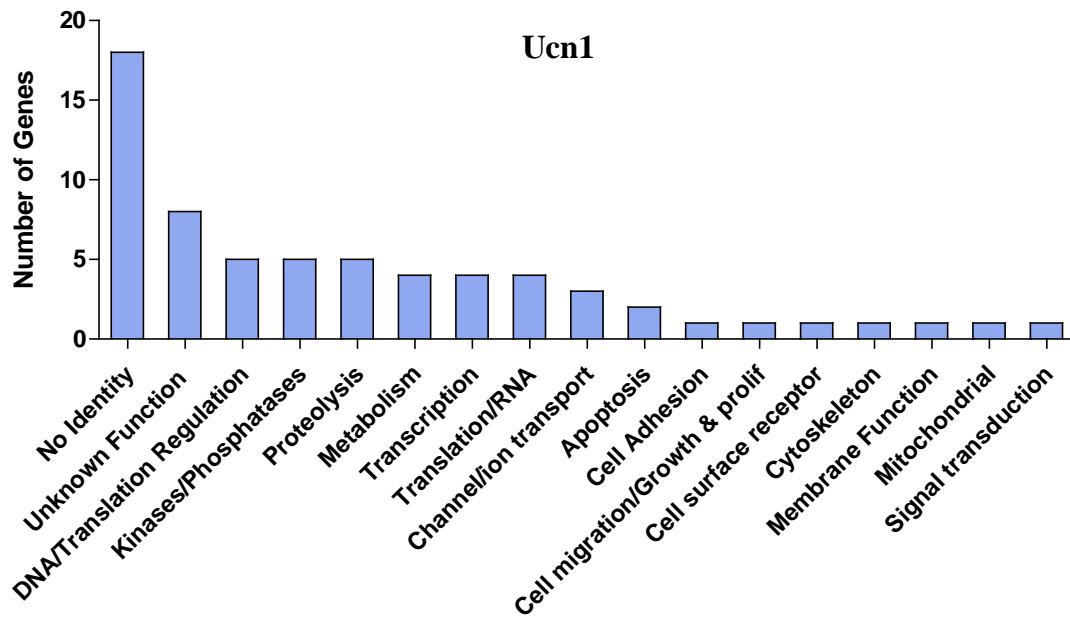


Fig 4.8. Manual GO analysis of differential expression by Ucn1 and Ucn2 compared to I/R. GO terms were assigned to the 67 probe sets for Ucn1 and 142 probe sets for Ucn2 and based on manual searching of the literature to define the most common function of each gene.

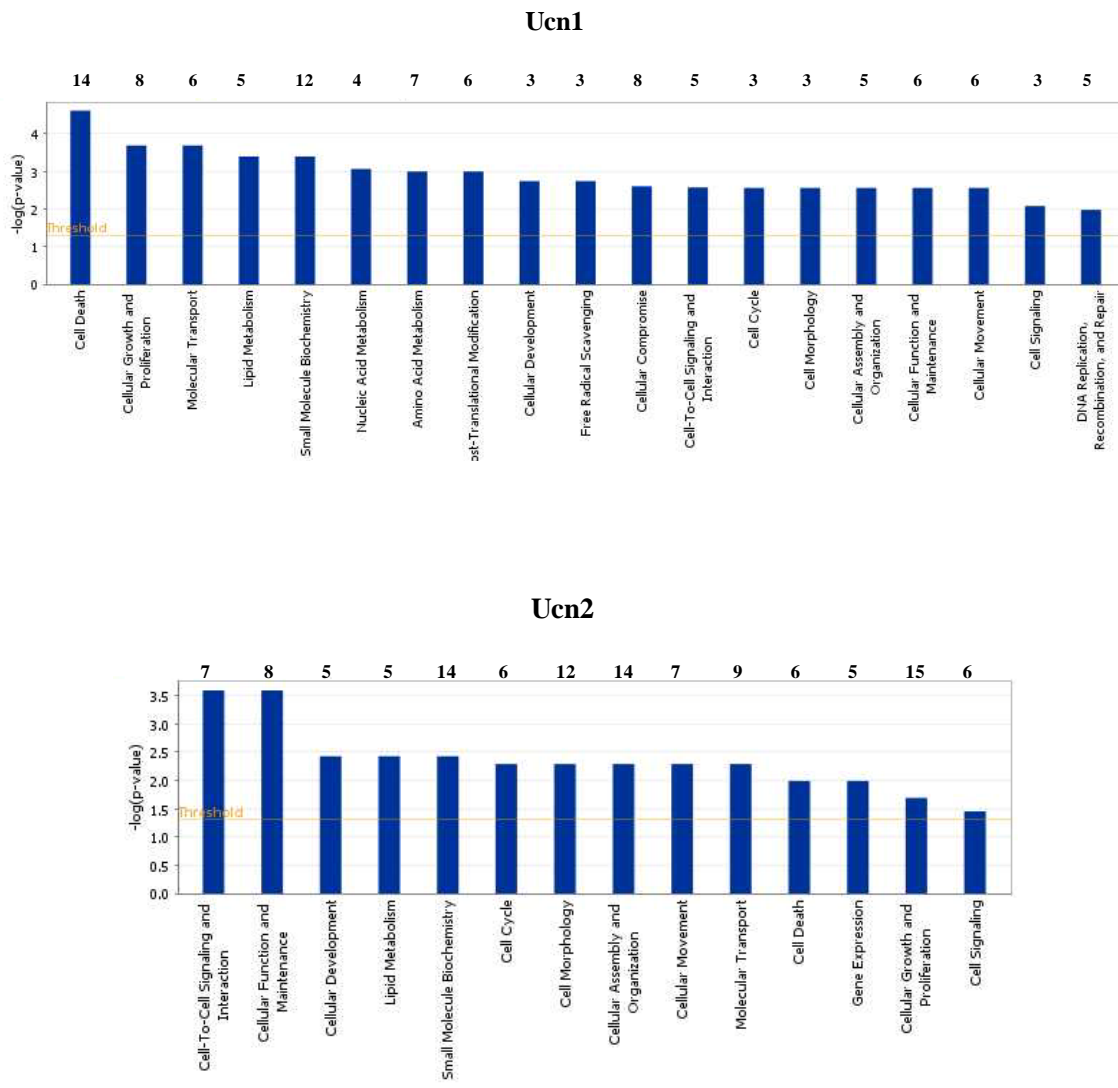
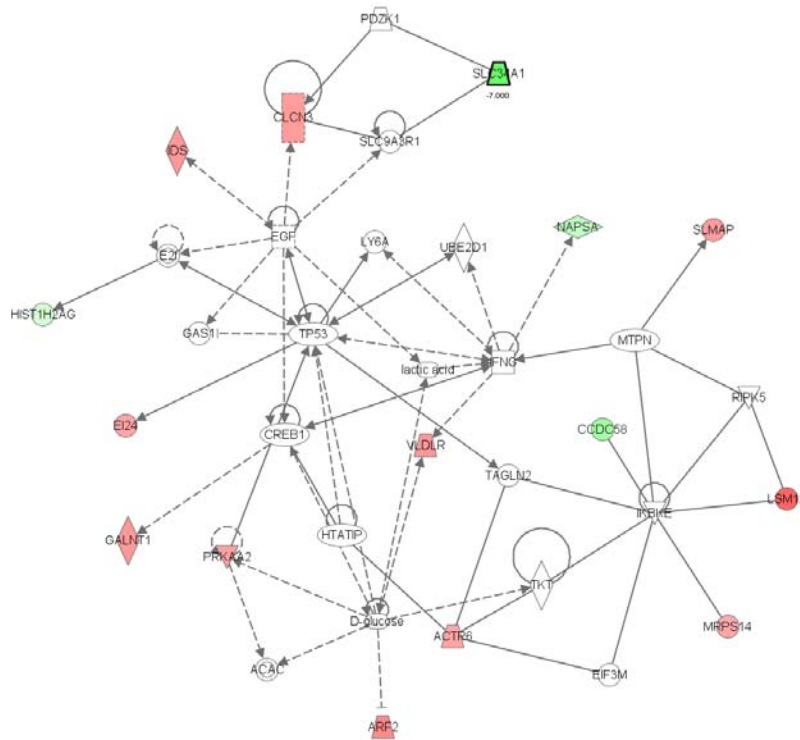


Fig 4.9. Ingenuity analysis of differential expression by induced by Ucn1 and Ucn2. Functional annotation of the 67 probe sets in the Ucn1 group and 142 probe sets in the Ucn2 group identified as being differentially expressed when compared to saline infusion during I/R. Groups are ranked according to p value significance, the $p < 0.05$ threshold is shown, on top are the number of genes in each grouping.

Ucn1



Ucn2

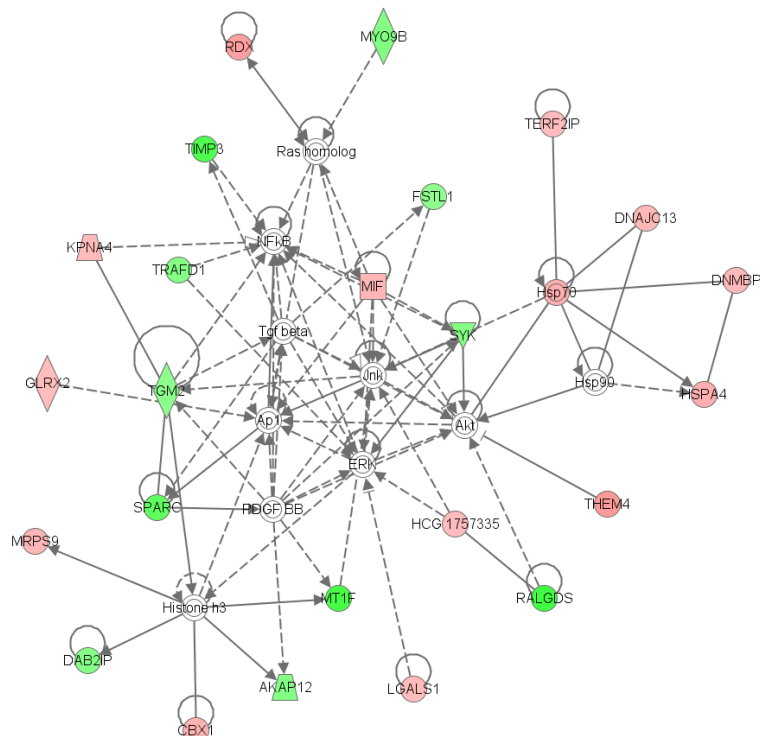


Fig 4.10 Network analysis of the Ucn1 and Ucn2 groups. A single network was identified from the 67 probe sets in the Ucn1 group and the 142 probe sets from the Ucn2 group. Interactions are defined from the curated Ingenuity database and comprise referenced published protein-protein interactions and transcriptional regulation. Upregulated genes are shown in red and downregulated genes are shown in green.

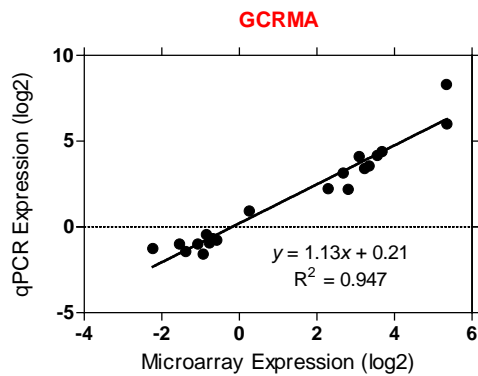
4.7 Validation of Microarray Data by qPCR

Before making any general inferences on regulation of specific genes, qPCR analysis was carried out in order to confirm some of the gene changes seen on the microarray. Fig 4.11a shows a list of 23 genes which were tested for differential expression between sham and I/R. With this data at hand, the effect of three common algorithms were examined to ensure that GCRMA was indeed the best method of normalization to choose for this dataset. Both GCRMA and RMA normalizations were carried out in Bioconductor and MAS5.0 normalization was carried out using Genespring 7.3. The log of the microarray fold change between sham and I/R was plotted on the *x*-axis versus the log qPCR fold change on the *y*-axis. Nonlinear regression analysis was used to test the correlation between the microarray data and qPCR levels (Fig 4.11b,c,d). Taking all 23 genes into account, the r value was highest for GCRMA at 0.947, followed by RMA at 0.943 and MAS 5.0 at 0.857. With a few exceptions (Bcl-2, XIAP), the qPCR data verifies the microarray results and thus some general conclusions can be drawn from the dataset as a whole. The following sections therefore will deal with regulation of specific genes and what effects they may have on I/R injury. It must be noted here that due to sample problems, it was not possible to confirm the gene expression changes seen with Ucn2 by qPCR.

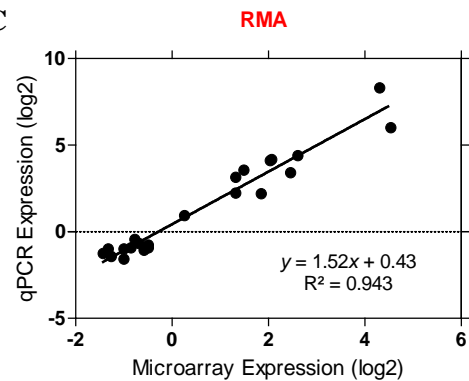
A

	MAS5.0	RMA	GCRMA	qPCR
HSP70	16.6	19.8	40.4	316.0
c-Fos	13.4	23.3	40.8	64.1
IL-1B	5.1	6.1	12.8	21.1
iNos	15.9	4.2	11.8	18.0
MMP8	4.6	4.1	8.5	17.1
MMP9	14.7	2.8	10.2	11.7
IL-6	4.1	5.5	9.4	10.6
Socs3	-	2.5	6.4	8.8
DUSP1	3.7	2.5	4.9	4.7
IL-17 R	3.5	3.6	7.0	4.6
Bcl-2	-	-	-	3.3
Icos	2.2	1.2	1.2	1.9
Map4k2	-3.0	-1.7	-1.8	-1.4
Tim23	-2.2	-1.6	-1.6	-1.6
Scn5a	-2.3	-1.4	-1.5	-1.7
Tom20	-	-1.4	-	-1.9
Timm8a	-2.3	-1.8	-1.7	-1.9
BNip3	-3.1	-2.0	-2.1	-2.0
Timm44	-9.6	-2.5	-2.9	-2.0
Xiap	-	-1.5	-	-2.1
Dut	-4.2	-2.7	-4.7	-2.4
Timm13	-3.3	-2.4	-2.6	-2.7
Timm8b	-2.5	-2.0	-1.9	-3.0

B



C



D

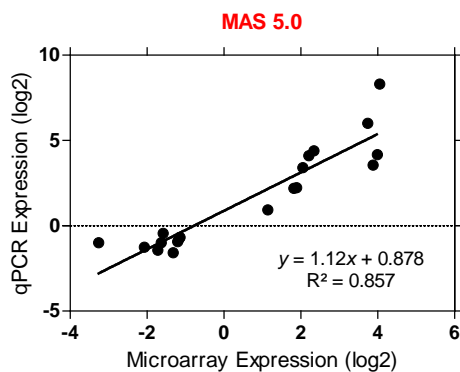


Fig 4.11. Fold changes obtained by three separate normalisation methods compared with qPCR. (A) Fold changes between I/R and sham were obtained using MAS5.0 in Genespring and RMA or GCRMA in Bioconductor and compared against qPCR data. (B, C and D) Linear regression analysis was carried out between qPCR data and microarray data and the correlation co-efficient was calculated.

4.8 Activation of a STAT3 Transcriptional Programme Following I/R Injury

Ingenuity pathway analysis identified the IL-6 and IL-10 pathways as being highly represented in the I/R dataset (Fig 4.4b) with approximately 15% of the genes in these pathways being upregulated by I/R. Both IL-6 and IL-10 have a commonality in requiring STAT3 to mediate their cellular effects (Murray, 2007) and therefore an analysis of STAT3 target genes differentially regulated by I/R injury was conducted. The list of 796 differentially expressed annotated genes was manually cross-referenced against genes which have been shown to be targets of STAT3 in the literature. This identified 46 STAT3 target transcripts comprising 5.8% of the differentially expressed annotated genes (Table 4.5), it is likely however that this is an underrepresentation of the true figure, since additional STAT3 target genes are being continually characterised. In the previous chapter it was shown that STAT3 was phosphorylated and transcriptionally active following I/R injury, this genomic expression data therefore extends these findings in identifying a large set of STAT3 dependent genes upregulated by I/R injury. While the genes identified in table 4.5 can be upregulated or repressed by STAT3, other transcription factors may be involved in their regulation, and individual chromatin immunoprecipitation would need to be conducted on each individual target to verify STAT3 binding to their promoter regions during I/R. Nonetheless the data suggest that during I/R injury STAT3 has a large impact on the resulting transcriptional programme.

Table 4.5. Genes differentially regulated by I/R previously been shown to be targets of STAT3

Symbol	Gene Name	FC	p value	Reference
Alox15	arachidonate 15-lipoxygenase	12.9	0.00	Xu B et al., 2003
Angpt2	angiopoietin 2	4.6	0.01	Synder et al., 2008
Bmp4	bone morphogenetic protein 4	2.3	0.01	Synder et al., 2008
Calm3	calmodulin 3	-2.4	0.00	Synder et al., 2008
Ccl2 (MCP-1)	chemokine (C-C motif) ligand 2	4.9	0.00	Burysek et al., 2002
Ccng2_predicted	cyclin G2 (predicted)	-2.1	0.01	Paz et al., 2004
Ccr1	chemokine (C-C motif) receptor 1	7.2	0.00	D'Amico et al., 2000
Cd44	CD44 antigen	4.0	0.00	Synder et al., 2008
Cdh2	cadherin 2	-2.0	0.03	Synder et al., 2008
Cox-2 (Ptgs2)	prostaglandin-endoperoxide synthase 2	2.7	0.02	Xuan et al., 2005
Dusp1	dual specificity phosphatase 1	5.0	0.00	Lam et al., 2007
Egr1	early growth response 1	17.2	0.00	Ng et al., 2006
Fgfr1	Fibroblast growth factor receptor 1	3.9	0.02	Synder et al., 2008
Fgl2	fibrinogen-like 2	7.6	0.00	Synder et al., 2008
Fos	FBJ murine osteosarcoma viral oncogene homolog	40.7	0.00	Joo et al., 2004
Fosl1	fos-like antigen 1	30.2	0.00	Paz et al., 2004
Ft11	ferritin light chain 1	2.6	0.00	Minami et al., 1996
Gadd45g	growth arrest and DNA-damage-inducible 45 gamma	4.5	0.00	Nakayama et al., 1999
Gata6	GATA binding protein 6	-2.3	0.01	Synder et al., 2008
H2a	histone 2a	2.1	0.00	Paz et al., 2004
Hif1a	hypoxia inducible factor 1, alpha subunit	2.0	0.01	Xu et al., 2005
Ifrd1	interferon-related developmental regulator 1	3.8	0.00	Synder et al., 2008
Il4ra	interleukin 4 receptor, alpha	3.9	0.00	Lang et al., 2002
Jak2	Janus kinase 2	2.2	0.02	Synder et al., 2008
Jun	Jun oncogene	4.8	0.00	Alvarez et al., 2005
Junb	Jun-B oncogene	4.0	0.00	Ng et al., 2006
Lbp	lipopolysaccharide binding protein	3.2	0.01	Schumann et al., 1995
Lyz	lysozyme	2.5	0.00	Minami et al., 1996
Mcl1	myeloid cell leukemia sequence 1	2.6	0.00	Niu et al., 2002
Mmp9	matrix metalloproteinase 9	10.2	0.00	Landen et al., 2007
Myc	myelocytomatosis viral oncogene homolog (avian)	6.5	0.00	Bownman et al., 2001
Nfil3	nuclear factor, interleukin 3 regulated	3.8	0.01	Alvarez et al., 2005
Nfkb1	Nfkb light polypeptide gene enhancer in B-cells 1, p105	2.0	0.02	Synder et al., 2008
Oasl1	2'-5' oligoadenylate synthetase-like 1	2.2	0.04	Dauer et al., 2005
Phlda1	pleckstrin homology-like domain, family A, member 1	9.4	0.00	Li et al., 2002
Plaur	plasminogen activator, urokinase receptor	25.5	0.00	Dauer et al., 2005
Plscr1	phospholipid scramblase 1	3.5	0.00	Lang et al., 2002
Ralgds	ral guanine nucleotide dissociation stimulator	4.8	0.00	Senga et al., 2001
S100a9	S100 calcium binding protein A9	8.0	0.00	Li et al., 2004
Slpi	secretory leukocyte peptidase inhibitor	9.0	0.00	Clarkson et al., 2006
Smad1	MAD homolog 1 (Drosophila)	2.0	0.01	Synder et al., 2008
Socs3	suppressor of cytokine signaling 3	6.4	0.05	Synder et al., 2008
Stat3	signal transducer and activator of transcription 3	2.3	0.00	Synder et al., 2008
Tfpi2	tissue factor pathway inhibitor 2	7.7	0.00	Dauer et al., 2005
Timp1	tissue inhibitor of metalloproteinase 1	6.4	0.00	Dien et al., 2006
Tnfrsf12a	tumor necrosis factor receptor superfamily, member 12a	7.2	0.00	Synder et al., 2008

Microarray analysis showed that IL-6 (9.6 ± 1.4), the IL-6 receptor (1.9 ± 0.0) and gp130 (3.0 ± 0.3) were all upregulated by I/R as was the IL-6 signaling antagonist SOCS3 (6.4 ± 1.9). qPCR showed that IL-6 was upregulated 7.6 ± 1.3 fold by I/R and significantly reduced by tempol treatment (Fig 4.12a). Upregulation of IL-6 during I/R injury may be therefore be involved in STAT3 phosphorylation and inhibition of IL-6 expression by tempol may contribute to its ability to inhibit STAT3 phosphorylation. IL-6 has previously been shown to have beneficial effects in I/R injury and is also required for preconditioning (Matsushita et al., 2005, Dawn et al., 2004). Interestingly, the I/R mediated increase in IL-6 expression was paralleled by an increase in SOCS3 expression, this suggests that similarly to inflammation, I/R leads to concomitant upregulation of stimulators and inhibitors to the JAK/STAT pathway.

Ucn1 increased IL-6 expression 1.8 fold over and above the levels in the saline treated samples and also repressed SOCS3 expression by I/R (Fig 4.12b). Since IL-6 induces STAT3 phosphorylation and SOCS3 inhibits it, the effect of Ucn1 on STAT3 phosphorylation was tested. Fig 4.12d shows that as previously demonstrated, I/R injury increased STAT3 tyrosine and serine phosphorylation; surprisingly however, the addition of Ucn1 had no consistent effect on or levels. Ucn1 treatment did increase STAT3 mRNA levels compared to the sham or I/R groups (Fig 4.12c) but this was not reflected by increased STAT3 protein levels (Fig4.12d). While Ucn1 had no effect on STAT3 phosphorylation or protein levels in the 2 hr reperfusion samples, it may increase both STAT3 protein expression and phosphorylation if examined over a longer period.

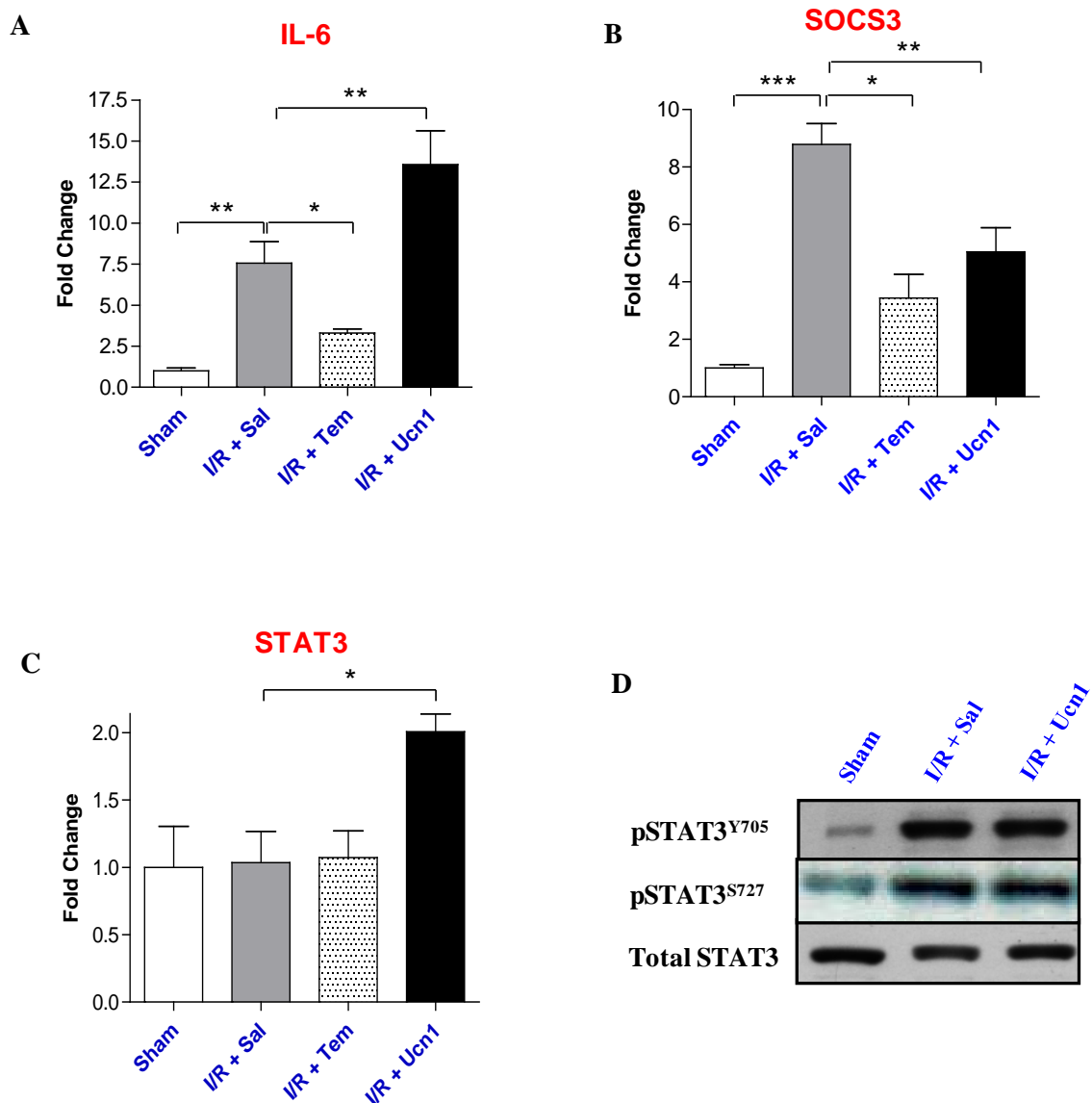


Fig 4.12. The IL-6/STAT3/SOCS3 axis is induced by I/R and enhanced by Ucn1. (A, and C) IL-6, SOCS3 and STAT3 expression was measured by qPCR and normalised to sham levels. Statistical analysis was carried out using a one-way ANOVA with Dunnett's post test, n=3 samples, * p<0.05, ** p<0.01, *** p<0.001 compared to I/R + Sal. (D) The expression of , and total STAT3 was measured by western blot.

Recently nitric oxide has come to the fore as a potent cardioprotective agent (Bolli, 2001). Nitric oxide synthase (NOS) is the enzyme responsible for producing nitric oxide and exists in three isoforms; NOS1 (nNOS), NOS2 (iNOS) and NOS3 (eNOS). Both eNOS and iNOS were upregulated on the microarray by 11.8 ± 1.1 and 3.3 ± 0.8 fold respectively. In epithelial and smooth muscle cells, IFN- \bullet and IL-1 \bullet have been shown to have a synergistic effect on iNOS expression and in addition, STAT1 and c-Fos interact with one another and bind to the iNOS promoter, thereby increasing iNOS expression (Tang et al., 2002, Xu et al., 2003). STAT1 activity was shown to be enhanced by I/R (see Fig 3.16b) and qPCR analysis found that IFN- \bullet , IL-1 \bullet , c-Fos and iNOS were markedly upregulated by I/R (Fig 4.13), thus confirming microarray data. During I/R, IL-1 \bullet and IFN- \bullet together with STAT1 and c-Fos may therefore co-operate to enhance iNOS expression. Cardioprotection by iNOS lies upstream of COX-2 (Li, 2007) and indeed COX-2 expression was also found to be upregulated by 2.7 ± 0.2 fold on the microarray. In addition, tempol-mediated inhibition of IFN- \bullet expression may contribute to the reduction in STAT1 phosphorylation by tempol.

The data therefore suggests that the JAK/STAT-iNOS/COX2 axis, one of the major cardioprotective pathways is induced by oxidative stress. It may seem counter-intuitive that tempol should inhibit a cardioprotective pathway such as this, however tempol treatment is expected to affect all pathways which are responsive to oxidative stress and therefore will reduce the activity of many cardioprotective molecules, on balance however it is expected to block the activity of more of the damaging pathways.

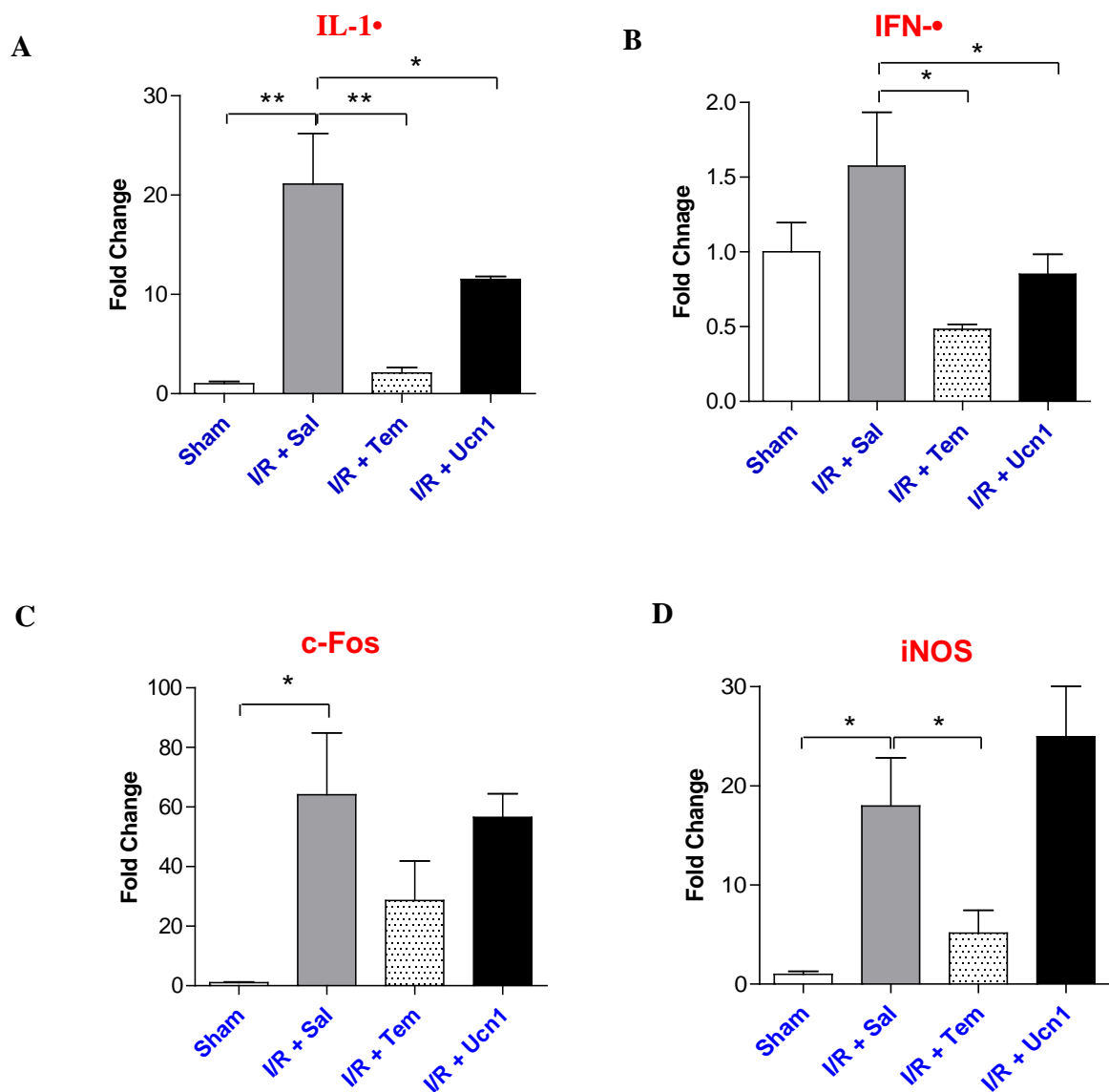


Fig 4.13. Regulation of the Nitric Oxide pathway by I/R injury. (A-D) The expression of the indicated genes was measured by qPCR and normalised to sham levels. Statistical analysis was carried out using a one-way ANOVA with Dunnett's post test, n=3 samples, * p<0.05, ** p<0.01, compared to I/R + Sal.

4.9 IL-17 Regulation in I/R injury

The IL-17 receptor was found to be upregulated by I/R (microarray 7.0 ± 1.1) and regulation of the IL-17 axis in I/R injury has not previously been reported. Huge interest has recently been generated in the newly identified subset of IL-17 producing T cells (termed Th17 cells) which are crucial to inflammatory responses and autoimmune disease. Differentiation of Th17 cells is controlled by TGF- β and IL-6 and stabilized and reinforced by IL-21 and IL-23 (Dong, 2008). STAT3 has been shown to be necessary for both the differentiation and stabilization of Th17 cells via transactivation of the Th17 specific transcription factors retinoic acid receptor-related orphan receptor gamma (ROR γ) and ROR α (Yang et al., 2007, 2008, Nurieva et al., 2007). Moreover, STAT3 is necessary for the subsequent production of IL-17A and IL-17F which mediate Th17 cell's biological effects (Chen et al., 2006). This is evidenced by the recurrent infections which occur in patients with hyper IgM syndrome, these patients harbor dominant negative mutations in the STAT3 DNA binding domain resulting in impaired IL-17 production and inability to clear infections (Ma et al., 2008). Little is known about IL-17 pathway regulation in the cardiovascular system, however one report has demonstrated upregulation of IL-17A following middle cerebral artery occlusion in rats and in ischaemic lesions in human brain (Li et al., 2005).

Upregulation of the IL-17R was verified by PCR (4.6 ± 0.8) Fig 4.14a. There were no probes present for IL-17A or IL-17F on the RAE 230A microarrays, but their expression was measured by qPCR. Fig 4.14 b and c show that both IL-17A and IL-17F were upregulated by I/R injury 8.3 ± 3.2 fold and 4.3 ± 1.3 fold respectively. A search for downstream IL-17 targets revealed upregulation of a host of IL-17 mediators upregulated by I/R injury on the microarray, including; Cxcl1, Cxcl2, Cxcl3, Ccl2, IL-1 β , iNOS, IL-6, S100a8, S100a9, Ccr1, P-selectin, ICAM-1, MMP-9, Ptgs2, Timp1, lcn2, Cotl1 and Spsb1 (Huang et al., 2007, Jovanovic et al., 1998, Hwang et al., 2004, Fossiez et al., 1996, Lubberts et al., 2005, Shen et al., 2005, Albanesi et al., 1999 McAllister et al., 2005).

To examine the kinetic expression of the IL-17 axis during I/R injury, their expression was measured following I/R injury *in vitro*. The mRNA expression of the IL-17R was time-dependently increased during I/R injury in NRVMs, reaching a maximum at 4 hr (Fig 4.14d). Analysis of IL-17A and IL-17F mRNA levels could not be accurately and consistently determined since the Ct threshold for these PCRs was in the range 38-40 cycles. IL-17A and IL-17F mRNA have been shown to be regulated by STAT3 (Yang et al., 2007), therefore in

order to examine if neonatal cardiac myocytes are capable of expressing IL-17A and IL-17F mRNA, NRVMs were transduced for 24 hr with a constitutively active STAT3 adenovirus (STAT3C). STAT3C transduction allowed for consistent measurements by qPCR (Fig 4.17 e, f), IL-17A was upregulated 3.5 ± 0.5 fold, IL-17F was upregulated 9.5 ± 1.3 fold and STAT3C had no effect on the IL-17R (Fig 4.14 e-g). This qPCR data shows that cardiac myocytes, although they express low constitutive levels, can still produce IL-17A and IL-17F mRNA when their transcriptional regulator is overexpressed. In the future, analysis of IL-17 levels using flow cytometry will allow more careful examination of the effect of *in vitro* I/R injury on IL-17 levels.

Taken together this data shows that the IL-17 axis is upregulated during IR injury *in vivo*, cardiac myocytes express IL-17A, IL-17F and the IL-17R and upregulate the receptor following I/R injury. What effect this has on cardiovascular biology is currently unknown. Likewise it is unknown what are the major cell types affected by IL-17 in the heart. Endothelial cells and fibroblasts have been shown to express a functional receptor and one report has shown that conditioned medium from cardiac fibroblasts contains IL-17 (Honorati et al., 2000, La Framboise et al., 2007, Chang et al., 2006). Since cardiac myocytes upregulate the receptor *in vitro* and *in vivo* following reperfusion injury, it is likely that IL-17 does affect cardiac myocyte physiology. Detailed examination of IL-17 production by flow cytometry and analysis of the effect of IL-17A and IL-17F production on cardiac myocyte survival following I/R injury should greatly add to the understanding of the role of this cytokine family in I/R injury.

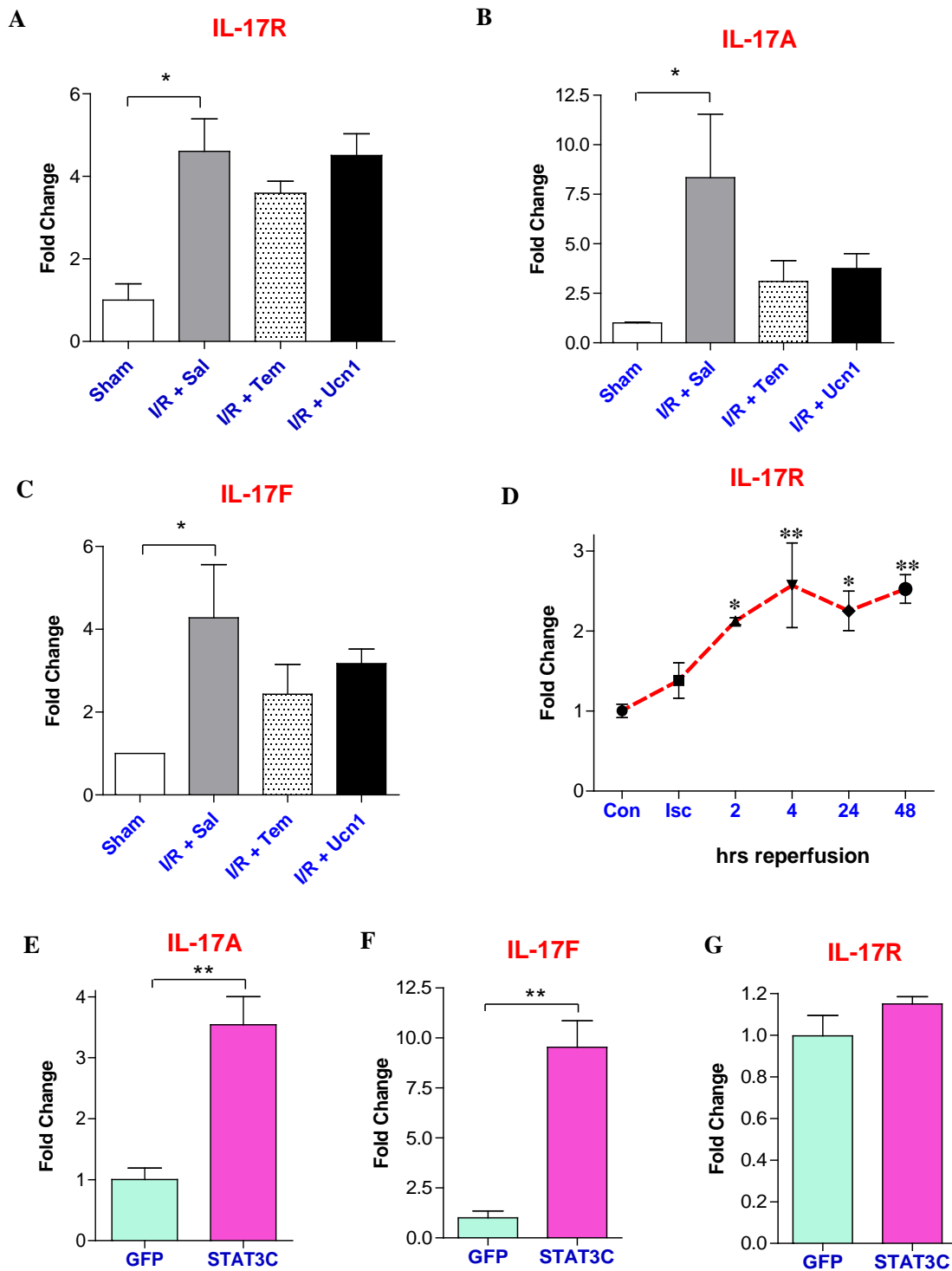


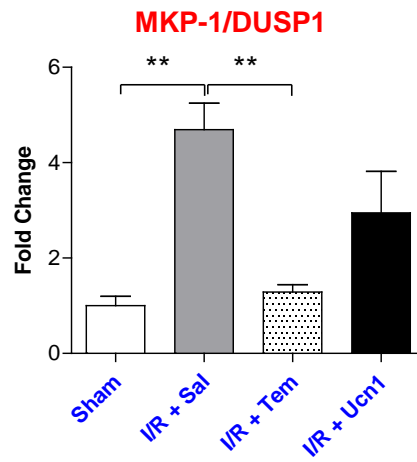
Fig 4.14. The IL-17 axis is regulated by I/R injury. (A-C) The expression of IL-17R, IL-17A and IL-17F was measured by qPCR and normalized to sham. (D) IL-17R expression was measured following a time course of *in vitro* I/R injury in NRVMs. (E-G) NRVMs were transduced with STAT3C at moi=100 for 24 hr and the expression IL-17A, IL-17F and IL-17R.

4.10 Differential Regulation of MAPKs and MKP-1 during I/R Injury

MAPK phosphatases (MKPs also known as dual-specificity phosphatases -DUSPs) are endogenous inhibitors of JNK, p38 MAPK and ERK activity. p38 MAPK and JNK have both been shown to be pro-apoptotic factors in the myocardium and mice deficient in MKP-1 had increased infarct sizes after I/R injury due to excessive p38 MAPK activity (Kaiser et al., 2004). Although, the activity of MAPKs in I/R injury has been addressed previously, there is little published information regarding the expression of MKP/DUSPs during I/R. The microarray results showed that the expression of 4 DUSPs was elevated by I/R; DUSP1/MKP-1 (4.9 ± 0.5), Dusp5 (16.6 ± 0.9), Dusp6/MKP-3 (5.3 ± 0.9) and Dusp16/MKP-7 (2.8 ± 0.5). Each phosphatase has a distinct specificity for each of the MAPKs, DUSP1 preferentially dephosphorylates p38 and JNK (Franklin et al., 1997), DUSP 5 and DUSP6 are selective for ERK (Camps et al., 1998, Mandl et al., 2005) and DUSP16 interacts with p38-• and JNK1 but not ERK (Tanoue et al., 2001). The expression of DUSP1/MKP-1 was examined by qPCR, which showed a 4.7 ± 0.6 fold induction during I/R, this was significantly inhibited by tempol but not Ucn1 (Fig 4.15a).

The phosphorylation status of ERK and p38 MAPK was also examined. Fig 4.15b shows that ERK was maximally phosphorylated within 15 min of reperfusion and by 30 min dephosphorylation had started to occur. Phosphorylation of p38 MAPK was found to be regulated in a more complex fashion; p38 MAPK was phosphorylated during ischaemia then rapidly dephosphorylated within 5 min of reperfusion. During reperfusion, phospho-p38 MAPK levels increased up to 60 min and were once again reduced by 2 hr, with total p38 MAPK levels remaining constant. Thus both ERK and p38 MAPK phosphorylation was reduced by 2 hr reperfusion, coinciding with increased DUSP expression. Upregulation of 4 separate DUSPs highlights the complex regulation of the MAPK cascade in I/R and shows that during I/R injury, the heart induces both activators and inhibitors to precisely control the temporal activation of MAPKs.

A



B

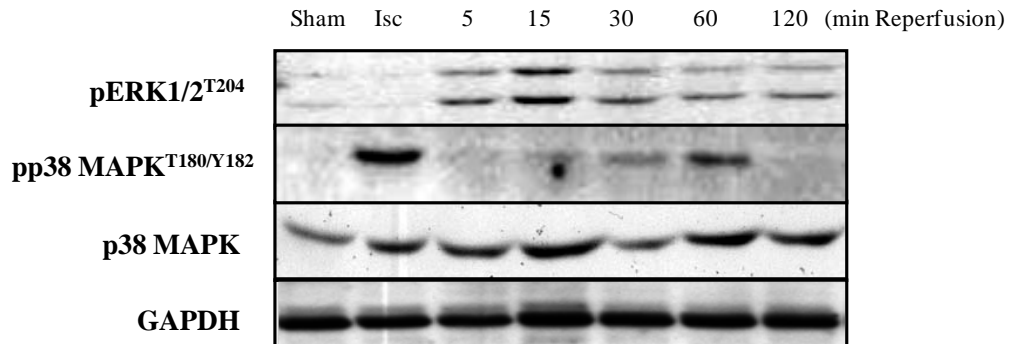


Fig 4.15 MAPK activity during I/R injury. (A) The expression of MKP-1 was analysed by qPCR and normalised to sham levels. Statistical analysis was carried out using a one-way ANOVA with Dunnett's post test, n=3 samples, ** p<0.01 compared to I/R + Sal. (B) Rats were subjected to a time course of I/R injury up to 2 hr. The indicated antibodies were used to measure the levels of MAPKs, GAPDH was used as a loading control.

4.11 Uracil Metabolism is Altered by I/R Injury

Although the effect of purines on myocardial physiology has been extensively studied, less is known about the effect on heart function of pyrimidines such as uridine triphosphate (UTP) and uridine diphosphate (UDP). Extracellular pyrimidines activate the membrane bound P2Y G-protein coupled purinoceptors leading to increases in adenylyl cyclase and phospholipase C activity (Mazzola et al., 2008). UTP acts through the P_2U_1 receptors while UDP is an agonist for the P_2U_1 receptor. Both UTP and UDP have been shown to have positive inotropic effects on cardiac myocytes and measurements of plasma levels of UTP showed an increase of 57% in patients with myocardial infarction (Wihlborg et al., 2006). UTP influences vascular tone and blood pressure through its effects on smooth muscle and endothelial cells and also promotes hypertrophy of cardiac myocytes (Pham et al., 2003). In addition, UTP has been shown to protect cardiac myocytes from hypoxic cell death by acting on the P_2U_1 receptor (Yitzhaki et al., 2005). UTP also reduces infarct size *in vivo* when administered both before and after I/R, preserving ATP levels and maintaining mitochondrial function. (Yitzhaki et al., 2006). In the I/R group, ATP was upregulated by 4.3 ± 0.3 fold and ADP was upregulated 3.4 ± 1.2 fold, there was no change in AMP levels. Since pharmacological inhibition of P2Y receptors during *in vivo* I/R injury increased contractile dysfunction and UDP and UTP are cardioprotective (Wee et al., 2007, Mazzola et al., 2008), it is possible that upregulation of ATP and ADP represents a novel endogenous cardioprotective mechanism initiated during I/R injury.

Deoxyuridine triphosphatase (Dut), also known as dUTPase, hydrolyses dUTP to give dUMP and pyrophosphate and is essential to cell survival by maintaining a constant dUTP/dTTP balance (Tooth et al., 2007). dUTPase prevents excess uracil from getting incorporated into newly synthesized DNA, which would cause DNA fragmentation and cell death (Curtin et al., 1991). Although dUTPase is necessary to maintain genomic stability, very little is known about its transcriptional regulation. It is known that alternative splicing produces distinct nuclear and mitochondrial isoforms but how their expression is controlled has not been ascertained (Ladner et al., 1997). Likewise, the role of dUTPase in the myocardium or its regulation by I/R injury has never been addressed. I/R injury was found to decrease the expression of dUTPase by $78.3 \pm 2.5\%$, suggesting that dUTP levels are likely to be elevated in the myocardium during I/R injury. Alignment analysis of the affymetrix probe sets for dUTPase showed that the probes are not specific to either isoform and therefore this figure represents a reduction in total dUTPase RNA levels. By microarray, tempol, Ucn1 and Ucn2

increased the expression of dUTPase by 3.8 ± 0.3 , 3.2 ± 0.2 and 3.3 ± 0.4 fold respectively. qPCR analysis confirmed repression of dUTP by I/R and increased expression by tempol, however qPCR did not show elevated levels of dUTPase after Ucn1 treatment (Fig 4.16). The reasons for this are unknown; the qPCR primers were designed to an area of the dUTPase gene common to both isoforms. It is clear however that dUTPase mRNA expression is lowered during I/R, the reasons for this reduction and the resulting physiological outcome are unknown but it is likely that persistent inhibition of dUTPase would result in significant DNA damage. Increased dUTPase expression by tempol may be a novel effect of antioxidant treatment during I/R injury. It is of course necessary to measure dUTP levels directly in the myocardium following I/R injury to formally show that this is the case, nonetheless it may represent a previously unappreciated role for dUTPase in cardiac pathology.

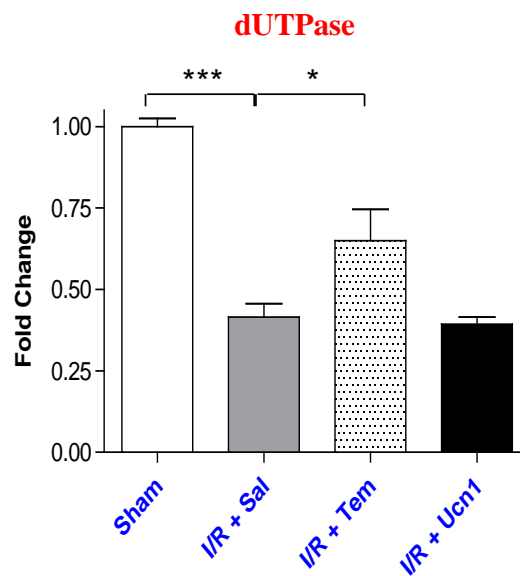


Fig 4.16. dUTPase levels are reduced by I/R and partially restored by tempol. dUTPase expression was measured by qPCR and normalised to sham levels. Statistical analysis was carried out using a one-way ANOVA with Dunnett's post test, n=3 samples, * $p < 0.05$, *** $p < 0.001$ compared to I/R + Sal.

4.12 Reduced Expression of Mitochondrial Translation Genes Following I/R Injury

Mitochondrial dysfunction during I/R injury results in reduced ATP synthesis and initiation of apoptosis, thus recovery of mitochondrial function is necessary to restore contractility after an ischemic episode (Solaini et al., 2005). The majority of mitochondrial proteins are encoded in the nucleus while the mitochondrial genome encodes 13 proteins, 22 tRNAs and 2 rRNAs. Mitochondrial mRNAs are translated by the 12 S and 16 S mitochondrial rRNAs and approximately 80 nuclear encoded mitochondrial ribosomal proteins (MRPs) which must be imported into the mitochondria (Wang et al., 2007). Mitochondrial encoded proteins form an essential part of the mitochondrial respiratory chain (Emdadul Haque et al., 2008) and require a specialized mitochondrial translation system. Mitochondrial genes were the third highest differentially expressed annotated group following I/R injury (Fig 4.3) and examination of genes in this group suggested that mitochondrial translation may be reduced during I/R injury. There are 68 MRPs represented on the RAE230A arrays and of these, 47 had reduced expression following I/R. The expression of MRPs L1, L3, L4, L9, L11, L12, L13, L14, L15, L16, L18, L20, L21, L22, L23, L27, L28, L30, L32, L35, L36, L37, L40, L41, L42, L43, L44, L46, L50, L53, L54, S9, S14, S16, S17, S18A, S21, S23, S24, S25, S27, S30, S33, S35, S36 and MRP63 were downregulated on average 51.3 ± 1.7 % by I/R injury. With such a large number of mitochondrial ribosomal proteins having reduced mRNA levels, it is likely that this results in a global reduction in the availability of mitochondrial proteins. In addition to MRPs, mitochondrial translational requires the elongation factors EF-Tu (TUFM), EF-Ts (TSFM) and EF-G (GFM1). Following I/R, EF-Tu expression was reduced by 51.3 ± 5.4 % and EF-G expression was reduced by 55.6 ± 10.7 %; however there are no probes for EFTs present on the Affymetrix RAE 230A arrays. This suggests that the entire mitochondrial translational machinery is transcriptionally downregulated following I/R injury and may represent a heretofore unrecognized facet of mitochondrial dysfunction during I/R.

4.13 Reduced Expression of Mitochondrial and Respiratory Chain Genes Following I/R Injury

During I/R injury, mitochondrial respiration is compromised, superoxide production is increased and the MPT pore opens, leading to cytochrome c release and dysregulation of calcium homeostasis (Di Lisa et al., 2007). The mitochondrial respiratory chain is the main source of ROS generation in the cell and at the same time is a major target of ROS damage (Ott et al., 2007). Approximately 1-2% of molecular oxygen used during normal mitochondrial respiration is converted to free radicals; this is increased during I/R injury and can contribute significantly to cardiac damage (Ott et al., 2007). Oxidative phosphorylation occurs through the mitochondrial respiratory chain which consists of five enzymatic complexes (I to V) embedded in the inner mitochondrial membrane (Fontanesi et al., 2006). It is widely accepted that mitochondrial respiration and oxidative phosphorylation are compromised during ischaemia and all five of the respiratory complexes have been shown to be affected by ischemic damage (Paradies et al., 2004, Petrosillo et al., 2003).

NADH-ubiquinone oxidoreductase (complex I) reduces ubiquinone using NADH as the electron donor. A significant reduction in complex I activity has been demonstrated *in vitro* and *in vivo*, for example Maklashina et al. demonstrated a 40% reduction in Complex I activity following 30 min of ischaemia (Maklashina et al., 2002). Currently the exact cause for this reduction is unknown but it has been attributed to both ROS production and damage from peroxynitrite intermediates (Paradies et al., 2002, Jekabsone et al., 2003). I/R injury was found to significantly downregulate 19 out of the 33 complex I genes represented on the RAE 230A microarrays by an average of $45.1 \pm 1.7\%$ (Table 4.6). Out of the three cardioprotective agents, only Ucn2 changed the expression of any of these genes significantly; Ndufb6 by 2.0 ± 0.1 fold and Ndufs8 by 1.9 ± 0.4 fold. This suggests that a facet of complex I functional inhibition during I/R may be attributable to transcriptional downregulation of a large number of NADH dehydrogenase genes.

Complex II (succinate dehydrogenase) oxidizes succinate to fumarate, releasing two electrons which are used to reduce ubiquinone to ubiquinol. There have been conflicting reports as to the effect of I/R injury on complex II activity but a study by Abe et al. demonstrated a reduction in activity following I/R injury in rats (Abe et al., 1999). One component of complex II, succinate dehydrogenase complex D (Sdhd), was found to be downregulated $47.5 \pm 6.6\%$ by I/R injury.

	Gene	Gene Title	FC	p value
	Nqo2	NAD(P)H dehydrogenase, quinone 2	-2.56	0.02
	Ndufa2	NADH dehydrogenase (ubiquinone) 1 alpha subcomplex, 2 (predicted)	-1.51	0.00
	Ndufa6	NADH dehydrogenase (ubiquinone) 1 alpha subcomplex, 6 (B14) (predicted)	-1.65	0.04
	Ndufa7	NADH dehydrogenase (ubiquinone) 1 alpha subcomplex, 7 (B14.5a) (predicted)	-1.53	0.09
	Ndufa9	NADH dehydrogenase (ubiquinone) 1 alpha subcomplex, 9	-2.07	0.01
	Ndufa11	NADH dehydrogenase (ubiquinone) 1 alpha subcomplex 11	-1.78	0.04
Complex I	Ndufa12	NADH dehydrogenase (ubiquinone) 1 alpha subcomplex, 12 (predicted)	-1.57	0.01
	Ndufb6	NADH dehydrogenase (ubiquinone) 1 beta subcomplex, 6 (predicted)	-2.12	0.00
	Ndufb7	NADH dehydrogenase (ubiquinone) 1 beta subcomplex, 7 (predicted)	-1.79	0.01
	Ndufb11	NADH dehydrogenase (ubiquinone) 1 beta subcomplex, 11 (predicted)	-1.74	0.03
	Ndufc2	NADH dehydrogenase (ubiquinone) 1, subcomplex unknown, 2	-1.55	0.04
	Ndufs1	NADH dehydrogenase (ubiquinone) Fe-S protein 1	-1.82	0.04
	Ndufs2	NADH dehydrogenase (ubiquinone) Fe-S protein 2	-1.65	0.01
	Ndufs3	NADH dehydrogenase (ubiquinone) Fe-S protein 3 (predicted)	-2.00	0.02
	Ndufs5	NADH dehydrogenase (ubiquinone) Fe-S protein 5	-1.76	0.02
	Ndufs7	NADH dehydrogenase (ubiquinone) Fe-S protein 7	-1.98	0.00
	Ndufs8	NADH dehydrogenase (ubiquinone) Fe-S protein 8 (predicted)	-2.32	0.00
	Ndufv1	NADH dehydrogenase (ubiquinone) flavoprotein 1	-1.67	0.01
	Ndufv3l	NADH dehydrogenase (ubiquinone) flavoprotein 3-like	-2.28	0.00
Complex II	Sdhb	succinate dehydrogenase complex, subunit D, integral membrane protein	-1.94	0.05
	Coq3	coenzyme Q3 homolog, methyltransferase (yeast)	-2.82	0.01
	Coq6	coenzyme Q6 homolog (yeast)	-1.69	0.03
Complex III	Coq10a	coenzyme Q10 homolog A (yeast) (predicted)	-1.98	0.04
	Uqcr	ubiquinol-cytochrome c reductase, 6.4kDa subunit	-1.61	0.00
	Uqcrc	ubiquinol-cytochrome c reductase, complex III subunit VII	-1.80	0.00
	Cox6b1	cytochrome c oxidase, subunit VIb polypeptide 1	-1.89	0.00
	Cox15	COX15 homolog, cytochrome c oxidase assembly protein (yeast)	-2.66	0.00
Complex IV	Cox17	cytochrome c oxidase, subunit XVII assembly protein homolog (yeast)	-1.75	0.00
	Cox18	COX18 cytochrome c oxidase assembly homolog (S. cerevisiae)	-1.45	0.04
	Cox19	COX19 cytochrome c oxidase assembly homolog (S. cerevisiae)	-2.05	0.04
	Atpaf1	ATP synthase mitochondrial F1 complex assembly factor 1 (predicted)	-2.49	0.00
F1/F0 ATP	Atpaf2	ATP synthase mitochondrial F1 complex assembly factor 2 (predicted)	-2.16	0.01
Synthase	Atp5s	ATP synthase, H+ transporting, mitochondrial F0 complex, subunit s	-2.03	0.03
	Atp5d	ATP synthase, H+ transporting, mitochondrial F1 complex, delta subunit	-1.84	0.01

Table 4.6 Mitochondrial respiratory complex genes differentially expressed during I/R injury.

Complex III (coenzyme Q: cytochrome c - oxidoreductase) uses ubiquinol to reduce cytochrome c, thereby pumping 4 from the mitochondrial matrix to the intermembrane space, resulting in the production of a proton gradient across the membrane. Veitch et al. recorded a 34% reduction in complex III activity after 1 hr ischaemia and 5 min reperfusion (Veitch et al., 1992). Reduction in complex III activity has been attributed to a decreased content of mitochondrial cardiolipin which is necessary for complex III function (Petrosillo G et al., 2003). I/R injury was found to decrease the expression of 5 of the 13 subunits of complex III by an average of $50.0 \pm 2.0\%$ (Table 4.6), showing that reduced complex III activity may be in part due to decreased subunit expression. In addition, there is a slight reduction ($41.1 \pm 15.4\%$) in cardiolipin synthase expression following I/R which may account for some of the reduced abundance of cardiolipin and hence reduced complex III activity following I/R injury. Cardiolipin is also important in retaining cytochrome c within the mitochondrial intermembrane space (Paradies et al., 2000) and therefore reduced cardiolipin synthase expression might also contribute to cytochrome c release from the mitochondria and subsequent apoptosis.

Complex IV consists of the 13 subunits of the cytochrome c oxidase (COX) enzyme which is the rate limiting enzyme in mitochondrial respiration. Complex IV transfers electrons from cytochrome c to oxygen, reducing oxygen to in the process. The energy generated by this electron flux is used to pump protons from the mitochondrial matrix into the inter-membrane space and the resulting proton gradient is used by complex V to catalyze the conversion of ADP and inorganic phosphate into ATP (Fontanesi et al., 2006). Some studies have shown that COX activity remains unaltered after ischaemia (Lesnefsky et al. 1997) although there is loss of cytochrome c which mediates electron transfer between complexes III and IV (Solaini 2005). Other studies have on the other hand demonstrated a reduction in complex IV activity after I/R (Sadek et al., 2002). Following I/R injury, 5 of the 13 COX subunits was found to be significantly downregulated including Cox15 ($61.9 \pm 4.6\%$), Cox17 ($41.9 \pm 6.7\%$), Cox19 ($48.6 \pm 10.4\%$) Cox6b1 ($47.0 \pm 2.2\%$) and Oxa1L ($54.1 \pm 4.7\%$).

The final step of the mitochondrial respiratory chain involves -ATPase which is responsible for the production of over 90% of the ATP needs of the myocardium (Solaini et al. 2005). I/R injury reduced expression of subunits of both the and ATPase by an average of $54.2 \pm 2.9\%$ (Table 4.7). It is currently unclear what effect reduced expression of the 4 ATPase genes has on cardiac function after I/R injury. During ischaemia, the -ATPase reverses and hydrolyses

ATP thus allowing protons to be pumped from the mitochondria. (Solaini et al. 2005). While total inhibition of the F_1F_0 -ATPase slows the rate of ATP depletion during ischaemia, it also inhibits ATP recovery after reperfusion (Grover et al., 2008.) Selective inhibition of the F_1F_0 -ATPase activity however allows the heart to restore ATP levels at a faster rate during reperfusion and leads to a reduction in cell death following I/R. (Gary et al., 2004). Reduced expression of F_1F_0 -ATPase may therefore reduce the level of ATP hydrolysis during ischaemia; on the other hand it may also decrease the production of ATP following the onset of reperfusion. Thus it appears that the transcriptional regulation of genes vital to the activity of the electron transport chain is affected by I/R injury. The reduced expression of 37 genes which are integral to all stages of mitochondrial respiration may contribute significantly to the documented decreases in activity.

4.14 Reduced Expression of Mitochondrial Import Machinery Genes Following I/R Injury

The Tim Tom and SAM family of genes are mitochondrial pore proteins which facilitate mitochondrial biogenesis by controlling the import and assembly of proteins into the mitochondria. Thirteen members of the mitochondrial transport machinery were found to be downregulated by I/R injury (Table 4.7). qPCR analysis confirmed the microarray data, showing significant repression of Tim8a, Tim8b, Tim13, Tim23, Tim44 and Tom20 (Fig 4.17). There was a trend towards reduced repression of the Tim proteins in the tempol group, however this only reached significance with Tim44, Ucn1 also increased the expression of Tim23 and Tim44 compared to saline infusion. The repression of Tim23 and Tim44 by was confirmed in a second *ex vivo* model of I/R injury using the Langendorff perfusion system (samples obtained from Dr Naushaad Suleman ICH). In these experiments mice hearts were subjected to 30 min of ischaemia and 45 min of reperfusion. Although the period of reperfusion was much less than the *in vivo* model, the expression of Tim23 and Tim44 was still reduced by $30.2 \pm 6.6\%$ and $47.7 \pm 4.7\%$ respectively (Fig 4.18).

The voltage-dependent anion channel (VDAC) is central in the transport of metabolites and ions across the outer mitochondrial membrane, has important roles in apoptosis and may be a component of the mitochondrial permeability transition pore (Shoshan-Barmatz et al. 2003). VDAC1 was downregulated $64.5 \pm 13.9\%$ by I/R; in addition the SAM complex proteins

Sam50, metaxin1 and metaxin2 were also downregulated (Table 4.7) and these have been shown to be necessary for import and assembly of VDAC into the mitochondria (Kozjak-Pavlovic et al., 2007). Reduced VDAC1 expression and insertion into the mitochondria may therefore affect MPT opening and release of apoptogenic factors from the mitochondria during I/R injury.

These data show that a large portion of the mitochondrial import machinery is repressed during I/R injury. This is likely to have significant effects on mitochondrial function since the Tim/Tom/SAM complexes control entry of almost all proteins into the mitochondria. Therefore reduced mitochondrial function during I/R may actually stem from a reduction in the availability of necessary components of the respiratory transport chain since they cannot be inserted into the mitochondria at the normal rate.

Table 4.7. Mitochondrial import genes are differentially regulated during I/R injury.

	FC	p value
Tim8a	-1.68	0.020
Tim8b	-1.94	0.004
Tim9	-1.80	0.230
Tim10	-1.55	0.089
Tim13	-2.60	0.000
Tim17a	-1.79	0.016
Tim22	-1.95	0.003
Tim23	-1.58	0.086
Tim44	-2.93	0.000
Tom7	-1.57	0.010
Metaxin1	-4.22	0.007
Metaxin2	-1.81	0.074
Oxa1l	-2.20	0.001

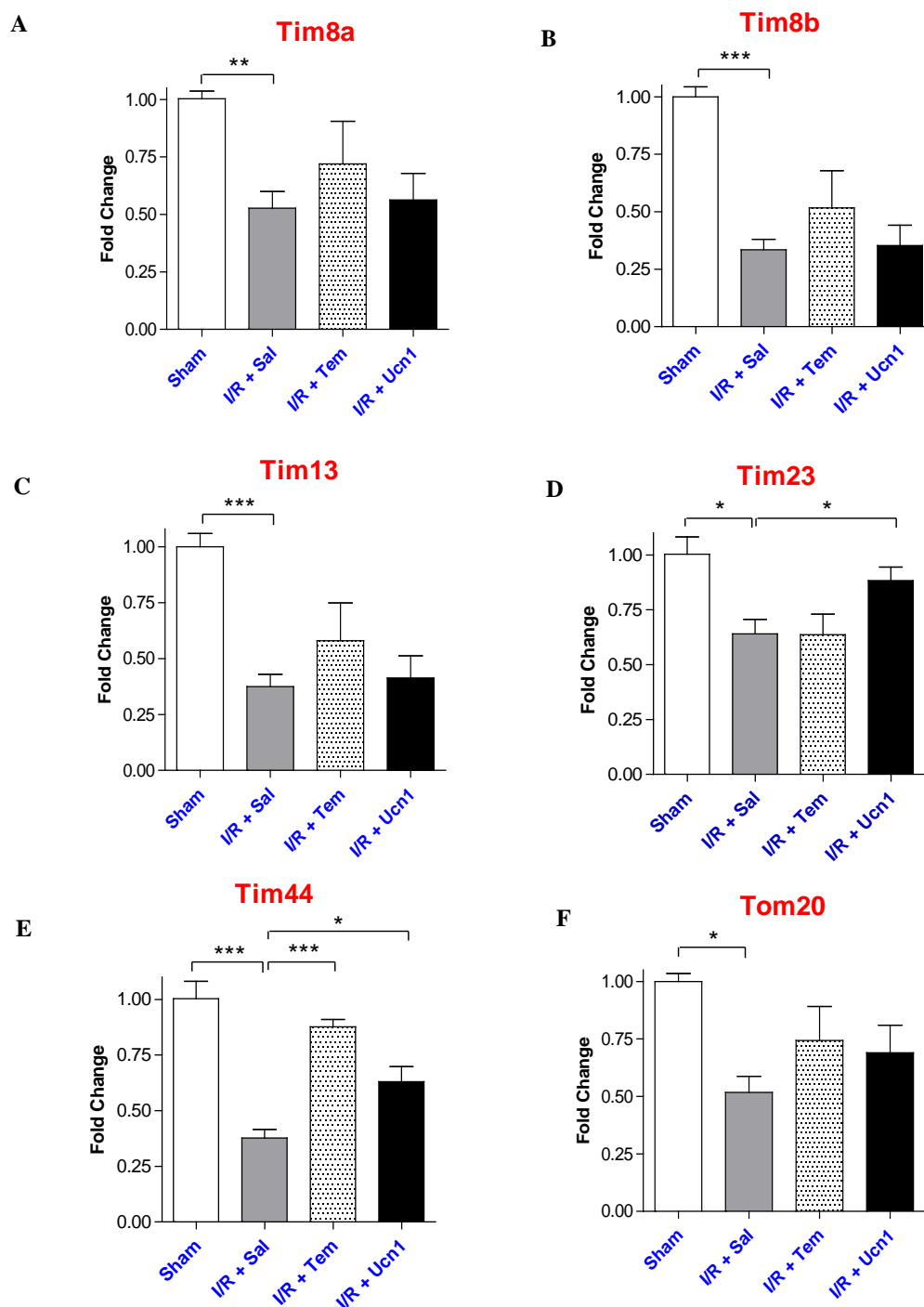


Fig 4.17. I/R injury represses the expression of mitochondrial transport genes. The expression of indicated genes was analysed by qPCR and normalised to sham levels. Statistical analysis was carried out using a one-way ANOVA with Dunnett's post test, n=3 samples, * p<0.05, ** p<0.01, *** p<0.001 compared to I/R + S.

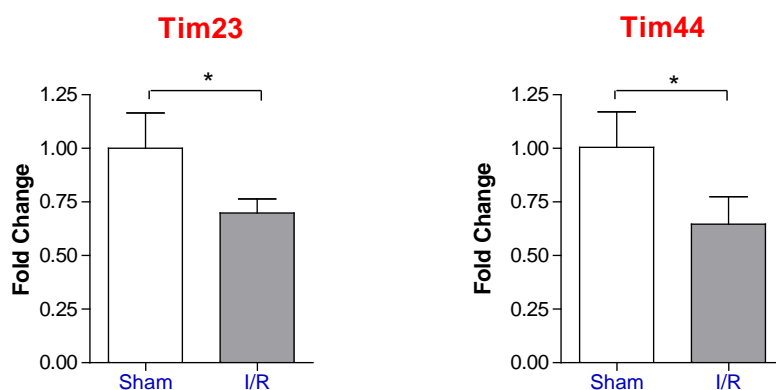


Fig 4.18. Tim23 and Tim44 are repressed in an ex vivo model of I/R injury. Mouse hearts were subjected to 30 min of ischaemia and 45 min of reperfusion using the Langendorff perfusion system. The mRNA levels of Tim23 and Tim44 were then examined by qPCR and normalised to sham levels. Statistical analysis was carried out using a student's t-test, n=5 animals, * p<0.

4.15 Cardioprotective Genes Induced by Ucn1 and Ucn2

Out of the list of potential cardio-protective genes differentially regulated by Ucn1 and Ucn2, several have not been previously shown to have a role in I/R injury and were examined in greater detail. One of the highest differentially expressed genes in the Ucn1 group is Birc4 (4.8 ± 0.3 fold) also known as X-linked inhibitor of apoptosis protein (XIAP), one of a family of 6 inhibitors of apoptosis (IAP) proteins. XIAP functions by inhibiting the effector caspases-3, -7 and -9 through ubiquitin mediated degradation (Martins et al., 2002). There are few studies addressing the role of XIAP in the myocardium, however Scarabelli et al. demonstrated that cardioprotection by minocycline was associated with increased expression of XIAP (Scarabelli et al. 2004). XIAP has also been shown to function as an anti-apoptotic factor in cerebral I/R (Zhu C et al., 2007, Guegan et al., 2006). Although XIAP expression was not reduced by I/R on the microarray, qPCR data showed that XIAP expression was reduced $51.3 \pm 8.5\%$ by I/R and increased 1.8 ± 0.2 fold by tempol and 1.6 ± 0.1 fold by Ucn1 which represents a restoration of XIAP expression to near sham levels (Fig 4.19). Urocortin administration has previously been shown to lower the number of caspase-3 positive endothelial cells and cardiac myocytes following I/R injury *in vivo* (Scarabelli et al., 2002) and it is therefore tempting to speculate that some of the anti-apoptotic effects of tempol and Ucn1 may be mediated through reduced executioner caspase activity via XIAP upregulation.

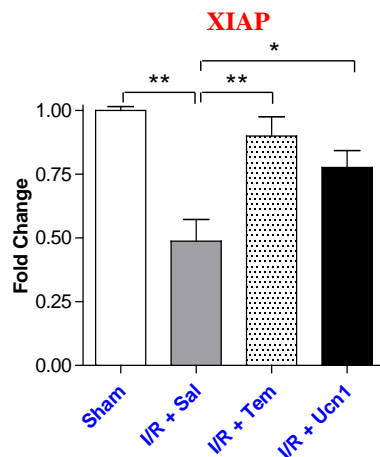


Fig 4.19. Tempol and Ucn1 upregulate XIAP expression. XIAP expression was measured by qPCR and normalised to sham levels. Statistical analysis was carried out using a one-way ANOVA with Dunnett's post test, n=3 samples, * p<0.05, ** p<0.01 compared to I/R + Sal.

AMP-activated protein kinase (AMPK) is responsible for promoting fatty acid oxidation and increasing glucose uptake and glycolysis (Dyck et al. 2006). AMPK- α 2 (Prkaa2), which is the main cardiac isoform, was upregulated 2.3 ± 0.2 fold by Ucn1 and 1.9 ± 0.1 fold by Ucn2. Several reports have demonstrated that AMPK- α 2 can protect the myocardium from I/R injury. Carvajal et al. found that AMPK- α 2 deficiency resulted in reduced myocardial glucose uptake and glycogen content during I/R, leading to accelerated contracture (Carvajal et al., 2007). Mice expressing a kinase dead form of AMPK- α 2 had exacerbated contractile dysfunction following I/R, accompanied with elevated TUNEL positivity and caspase-3 activity (Russell et al. 2004). Scarabelli et al. previously reported improved myocardial energetics when administering Ucn1 before reperfusion (Scarabelli et al., 2002) and this energetic recovery of the ischaemic myocardium might therefore be linked to increased AMPK levels.

Nuclear factor erythroid 2-related factor 1 (Nfe2l1), also known as Nrf1, is a member of the CNC (cap 'n' collar)-basic leucine zipper family of transcription factors. Nrf1 is a crucial mediator of oxidative stress and is required for free radical scavenging and maintenance of redox potential. It achieves this through binding to the antioxidant response element (ARE) in a number of oxidative stress regulated gene promoters, including NAD(P)H:quinone oxidoreductase, glutathione-S-transferase, haem oxygenase-1, glutathione peroxidase, thioredoxin reductase 1 and aldo-keto reductases (Mathers et al., 2004). There are no reports

pertaining to the role of Nrf1 in I/R injury; however the related transcription factor Nrf2 has been shown to protect rats from cerebral I/R injury in a stroke model (Shih et al., 2005). I/R injury reduced the levels of Nrf1 by $84.5 \pm 6.1\%$ (-7.6 ± 1.2 fold) while tempol (6.2 ± 0.8), Ucn1 (4.0 ± 0.83) and Ucn2 (5.2 ± 0.8) all increased it and this was confirmed by qPCR (Fig 4.20a). The physiological effect of such a large reduction in Nrf1 levels during I/R is unknown but some conclusions can be drawn from studies of Nrf1 deficiency. Nrf1 knockout mice die mid gestation; however Nrf1^{-/-} fibroblasts display increased levels of cell death when treated with oxidants such as paraquat and cadmium chloride (Kwong et al., 1999). Likewise Nrf1^{-/-} foetal liver cells have been shown to be extremely sensitive to oxidative stress (Chen et al., 2003). Taken together this suggests that during I/R, transcriptional repression of Nrf1 leads to reduced levels of anti-oxidants which may sensitize cardiac myocytes to oxidative stress. In this setting, upregulation of Nrf1 levels by tempol, Ucn1 or Ucn2 may be important in aiding free radical scavenging and protecting from I/R injury.

Since Nrf1 is a major regulator of anti-oxidant proteins and both Ucn1 and Ucn2 upregulated Nrf1 to nearly the same level as tempol, the question was asked whether Ucn1 and Ucn2 could also afford some level of protection from oxidative stress. To address this question the levels of MDA in the left ventricle were measured in each group. Fig 4.20b shows that I/R injury increased MDA levels from 0.46 ± 0.05 to 0.91 ± 0.08 $\mu\text{mol MDA/g protein}$. As expected, tempol lowered the MDA concentration back to sham levels (0.44 ± 0.03 $\mu\text{mol/g}$); surprisingly though, Ucn1 lowered MDA levels to 0.52 ± 0.13 and Ucn2 to 0.38 ± 0.08 . This data shows that Ucn1 and Ucn2 are as efficient at inhibiting free radical formation as the SOD mimetic tempol and this previously unappreciated activity of urocortins may be central to their cardioprotective effects. It is likely that urocortins inhibit oxidative stress via an intermediary rather than possessing antioxidant activity *per se* and upregulation of Nrf1 may be a likely candidate for this effect. Therefore it would be of interest to examine the anti-oxidant capacity of Ucn1 in Nrf1 deficient cells.

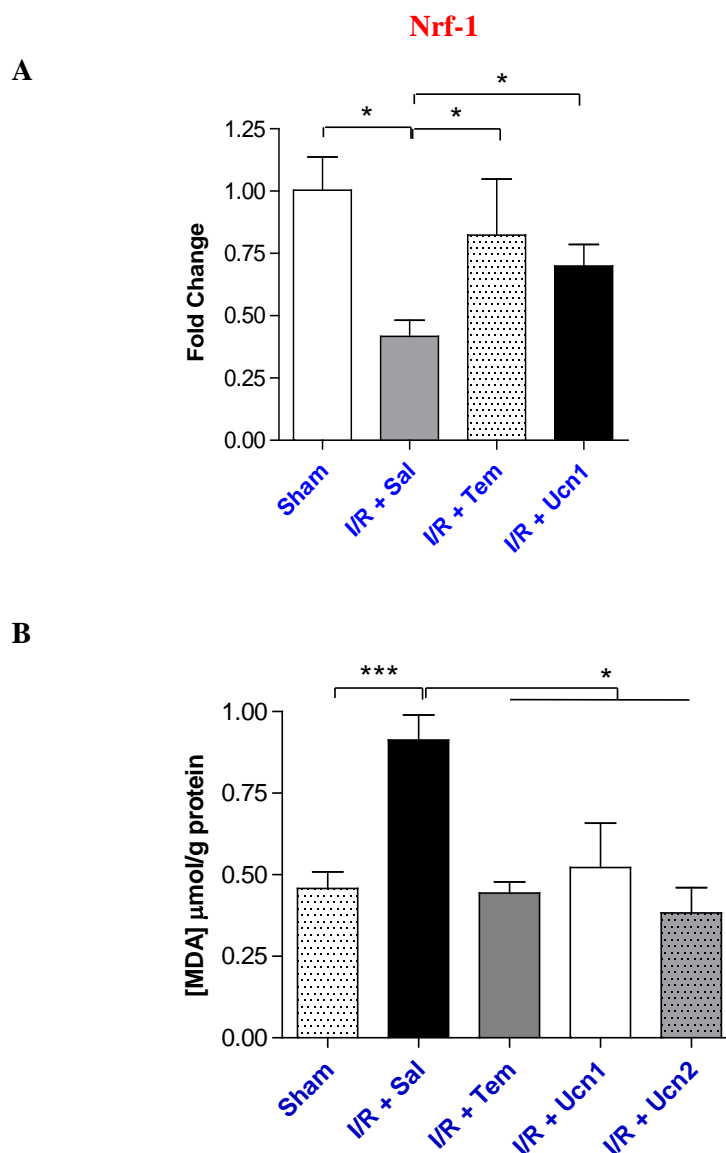


Fig 4.20. Ucn1 and Ucn2 inhibit free radical formation following I/R injury. (A) Nrf-1 levels were measured by qPCR and normalized to Sham. (B) Saline, tempol, Ucn1 or Ucn2 were infused after 25min ischaemia and was followed by 30min reperfusion. Tissue MDA levels were measured by HPLC from each of the indicated treatment groups n=5 animals. Statistical analysis was carried out using a one way ANOVA with Dunnet's post test, * p<0.05, *** p<0.001 compared to I/R + saline.

4.16 Discussion

Affymetrix microarray analysis was used to examine the change in MI induced gene expression in left ventricular tissue from rats. Detailed discussion of all differentially expressed genes is not possible due to the numbers involved, therefore I will discuss differential expression which is both novel and of interest to the pathogenesis of I/R injury. From the outset it must be acknowledged that the conclusions of this work are based on mRNA data which may not necessarily be mirrored by changes in protein expression. Being that as it may, novel transcriptional changes will be discussed with a view to confirming many of these changes by other means in the future.

One of the initial goals of the study was to ascertain if STAT3 target genes were induced during I/R injury and altogether a total of 46 known STAT3 targets were found to be differentially regulated by I/R. Therefore the increased phosphorylation of STAT3 described in chapter 3 was accompanied by induction of a STAT3 transcriptional programme. IL-6 and SOCS3 were highly upregulated by I/R injury, demonstrating that both activators and inhibitors of STAT3 activity are induced at the same time. The IL-6/SOCS3 balance may be in part responsible for controlling the levels of STAT3 phosphorylation shown in Fig 3.16a and a detailed kinetic analysis of IL-6 and SOCS3 levels during I/R injury would aid in understanding the dynamics of STAT3 activity. Tempol lowered the levels of both IL-6 and SOCS3 and this may impact on tempol mediated reduction in STAT3 phosphorylation. In contrast, Ucn1 increased mRNA levels of STAT3 and IL-6 while decreasing levels of SOCS3 and although there was no effect on STAT3 phosphorylation by 2 hr of reperfusion, examination of STAT3 activity over an extended time period might reveal novel effects of Ucn1 on STAT3 functionality. Recently Ucn1 has been shown to increase expression from a STAT3 dependent luciferase reporter in HEK293 cells suggesting that Ucn1 can indeed augment STAT3 activity (Pan et al., 2007).

The IL-17 receptor, IL-17A and IL-17F were all found to upregulated at the mRNA level *in vivo*. IL-17R was also found to be time-dependently increased by reperfusion in an *in vitro* model of I/R injury in NRVMs, however detailed examination of IL-17A and IL-17F expression by qPCR in this model proved to be problematic. These cells were shown to be capable of expressing both cytokines when using forced expression of STAT3. The effects of IL-17 on cardiac physiology are currently unknown. One recent report demonstrated that

exogenously added IL-17 could induce upregulation of MMP-1 in human cardiac fibroblasts, suggesting that it may play a role in cardiac remodeling (Cortez et al., 2007). IL-17 may also play a role in growth of vascular endothelial cells (Takahashi et al., 2005) and has also been implicated in the pathology of auto-immune myocarditis (Rangachari et al., 2006). Studies aimed at understanding the role of IL-17 in cardiac physiology and pathophysiology should give a greater insight into immunological responses during I/R. Experiments such as administering IL-17 or an IL-17 receptor antagonist during I/R injury *in vivo* or *ex vivo* will clarify if this cytokine is protective or detrimental to I/R-mediated pathology. Analysis of IL-17 plasma levels in patients suffering from myocardial infarction would also be of help to clarify if IL-17 is secreted during cardiac pathology in humans. It is not yet clear what are the major cell types which produce IL-17 during I/R injury. It is therefore of interest to address in more detail if cardiac myocytes can truly express IL-17A and IL-17F and to examine if IL-17A and IL-17F work in an autocrine or paracrine manner in the myocardium during I/R injury. Increased activity of STAT3 in the myocardium may also contribute to increased IL-17A and IL-17F levels, this could be tested directly by inhibiting STAT3 *in vivo* during I/R injury and measuring both serum levels and intracellular levels of these cytokines by flow cytometry.

One of the main gene ontology groupings in I/R mediated differential expression encompassed genes involved in mitochondrial regulation. Three main families of genes were affected; those involved in mitochondrial translation, the respiratory chain, and mitochondrial import; together totaling 95 separate gene expression changes. Although there is a large body of literature addressing general mitochondrial dysfunction during I/R injury, there is little information regarding changes in mRNA levels of genes involved in these three processes. In all three groups, the expression of genes was reduced and while the physiological effects of this reduction are currently unclear, it is likely that a decrease in components of the respiratory chain, translation and transport would all contribute to mitochondrial dysfunction. Again, this would need to be confirmed by western blot to make more definitive conclusions.

A large number of mitochondrial ribosomal proteins were downregulated by I/R. MRPs are thought to form a regulatory network and may all be coordinately regulated (Hi et al. 2007), suggesting the possibility that the reduced expression of 47 MRP genes may be due to alterations in one or a few MRP transcriptional regulators. The outcome of decreased MRP expression is unclear, but since MRPs are necessary for correct translation of mitochondrial

proteins, it is highly likely that this may slow or block mitochondrial biogenesis and thus contribute to reduced mitochondrial function during I/R injury. The biology of the MRP proteins is poorly understood at present and although their main function lies in regulation of mitochondrial gene translation, other functions have recently been ascribed to them. For example, MRPL41 increases p53 stability and enhances its translocation to the mitochondria where it promotes p53 mediated apoptosis (Yoo et al., 2005). MRPS36 plays a role in cycle progression by promoting increased expression of p21 (Chen et al., 2007). MRPL12, in addition to its role in translation, regulates mitochondrial transcription through binding bacteriophage-related RNA polymerase (POLRMT) (Wang Z 2007). Since MRPL12 is involved in both mitochondrial gene transcription and ribosome biogenesis, its reduction during I/R may play a key role in inhibiting mitochondrial protein synthesis. In humans, a mutation in MRP22 causes respiratory chain dysfunction, manifesting in hypotonia, cardiomyopathy and tubulopathy (Miller et al., 2004). A mutation in MRPS16 likewise damages the respiratory chain and leads to fatal neonatal lactic acidosis (Saada et al., 2007). These defects highlight the important role of MRPs in maintaining a functional respiratory chain and thus the I/R mediated repression of MRPs is suggested to compromise mitochondrial energetics and have direct effects on apoptosis and the cell cycle.

A total of 34 genes from all five of the mitochondrial respiratory chain complexes were repressed during I/R injury; none of these genes have been previously shown to be transcriptionally regulated by ischaemic injury in the myocardium. Reduced activity of the mitochondrial respiratory system has been well documented; however mitochondrial dysfunction has never been attributed to decreased mRNA levels of complex I-V components. At present it is not known what effect reduced expression of individual components of the respiratory complex has on mitochondrial energetics; reduced availability of 34 components in combination however would clearly be expected to perturb normal mitochondrial function. To fully understand the role of these individual genes it would be necessary to inhibit their expression (through RNAi for example) individually or in combination and then assess the state of mitochondrial respiration during I/R. It is also worth considering that although mitochondrial respiration is obligatory for maintaining cell viability, it can also contribute to ischaemic damage. For example, inhibition of complex I with rotenone reduces the production of ROS from complex I substrates, thereby protecting the heart from ischaemic damage (Lefensky et al., 2004). This suggests that the mitochondrial electron transport chain can contribute to the deleterious effects of ischemic damage.

The subunits that comprise the mitochondrial electron transport chain (ETC) are encoded by both the nuclear and mitochondrial genomes. Correct 1:1 stoichiometry is necessary to form functional complexes and this is governed by coordinated transcription from both genomes. Recently it has become clear that genes involved in oxidative phosphorylation are co-coordinately regulated. The transcription factors Nrf1, EREF, YY1F, PGC1 and CREB all correlate significantly with oxidative phosphorylation gene expression pattern and are thought to be the main regulators of this coordinated expression (van Waveren et al., 2008). Of these genes, only Nrf1 gave a signal on the microarray, mRNA levels being highly repressed by I/R. Nrf1 and the related transcription factor Nrf2 have previously been suggested to control the coordinated transcription of respiratory chain factors encoded by both the mitochondrial and nuclear genomes (Evans et al., 1990). Moreover, Nrf1 is known to play a pivotal role in regulating the expression of transcription and mitochondrial DNA maintenance factor (TFAM) and transcription specificity factors (TFB1M and TFB2M), both of which control mitochondrial gene expression (Dhar et al., 2008). Nrf1 has been shown to regulate all ten nuclear encoded COX subunits in neurons and Nrf1 binding sites have been found in Complex I, complex II and cytochrome C genes (Dhar et al., 2008, Elbehti-Green et al., 1998, De Sury et al., 1998, Xia et al., 1998, Venugopal et al., 1996). Nrf1 knock-out mice are not viable but analysis of Nrf1 deficient foetal livers demonstrated exuberant oxidative stress due to insufficient expression of the antioxidant genes GHS and GSSG (Chen et al., 2003). These studies all underscore the concept that Nrf1 is a master regulator of mitochondrial biogenesis and the novel finding that its expression is reduced during I/R may account in a large part for the reduced expression of oxidative phosphorylation genes. Nrf1 may also play a role in controlling the expression of mitochondrial transport proteins, for example the 5' flanking region of the Tom20 gene contains an Nrf1 binding site that controls its expression in conjunction with Nrf2 (Blesa et al., 2007).

I/R injury was found to downregulate several genes involved in controlling entry of proteins into the mitochondria. The TOM complex sits in the mitochondrial outer membrane and regulates protein transport into the intermembrane space. Two TOM components were downregulated by I/R, Tom7 and Tom20. Tom20 binds to mitochondrial presequences and Tom7 stabilises the main Tom40 translocase channel. Increasing or reducing levels of Tom20 in C2C12 skeletal muscle cells lead to a corresponding increase or decrease in malate dehydrogenase import into the mitochondria (Grey et al., 2000). At present there is only one

publication addressing the mitochondrial transport channel function during I/R. Boengler and colleagues showed that following 90 min of low-flow ischaemia in minipigs, the mitochondrial protein content of Tom20 was reduced and this effect was reversed by preconditioning. (Boengler et al., 2006). In skeletal muscle, contractile activity is associated with increased levels of Tom20 and inhibiting Tom20 expression reduced protein transport into the mitochondria (Grey et al., 2000). This lends weight to the argument that reduced Tom20 levels during I/R would result in a slower rate of mitochondrial import.

Proteins destined for the inner membrane and the matrix are transported by the TIM22 and TIM23 complexes respectively. Both the Tim23 channel and its regulatory subunit Tim17 were repressed by I/R. Tim44 which binds the mtHSP70 ATPase necessary to supply the energy for transport through the TIM23 complex was likewise downregulated by I/R. Interestingly, inhibition of Tim44 in human proximal tubular cells lead to a reduction in the mitochondrial import of SOD and glutathione peroxidase (Zhang et al., 2006). In addition, viral delivery of Tim44 reduced ROS production *in vivo* in both the balloon injury model of diabetic rats and in streptozotocin-induced diabetic CD-1 mice (Zhang et al., 2006, Matsuoka et al., 2005). Five components of the TIM22 complex also had reduced mRNA levels including the main Tim22 pore and the so called Tiny Tim accessory proteins Tim8a, Tim8b, Tim10 and Tim13 which aid in guiding proteins across the intermembrane space. Therefore, not only is there reduced availability of outer membrane pore components, correct trafficking of proteins inside the mitochondria is also likely to be disrupted during I/R injury.

The SAM complex controls the insertion of β -barrel proteins into the outer membrane and the three main components of this pore, Sam50, metaxin-1 and metaxin-2 were all reduced in expression. The SAM complex controls insertion of MPT pore proteins such as VDAC into the outer membrane; closure of VDAC is associated with reduced ATP exchange with the cytosol and the antiapoptotic Bcl-xL can maintain metabolite exchange across the outer membrane by maintaining VDAC in an open configuration (Vander Heiden et al., 2000, 2001), although this has recently been disputed (Baines et al., 2007). It is clear that reduced levels of the SAM complex will affect the constituents of the mitochondrial outer membrane and therefore may have a significant impact on the intrinsic pathway of apoptosis through the opening of the MPT pore.

Taken together, these observations all point to the fact that transport of proteins into the mitochondria may be reduced during I/R injury. Reduced availability of Tim, Tom and SAM proteins may represent a fundamental cause of decreased mitochondrial biogenesis during I/R. Further experiments aimed at addressing the role of mitochondrial import in I/R injury are likely to aid our understanding of mitochondrial biology and I/R injury. For example, GFP linked to mitochondrial pre-sequences could be used to measure the effect of ischaemic damage on the rate of import into the mitochondria. Likewise, inhibiting individual components of the import pathway could be used to assess the effects of TIM, TOM and SAM complex subunits on mitochondrial biogenesis, energy usage and ROS production. Since ischaemic preconditioning (IPC) is associated with increased rates of mitochondrial biogenesis (McLeod et al., 2005) it would also be informative to examine the expression of TOM, TIM and SAM complex components following IPC. Increased mitochondrial biogenesis during IPC might be linked to the expression of the mitochondrial transport apparatus and strategies aimed at restoring the mitochondrial import apparatus may prove to be cardioprotective. Reduced levels of mitochondrial transport proteins in conjunction with decreases in electron transport chain proteins and inhibition of the mitochondrial translation apparatus all represent previously unappreciated causes of mitochondrial dysfunction during I/R injury. Elucidation of the signalling pathways involved in these three processes will greatly add to our understanding of mitochondrial dysfunction and altered energy usage in myocardial infarction.

Although tempol is thought to exert its anti-oxidant properties by acting as a SOD mimetic, its affect on global gene expression has never been examined. Tempol was found to affect several genes of the contractile apparatus and genes involved in Ca^{2+} regulation. In cardiac myocytes, myofilament contraction occurs via sarcolemmal membrane depolarisation and release of Ca^{2+} from the sarcoplasmic reticulum stores through the ryanodine receptor (RyR). During diastole, ATP2a2 also known as Sarcoplasmic Reticulum Ca^{2+} -ATPase 2 (SERCA2) is responsible for pumping Ca^{2+} from the cytosol back to the sarcoplasmic reticulum to maintain intracellular Ca^{2+} homeostasis (Vangheluwe et al., 2006). Tempol was found to restore the expression of both SERCA2 and RyR. This is in agreement with a previous study where infusion of the antioxidants superoxide dismutase and catalase restored the levels of both RyR and SERCA2 after I/R injury (Temsah et al., 1999). Moreover, this underscores

the concept that a main focal point for anti-oxidant treatment is maintaining calcium homeostasis and restoring normal contractility to the heart.

Interestingly p53 was present as a central node in the single statistically significant networks identified in both the tempol and Ucn1 group. Neither tempol nor Ucn1 had any direct effects on p53 expression, however tempol has previously been shown to phosphorylate p53 on serine 18 in thymocytes, thereby stabilising its expression (Erker et al., 2005). Although phosphorylation of p53 by tempol or Ucn1 in the myocardium has not been demonstrated, its appearance in a central network is nonetheless intriguing. While p53 is undoubtedly central to apoptosis, it is also necessary for maintaining mitochondrial respiration via upregulation of Synthesis of Cytochrome c Oxidase 2 (SCO2) and in the absence of p53, SCO2 levels are reduced and cells switch their energy production from oxidative phosphorylation to glycolysis (Matoba et al., 2006). Therefore, examination of the effects of tempol and Ucn1 on p53 function in the myocardium warrant further investigation.

Both Ucn1 and Ucn2 lowered MDA concentration to near sham levels, demonstrating that urocortin administration significantly reduces free radical damage during I/R injury. The exact mechanism for this is unknown at the present time. Of the 67 genes which were differentially regulated in the tempol group, 21 were also changed by Ucn1 and 40 by Ucn2, demonstrating significant overlap between the groups. There was a total of 18 genes common to all three and of these, only 9 are currently annotated; Rpl7, H2A, Nfe2l1, Gbe1, Actr6, Orc4, Tmem98, Pja2 and Dut. From this list, Nfe2l1 (Nrf1) represents the most likely candidate gene common to all three which might be responsible for inhibiting free radical formation. In addition to its effects on mitochondrial gene expression, Nrf1 is a regulator of several anti-oxidant enzymes and the finding that tempol, Ucn1 and Ucn2 all increase its expression point to the fact that Nrf1 may represent a common mediator of anti-oxidant effects. Ucn1 treatment has recently been shown to prevent MPTP opening during I/R injury (Townsend et al., 2007) and upregulation of Nrf1 could conceivably contribute to this effect by increasing mitochondrial biogenesis and upregulating antioxidant levels in the heart. It would therefore be of great interest to examine the extent of urocortin mediated free radical inhibition in Nrf1-deficient cells. Thus it could be determined if urocortins are still capable of reducing free radical damage in the absence of Nrf1 and also if Nrf1 deficiency has any impact on urocortin mediated cardioprotection. If Nrf1 did indeed represent a common

mediator of Ucn1 and Ucn2 cardioprotection it could represent a novel downstream therapeutic target.

Taken together these observations identify novel transcriptional changes which occur during I/R injury. The documented changes in mitochondrial genes, uracil metabolism and the IL-17 pathway represent fruitful avenues of future research. The identification of a common transcription factor regulated by tempol, Ucn1 and Ucn2 may hold promise for future therapeutic intervention and the identification of a STAT3 transcriptional programme supports the findings of the previous chapter. In the future it will be necessary to also confirm the Ucn2 microarray changes by qPCR and confirm mRNA expression by western blot.

Chapter 5: Regulation of the DNA Damage Response by STAT3

5.1 Aims

In chapter 3 it was shown that STAT3 deficient MEFs were more sensitive to oxidative stress than wild type cells. A key feature of oxidative stress involves DNA damage and repair; following strand breaks, the DNA damage pathway is rapidly activated and generates signals to initiate both DNA repair and apoptosis. Although several studies have addressed the role of STAT3 in apoptosis, its contribution to the DNA damage response and DNA repair has never been investigated. This chapter addresses this by examining the DNA damage response pathway in STAT3 deficient MEFs.

5.2 STAT3^{-/-} MEFs Repair DNA Less Efficiently Than Wild Type Cells

In order to ascertain what effect STAT3 has on the DNA repair pathway, the host-cell reactivation assay (HCR) was used (Qiao et al., 2002). The HCR assay involves introducing strand breaks in luciferase plasmids followed by transfection into cells. The damaged plasmids are repaired by the cell's DNA repair machinery and only fully repaired plasmids will be transcribed correctly to generate active luciferase. The resulting luciferase activity is then compared against an undamaged control plasmid (set to 100%) to calculate a % of repair (known as % HCR). Initially a dose response of UVB irradiation was carried out; plasmids were irradiated with 25-1000 J/ UVB, transfected into wild type MEFs for 24 hr and the % HCR was calculated. Fig 5.1 shows that there was a dose dependent decrease in HCR with increasing UV irradiation; at the highest dose, 1000 J/ reduced the HCR to 3.4%.

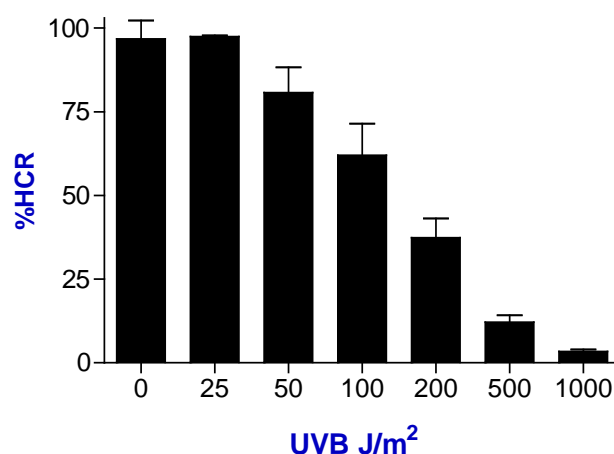


Fig 5.1. Rate of HCR in MEF cells with a dose response of UV irradiation. A luciferase plasmid was irradiated with the indicated dose of UV and transfected into MEF cells; 50 ng of luciferase plasmid and 20 ng renilla plasmid were used per well and values were measured 24 hr later with a luminometer. All values are relative to the non-irradiated control which was set to 100%.

Next the dose response was repeated and plasmids were transfected into both STAT3^{+/+} and STAT3^{-/-} MEFs for 16-48 hr. Fig 5.2 shows that at 16 hr and 24 hr there are no differences between cell types. However as the time for DNA repair increased between 32 hr and 48 hr, it was apparent that STAT3^{-/-} MEFs had a lower %HCR, indicating a reduced efficiency of DNA repair. This data shows that STAT3 deficient MEFs, although they are capable of repairing damaged DNA, do so at a slower rate and may be defective in the late phase of DNA repair. Accumulation of damaged DNA in STAT3 deficient cells may therefore have effects on the rate of apoptosis in these cells.

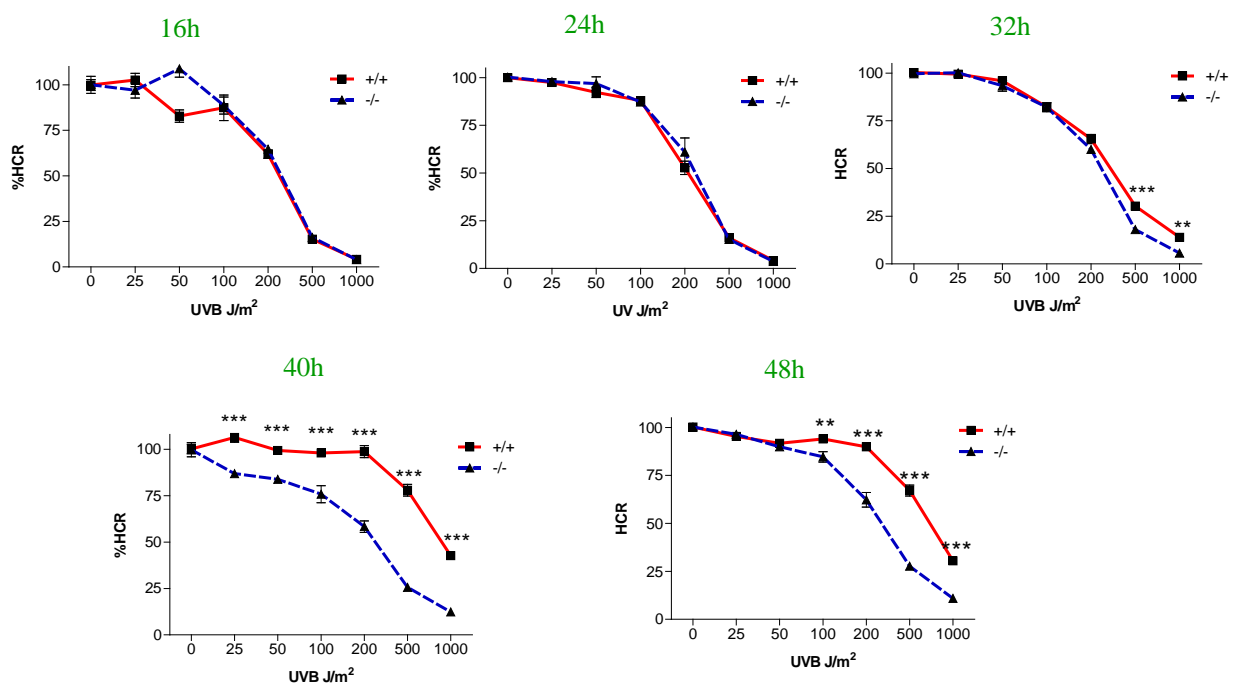


Fig 5.2. STAT3^{-/-} MEFs have reduced capacity to repair damaged DNA. STAT3^{+/+} and STAT3^{-/-} MEFs were transfected for 16-48 hr with 50 ng luciferase plasmids which were irradiated with the indicated doses of UV and 20 ng renilla plasmid in 96 well plates. Luciferase values were read with a luminometer, normalized to renilla and expressed as a percentage of un-irradiated control. A representative experiment is shown, n=6 per experiment, repeated in triplicate. Error bars represent mean ± SEM, statistical analysis was carried out using a Two-way ANOVA with Bonferroni post test, * p<0.05, ** p<0.01, *** P<0.005.

To show that reduced DNA repair in the STAT3^{-/-} cells was directly attributable to reduced STAT3 levels, STAT3^{-/-} MEFs were transfected with increasing concentration of STAT3 and a luciferase plasmid irradiated with 500 J/ UV; the HCR assay was carried out after 48 hr. Transfection of 100 ng STAT3 increased the % HCR from 31.8% to 43.5% and 300 ng STAT3 significantly increased the HCR to 74.4%, showing that STAT3 directly contributes to DNA repair (Fig 5.3). These results are consistent with the previous data (Fig 5.2) which showed that at 500 J/ after 48 hr, the % HCR in STAT3^{+/+} MEFs was 67.1% and in STAT3^{-/-} MEFs was 27.7%. Importantly this experiments shows for the first time that the level of STAT3 directly correlates with the level of DNA repair. This data thus predicts that cells which increase their expression of STAT3 (such as certain cancer cells) should repair damaged DNA more efficiently.

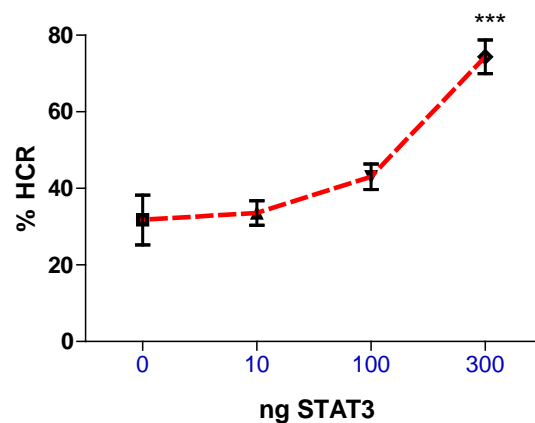


Fig 5.3. STAT3 increases the rate of DNA repair. Luciferase plasmids were treated with 500 J/ UV and transfected into STAT3^{-/-} MEFs with 10, 100 or 300 ng STAT3-pcDNA3 or pcDNA3 along with 20 ng renilla plasmid in 96 well plates. After 48 hr luciferase activity was measured with a luminometer, normalized to renilla and expressed as a percentage of non-irradiated control plasmid. The values were further normalized against pcDNA3 control values. Error bars represent mean \pm SEM, statistical analysis was carried out using a One-way ANOVA with Dunnett's post test. n=4 per experiment, repeated in duplicate. *** p<0.001.

5.3. STAT3^{-/-} MEFs Show Reduced Activity of the ATM/H2AX Pathway

Following DNA strand breaks, the DNA damage response pathway is quickly activated. The apical kinase in this pathway is ATM which phosphorylates several key proteins involved in DNA repair and apoptosis. Since STAT3 deficient cells repair DNA at a slower rate, the levels of activated ATM were examined in STAT3^{-/-} MEFs to ascertain whether this key DNA damage kinase is altered in these cells. STAT3^{+/+} and STAT3^{-/-} MEFs were treated for up to 4 hr with 10 μ M etoposide, a topoisomerase II inhibitor which induces DNA strand breaks. Etoposide treatment resulted in a time dependent increase in ATM phosphorylation in both STAT3 WT and knock-out cells; however the levels of phosphorylated ATM (pATM) were far lower at each time point in the STAT3^{-/-} cells (Fig 5.4a). Densitometric analysis for three separate experiment revealed that on average, pATM levels were 2.5 times higher in wild type cells (Fig 5.4b).

The histone H2AX is a major ATM substrate which becomes phosphorylated at serine 139 following strand breaks (known as γ -H2AX) and serves as a molecular beacon for the accumulation of DNA repair factors around the site of the break (Lowndes et al., 2005). Similarly to ATM, γ -H2AX was activated by etoposide in a time dependent manner, and again the levels were reduced in STAT3^{-/-} cells (Fig 5.4c). Densitometry showed that γ -H2AX levels were on average 3.5 times higher in wild type cells when examined over three experiments (Fig 5.4d).

Two other downstream targets of ATM are Chk1 which is involved in blocking the cell cycle following DNA damage and p53 which mediates both cell cycle arrest and apoptosis. Phosphorylation of Chk1 was seen within 30 min of etoposide treatment in WT MEFs and was dephosphorylated by 2 hr (Fig 5.5). The levels of γ -H2AX in STAT3^{-/-} MEFs however were far lower at 0.5 hr and 1 hr, suggesting that like γ -H2AX, ATM mediated Chk1 phosphorylation may be reduced in the absence of STAT3. ATM phosphorylates p53 on serine 15; examination of p53 levels in STAT3^{-/-} MEFs however revealed no difference to wild type cells (Fig 5.5). Taken together this shows that reduced activity of ATM in STAT3 deficient MEFs may result in lower levels of phosphorylated H2AX and Chk1 but not p53, underscoring a complex regulation of the DNA damage response pathway in these cells.

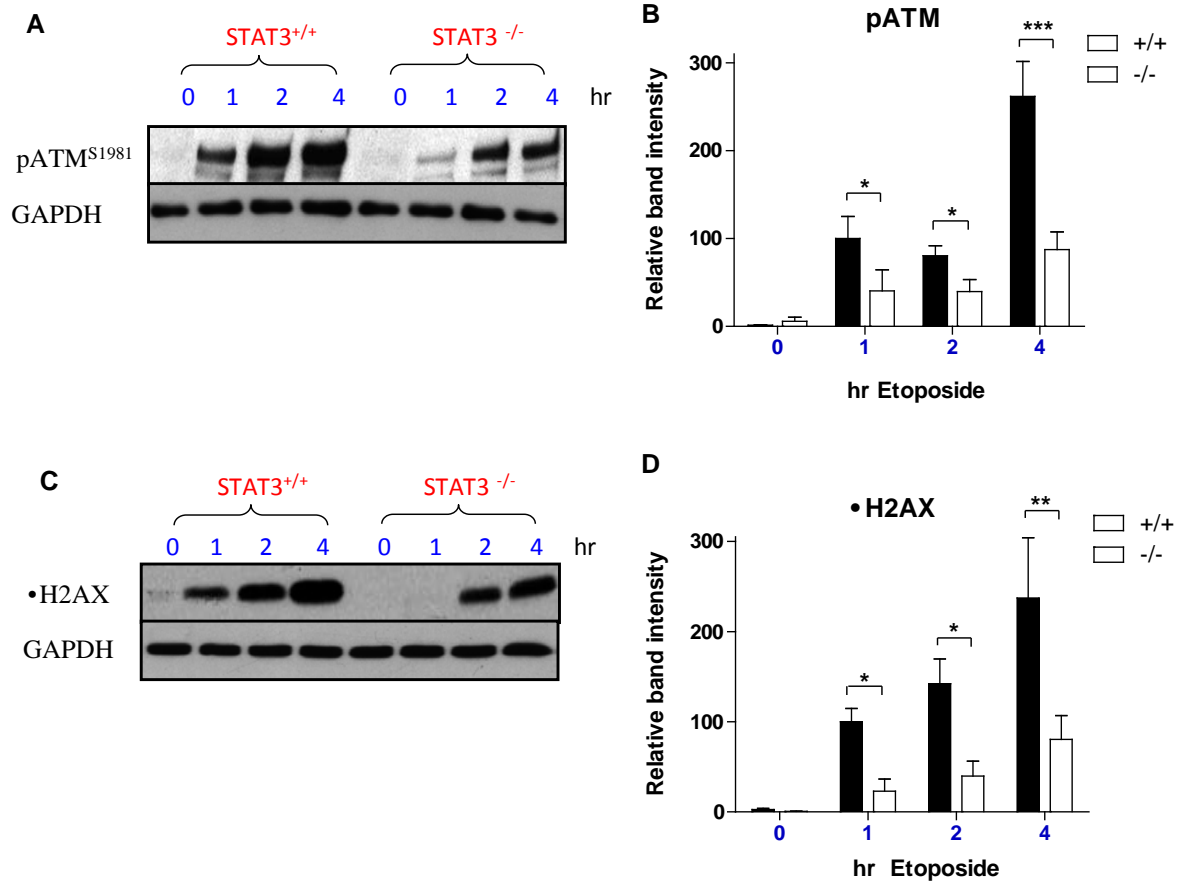


Fig 5.4. Phosphorylation of ATM and H2AX are reduced in STAT3^{-/-} MEFs. STAT3^{+/+} and STAT3^{-/-} MEFs were treated with DMSO (0 hr) or 10 μM etoposide for 1, 2 or 4 hr and western blots were carried out on cell lysates using antibodies for the phosphorylated forms of (A) ATM (pATM) and (C) H2AX (•H2AX), equal loading was confirmed using GAPDH. (B and D) Densitometry was carried out on three separate experiments by firstly normalizing to GAPDH levels and normalizing again to the band intensity at 1 hr which was arbitrarily set to 100. Error bars represent mean ± SEM, statistical analysis was carried out using a Two-way ANOVA with Bonferroni post test. * p<0.05, ** p<0.01, *** p<0.001

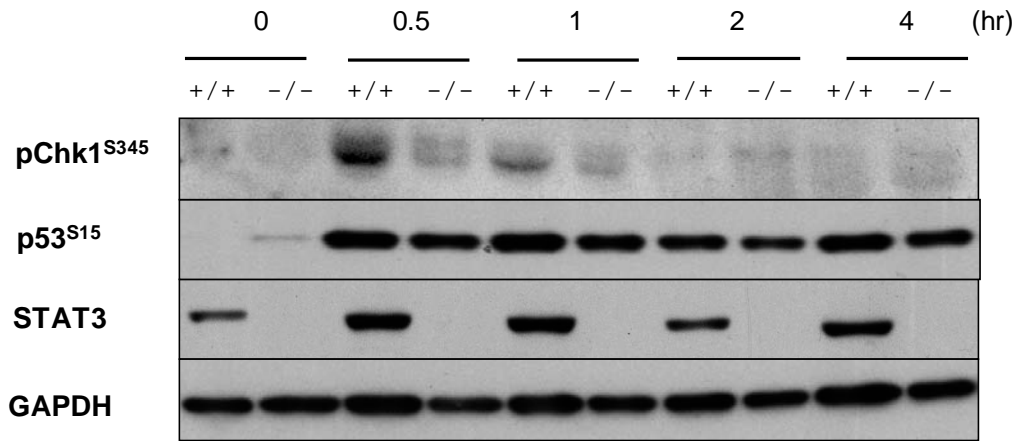


Fig 5.5. Phosphorylation of Chk1 but not p53 is reduced in STAT3^{-/-} MEFs. STAT3^{+/+} and STAT3^{-/-} MEFs were treated with DMSO (0 hr) or 10 μ M etoposide for 0.5, 1, 2 or 4 hr and western blots were carried out on cell lysates using antibodies for the phosphorylated forms of Chk1 (pChk1^{S345}), p53 (p53^{S15}) and total STAT3, equal loading was confirmed with GAPDH. The experiment was repeated in duplicate.

5.4. STAT3 Facilitates DNA Damage Mediated Upregulation of MDC1

The previous sections have demonstrated that activation of ATM and its downstream substrates are reduced in STAT3 deficient MEFs. MDC1 functions to amplify DNA damage signals by binding to γ -H2AX through its BRCT domain and to ATM via its FHA domain (Lou et al., 2006). This allows further recruitment of ATM to the sites of strand breaks and enhances the ATM mediated DNA damage response by facilitating ATM dependent phosphorylation of Nbs1, 53BP1 and BRCA1 (Stucki et al., 2005). Although MDC1 has no effect on the initial activation of ATM and H2AX, it is required to maintain the DNA damage response past the initial activation phase (Lou et al., 2006). Since several other mediators of the DNA damage response were dysregulated in STAT3^{-/-} MEFs, it was of interest to examine the regulation of MDC1 in these cells.

The mRNA levels of MDC1 were measured in STAT3^{+/+} and STAT3^{-/-} MEFs by qPCR and no difference was seen between cell types (Fig 5.6a). Next, the regulation of MDC1 levels by STAT3 following DNA damage was assessed. It is unknown whether the expression of MDC1 is altered by DNA damage, therefore WT MEFs were treated with 10 μ M etoposide for up to 24 hr and MDC1 mRNA levels were measured. Fig 5.6b shows that MDC1 levels increased over time following DNA damage with etoposide, and a significant increase could be seen by 12 hr. STAT3^{-/-} MEFs were then treated with 10 μ M etoposide for 12 hr and compared to wild type cells (Fig 5.6c). In contrast to the 2 fold increase in MDC1 levels in WT cells, STAT3^{-/-} MEFs did not show any increase in MDC1 levels at 12 hr. To ascertain if increased MDC1 levels is a general feature of DNA damage, WT MEFs were irradiated with 10 Gy γ -IR and allowed to recover for 2, 8 and 24 hr (Fig 5.6d). At 8 hr and 24 hr after irradiation, MDC1 levels were significantly increased. Comparison of γ -IR mediated MDC1 upregulation showed that MDC1 failed to be upregulated in STAT3^{-/-} MEFs which supports the findings with etoposide (Fig 5.6e).

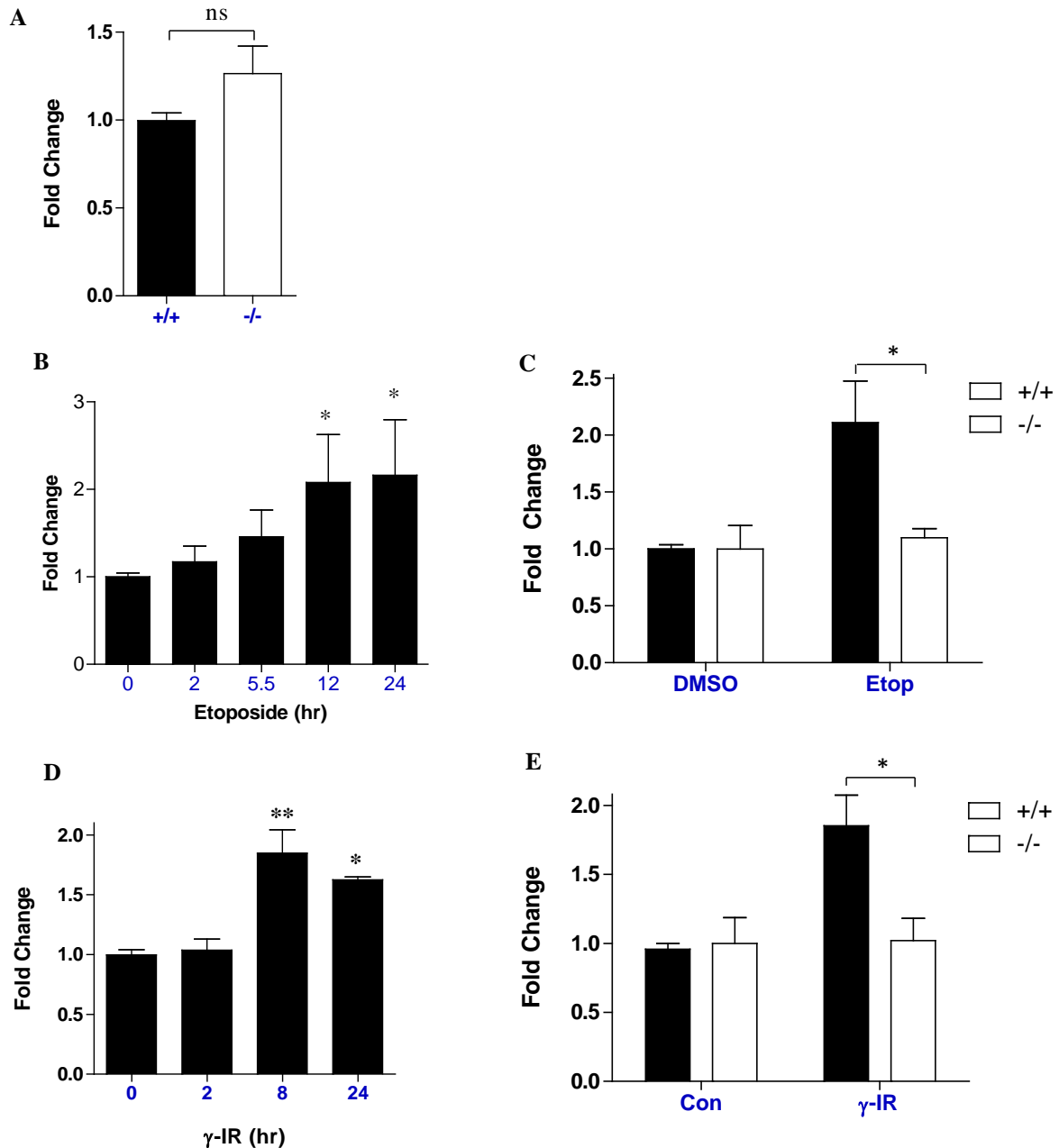


Fig 5.6. DNA damage mediated increase in MDC1 expression is compromised in STAT3^{-/-} MEFs. (A) Basal MDC1 expression was measured in STAT3^{+/+} and STAT3^{-/-} MEFs by qPCR. (B) Wild type MEFs were treated with 10μM etoposide for the indicated times and MDC1 levels were measured by qPCR. (C) STAT3^{+/+} and STAT3^{-/-} MEFs were treated for 12 hr with 10μM etoposide and MDC1 levels were measured by qPCR. (D) Wild type MEFs were treated with 10 Gy •-irradiation for the indicated times and MDC1 levels were measured by qPCR. (E) STAT3^{+/+} and STAT3^{-/-} MEFs were treated for 8 hr with 10 Gy •-irradiation and MDC1 levels were measured by qPCR. Error bars represent mean ± SEM, Statistical analysis was carried out using a student's t-test (A), one-way ANOVA with Dunnett's post test (B, D) or a two-way ANOVA with Bonfferoni post test (C,E), n=2 per experiment, repeated in triplicate. * p<0.05, ** p<0.01.

The STAT3 dependent regulation of MDC1 expression was examined in greater detail using an MDC1 promoter luciferase construct (Townsend et al., 2005). The MDC1 luciferase reporter was co-transfected with pcDNA3, STAT1, STAT3[•] or STAT3[•] into four separate cell lines; Chinese hamster ovary cells (CHOs), MEFs and the fibrosarcoma cell lines 2ftgh and U3A (Fig 5.7a). Luciferase activity was measured after 24 hr and in each cell line tested, both STAT3[•] and STAT3[•] increased MDC1 promoter activity. In contrast, STAT1 had no effect on MDC1 promoter levels.

Next, STAT3^{-/-} MEFs were co-transfected with 10, 50 or 300 ng of STAT3 expression plasmid and the MDC1 reporter, treated with 10 Gy of •-IR and assessed for luciferase activity after 24 hr (Fig 5.7b). STAT3 dose dependently increased MDC1 promoter activity and this effect was enhanced by •-IR, reaching a maximum level of 5 fold over control levels when transfected with 300 ng STAT3. In order to see if both tyrosine 705 and serine 727 were necessary for this STAT3 dependent effect, the MDC1 promoter construct was co-transfected with STAT3 mutant plasmids; Y705F, S727A and a plasmid with both mutations (Y705F/S727A) (Fig 5.7c). Mutation of the Y705 site had no effect when compared to wild type STAT3, both enhanced MDC1 promoter activity by 2.5 fold. This suggests that phosphorylation at Y705 may not be necessary for STAT3 mediated upregulation of MDC1. Surprisingly, mutation of the serine 727 site or mutation of both sites led to a 40% increase over WT STAT3 levels, suggesting that phosphorylation of STAT3 at serine 727 reduces STAT3 mediated upregulation of the MDC1 promoter.

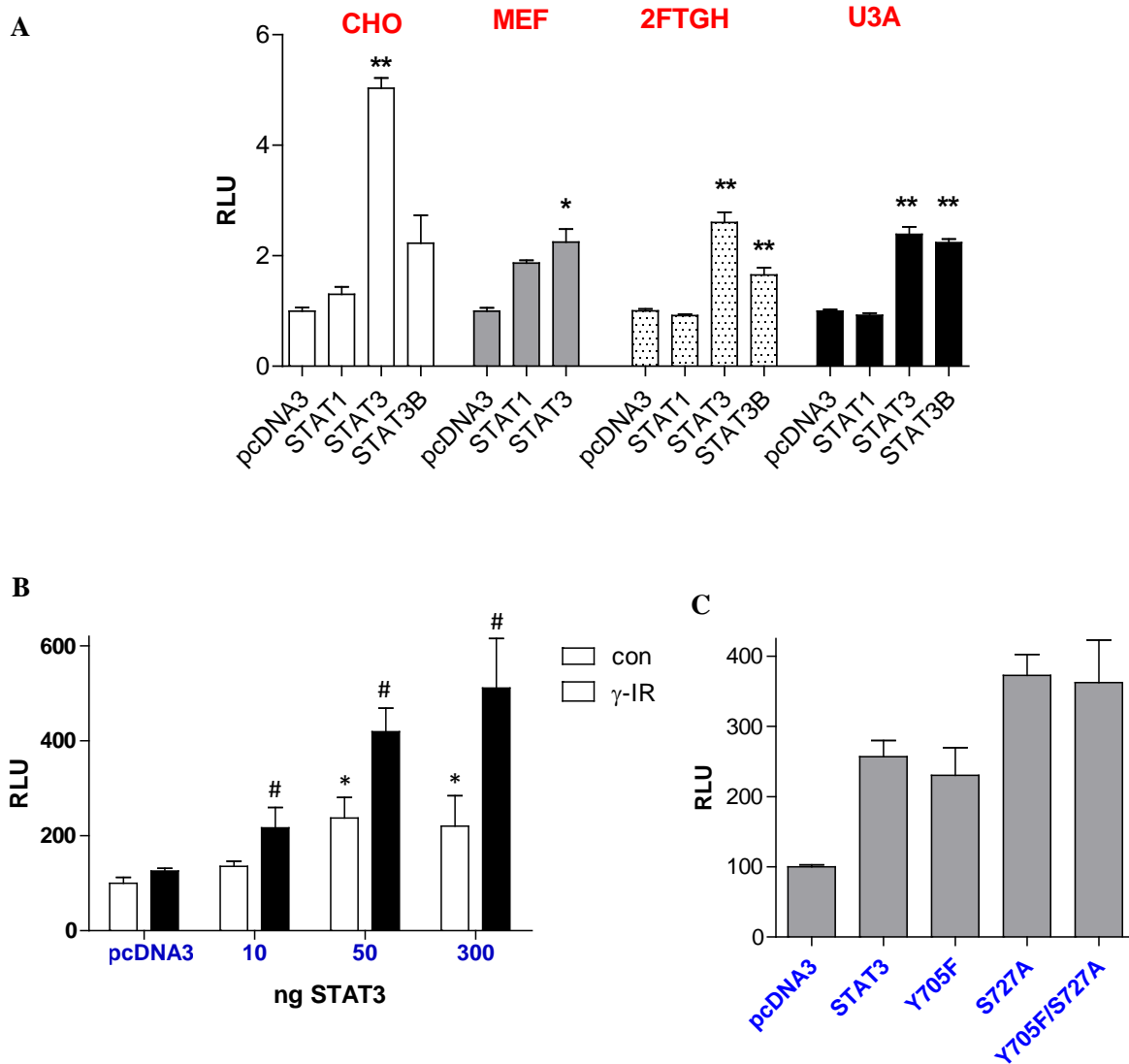


Fig 5.7. STAT3 regulates the MDC1 promoter. (A) CHO, MEF, 2FTGH or U3A cells were transfected with 50 ng pcDNA3, STAT1, STAT3 or STAT3 \bullet expression plasmids together with 50 ng of MDC1 reporter and 20 ng of renilla plasmid. Luciferase activity was measured after 24 hr. (B) STAT3 $^{-/-}$ MEFs were transfected with 50 ng MDC1 expression plasmid, 20 ng renilla plasmid and 10, 50 or 300 ng STAT3 expression plasmid or the corresponding amount of pcDNA3 for 24 hr and then left untreated (con) or treated with 10 Gy \bullet -IR, luciferase activity was measured after 48 hr. (C) STAT3 $^{-/-}$ MEFs were transfected with 50 ng MDC1 reporter, 20 ng renilla and 50 ng of pcDNA3, STAT3, Y705F, S727A or Y705F/S727A in 96 well plates and luciferase activity was measured after 24 hr. Experiments were repeated in triplicate, n=6 per experiment, luciferase values were normalized to renilla levels and then re-normalised to appropriate pcDNA3 controls and expressed as relative luciferase units (RLU). Statistical analysis was carried out using a student's t-test (A and C) or a Two-way ANOVA with Bonfferoni post correction. * p<0.05, ** p<0.01. In B, * is compared to pcDNA3 control and # is compared to pcDNA3 \bullet -IR.

5.5 Discussion

Efficient repair of damaged DNA is essential to maintain genomic stability and cell survival. Although STAT3 has been shown to function as an anti-apoptotic transcription factor, there is little published data regarding its role in the DNA damage response. STAT3 deficient MEF cells were found to be less efficient at repairing damaged DNA from a transfected reporter construct, suggesting that STAT3 is necessary for optimum DNA repair. Since STAT3^{-/-} MEFs are less efficient at repairing damaged DNA, it is possible that DNA breaks may persist for longer in STAT3 deficient cells. In addition, artificially increasing the levels of STAT3 correlated with increased ability to repair DNA and restored the repair defect phenotype of knock-out cells.

Several cancers are associated with elevated STAT3 levels, including multiple myelomas, lymphomas, breast, head and neck, lung, pancreatic and prostate cancers (Yu and Jove, 2004). Moreover, elevated STAT3 activity is thought to contribute to chemoresistance in these malignancies (Barre et al., 2007) and targeting of STAT3 has been shown to restore sensitivity to chemotherapeutic drugs (Gariboldi et al., 2007, Alas et al., 2003). Thus over the past 5 years, STAT3 has emerged as a major new target for anti-cancer therapy (Yu and Jove, 2004). STAT3 mediated chemoresistance has been attributed to upregulation of anti-apoptotic STAT3 target genes such as cyclin D1, Bcl- and survivin (Gritsko et al., 2006, Turkson et al., 2005) and the data presented here now add to the understanding of how STAT3 may contribute to chemoresistance. Although the experiments were done in mouse embryonic fibroblasts, speculation can be made as to how these results elucidate the contribution of STAT3 to chemoresistance. Expression of STAT3 was associated with an enhanced ability to repair damaged DNA. By inference this suggests that cancer cells which overexpress STAT3 may be resistant to chemotherapeutics through their increased efficiency of DNA repair and greater resistance to genotoxic stress. It would therefore be of interest to examine the rate of DNA repair following treatment with chemotherapeutic drugs in tumor cells with elevated STAT3 expression. Thus the HCR assay could be conducted on cancer cell lines which have varying expression of STAT3 to examine the correlation between STAT3 expression and DNA repair. If the conjecture that elevated STAT3 levels in cancer contribute to increased efficiency of DNA repair, it would offer an alternative explanation for chemoresistance in these tumors.

Molecular analysis of the DNA damage response pathway in $STAT3^{-/-}$ MEFs revealed several possible explanations for the reduced repair efficiency. The apical kinase in the DNA damage response is ATM which undergoes autophosphorylation after DNA damage, followed by dimer dissociation and activation (Bakkenist and Kastan, 2003). ATM is responsible for phosphorylation of a host of proteins involved in DNA repair and cell cycle arrest and skin fibroblasts from Ataxia-telangiectasia patients have a reduced capacity to repair damaged DNA in conjunction with decreased HCR levels (Hannan et al., 2002). The reduced activity of ATM in $STAT3^{-/-}$ MEFs may therefore lead to dysregulation of repair proteins resulting in sub-optimal efficiency of DNA repair.

The activity of several downstream proteins in the ATM pathway were analysed in $STAT3^{-/-}$ MEFs. Phosphorylation of both H2AX and Chk1 was decreased in the absence of STAT3; however there was no effect on phosphorylation of p53. Phosphorylation of H2AX by ATM is a key event in the DNA damage response; it leads to the recruitment of repair factors directly to the site of strand breakage (Celeste et al., 2002). Thus H2AX deficient cells are sensitive to radiation and have a reduced capacity to repair double strand breaks (Bassing et al., 2002). The level of both γ -H2AX and pATM activity after 1 hr etoposide treatment in wild type cells was only reached after 4 hr in $STAT3^{-/-}$ cells (Fig 5.4b,d), suggesting that DNA damage signaling occurs at a slower rate in STAT3 deficient cells. This reduced phosphorylation of H2AX in $STAT3^{-/-}$ MEFs following etoposide treatment in conjunction with reduced active ATM might in part account for the slower rate of DNA repair in these cells. Reduced activity of H2AX would be expected to slow the rate of accumulation of DNA repair factors around the site of strand breakage, thereby hampering the DNA repair process. One caveat to this observation however is that since plasmid DNA does not contain histones it is unclear whether transfection of a plasmid with double strand breaks activates endogenous γ -H2AX. It would therefore be of interest to examine the rate of endogenous DNA repair in $STAT3^{-/-}$ MEFs to confirm that the decreased activity of ATM and H2AX does indeed lead to decreased repair efficiency, this could be achieved using the comet assay for example (Singh et al., 1998).

Chk1 phosphorylation at serine 345 was also shown to be reduced in $STAT3^{-/-}$ MEFs. Chk1 phosphorylation leads to its release from chromatin where it in turn phosphorylated the CDC25 phosphatases and targets them for destruction by ubiquitin-mediated proteolysis (Cimprich and Cortez, 2008). This promotes CDK activation and cell cycle checkpoint block

(Cimprich and Cortez, 2008). Chk1 can be phosphorylated by both ATM and ATR and although ATR phosphorylation was not examined in STAT3^{-/-} MEFs, it has been shown to lie downstream of ATM following DSB formation (Jazayeri et al., 2006). The importance of serine 345 phosphorylation in Chk1 is underscored by the finding that mutation of this site on Chk1 dysregulates checkpoint control and leads to mitotic catastrophe (Niida et al., 2007). Reduced phosphorylation of Chk1 in STAT3^{-/-} cells would be expected to abrogate cell cycle arrest through the checkpoint system and examination of cell cycle profiles from STAT3 deficient cells could be used to address this.

Active ATM phosphorylates p53 on serine 15 following ionizing radiation or radiomimetic drug treatment and this appears to be necessary for fully fledged activation of p53 (Banin et al., 1998, Fiscella et al., 1993). p53 serine 15 phosphorylation proceeded with equivalent kinetics following etoposide treatment in both WT and knock-out STAT3 cells. This finding demonstrates that not all aspects of the ATM pathway are affected. Why •H2AX and Chk1 phosphorylation is reduced but p53 phosphorylation is unaltered in STAT3^{-/-} MEFs is currently unknown. Other p53 kinases may be involved in regulating p53 activity in STAT3 deficient cells, for example both ERK and p38 MAPK have been shown to be capable of phosphorylating (She et al., 2000)

STAT3 was also shown to be capable of modulating MDC1 expression. Although MDC1 levels were not increased over the time frame in which pATM and •H2AX activity were examined (1-4 hr), the increased expression of MDC1 by 12 hr is expected to promote further recruitment of DNA repair factors to the site of strand breakage. STAT3 deficient MEFs failed to upregulate MDC1 expression in response to etoposide and •-IR. Furthermore, STAT3 but not STAT1 upregulated the activity of an MDC1 promoter construct and transfection of STAT3 enhanced •-IR mediated MDC1 upregulation. It is not yet clear whether STAT3 directly regulates the MDC1 promoter or if it does so through an intermediate STAT3 dependent protein. This could be addressed in two ways, firstly through the use of chromatin immunoprecipitation to ascertain if STAT3 can bind directly to the MDC1 promoter. In addition transfection of constitutively active STAT3 in the presence of transcriptional inhibitors would reveal whether MDC1 upregulation occurs through STAT3 mediated transactivation of an MDC1 regulator. Recently Sp1 has been identified as a direct transcriptional activator of the MDC1 promoter (Bu et al., 2008). STAT3 might therefore co-

operate with Sp1 at the MDC1 promoter, indeed STAT3 has previously been shown to bind to Sp1, thereby enhancing Sp1 mediated upregulation of VEGF (Loeffler et al., 2005). Surprisingly neither the Y705 or S7272 sites of STAT3 appeared to be necessary for MDC1 upregulation. Indeed mutating the S727 site to an alanine actually enhanced STAT3 mediated MDC1 upregulation (Fig 5.7c) suggesting that phosphorylation at this site may reduce the transactivation capacity of STAT3. It has previously been demonstrated that phosphorylation of STAT3 may not be necessary to induce transcriptional upregulation (Chatterjee-kishore et al., 2000, Yang et al., 2005). Indeed if STAT3 does prove to upregulate MDC1 indirectly, it may be through protein-protein binding which might not require Y705 phosphorylation.

Taken together, this shows that STAT3 is necessary for the upregulation of MDC1 levels following DNA damage and impaired MDC1 expression may contribute to the reduced efficiency of DNA repair in STAT3^{-/-} MEFs. In addition, it can be speculated that cancer cells overexpressing STAT3 might also have elevated MDC1 levels, allowing more efficient DNA repair and thus contributing to chemo-resistance. However analysis using both the Cancer Genome Anatomy Project and Oncomime cancer expression databases revealed few MDC1 overexpressing cancers and none of these was associated with increased STAT3 expression. More detailed analysis of cancer cells from patients with chemoresistance may prove more informative.

Although these studies were limited to mouse embryonic fibroblasts and DNA damage was induced predominantly with etoposide; some general conclusions can still be made. These studies have demonstrated that STAT3 is necessary for efficient repair of damaged DNA. Several candidate proteins which could mediate this affect have been highlighted, including ATM, H2AX, Chk1 and MDC1. Increased expression and/or activity of STAT3 in tumors is suggested to contribute to chemoresistance through the possibility of increasing the activity of ATM and its downstream targets and upregulating MDC1 expression, allowing more efficient localization of repair proteins to sites of damaged DNA. In future studies, direct imaging of DNA damage response factors at the sites of DNA breaks in tumor cells with varying levels of STAT3 will highlight any differences in duration of chromatin occupancy which might be influenced by STAT3.

Chapter 6: Regulation of the MAPK Pathway in Inflammation

6.1 Aims

During the course of doctoral work the opportunity arose to carry out research at the lab of Prof Richard Flavell at Yale University. The experiments described in this chapter were all carried out in the Flavell lab and thus represent a separate body of work from the previous chapters. In chapter 4, MAPK phosphatase-1 (MKP-1) was found to be upregulated by I/R injury and inhibited by antioxidant treatment. MKP-1 upregulation coincided with reduced phosphorylation of p38 MAPK and ERK. In this chapter, the effect of MKP-1 deletion on MAPK activity is explored. The aims were to characterise the immune phenotype of MKP-1 deficient mice and explore the relationship between altered MAPK responses and inflammation. In addition, the effect of MKP-1 on acquired immunity was also examined.

6.2 MKP-1 Deficient Mice have Elevated Cytokine Production, are Hyper-responsive to Endotoxic Shock and are Less Susceptible to *Listeria Monocytogenes* Infection *in vivo*.

The reaction to bacterial LPS is a well characterised innate immune response which can lead to endotoxic shock due to systemic overproduction of pro-inflammatory cytokines. Cytokine production by LPS is dependent on activation of MAPKs which in turn are suppressed by the activity of MKPs. In order to further characterise the role of MAPK in cytokine production, MKP-1 deficient mice were used, Fig 6.1 shows genotyping of MKP-1^{+/+}, MKP-1^{+/-} and MKP-1^{-/-} mice. Age and sex matched MKP-1^{+/+} and MKP-1^{-/-} mice were treated with 10 mg/kg LPS and serum cytokine levels were measured after 3 hours (Fig 6.2). MKP-1^{-/-} mice showed 8 fold and 4 fold higher levels of TNF-• and IL-6 respectively. Although less pronounced, there were significant increases in IL-1•, IL-12, IL-10, IL-4 and GM-CSF in MKP-1^{-/-} mice while no significant difference was observed in the levels of IL-2, IL-5 and IFN-•. Thus the absence of MKP-1 has a dramatic effect on the cytokine profile following LPS challenge and the results clearly demonstrate that MKP-1 negatively regulates cytokine production *in vivo*. Interestingly, although the majority of cytokines that were enhanced in MKP-1^{-/-} mice were pro-inflammatory, the levels of the anti-inflammatory IL-10 were elevated 8 fold, this suggests that MKP-1 does not simply function to inhibit pro-inflammatory mediators, rather it may have a more complex regulatory role in controlling the response of the innate immune system.

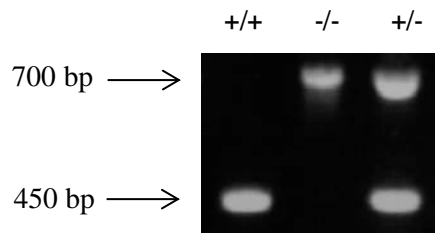


Fig 6.1 MKP-1 genotyping. Genotyping was carried out as described in methods, wild type mice had a PCR product of 450bp, MKP-1 deficient mice had a PCR product of 700 bp and heterozygote DNA contained both bands

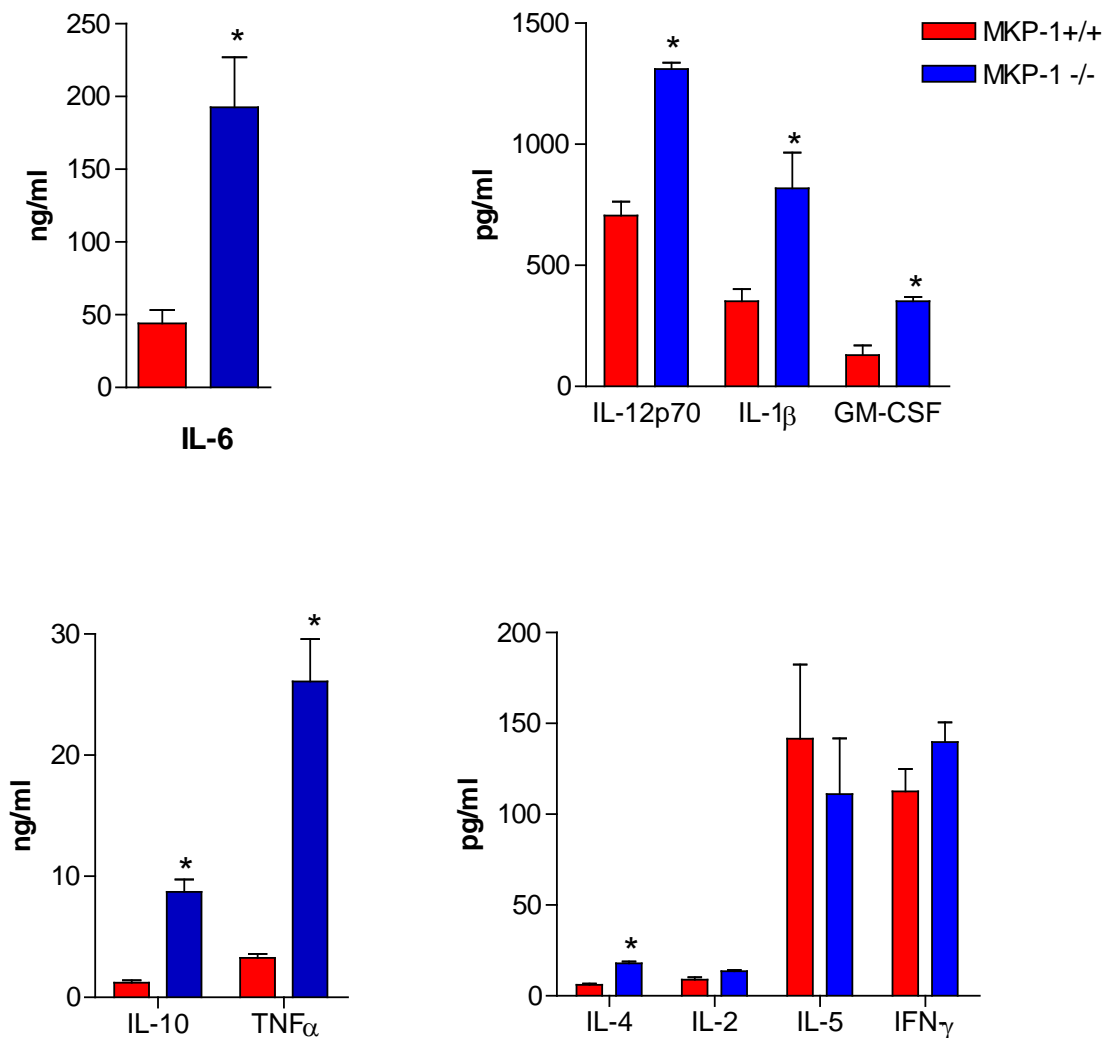


Fig 6.2 MKP-1^{-/-} mice show enhanced cytokine production following LPS challenge. Serum cytokine levels were measured by Bioplex assay following 3 hr challenge with 10 mg/kg LPS. Data show mean \pm SD for 5 mice per group, * $p < 0.05$ determined using students *t*-test.

In order to ensure that the results obtained were not due to differences in generation of the myeloid and dendritic cell lineages in MKP-1^{-/-} mice, total spleen and lymph node were stained with CD11b and CD11c. No difference in cell numbers were seen in CD11b⁺ myeloid cells, and CD11b⁻CD11c⁺ and CD11b⁺CD11c⁺ dendritic cell populations between genotypes (Fig 6.3). Therefore the increase in cytokine levels are in fact due to elevated cytokine production and not due to increased cell numbers.

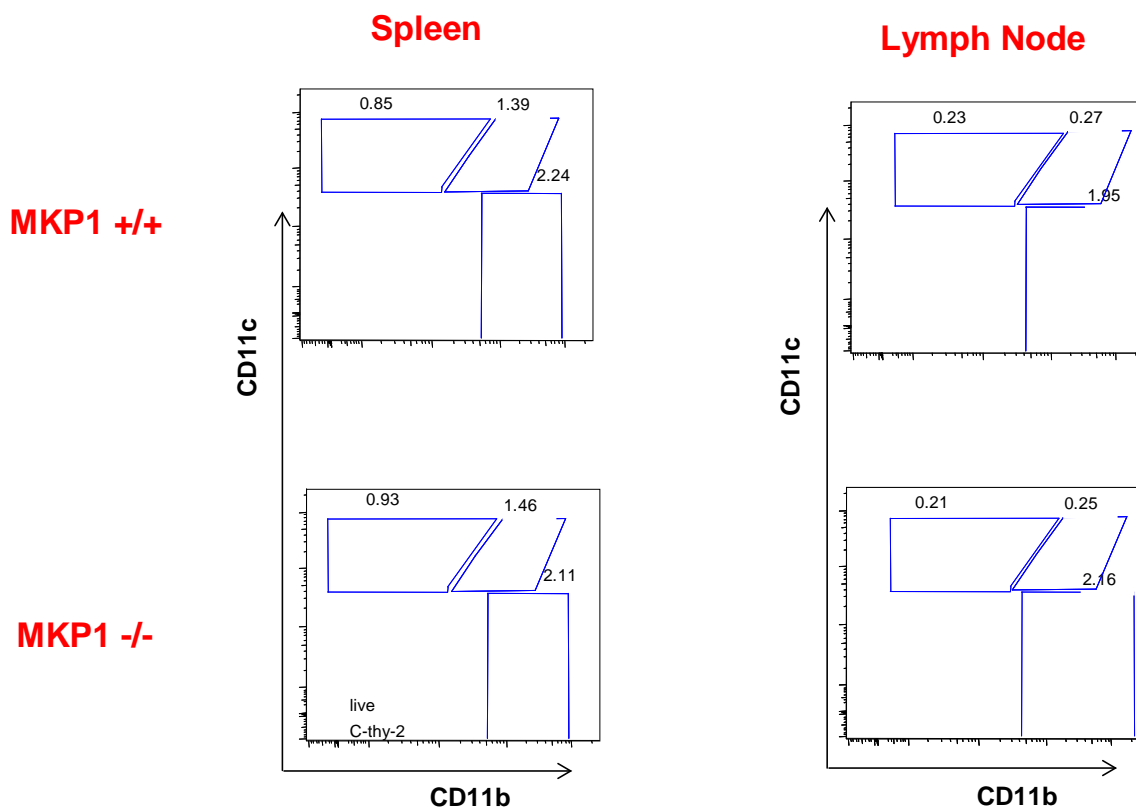


Fig 6.3 Flow cytometry analysis of myeloid cells markers in MKP-1^{+/+} and MKP-1^{-/-} mice. Total spleen and lymph nodes were harvested from MKP-1^{+/+} and MKP-1^{-/-} mice, digested with collagenase, stained with CD11b and CD11c antibodies and analysed by flow cytometry. Percentages of CD11b⁺ myeloid cells, and CD11b⁻CD11c⁺ and CD11b⁺CD11c⁺ dendritic cell populations are shown. Representative flow cytometry plot from 3 mice.

The pathological consequences of endotoxic shock are attributed to the damaging effects of high levels of TNF- α , IL-6 and IL-1 β induced by LPS. Since these three cytokines were elevated in MKP-1 $^{-/-}$ mice, the question was asked whether MKP-1 has a role to play in the mortality induced by toxic shock. MKP-1 $^{+/+}$ and MKP-1 $^{-/-}$ mice were injected *i.v* with two doses of LPS and survival was monitored over 48 hours. Administration of 10 mg/kg LPS resulted in 100% mortality in MKP-1 $^{-/-}$ by 18 hr, whereas wild type mice died between 24 and 48 hr. At the lower dose of 2.5 mg/kg LPS, all the MKP-1 $^{-/-}$ died within 24 hr whereas wild type mice survived significantly longer (Fig 6.4). This suggests that MKP-1 plays a distinct role in controlling the innate inflammatory response following endotoxic shock and in the absence of MKP-1, elevated levels of pro-inflammatory cytokines have significant detrimental effects on mortality.

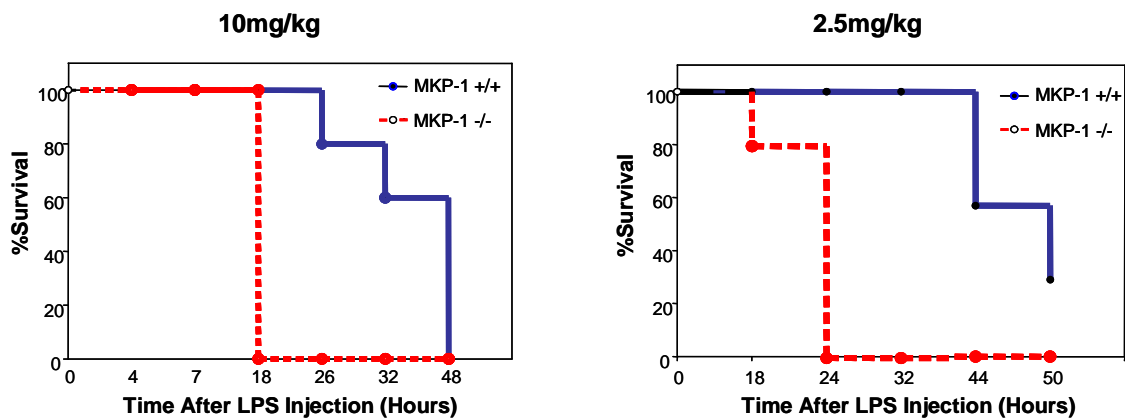


Fig 6.4. MKP-1 $^{-/-}$ mice are hyper-responsive to endotoxic shock *in vivo*. MKP-1 $^{+/+}$ (solid line) and MKP-1 $^{-/-}$ mice (dotted line) were injected *i.p* with either 10 mg/kg or 2.5mg/kg LPS and survival was monitored up to 50 hours. Both treatments resulted in significant differences between groups, $p=0.008$ and $p=0.004$ for 10 mg/kg and 2.5 mg/kg respectively, log-rank (Mantel-Cox) test, $n=5$.

To determine if overproduction of pro-inflammatory cytokines in MKP-1^{-/-} affects the outcome of bacterial infection, MKP-1^{-/-} and wild type mice were inoculated with 1.0 x 10⁸ particles of *Listeria monocytogenes*. Although the natural route of *L. monocytogenes* infection is through mucosal surfaces following ingestion, for experimental purposes *i.v* injection is used. This facilitates uptake of bacteria from the bloodstream by splenic and hepatic macrophages (Pamer, 2004). Examination of bacterial burden in the spleen and liver revealed that MKP-1^{-/-} mice had a reduced bacterial load following 72 hours of infection. This suggests that elevated levels of pro-inflammatory cytokines in MKP-1^{-/-} mice may be effective in slowing the progress of bacterial infection through enhanced bacterial killing and clearance.

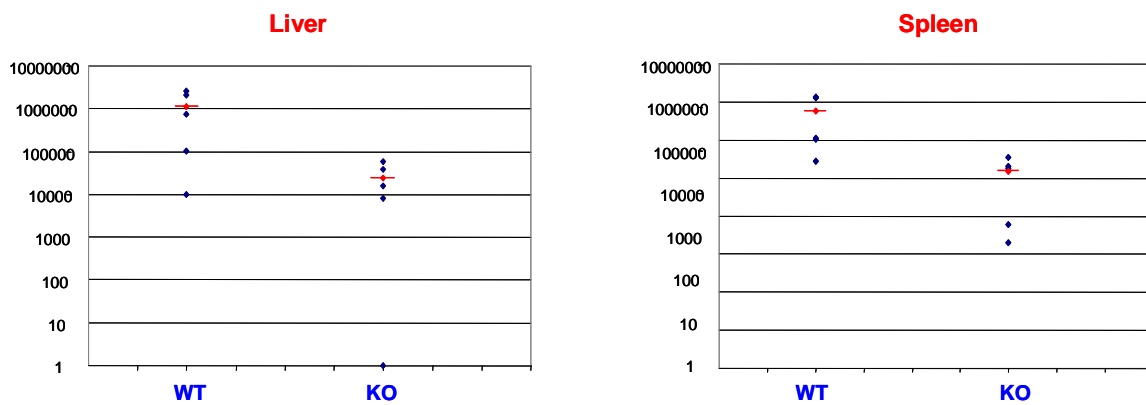


Fig 6.5. MKP-1^{-/-} mice are less susceptible to *Listeria* infection. Mice were injected *i.v* with 1.0 x 10⁸ particles of *Listeria monocytogenes*. 72 hr later, animals were sacrificed and the spleen and liver removed and homogenised. Serial dilutions of tissue homogenates were plated on brain-heart infusion agar plates and cultured at 37°C, colony numbers were counted following 24 hours of incubation, the results are expressed as cfu per organ.

6.3 MKP-1 Negatively Regulates p38 MAPK, JNK and AP-1 Activity and iNOS expression

LPS is a potent activator of the MAPK family; including p38, ERK and JNK. Therefore, to determine if MKP-1 activity affects MAPK signalling following TLR stimulation, bone marrow derived macrophages (BMDM) from MKP-1^{-/-} and wild type mice were treated with 10 ng/ml LPS and MAPK activity was determined using antibodies which recognise the active (phosphorylated) form of these proteins. No difference in the initial phase of MAPK activation (20 min) was seen between genotypes, however both p38 MAPK and JNK activity was prolonged in MKP-1^{-/-} BMDM (Fig 6.6). By 2 hr LPS stimulation both active p38 and JNK levels had almost returned to baseline, whereas in the MKP-1^{-/-} macrophages they were still elevated. In contrast, ERK activity was equivalent in wild type and knockout BMDM, suggesting that in macrophages, MKP-1 does not affect ERK activity in response to LPS. MKP-1 is therefore essential for the inactivation of p38 MAPK and JNK following LPS stimulation and as such provides an endogenous brake on prolonged MAPK signalling which would otherwise be deleterious by allowing overproduction of pro-inflammatory cytokines.

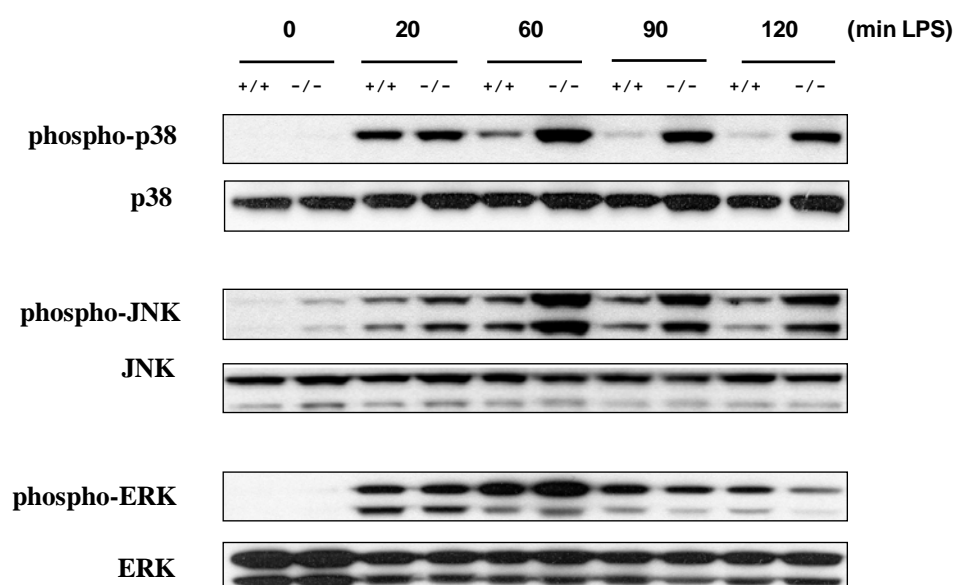


Fig 6.6. Prolonged MAPK activity in MKP-1^{-/-} BMDM in response to LPS. BMDM were harvested from MKP-1^{+/+} and MKP-1^{-/-} mice and treated with 10 ng/ml LPS for the indicated times. Cells were lysed in RIPA buffer and western blot was carried out using the indicated antibodies. Representative gel from 3 separate experiments.

AP-1 is a well described transcription factor composed of c-jun and fos subunits, it is known to be strongly induced by MAPKs and is a potent transcription factor for several important cytokines (Hess et al., 2004). AP-1 activity was examined using a gel shift (EMSA) assay which revealed a substantial increase in AP-1 DNA binding at both 30 and 90 min LPS stimulation in MKP-1^{-/-} BMDM in comparison with wild type cells (Fig 6.7a). This suggests that MKP-1 controls cytokine expression through its effects on MAPKs and their downstream targets such as AP-1.

JNK, p38 MAPK and AP-1 have all been shown to be necessary for iNOS upregulation in macrophages following LPS stimulation (Chan and Riches, 2001, Chen et al., 1999). iNOS levels were therefore measured in MKP-1 deficient macrophages by qPCR (Fig 6.7b). LPS stimulation resulted in significant overproduction of iNOS in MKP-1^{-/-} macrophages. Maximum iNOS levels were reached by 5 hr in wt cells, in MKP-1 deficient macrophages iNOS mRNA levels continued to rise until 12 hr at which time MKP-1 deficient cells produced 55 fold more iNOS mRNA than wt cells. Nitric oxide production is protective against listeria infection and iNOS deficient mice fail to restrain listeria growth (Boockvar et al., 1994, MacMicking et al., 1995). Therefore elevated iNOS levels in MKP-1 deficient mice may contribute to the reduced bacterial load of these mice following listeria infection.

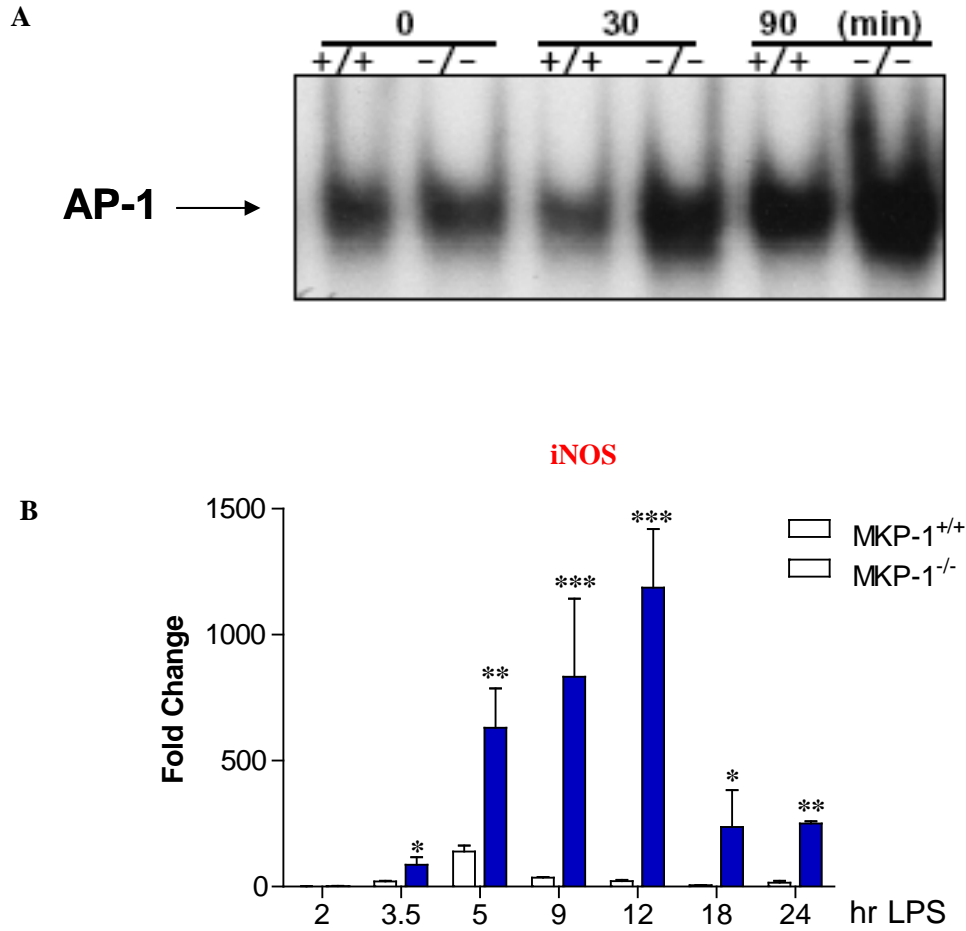


Fig 6.7. Increased AP-1 DNA binding activity in MKP-1^{-/-} BMDM. (A) MKP-1^{+/+} and MKP-1^{-/-} BMDM were treated for the indicated times with 10 ng/ml LPS, nuclear fractions were obtained and AP-1 binding activity was determined using a gel shift assay with a consensus AP-1 oligonucleotide. A representative gel is shown from 3 separate experiments. (B) MKP-1^{+/+} and MKP-1^{-/-} macrophages were treated with LPS for up to 24 hr. iNOS mRNA levels were measured by qPCR and normalised to the levels of wt cells at 2 hr. Error bars represent mean \pm SEM, statistical analysis was carried out using a Two-way ANOVA with Bonfferoni post test, * $p < 0.05$, ** $p < 0.01$, *** $p < 0.001$.

6.4 TLR Mediated MKP-1 Expression Proceeds Through TRIF and MyD88

In order to understand the temporal regulation of MKP-1, BMDM were treated with 10 ng/ml LPS over 24 hr, followed by qPCR analysis of MKP-1 expression. MKP-1 expression peaked following 1 hr of LPS stimulation with a 15 fold induction in mRNA levels, this was followed by rapid downregulation and return to basal levels 3-4 hr post LPS treatment (Fig 6.8a). MKP-1 protein showed a similar pattern of strong induction followed by rapid downregulation (Fig 6.8b). Such rapid induction of MKP-1 has presumably evolved to effectively limit prolonged MAPK activation which could lead to aberrant cytokine overproduction. Interestingly a second smaller peak of expression was consistently seen 5 hr following LPS treatment which may be associated with secondary cytokine release, possibly IL-10 which has recently been shown to induce MKP-1 expression (Hammer et al., 2005)

TLRs can transduce their signals through the use of two adaptor proteins, MyD88 in the case of TLRs 2, 5, 6 and 9 or through Trif in the case of TLR3, while LPS can induce signal transduction through either adaptor (Fig 1.4). It was therefore of interest to examine which adaptor molecules are required for TLR induced upregulation of MKP-1. To examine this aspect of TLR signalling, two mouse lines were employed; MyD88^{-/-} mice and the TRIF null mutant line. Treatment of BMDM from wild type, MyD88^{-/-} and mice with LPS revealed that both pathways are required for maximal MKP-1 induction (Fig 6.8b). MKP-1 expression was reduced in both MyD88 and TRIF deficient cells by 1 hr post LPS treatment and by 2 hr MKP-1 expression was almost completely inhibited.

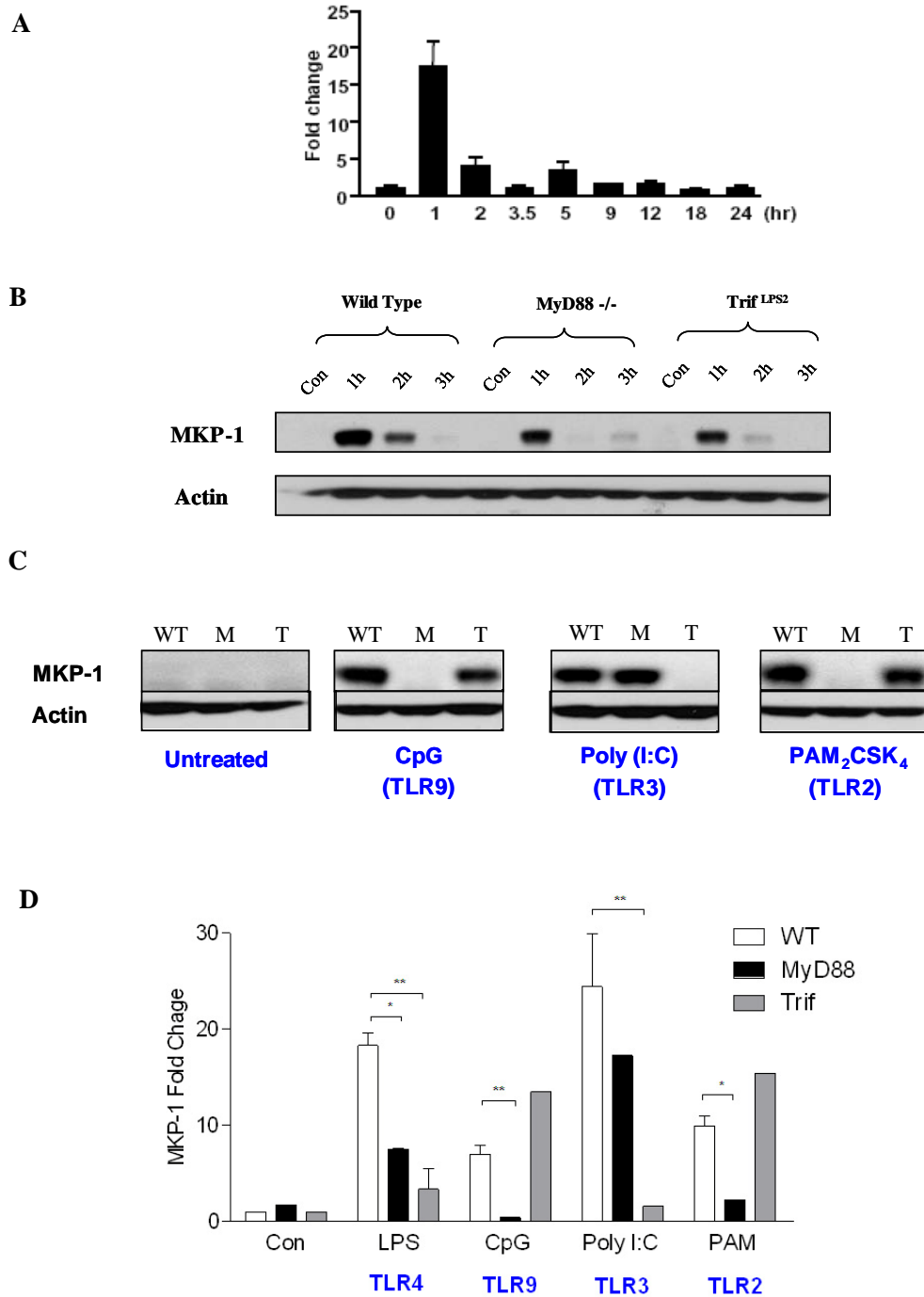


Fig 6.8. MKP-1 Expression can be Stimulated Through both the MyD88 Dependent and Independent Pathways. (A) BMDM were treated with 10 ng/ml LPS for the indicated times and MKP-1 expression was determined by qPCR. (B) Wild type, MyD88^{-/-} and BMDM were left untreated (con) or stimulated for the indicated times with 10 ng/ml LPS followed by western blotting for MKP-1 (C,D) Wild type, MyD88^{-/-} and BMDM were left untreated (con) or stimulated for 1 hr with 10 ng/ml LPS, 1 μ M CpG, 50 μ g/ml Poly(I:C) or 200 ng/ml PAM3CSK4 and MKP-1 expression was determined by western blot (C) or qPCR (D). For qPCR data, error bars represent mean \pm SEM, statistical analysis was carried out using a student's t-test, *p <0.05, ** P<0.01, n=3 per experiment, repeated in triplicate.

In order to ascertain if this mode of MKP-1 regulation is particular to LPS or is a facet of TLR signalling in general, wild type, MyD88^{-/-} and BMDM were treated with the TLR 9 agonist CpG, the TLR3 agonist poly(I:C) or the TLR2 agonist . All three agonists potently upregulated MKP-1 expression within 1 hr (Fig 6.8c). This demonstrates that a variety of bacterial and viral TLR ligands are capable of inducing MKP-1 expression and therefore upregulation of MKP-1 is a general phenomenon of inflammatory responses in macrophages during innate immunity. As expected, no MKP-1 upregulation was seen in MyD88^{-/-} mice treated with CpG or since they both require MyD88 to transduce their signal and similarly no upregulation was seen in mice treated with CpG which requires TRIF as an adaptor protein. These results were also confirmed by qPCR (Fig 6.8d). Taken together these results indicate that MKP-1 can be induced through MyD88 and TRIF dependent pathways in response to TLR stimulation.

Since it was established that both TRIF and MyD88 contribute to induction of MKP-1 expression, downstream components of the signalling cascade were analysed for their contribution to MKP-1 expression. Thus BMDM were treated with LPS for 1 hr in the presence of SP600125 (a JNK inhibitor), SB203580 (a p38 MAPK inhibitor), U0126 (a MEK1/2 inhibitor) and Ro106-9920 (an NF- κ B inhibitor) and MKP-1 expression was evaluated by western blot and qPCR (Fig 6.9). Inhibition of JNK was found to have little effect on MKP-1 expression, however inhibition of p38, ERK or NF- κ B all reduced the expression of MKP-1 at both the protein and RNA level. p38 and ERK have previously been shown to be involved in MKP-1 upregulation in other cell types (Lin and Yang, 2006). This is the first report of NF- κ B mediated MKP-1 expression and suggests a previously unappreciated level of cross-talk between the MAPK and NF- κ B family and as such warrants further investigation.

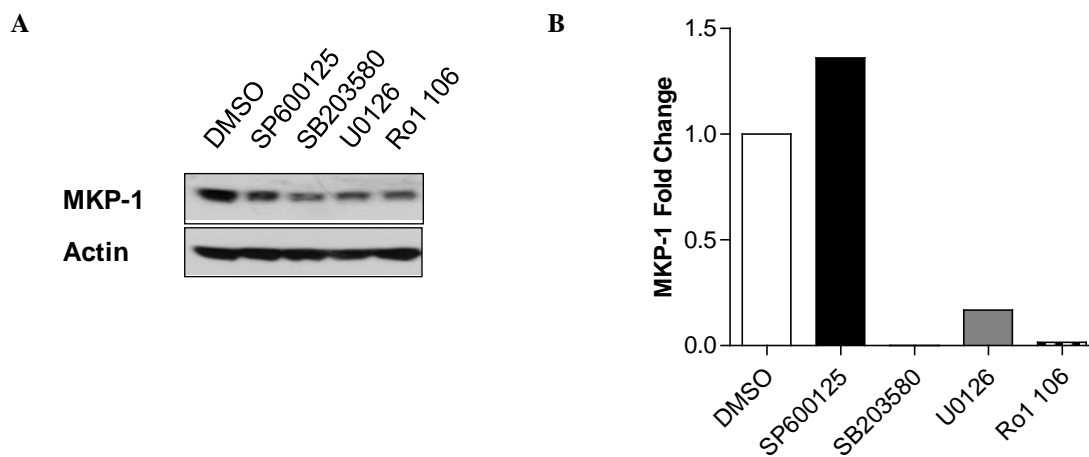


Fig 6.9. MKP-1 upregulation by LPS is dependent on MAPKs and NF- κ B. BMDM were pre-treated for 30 min with 10 μ M of indicated inhibitors or DMSO control, then stimulated for 1 hr with 10 ng/ml LPS and the expression of MKP-1 was analysed by (A) western blot and (B) qPCR

Since dendritic cells (DCs) are a vital part of the innate immune responses and serve as a bridge between innate and adaptive immunity, it was of interest to examine the regulation of MKP-1 in DCs. DCs were treated with 10 ng/ml LPS for up to 24 hr and MKP-1 expression was determined at the protein and RNA level. Interestingly, the temporal regulation of MKP-1 mRNA in DCs was very distinct to that of macrophages, there was a modest 3 fold increase in MKP-1 expression at 1 hr but surprisingly a 15 fold increase was seen at 12 hr which was sustained up to 24 hr (Fig 6.10a). This is in contrast to macrophages, where MKP-1 expression returns to baseline levels from 9 hr LPS stimulation (Fig 6.8a). Intriguingly, analysis of MKP-1 protein expression in DCs did not recapitulate the temporal expression seen at the mRNA level (Fig 6.10b). MKP-1 protein was still evident at 12 and 24 hr LPS stimulation but was greatly reduced in comparison to levels seen at 1 hr. Since increased mRNA levels are not reflected by increased protein levels it suggests that MKP-1 may be regulated post-translationally in DCs. The functional significance of this is currently unknown but highlights the fact that the regulation of MKP-1 during inflammation may be distinct in different immune cell types.

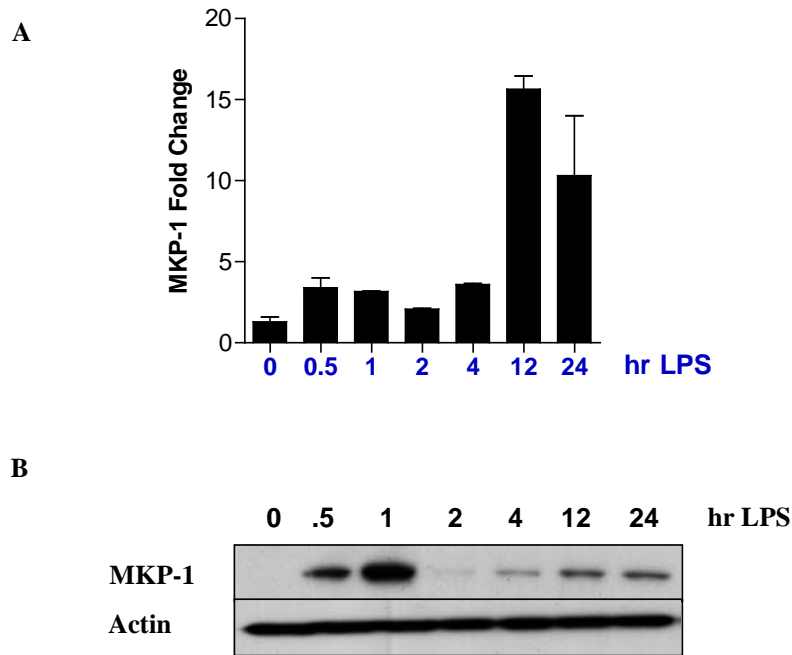


Fig 6.10. LPS induced MKP-1 expression in dendritic cells. BMDC were treated for the indicated times with LPS and MKP-1 expression was analysed by (A) qPCR and (B) western blot. Error bars represent mean \pm SEM, n=3. Statistical analysis of qPCR was carried out by ANOVA with Dunnett's post test and at all time points MKP-1 was significantly upregulated ($p < 0.05$) compared to the 0 hr control.

6.5 Regulation of IL-10 by MKP-1

LPS treatment *in vivo* revealed that MKP-1 controls the expression of both pro and anti-inflammatory cytokines, it was therefore of interest to examine cytokine responses in MKP-1^{-/-} mice in more detail. IL-10 is a potent anti-inflammatory cytokine released by macrophages and TH2 cells which serves to inhibit pro-inflammatory cytokine release from macrophages and attenuate TH1 cell function (Couper et al., 2008). IL-10 expression was increased 8 fold in serum from MKP-1^{-/-} mice compared to wild type mice. To further investigate the effect of MKP-1 on IL-10 expression in response to innate immune signalling, MKP-1^{+/+} and MKP-1^{-/-} BMDM were treated with a panel of TLR agonists; activation of TLRs 2, 3, 4, 5, 7 and 9 was induced for 12 hr and IL-10 in the culture supernatants was measured by ELISA. All TLR agonists tested resulted in elevated expression of IL-10 in MKP-1^{-/-} BMDM, the biggest increase was seen with LPS (6 fold) and flagellin (5 fold) (Fig 6.11a). Interestingly, there is a gene dosage effect of MKP-1 on IL-10 expression; treatment of MKP-1^{+/-} mice with LPS *in vivo* or treatment of MKP-1^{+/-} BMDM with LPS *in vitro* resulted in IL-10 levels which were intermediate between that of MKP-1^{+/+} and MKP-1^{-/-} mice (4.11b).

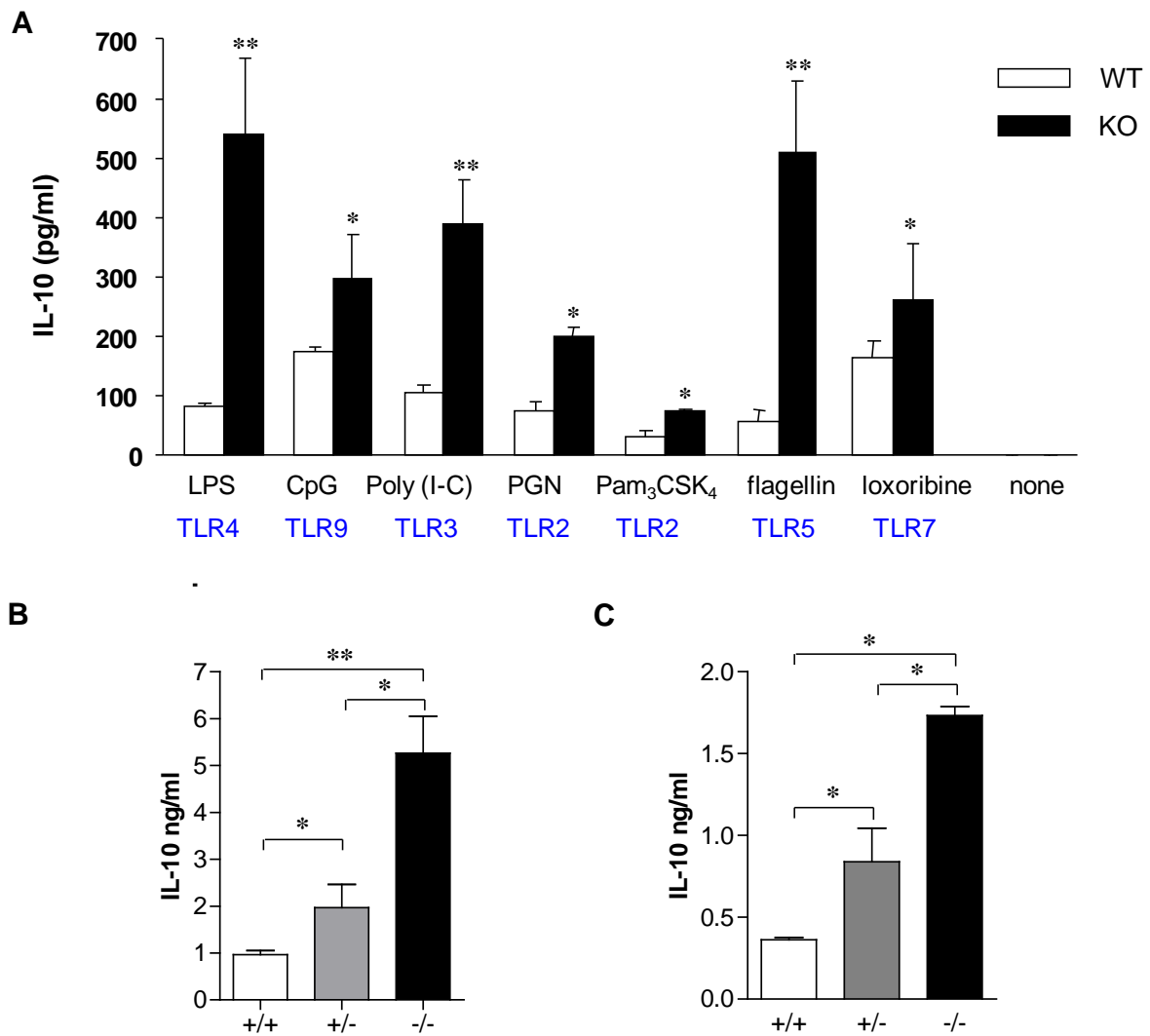


Fig 6.11. MKP-1 inhibits TLR induced IL-10 expression and has gene dosage effects. (A) BMDM from MKP-1^{+/+} and MKP-1^{-/-} mice were treated for 12 hr with 10 ng/ml LPS, 1 μ M CpG, 50 μ g/ml Poly(I:C), 10 μ g/ml peptidoglycan (PGN), 200 ng/ml Pam₃CSK₄, 100 ng/ml flagellin, 200 μ M loxoribine or left untreated and IL-10 in the culture supernatant was measured by ELISA. (B) Serum from MKP-1^{+/+}, MKP-1^{+/-} and MKP-1^{-/-} mice was collected 3 hr following 2.5 mg/kg LPS challenge and IL-10 measured by ELISA. (C) BMDM from MKP-1^{+/+}, MKP-1^{+/-} and MKP-1^{-/-} mice were treated with 10 ng/ml LPS for 12 hr and IL-10 in the culture supernatant was measured by ELISA. Error bars represent mean \pm SEM, n=3. Statistical analysis was carried out using a student's t-test (A) and an ANOVA with Bonferroni post test (B) * p<0.05, ** p<0.01.

A time course of LPS treatment in BMDMs revealed increased IL-10 protein levels in MKP-1^{-/-} at all times examined, with an 8 fold increase by 5 hr (Fig 6.12a). Detailed analysis of IL-10 mRNA levels were in agreement with the ELISA data, with the greatest difference (10-20 fold) observed 5-9 hr following LPS treatment, mRNA levels were equivalent between genotypes by 18-24 hr LPS treatment (Fig 6.12b). Since MKP-1 deficient macrophages showed enhanced MAPK activity, it was of interest to determine if the increased MAPK activity was responsible for the elevated IL-10 levels in MKP-1^{-/-} macrophages. Therefore, MKP-1^{-/-} BMDM were treated with the p38 MAPK inhibitor SB203580, the JNK inhibitor SP600125 or the MEK inhibitor U0126 at doses ranging from 1-20 μM, followed by LPS challenge (Fig 6.13). All the MAPK inhibitors dose-dependently decreased IL-10 expression, however p38 inhibition had the largest effect. At the lowest dose tested (1 μM), inhibition of JNK and ERK reduced IL-10 expression in MKP-1^{-/-} macrophages by an average of 50% whereas inhibition of p38 MAPK reduced IL-10 levels to that of wild type cells. This suggests that the inhibitory effect of MKP-1 on IL-10 expression is mainly mediated through the inhibition of p38 MAPK by MKP-1, although there are contributory effects from JNK and ERK.

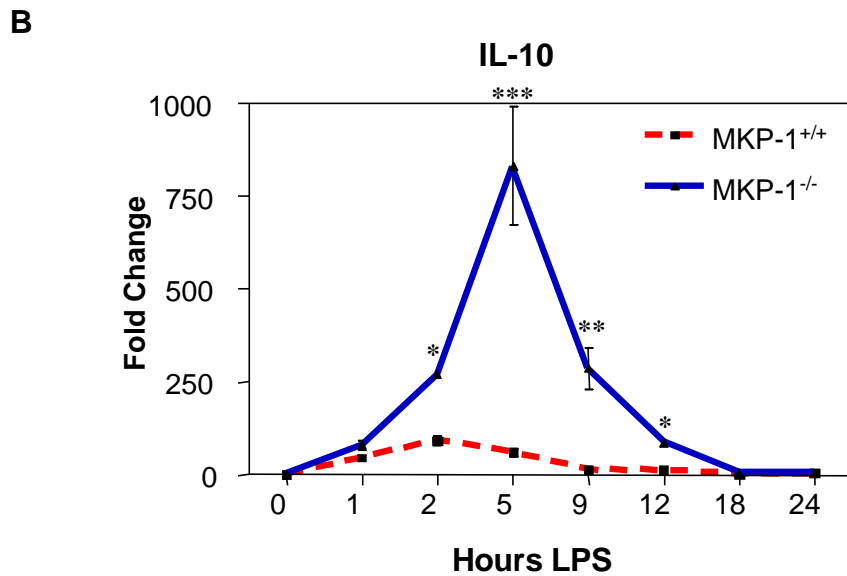
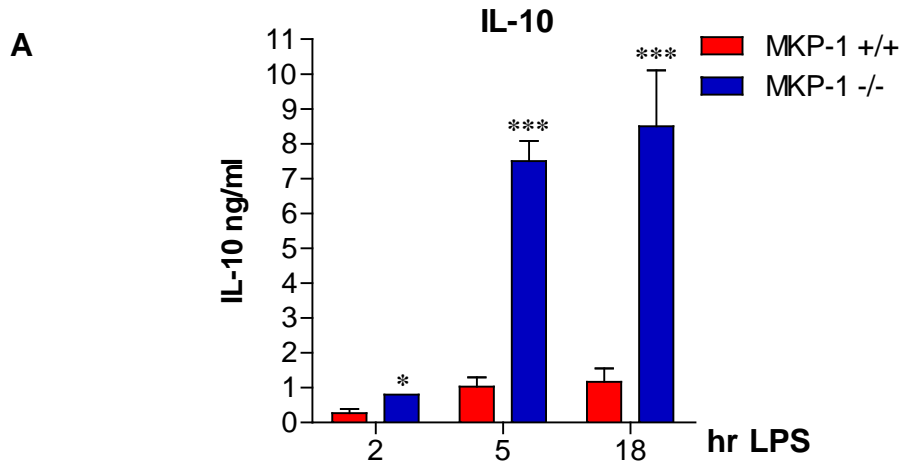


Fig 6.12. Temporal regulation of IL-10 by MKP-1. MKP-1^{+/+} and MKP-1^{-/-} BMDM were treated for the indicated times with 10 ng/ml LPS and IL-10 was measured in the culture supernatant by ELISA (**A**) or by qPCR (**B**). Error bars represent mean \pm SEM, n=3, experiments repeated in triplicate. Statistical analysis was carried out using a two-way ANOVA with Bonferroni post test, * p<0.05, ** p<0.01, *** p<0.001.

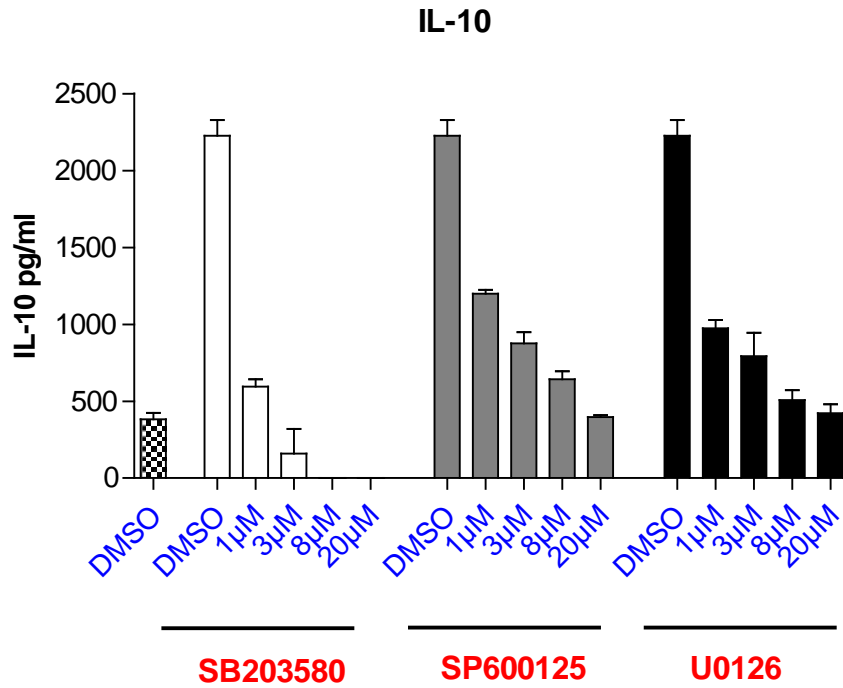


Fig 6.13. MKP-1 inhibition of IL-10 is controlled through MAPK. MKP-1^{+/+} (hatched bar) or MKP-1^{-/-} (white, grey, black bars) BMDM were pretreated for 1hr with 1 μ M, 3 μ M, 8 μ M or 20 μ M SB203580, SP600125, U0126 or DMSO control, followed by 12 hr treatment with 10 ng/ml LPS and IL-10 levels in the culture supernatant was measured by ELISA. Error bars represent mean \pm SEM, n=3, experiments repeated in triplicate.

6.6 Dynamic Regulation of TNF- \bullet is Mediated Through IL-10 in MKP-1 $^{-/-}$

TNF- \bullet is a potent pro-inflammatory cytokine which leads to strong macrophage induction, activates the endothelium and can cause to septic shock when released systemically. Since it is such a potent cytokine, multiple levels of control are employed by cells to tightly control TNF- \bullet expression, including stabilisation of its mRNA by the p38 MAPK dependent protein MK1, which stabilises TNF- \bullet message by inhibiting 3' AU-rich element (ARE) dependent mRNA degradation. Another method to control TNF- \bullet expression is the release of IL-10 from macrophages and TH2 cells which inhibits TNF- \bullet production from macrophages. To further determine the regulation of TNF- \bullet by MKP-1, MKP-1 $^{+/+}$ MKP-1 $^{-/-}$ BMDM were treated for 2, 5 and 18 hr with 10 ng/ml LPS and TNF- \bullet protein was measured (Fig 6.14a). At earlier time points there was 3 fold increased TNF- \bullet expression in MKP-1 $^{-/-}$ BMDM, however by 18 hr LPS treatment, TNF- \bullet expression was equal between genotypes To further elucidate the temporal regulation of TNF- \bullet , a time course of LPS treatment was carried out and TNF- \bullet mRNA levels were measured b qPCR. Compared with ELISA which measures the accumulative amounts of protein secreted into the culture medium, RNA analysis can reveal additional kinetic information concerning cytokine expression. qPCR analysis showed a 2-fold increase in TNF- \bullet expression in MKP-1 $^{-/-}$ cells 1 hr post LPS challenge which is reflected in the increased protein levels (Fig 6.14b). Interestingly by 2 hr post LPS challenge, levels were equal between genotypes and from 5 hr to 24 hr, MKP-1 $^{-/-}$ cells produced less TNF- \bullet mRNA than wild type cells. Therefore there is dynamic regulation of TNF- \bullet mRNA in MKP-1 $^{-/-}$ macrophages, with increased expression at earlier time points and decreased expression at later time points.

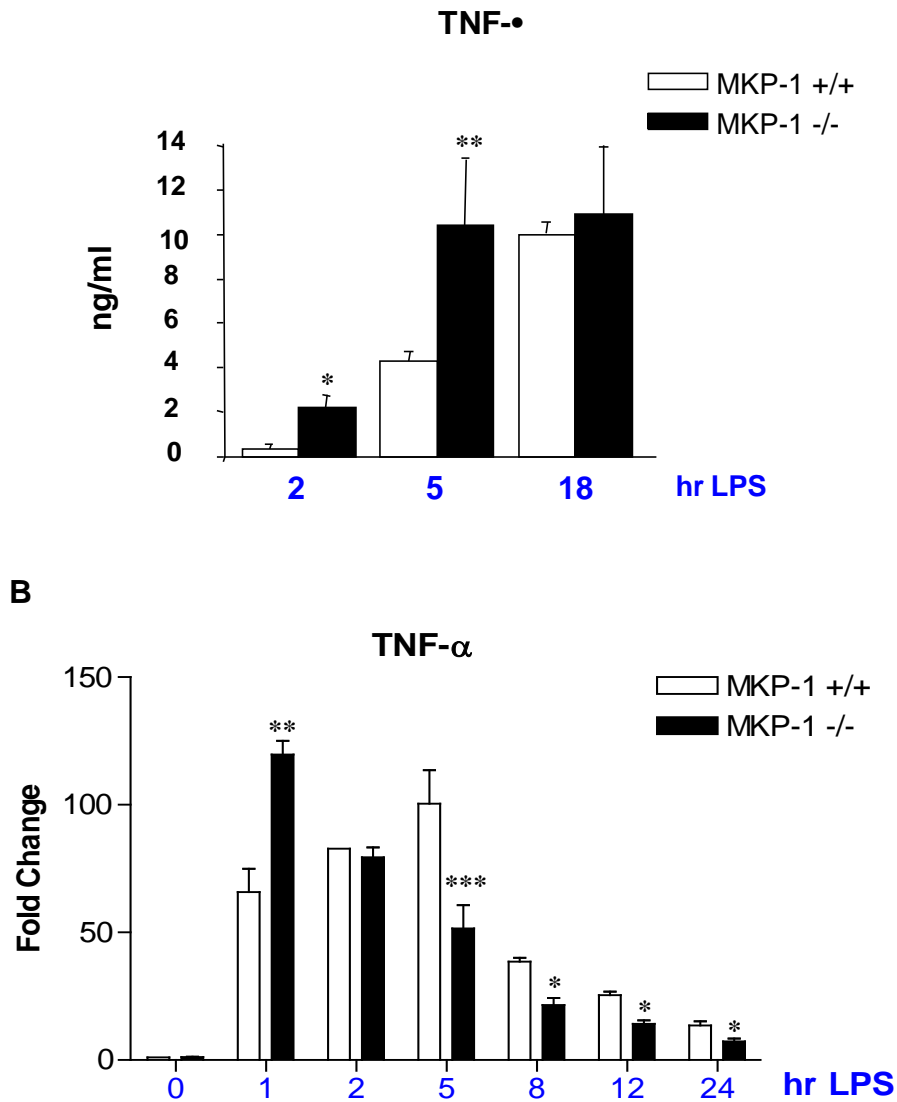


Fig 6.14. Temporal regulation of TNF- α in MKP-1 deficient cells. (A) MKP-1^{+/+} and MKP-1^{-/-} BMDM were treated for the indicated times with 10 ng/ml LPS and TNF- α protein levels were measured in the culture supernatant by ELISA. (B) MKP-1^{+/+} and MKP-1^{-/-} BMDM were treated for the indicated times with 10 ng/ml LPS and TNF- α mRNA levels were measured by qPCR. Error bars represent mean \pm SEM, n=3 per group, experiment was repeated in triplicate.

Since IL-10 is a potent downregulator of TNF- α and MKP-1^{-/-} macrophages secrete increased amounts of IL-10, it was thought that IL-10 may be responsible for the decline in TNF- α

levels seen by 5 hr LPS challenge in MKP-1^{-/-} macrophages. Overlaying the LPS time course of TNF-• and IL-10 mRNA expression was highly suggestive of a role for IL-10 in controlling TNF-• expression since IL-10 levels start to increase 1-2 hr following LPS treatment as TNF-• levels start to decline (Fig 6.15a). To test this further, MKP-1^{+/+} and MKP-1^{-/-} BMDM were pretreated with an IL-10 blocking antibody or control IgG followed by LPS challenge for 5 hr or 12 hr. At both time points, blocking IL-10 resulted in a two fold increase in TNF-• levels and inhibition of IL-10 completely abrogated the reduction of TNF-• mRNA in MKP-1^{-/-} cells (Fig 6.15b). These results show that in MKP-1^{-/-} macrophages, there is an early overproduction of TNF-• mRNA due to excessive MAPK activation, however by 5 hr LPS activation, IL-10 has started to be overproduced in MKP-1^{-/-} cells which leads to TNF-• mRNA inhibition. This highlights the complicated and dynamic nature of cytokine production in macrophages, which is subject to multiple levels of control.

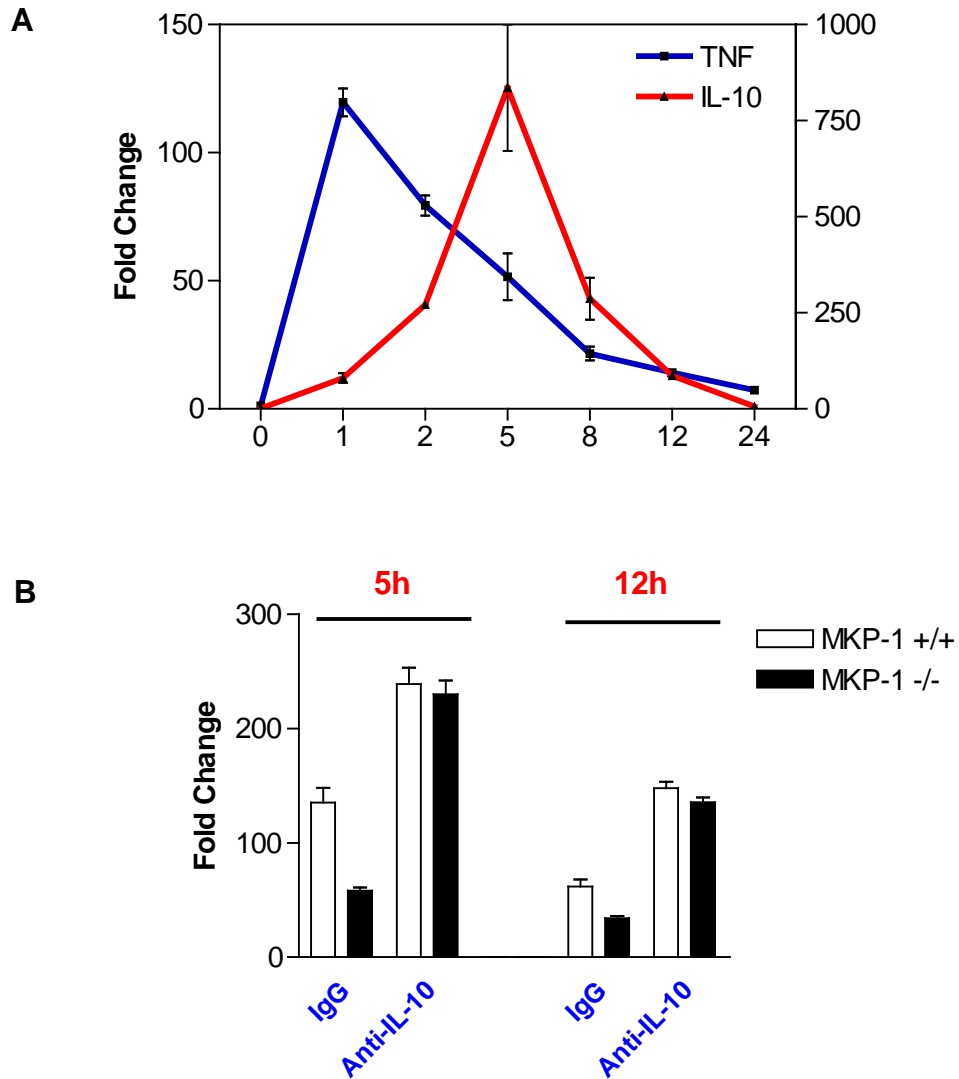


Fig 6.15. TNF- α expression in MKP-1^{-/-} macrophages is controlled through IL-10 upregulation. (A) Overlay of TNF- α and IL-10 mRNA expression profiles following LPS treatment. (B) MKP-1^{+/+} and MKP-1^{-/-} BMDM were pretreated with 10 ng/ml anti-IL-10 antibody or with IgG for 1 hr followed by 5 hr or 12 hr LPS treatment, TNF- α mRNA levels were then measured by qPCR. Error bars represent mean \pm SEM, n=3 per group, experiment was repeated in triplicate.

Previous studies have shown that IL-10 inhibits TNF- α activity through STAT3-mediated induction of the I κ B family member Bcl-3 (Kuwata et al., 2003). Bcl-3 binds to the p50 subunit of NF- κ B on the TNF- α promoter and inhibits NF- κ B induced TNF- α transcription (Fig 6.16a). Therefore, if increased IL-10 in MKP-1^{-/-} cells does indeed cause inhibition of TNF- α , Bcl-3 may also be increased in the absence of MKP-1. Bcl-3 mRNA levels were therefore measured in MKP-1^{+/+} and MKP-1^{-/-} macrophages following LPS challenge; 5 hr after LPS treatment, MKP-1^{-/-} macrophages produced 2.5 fold higher levels of Bcl-3 mRNA and levels remained significantly higher in MKP-1^{-/-} cells for up to 24 hr (Fig 6.16b). In MKP-1^{-/-} macrophages, between 2 hr and 5 hr after LPS treatment, IL-10 levels increase and TNF- α levels concomitantly decrease (Fig 6.15a); the finding that Bcl-3 levels are also increased between 2 hr and 5 hr strongly suggests that Bcl-3 is involved in IL-10 mediated TNF- α downregulation in these cells.

STAT3 is the main transcriptional regulator of Bcl-3, suggesting that STAT3 activity might be altered in the absence of MKP-1. To address this, MKP-1^{+/+} and MKP-1^{-/-} BMDM were treated with LPS and STAT3 activity was assessed with phospho-specific antibodies. STAT3 serine phosphorylation was induced within 30 min of LPS treatment and returned to baseline levels after 2 hr in wild type cells; however in the absence of MKP-1, S727 phosphorylation remained elevated at 2 hr (Fig 6.16c). In contrast, STAT3 Y705 phosphorylation showed a slower course of activity when compared to serine phosphorylation but at 2 hr LPS treatment Y705 levels were again enhanced in MKP-1^{-/-} macrophages compared to wild type cells. Thus as predicted STAT3 phosphorylation is enhanced in MKP-1 deficient macrophages. Dysregulated STAT3 phosphorylation was specific since neither STAT1 tyrosine nor serine phosphorylation was altered in MKP-1^{-/-} macrophages (Fig 6.16d).

It is likely that elevated STAT3 serine and tyrosine phosphorylation is brought about by distinct mechanisms. Since MKP-1 is responsible for dephosphorylating tyrosine and threonine residues, this precludes a direct effect on STAT3 serine phosphorylation. Therefore this must occur indirectly, possibly through elevated expression of MAPKs which have been shown to phosphorylate STAT3 at S727 after LPS treatment (Chung et al., 1997, Xu et al., 2003). Thus elevated levels of active JNK and p38 MAPK in MKP-1^{-/-} cells might account for increased STAT3 serine phosphorylation. In contrast, the elevated levels of STAT3 tyrosine phosphorylation are likely to be due to the higher levels of IL-10 and possibly IL-6 in MKP-1^{-/-} macrophages. This fits well with the IL-10 kinetic data in Fig 6.12 which showed

that IL-10 begins to be secreted by 2 hr LPS treatment with elevated levels being secreted from MKP-1^{-/-} macrophages. Taken together enhanced STAT3 705 and 727 phosphorylation in MKP-1^{-/-} macrophages may be involved in upregulation of Bcl-3 and subsequently inhibition of TNF-•.

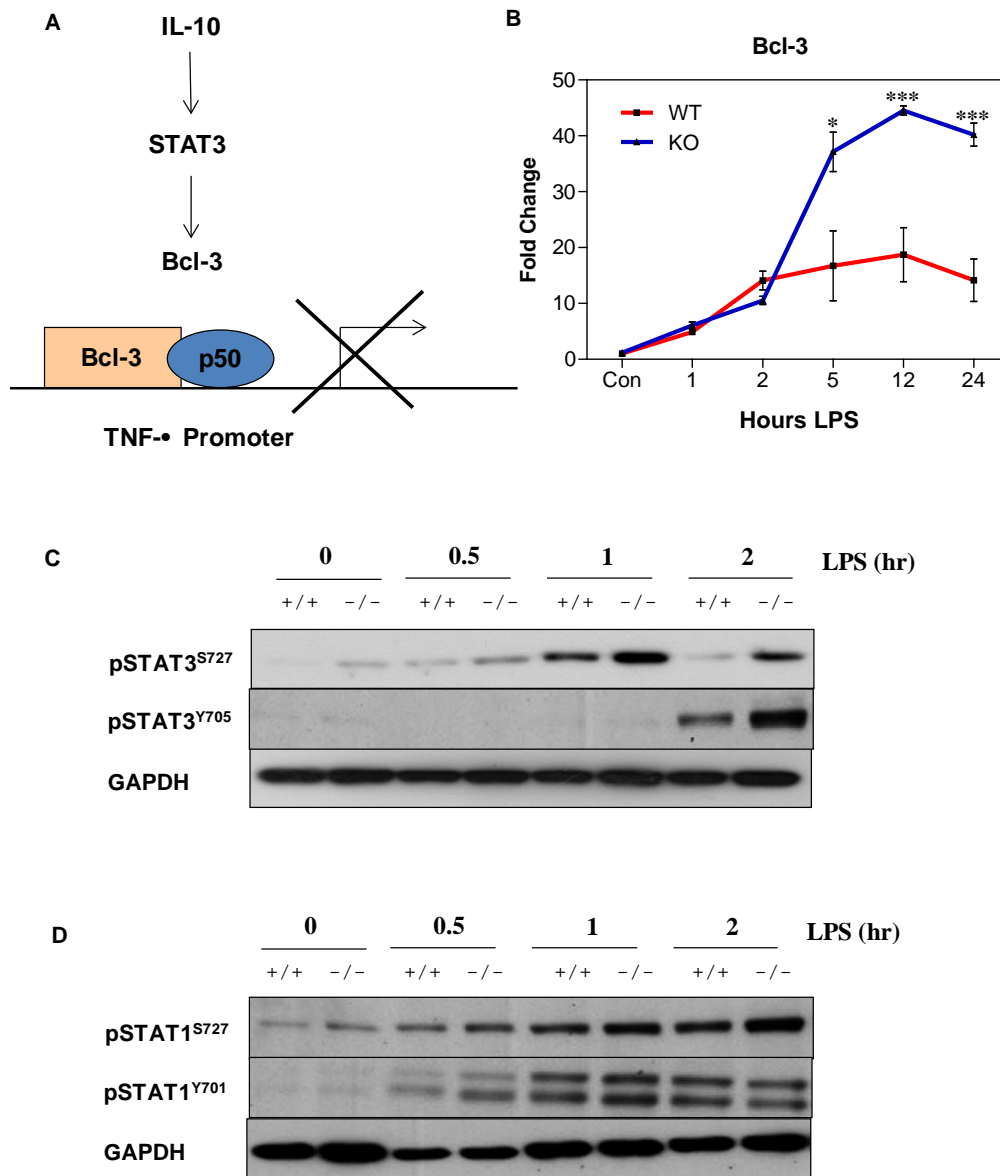


Fig 6.16. Increased IL-10 in MKP-1^{-/-} macrophages leads to overproduction of Bcl-3 through increased STAT3 activation. (A) Diagram of inhibitory effect of Bcl-3 on the TNF-• promoter. Bcl-3 is a STAT3 responsive gene, following IL-10 stimulation it binds to the TNF-• promoter where it inhibits p50 mediated transcription. (B) MKP-1^{+/+} and MKP-1^{-/-} BMDM were treated for the indicated times with 10 ng/ml LPS and Bcl-3 mRNA levels were assessed by qPCR, results are expressed as fold change over control. Error bars represent mean ± SEM, n=3 per group, experiment was repeated in triplicate. Statistical analysis was carried out using a Two-way ANOVA with Bonferroni post-test * p<0.001. (C and D) -1^{+/+} and MKP-1^{-/-} BMDM were treated with 10ng/ml LPS for the indicated times and western blots were carried out with the indicated antibodies.

6.7 MKP-1 Activity Promotes IL-12 Expression

IL-12 is composed of two subunits; p35 and p40 which form a functional p70 heterodimer. IL-12 is a potent pro-inflammatory cytokine and a strong inducer of Th1 responses, indeed IL-12 receptor expression is confined largely to activated T cells and NK cells (Trinchieri, 2003). It is expressed at low levels in resting T cells but is upregulated upon activation. Since IL-10 and IL-12 are often reciprocally regulated and MKP-1 deficient macrophages produce elevated levels of IL-10, IL-12 regulation was examined in MKP-1^{-/-} BMDM in response to TRL stimulation. MKP-1^{-/-} macrophages produced an average of 2-fold less IL-12p40 with all TLR ligands examined (Fig 6.17a). IL-12p70 levels were also interrogated, LPS mediated IL-12p70 expression was below the limits of detection in MKP-1^{-/-} macrophages, therefore to increase the levels of IL-12p70, macrophages were primed for 1 hr with IFN-• and then stimulated with LPS. Under these conditions, MKP-1^{-/-} macrophages produced an average of 3.5 fold less IL-12p70 compared to wild type (Fig 6.17b). Similarly to IL-10, there was also a gene dosage effect evident, with MKP-1^{+/-} macrophages producing intermediate levels of IL-12 (Fig 6.17c). Temporal analysis of IL-12 levels revealed that MKP-1^{-/-} produced reduced amounts of IL-12p40 protein when treated with LPS for 5 hr and 12 hr (Fig 6.18a). In addition, IL-12p40 and IL-12p35 levels were measured from 1-24 hr after LPS treatment (Fig 6.18b,c). The mRNA levels of both subunits were significantly lower over the entire course of LPS treatment. Interestingly, there was a second peak of IL-12p40 expression at 18 hr LPS stimulation which was not seen with IL-12p35. Since IL-23 also utilizes the IL-12p40 subunit there may also be distinct regulatory effects of this cytokine in MKP-1^{-/-} mice, however this has not yet been explored.

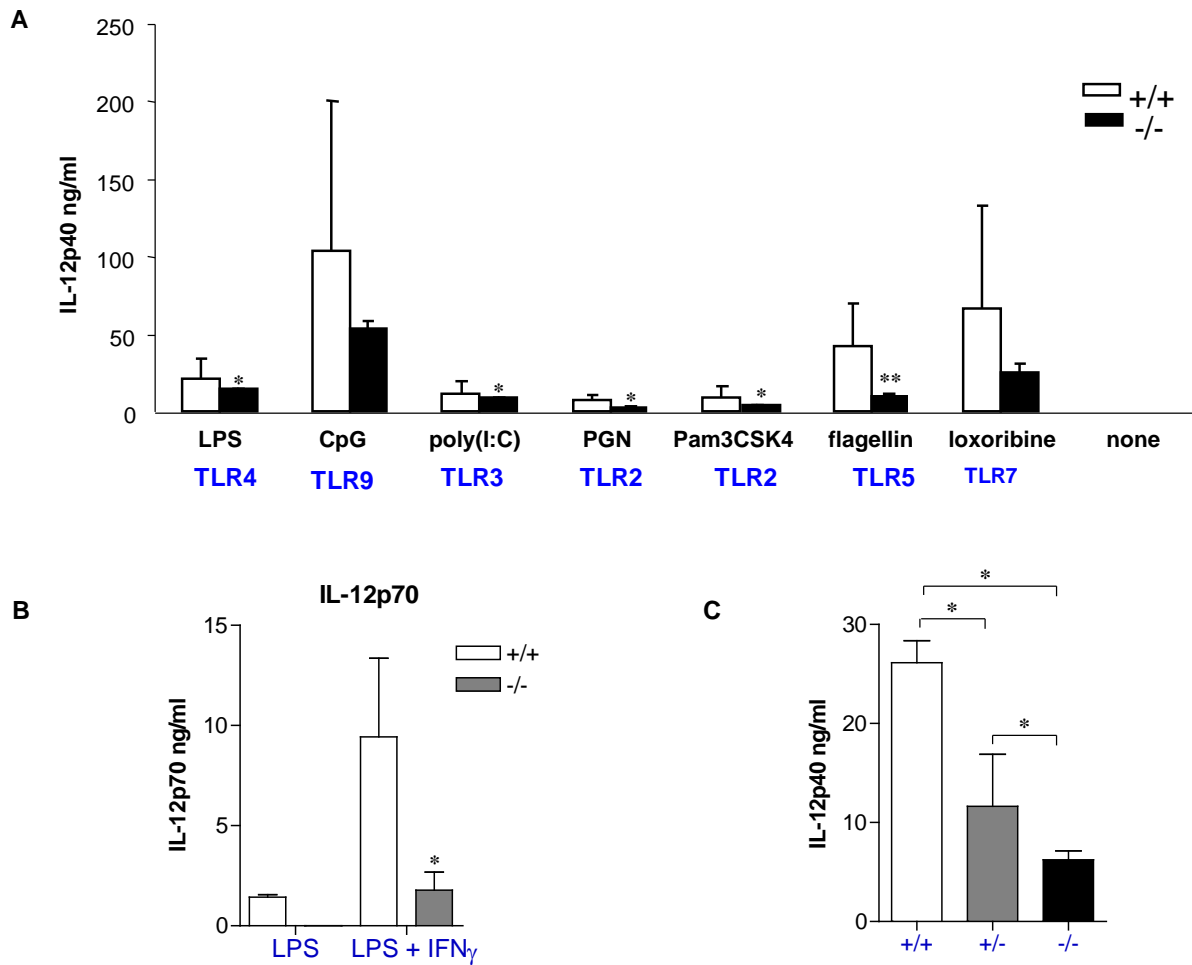


Fig 6.17. IL-12p40 expression is repressed in MKP-1^{-/-} mice following TLR stimulation. (A) BMDM from MKP-1^{+/+} and MKP-1^{-/-} mice were treated for 12 hr with 10 ng/ml LPS, 1 μ M CpG, 50 μ g/ml Poly(I:C), 10 μ g/ml petidoglycan (PGN), 200 ng/ml , 100 ng/ml flagellin, 200 μ M loxoribine or left untreated, IL-12p40 in the culture supernatant was measured by ELISA. (B) BMDM from MKP-1^{+/+} and MKP-1^{-/-} mice were treated with 10ng/ml LPS for 12 hr or pretreated for 1 hr with 10 ng/ml IFN- \bullet followed by 10 ng/ml LPS for 12 hr. IL-12p70 levels were then measured from the culture supernatant. (C) BMDM from MKP-1^{+/+}, MKP-1^{+/-} and MKP-1^{-/-} mice were treated with 10 ng/ml LPS for 12 hr and IL-12p40 in the culture supernatant was measured by ELISA. Error bars represent mean \pm SEM, n=3. Experiments repeated in triplicate. Statistical analysis was carried out with a One-way ANOVA with Bonfferoni post test, * p<0.05.

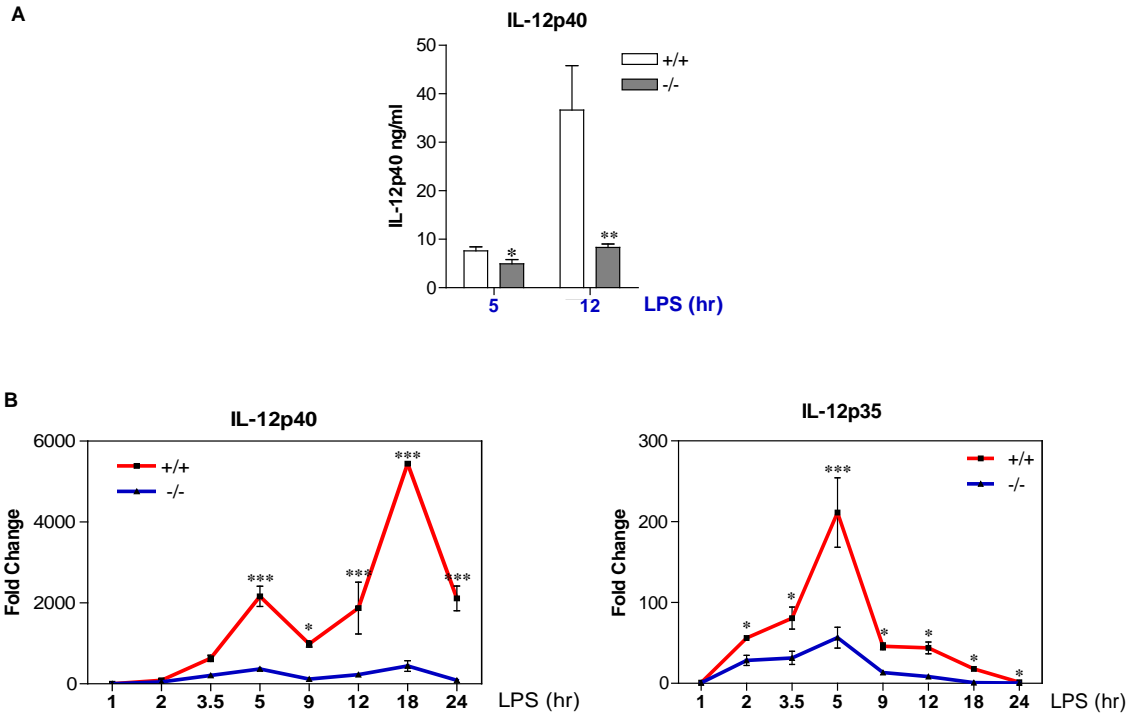


Fig 6.18. Time course of IL-12 expression in MKP-1^{-/-} mice. (A) BMDM from MKP-1^{+/+} and MKP-1^{-/-} mice were treated with 10 ng/ml LPS for 5 hr or 12 hr with LPS and IL-12p40 levels in the culture supernatant were measured by ELISA. (B) MKP-1^{+/+} and MKP-1^{-/-} BMDM were treated for the indicated times with 10 ng/ml LPS and IL-12p40 (left panel) or IL-12p35 (right panel) mRNA levels were measured by qPCR. Error bars represent mean \pm SEM, n=3 per group, experiments were repeated in triplicate. Statistical analysis was carried out using (A) t-test and (B) Two-way ANOVA with Bonferroni post test, * p<0.05, ** p<0.01, *** p<0.001.

Similarly to the experiments aimed at understanding which MAPKs control differentially regulation of IL-10 in MKP-1 deficient cells, MAPK inhibitors were again used to ascertain if the reduced IL-12 expression in MKP-1^{-/-} macrophages is linked to the elevated MAPK activity in these cells. IL-12p40 expression was found to be partially dependent on JNK activity in both wild type and knock out macrophages (Fig 6.19). Inhibition of p38 MAPK activity with sb203580, revealed that p38 MAPK represses IL-12 expression in both genotypes, this is most likely due to the fact that blocking p38 MAPK activity inhibits IL-10 expression, this reduction in IL-10 would then be expected to lead to a concomitant increase in IL-12 expression. As expected, inhibition of ERK activity with U0126 had no effect on IL-12p40 expression.

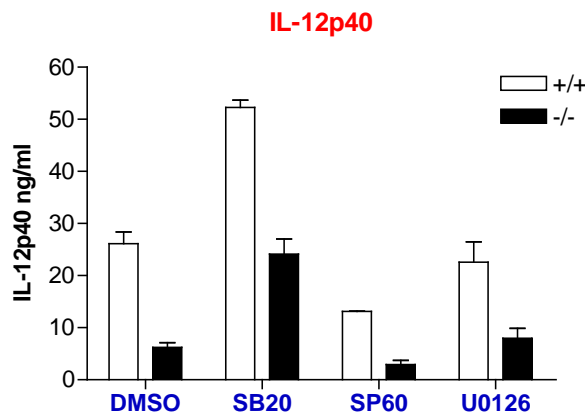


Fig 6.19. Effect of MAPK inhibition on IL-12p40 levels. MKP-1^{+/+} and MKP-1^{-/-} BMDM were treated for 1 hr with 10 μ M of the indicated inhibitors or DMSO control followed by LPS stimulation for 12 hr. IL-12p40 levels in the culture supernatant were assessed by ELISA. Experiment was repeated in triplicate.

The reciprocal regulation of IL-10 and IL-12 in MKP-1^{-/-} cells suggested that the decreased IL-12 levels seen in MKP-1^{-/-} macrophages might be directly attributable to the increased expression of IL-10 in these cells. To address this, IL-10 was inhibited using a blocking antibody, and cells were then stimulated with LPS for 12 hr. Inhibition of IL-10 increased IL-12p70 production 11-fold (Fig 6.20a left panel), however it did not lead to equivalent production of IL-12 from both genotypes as was the case for TNF- \bullet (Fig 6.14b). This result was recapitulated for IL-12p40 protein expression and IL-12p40 and IL-12p35 mRNA expression (Fig 6.12), suggesting that reduced IL-12 expression in MKP-1^{-/-} macrophages is not directly related to elevated IL-10 and may be a primary effect of increased p38 MAPK activity.

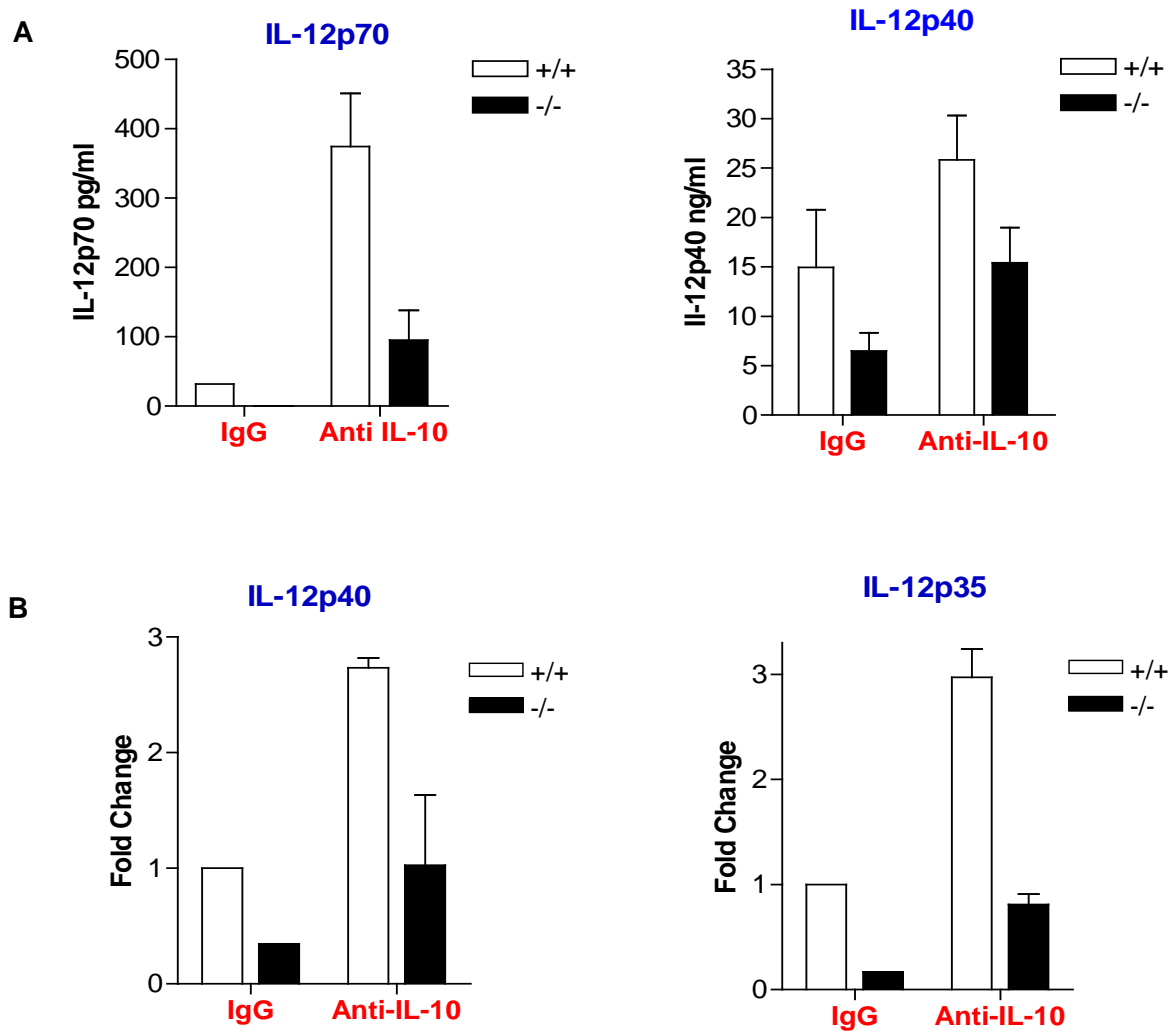


Fig 6.20 Reduced IL-10 expression in MKP-1^{-/-} macrophages may not be responsible for the increased levels of IL-12. MKP-1^{+/+} and MKP-1^{-/-} BMDM were pretreated for 1 hr with 10 ng/ml anti-IL-10 or IgG control, followed by 12 hr stimulation with LPS. (A) IL-12p70 and IL-12p40 levels were measured by ELISA, (B) IL-12p40 and IL-12p35 expression was measured by qPCR.

6.8 MKP-1 Deficiency has no Effect on the Outcome of DSS Induced Colitis

Inflammatory bowel disease (IBD) comprises two main disorders; Crohn's disease and ulcerative colitis, both confer significant chronic morbidity on patients. IBD is characterised by chronic inflammation of the digestive tract, mainly the bowel and is thought to occur when tolerance to comensal flora breaks down, eliciting an inflammatory response. A central role for TNF- α and IL-10 has been demonstrated in IBD and indeed anti-TNF- α therapy is one of the main treatments in Crohn's disease (Peyrin-Biroulet et al., 2008). Since cytokine expression is dysregulated in MKP-1 null mice in response to inflammatory stimuli, it was hypothesised that clinical outcome of colitis might be affected in these animals.

To address this question, MKP-1^{+/+} and MKP-1^{-/-} mice were fed dextran sulphate (DSS) in their drinking water for 7 days. DSS induces colitis by damaging the epithelial lining of the digestive tract, thus allowing access of the comensal flora to the gut which initiates an immune response. This inflammatory response includes neutrophils, macrophages B and T cell and manifests itself clinically as weight loss, sometimes accompanied by bloody stool. DSS was administered for the first 7 days of the protocol and weight loss was monitored up to 18 days. Weight loss began to occur by day 5 and continued up until day 10 when the mice started to regain weight (Fig 6.21). Over the course of the protocol, no significant differences in weight loss were observed between genotypes. This is quite a surprising finding in light of the fact that IL-10 therapy reduces DSS induced weight loss in mice and IL-10 deficient mice are highly susceptible to colitis (Sasaki et al., 2005, Kühn et al., 1993). As such, increased IL-10 levels in MKP-1 deficient mice would be expected to elicit a level of protection by inhibiting the inflammatory cascade during colitis. This suggests that there may be other unappreciated regulatory mechanisms at play which preclude any protection afforded by increased IL-10 levels in this colitis model.

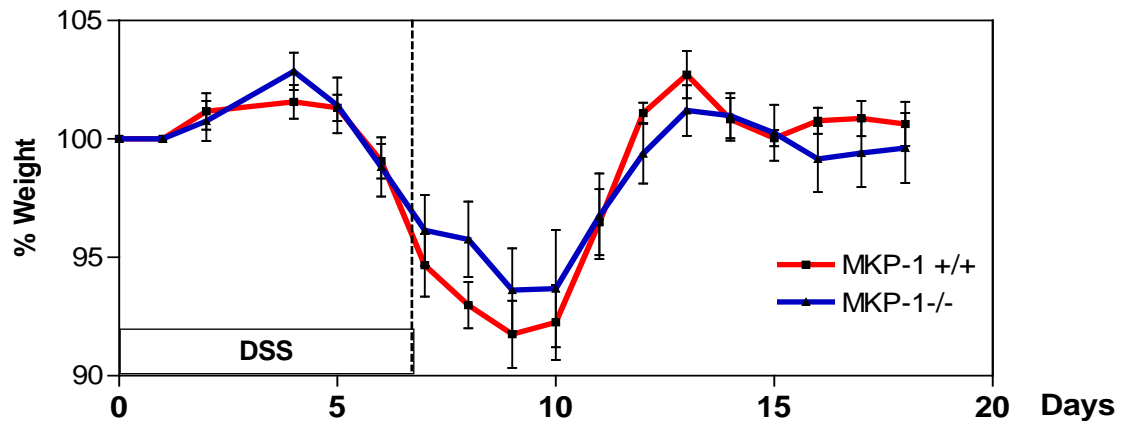


Fig 6.21. Loss of MKP-1 does not affect outcome of DSS induced colitis. MKP-1^{+/+} and MKP-1^{-/-} mice were given 2.5% DSS in drinking water for 7 days, weight loss was measured daily over 18 days. Error bars represent mean \pm SEM. n=5, experiment repeated in duplicate.

6.9 MKP-1 Deficiency Impairs Recovery from Experimental Autoimmune Encephalomyelitis

While MKP-1 was shown to have a significant role in innate immunity, it was of interest to examine what role if any MKP-1 might play in the adaptive immune response. To examine adaptive immunity *in vivo*, a mouse model of multiple sclerosis (MS) was used as this disease is characterised by dominant T cell responses. MS is a severely debilitating terminal disease which affects 85,000 individuals in the U.K alone. MS is characterised by severe muscle wasting and loss of neuronal function and is thought to be due to the overproduction of autoreactive T cells which attack the myelin sheath of neurons causing progressive neuronal loss over time (McFarland and Martin, 2007). Since neurons are terminally differentiated and non-dividing, progressive loss is irreversible.

Experimental autoimmune encephalomyelitis (EAE) is a mouse model of multiple sclerosis which closely resembles the human disease and is also characterised by muscle wasting and loss of motor function. Given the drastically altered cytokine profile in MKP-1^{-/-} mice, it was of interest to ascertain whether this might affect the pathology of EAE. Differences in cytokine production from the innate immune system would be expected to have an effect on the profile of effector T cells and thus possibly influence T cell responses to myelin. Therefore wild type and MKP-1 deficient mice were immunised with 50 μ g myelin oligodendrocyte glycoprotein (₋₅₅) peptide and 200 ng pertussis toxin followed 3 days later with another 200 ng pertussis toxin. Clinical score was measured daily over 35 days

according to the criteria shown in table 6.1. Clinical score began to increase from day 9, reaching a maximum at day 16 (Fig 6.22). No difference was seen between genotypes during the initiation phase of the disease, with clinical score being equivalent up to day 15 at the height of disease progression. From day 15 onwards, wild type mice showed a reduction in clinical score which is characteristic of this disease model (Stenman and Zamvil, 2005). Interestingly however, MKP-1 null mice did not show any recovery in symptoms, the clinical score remained close to day 15 levels for the duration of the protocol. This strongly suggests that MKP-1 plays a role in recovery from EAE and by inference, prolonged activation of MAPKs leads to a more severe pathology in MS. More detailed understanding of how MKP-1 contributes to MS may open up novel therapeutic avenues in the future.

Table 6.1. EAE clinical score measurement

0	No symptoms
1	Flacid Tail
2	One immobilised hind paw
3	Two immobilised hind paws
4	Upper body immobilisation
5	Moribund
6	Death

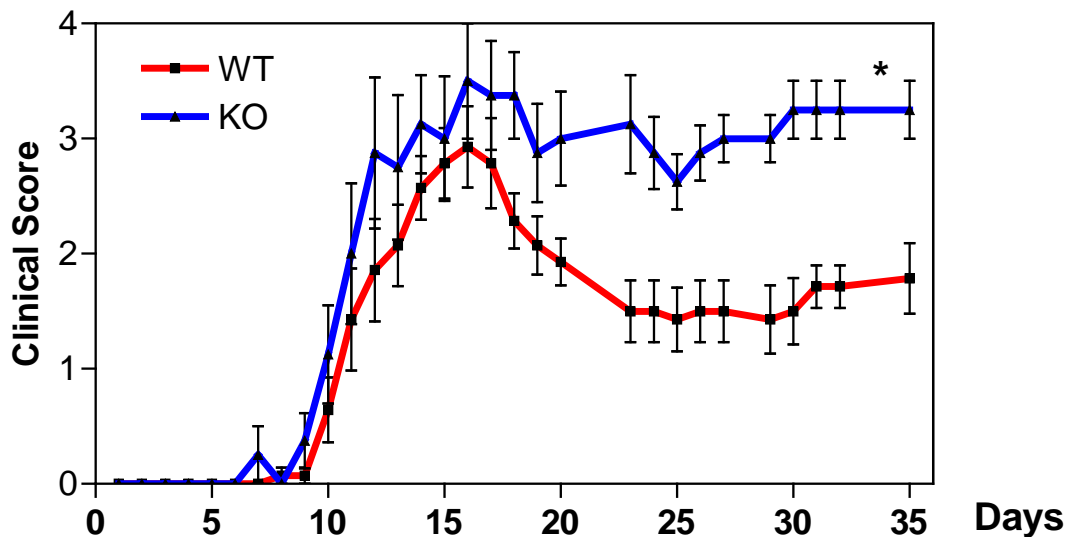


Fig 6.22. MKP-1 null mice show impaired recovery from EAE. MKP-1^{+/+} and MKP-1^{-/-} mice were immunized with 50 µg MOG injected *s.c* above 4 lymph nodes, mice were also injected with 200 ng pertussis toxin on day 0 and day 3. Clinical score was measured daily for 35 days. Error bars represent mean ± SEM, n=7 per group, experiment repeated in duplicate. Statistical analysis was carried out using a Mann-Whitney U test * p=0.01.

6.10 Loss of MKP-1 does not Effect T Cell Differentiation

Since EAE is dominated by T cell responses, one explanation for the severe phenotype seen in MKP-1 deficient mice may be dysregulated T cell production. To address this, the absolute numbers of lymphocytes in wild type and knock-out mice were examined; spleen, lymph nodes and thymus were stained with CD4 and CD8 antibodies and analysed by flow cytometry (Fig 6.23). No difference in single positive, double positive or double negative CD4 and CD8 cells was seen between genotypes demonstrating that MKP-1 does not affect CD4 or CD8 T cell generation.

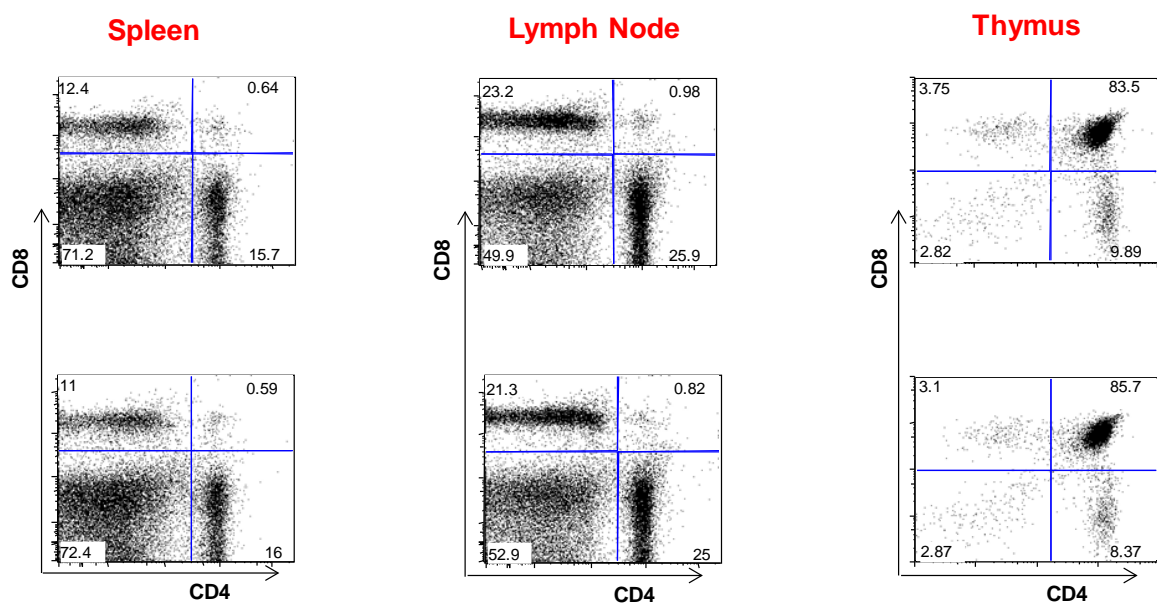


Fig 6.23. Flow Cytometry analysis of lymphoid cell Markers in MKP-1^{+/+} and MKP-1^{-/-} mice. Spleen, lymph node and thymus were harvested from MKP-1^{+/+} and MKP-1^{-/-} mice, digested with collagenase and cells were stained with CD4 and CD8 antibodies and analysed by flow cytometry. Representative plots are shown from 3 separate mice.

Although the generation of CD4⁺ and CD8⁺ T cells was not affected, MKP-1 might have a role to play in CD4⁺ T cell differentiation. Both JNK and p38 MAPK expression are necessary for Th1 differentiation (Dong et al., 2000, Rincon et al., 1998), suggesting that the prolonged phosphorylation of JNK and p38 in MKP-1 deficient mice might therefore lead to altered differentiation of T cell subsets. Taking this into account, it was thought that skewed T cell lineages might account for the difference in clinical outcome to EAE in MKP-1^{-/-} mice. Previously MKP-1 was shown to have no effect on the total numbers of Th1 and Th2 cells generated *in vitro* (Hongbo Chi, personal communication), however cytokine production from Th1 and Th2 cells has not been examined.

Initially the study was focused on IL-10 regulation, since IL-10 was shown to be highly elevated in MKP-1 deficient macrophages. To this end, MKP-1^{-/-} mice were crossed with the TIGER strain of IL-10 reporter mice (Kamanaka et al., 2006). TIGER mice have a GFP sequence fused to an internal ribosome entry site (IRES) inserted immediately before the polyadenylation site of the IL-10 gene, thereby allowing GFP fluorescence to be used as a marker of IL-10 expression. CD4⁺ T cells from TIGER⁺/MKP-1^{+/+} or TIGER⁺/MKP-1^{-/-} mice were separated using magnetic activated cell sorting (MACS) beads coated with anti-CD4 antibodies and incubated with irradiated splenocytes as a source of APCs along with IL-2 and soluble antibodies for CD3 and CD28. To induce Th1 and Th2 differentiation, cells were also incubated with IL-12 and anti-IL4 (Th1) or IL-4 and anti-IFN• (Th2). After 5 days in culture, viable effector cells were isolated using ficoll centrifugation and re-stimulated with PMA and ionomycin for 24 hr. The expression of GFP was then measured by flow cytometry. Fig 6.24a shows that as expected, Th1 conditions resulted in no GFP expression when compared to cells stimulated solely with anti-CD3, anti-CD28 and IL-2 (Th0), Th2 polarisation resulted in robust GFP staining, however there was no difference in GFP levels between MKP-1 wild type and knock- out mice.

To ensure that the results from the TIGER/MKP-1 mice were accurate, the experiment was repeated in MKP-1^{+/+} and MKP-1^{-/-} mice, this time using intracellular staining to measure the expression of IL-10 (Fig 6.24b). Th2 cells increased expression of IL-10 but again no difference was seen between genotypes. Expression of the Th1 signature cytokine IFN-• was also measured; Th1 cells upregulated IFN-•, with equal amounts being produced by wild type and MKP-1 deficient cells (Fig 6.24c).

Taken together, these results demonstrate that the macrophage IL-10 phenotype is not recapitulated in CD4⁺ T cells. Moreover, it appears that Th1 and Th2 cells differentiation is unaffected in the absence of MKP-1. The EAE phenotype in MKP-1^{-/-} mice can therefore not be accounted for by differences in intrinsic T cell responses. In addition, since IL-10 production from T cells is a major regulator of IBD pathology, the equivalent production of IL-10 from Th2 cells in both genotypes this may in part account for the unexpected lack of phenotype in MKP-1^{-/-} mice treated with DSS. Despite this, the TIGER/MKP-1^{-/-} mice will be extremely useful for future studies aimed at detailed understanding of the regulation of IL-10 in MKP-1 deficient mice.

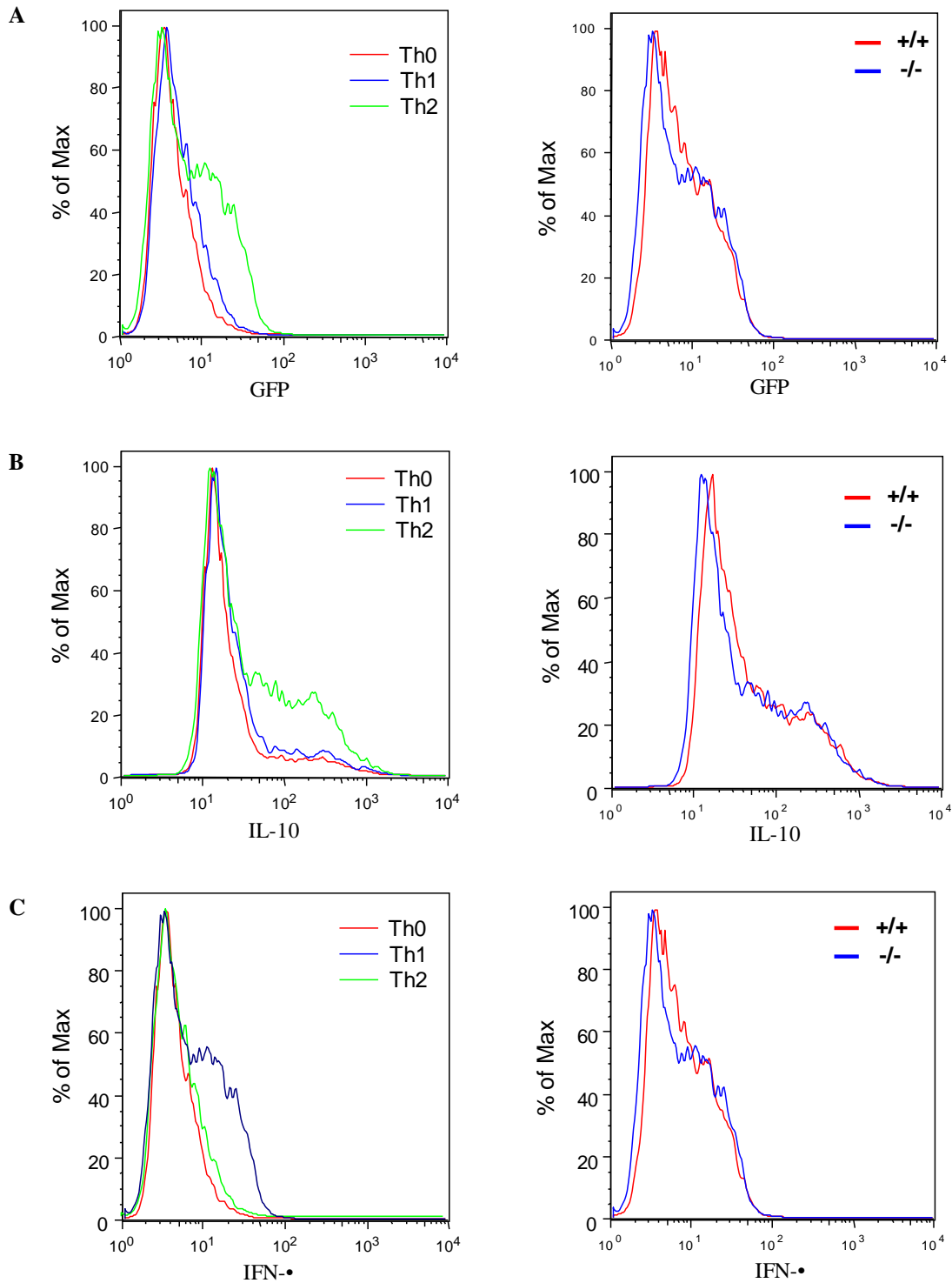


Fig 6.24. MKP-1 does not affect IL-10 expression from Th2 cells or IFN- γ expression from Th1 cells. (A) TIGER⁺/MKP-1⁺ or TIGER⁺/MKP-1^{-/-} CD4⁺ T cells were differentiated into Th0, Th1 or Th2 cells and GFP levels were measured by flow cytometry – left panel, the GFP expression from Th2 cells of both genotypes is shown in the right panel (B and C) IL-10 and IFN- γ levels were measured in wild type effector cells by intracellular staining –left panels, the levels of IL-10 (Th2 cells) and IFN- γ (Th1 cells) was compared between MKP-1^{+/+} and MKP-1^{-/-} mice – right panels. T cells were taken from 3 separate mice of each genotype, representative plots are shown. MKP-1

Since loss of MKP-1 does not appear to affect the differentiation of Th1 or Th2 cells, it was of interest to examine MKP-1 expression over the course of T cell activation. To examine the regulation of MKP-1 in T cells, total CD4 T cells were harvested from lymph nodes and spleen of wild type mice and activated with plate bound anti-CD3 and anti-CD28 antibodies over 28 hr and MKP-1 expression was analysed by qPCR. MKP-1 was transiently activated over 2 hours then time-dependently downregulated, by 28 hr only negligible levels of MKP-1 were expressed (Fig 6.25a). This suggests that MKP-1 may have a role to play in the early activation of T cells, however since expression is reduced over time it is unlikely that MKP-1 plays a significant role in fully differentiated effector T cells. To examine this further, total CD4 and CD8 T cells were grown in culture with irradiated splenocytes as a source of APCs along with IL-2 and soluble antibodies to CD3 and CD28 for up to 5 days. Both CD4 and CD8 cells downregulated MKP-1 mRNA levels following APC stimulation, showing almost no expression of MKP-1 over 5 days (Fig 6.25b,c). This finding that MKP-1 is normally downregulated in effector T cells explains why no difference was found in Th1 and Th2 differentiation i.e. MKP-1 deficient effector T cells are essentially the same as wild type T cells in terms of MKP-1 expression.

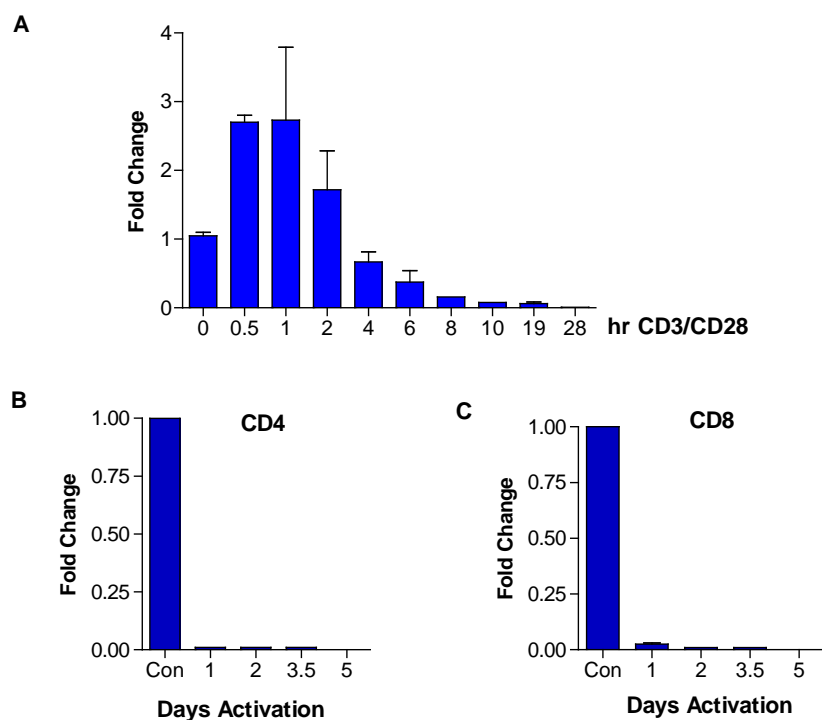


Fig 6.25. MKP-1 expression in activated T cells. (A) CD4⁺ T cells were incubated with 5 μ g/ml anti-CD3 and 2 μ g/ml anti-CD28 for the indicated times. MKP-1 expression was determined by qPCR. (B) Total CD4 or (C) CD8 T cells were incubated with irradiated splenocytes as a source of APC for the indicated times, MKP-1 expression was assessed by qPCR. Error bars represent mean \pm SEM, n=3 per group, experiment was repeated in triplicate.

6.11 Discussion

The family of MAP kinases comprises p38 MAPK, ERK and JNK, which are an integral part of the innate immune system and are all induced by TLR signalling. MAPKs phosphorylate several transcription factors, including ELK-1, MK2, 3 and 5, STATs, ATF2 and AP-1 and activation of these transcription factors leads to cytokine upregulation, comprising the first line of defense following pathogen infection. Cytokine release is obviously necessary and desirable to control the initial infection; however the resulting inflammation needs to be tightly regulated since uncontrolled cytokine release can have severely deleterious consequences. This is evidenced in many immunological diseases such as toxic shock, rheumatoid arthritis, IBD and multiple sclerosis, where prolonged cytokine release leads to severe pathology. Although the regulation of the NF- κ B pathway by TLRs has been extensively studied, the precise molecular control and regulation of the MAPK pathway in innate immunity is not as well defined.

Using knockout mice, it was found that following LPS challenge in macrophages, MKP-1 specifically inhibits p38 MAPK and JNK phosphorylation but had no effect on ERK phosphorylation. Increased activity of JNK and p38 MAPK in the absence of MKP-1 was accompanied by elevated DNA binding activity of the AP-1 transcription factor and enhanced production of several pro-inflammatory cytokines both *in vitro* and *in vivo*. This overproduction of cytokines resulted in MKP-1^{-/-} mice experiencing increased mortality during toxic shock, most likely due high systemic levels of TNF- α , IL-12 and IL-1 α . It is therefore suggested that during acute inflammation, the predominant role of MKP-1 is to serve as an endogenous brake on MAPK activation to suppress the production of pro-inflammatory cytokines. Although MKP-1^{-/-} mice produced increased levels of the anti-inflammatory cytokine IL-10, which has been previously shown to rescue mice from endotoxic shock, it may not be produced early enough or in sufficient amounts to counteract the effects of sustained release of several potent pro-inflammatory cytokines in these mice.

During toxic shock, nitric oxide levels are enhanced and cause a decrease in vascular resistance and hypotension, which along with activation of the procoagulation pathway can lead to ischaemia and multiple organ failure (Mackmicking et al., 1995). MKP-1^{-/-} mice had increased expression of iNOS, and although this study did not measure nitric oxide levels directly, two groups recently demonstrated that the increased iNOS expression in MKP-1^{-/-}

mice leads increased NO levels (Zhao et al. 2006, Calvert et al., 2008). MKP-1 deficient mice experienced increased hypotension during toxic shock compared to wild type mice and this was reversed by treating with nitric oxide inhibitors (Calvert et al., 2008). This suggests that in addition to elevated pro-inflammatory cytokine levels, increased NO may contribute to toxic shock mediated mortality in MKP-1^{-/-} mice.

This excessive pro-inflammatory cytokine production was also shown to have functional significance during bacterial infection, MKP-1 null mice suffered reduced bacterial load following *Lysteria Monocytogenes* infection compared with wild type controls. Clearance of *L. monocytogenes* infection is highly dependent on TNF- α and NO production from macrophages and DCs (Pamer, 2004), both of which are elevated in MKP-1^{-/-} mice. Therefore dysregulated cytokine release in the absence of MKP-1 can have both positive and negative effects. On the one hand, lack of MKP-1 can confer protection from infection, however if the infection is not efficiently cleared and spreads to the bloodstream, lack of MKP-1 will compound the deleterious effects of toxic shock. This may have important implications for MAPK modulating drugs which might be used to treat inflammatory conditions.

LPS challenge of macrophages showed that MKP-1 is upregulated within 1 hr and is then rapidly downregulated, suggesting tightly controlled temporal regulation of MAPK activity. It is interesting to note that LPS induced MKP-1 expression is dependent on both p38 and ERK. Since ERK phosphorylation is not affected by MKP-1 in the context of LPS stimulation, ERK mediated induction of MKP-1 may serve to limit the activity of p38 and JNK, suggesting an unappreciated level of cross regulation between MAPKs. Furthermore, MKP-1 expression was blocked by an NF- κ B inhibitor, suggesting cross-talk between the MAPK and NF- κ B pathways. Based on this data a model is proposed whereby following TLR stimulation, NF- κ B upregulates MKP-1 gene expression and p38 MAPK promotes transcript stabilization through the AREs located in the 3' UTR of MKP-1. More experiments will be need to verify this postulate, most importantly, examination of MKP-1 in cells deficient for components of the NF- κ B pathway as well as investigating MKP-1 transcript stability in cells which over- or under-express p38 MAPK. MKP-1 expression was found to be induced by all TLR ligands tested and this was dependent on the TLR signaling adaptors MyD88 and Trif. This demonstrates that MKP-1 induction occurs in response to a diverse range of pathogens and thus may be central to the inflammatory response.

TNF- \bullet production in macrophages is dynamically regulated by MKP-1, in the early part of an inflammatory response, MKP-1^{-/-} macrophages had increased mRNA and protein levels of TNF- \bullet , demonstrating that early expression of MKP-1 inhibits TNF- \bullet production. However, by 5 hr LPS challenge, the levels of TNF- \bullet mRNA produced by MKP-1^{-/-} macrophages was less than that of wild type cells. Analysis of TLR signalling showed that IL-10 was upregulated in MKP-1^{-/-} macrophages by all TLR ligands tested, again showing that this is a general feature of innate immunity and not confined to a single set of pathogens. Comparing expression profiles revealed that as the levels of IL-10 increased in MKP-1^{-/-} cells, the level of TNF- \bullet started to decrease. Blocking IL-10 with a neutralising antibody inhibited the downregulation of TNF- \bullet , clearly demonstrating that IL-10 was responsible for this effect. IL-10 inhibits TNF- \bullet induction via STAT3 mediated upregulation of Bcl-3 and both STAT3 tyrosine and serine phosphorylation and Bcl-3 expression were increased in MKP-1^{-/-} macrophages.

Based on chemical inhibitor studies, all three MAPK were found to contribute to IL-10 overproduction, however p38 MAPK appeared to be the main MAPK responsible. It should be noted however that MAPK inhibitors may sometimes have off target effects (Muniyappa and Das, 2008). However, drawing on the results of several experiments, a clear picture has emerged whereby MKP-1 influences cytokine production (Fig 6.26). Following TLR ligation, NF- \bullet B and MAPK are rapidly activated and in turn upregulate pro-inflammatory cytokines such as TNF- \bullet . By 1 hr post TRL ligation MKP-1 is upregulated, also by NF- \bullet B and MAPK, and begins to dephosphorylate p38 MAPK and JNK. By 2 hr TLR stimulation MKP-1 begins to be downregulated, most likely through feedback inhibition routed through MAPK inactivation. At this time, although p38 and JNK activity are reduced by MKP-1 they still have activity over basal levels; this enables the remaining active MAPK to induce IL-10 expression which can then limit TNF- \bullet production. Through the use of MKP-1, this negative feedback mechanism allows tight control of TNF- \bullet expression which is necessary to prevent the deleterious consequences of TNF- \bullet overproduction such as toxic shock.

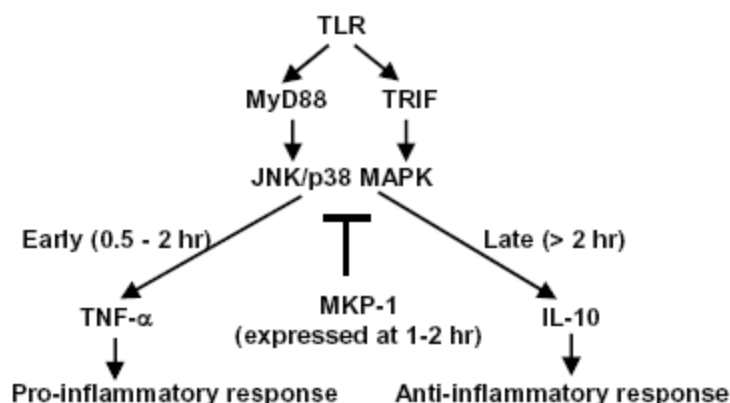


Fig 6.26. Model of MKP-1 mediated temporal regulation of cytokine production in TLR signaling. TLR signalling through the MAPK pathway induces two phases of cytokine production, an initial phase characterised by rapid production of pro-inflammatory cytokines such as TNF- \bullet and a second later phase involving IL-10 production. In the first phase p38 MAPK and JNK are rapidly activated (~20 min) leading to production of TNF- \bullet . This is followed by production of MKP-1 (~60 min) mediated through the MyD88 and TRIF pathways which serves as a negative feedback mechanism to downregulate MAPK signalling and TNF- \bullet production. In the second phase p38 MAPK and JNK activity are reduced due to MKP-1 but are still higher than basal levels whereas MKP-1 is downregulated to allow the remaining active p38 MAPK and JNK to promote IL-10 expression which in turn limits TNF- \bullet production.

There are at least four MKPs expressed in macrophages; MKP-1, MKP-2, PAC-1 and MKP-5. Each phosphatase appears to have different substrate specificity, for example MKP-1 prefers p38 and JNK as substrates whereas MKP-5 appears to be selective for JNK (Zhang et al., 2004). It is likely that induction of all the phosphatases co-coordinately regulates MAPK dephosphorylation, indeed in MKP-1^{-/-} cells, JNK and p38 MAPK dephosphorylation is delayed but does occur eventually, presumably through one of the other phosphatases. It is interesting to note that knockout of MKP-5 resulted in only a two-fold increase in TNF- \bullet serum levels following LPS challenge, whereas MKP-1^{-/-} mice produced 8 fold more. This may reflect the fact that MKP-5 only affects JNK activity, whereas MKP-1 affects both JNK and p38 MAPK, thereby effecting cytokine production more profoundly (Zhang et al., 2004). In the future, generation of double and triple knockouts will be of interest to tease apart the precise role of each and to get a better understanding of the level of redundancy within the MKP family.

While serum from LPS challenged MKP-1^{-/-} mice showed a 2 fold increase in the levels of IL-12, detailed analysis of MKP-1^{-/-} macrophages revealed that they in fact produced less IL-12 than wild type cells, a finding which has recently been confirmed by other investigators (Zhao et al., 2006). The source of the elevated levels of IL-12 in the serum is currently unknown, however CD8⁺ DCs are the first cells to synthesise IL-12 upon LPS stimulation (Trinchieri, 2003), this may account for the increased IL-12 production in MKP-1^{-/-} mice *in vivo*, more detailed analysis of MKP-1 deficient immune cell types is necessary to confirm this. Interestingly the reduction in IL-12 levels in MKP-1^{-/-} macrophages was not due to the concomitant increase in IL-10 levels; rather it may be a direct result of increased p38 MAPK and JNK activity.

IBD is characterised by excessive production of pro-inflammatory cytokines, including TNF- α , IL-12 and IFN- γ which induce an enhanced, chronic Th1 response. Furthermore, IL-6 promotes resistance to apoptosis in these T cells, exacerbating the chronic nature of the disease (Atreya et al., 2000). IL-10 has been shown to be beneficial in IBD, IL-10 deficient mice suffer from spontaneous colitis and IL-10 therapy has shown therapeutic promise in IBD (Kuhn et al., 1993, Steidler et al., 2000). STAT3 is indispensable for IL-10 signalling and mice where STAT3 is deleted in haematopoietic cells also suffer from colitis, demonstrating the important role of IL-10 in restraining the inflammatory response in IBD (Welte et al., 2003).

Since MKP-1^{-/-} mice have dysregulated production of TNF- α , IL-12, IL-6 and IL-10, all important cytokines in the pathogenesis of IBD, it was hypothesised that the response to IBD might be affected in MKP-1^{-/-} mice. However, no difference in weight loss was seen in MKP-1 deficient mice using a DSS model of colitis. This was especially surprising in light of the fact that JNK and p38 activation is enhanced in the colon of Crohn's patients and targeted MAPK inhibition has been shown to be of clinical benefit and was associated with reduced levels of TNF- α , IL-6 and IL-1 β (Hommes et al., 2002). There may be several explanations for this result. Firstly, there is overproduction of both pro- and anti-inflammatory cytokines in MKP-1^{-/-} mice and during colitis they may have the effect of balancing each other out. Secondly, excessive cytokine production may be transient and not sustained sufficiently long enough to have an effect on effector T cell function. Generation of effector T cells generally takes up to 96 hr and it is currently unknown if increased cytokine production in MKP-1^{-/-} mice is sustained to that extent during the initial innate immune phase

of DSS induced colitis. Other possibilities include effects of regulatory T cells or possibly a role for TGF- β .

Although no difference was seen in this model of colitis, use of additional colitis/IBD models should allow greater clarification of this issue. For example, transfer of naïve CD4⁺ T cells into lymphocyte-deficient Rag1^{-/-}/Rag2^{-/-} recipients leads to the development of a progressive Th1 cell-mediated IBD. (Annacker et al., 2003). Thus transfer of naïve T cells from MKP-1^{-/-} mice into Rag deficient mice or transfer of wt naïve T cells into MKP-1^{-/-}/Rag1^{-/-}/Rag2^{-/-} mice would more efficiently demonstrate if MKP-1 deficiency in T cells can affect the outcome of IBD.

Multiple sclerosis is a severely debilitating disease where autoreactive T cells attack the myelin sheaths of neurons. The EAE mouse model of multiple sclerosis is characterised by an initiation phase where the clinical symptoms worsen, followed by a period of remission where clinical symptoms improve but do not return to baseline. The clinical symptoms of EAE did not vary between genotypes in the early progression of the disease. There was a significant difference in the remission phase however, MKP-1^{-/-} mice did not show any amelioration of symptoms whereas wild type mice progressively improved over the course of 35 days. This suggests that MKP-1 may play an important role in the control of remission in EAE.

How MKP-1 controls EAE is currently unknown but several scenarios can be postulated. The number of infiltrating T cells into the spinal cord was not changed between MKP-1^{+/+} and MKP-1^{-/-} mice at day 35. However, it would be of interest to examine the number of infiltrating T cells earlier during the initiation phase, optimally at day 15, this might reveal increased T cell numbers in MKP-1^{-/-} mice in the spinal cord. By measuring at the end of the experiment, many of the autoreactive T cells may have already been removed by apoptosis. IL-10 production by B cells has been shown to be important in ameliorating the symptoms of EAE. Using bone marrow chimeric mice where the B cell compartment was deficient in IL-10, Fillatreau et al. found that these mice failed to recover from EAE even though IL-10 was being produced by other cell types (Fillatreau et al., 2002). Although it has been demonstrated that MKP-1 controls IL-10 signalling in macrophages, the role of MKP-1 in B cells has yet to be examined. Immunosuppressive regulatory T cells (Treg) are also

important producers of IL-10 and expand in numbers during the resolution phase of EAE, while immuno-depletion of Tregs delays recovery (McGeachy et al., 2005).

MKP-1 deficiency was not found to affect generation of naïve CD4⁺ or CD8⁺ T cells, nor did it affect the differentiation of Th1 or Th2 cells; this was surprisingly given the slew of evidence which highlights prominent roles for p38 and JNK in T cell differentiation (Rincon and Pedraza-Alva, 2003). While no intrinsic differences were found between Th1 and Th2 cells in the absence of MKP-1, differences in cytokine levels from macrophages and DCs may influence aspects of adaptive immunity. Using macrophages and DCs deficient in MKP-1 to present antigen and prime naïve T cells *in vitro* will address this question further.

Macrophage iNOS and NO play a prominent role in EAE, inhibition of NO reduces the severity of EAE and NO production by macrophages and brain microglia inhibit T cell proliferation (Rincon et al., 2003). It has also been suggested that NO might block conductance on hypomethylated axons (Redford et al., 1997). MKP-1^{-/-} macrophages were found to produce elevated levels of iNOS, however the contribution of this to EAE is currently unknown. Other possibilities include a role for MKP-1 in Treg function or an effect on the IL-23/IL-17 axis which has recently been shown to be paramount in EAE progression (Cua et al., 2003). In direct contrast to the results in MKP-1 mice, MKP-5 deletion confers protection from the onset of EAE, with MKP-5 deficient mice showing reduced disease incidence and reduced clinical score upon MOG immunization (Zhang et al., 2005). This may be due to reduced proliferation seen in MKP-5^{-/-} CD4 T cells and serves as a prime example of the functional heterogeneity seen within the MKP family.

Since this work was carried out, several publications have arisen concerning the immunological role of MKP-1. Three separate groups confirmed the findings that (i) MKP-1 regulates p38 MAPK and JNK activity in macrophages, (ii) MKP-1^{-/-} mice have increased mortality following endotoxic shock and (iii) serum levels of TNF- α , IL-6, IL-12 and IL-10 are elevated in MKP-1^{-/-} after LPS challenge (Zhao et al., 2006, Hammer et al., 2006, Salojin et al., 2006). In addition, MKP-1 was found to control the expression of the chemokines CCL3, CCL4 and CXCL12 and the cell surface markers CD40 and CD86 (Hammer et al., 2006, Salojin et al., 2006). Another recent study has shown that LPS induces p300 mediated acetylation of MKP-1 which enhances MKP-1 association with p38 (Cao et al., 2008). Interestingly, histone deacetylase inhibitors reduced inflammation and mortality in

wild type mice but failed to do so in MKP-1^{-/-} mice. MKP-1 has also been shown to be involved in limiting inflammation in the endothelium at sites of high shear stress (Zahhar et al., 2008). MKP-1 has been shown to be central to the anti-inflammatory effects of glucocorticoids. Glucocorticoids have been shown to both upregulate MKP-1 expression and attenuate MKP-1 proteasomal degradation (Kassel et al., 2001). In MKP-1 deficient cells, dexamethasone failed to inhibit p38 MAPK and JNK phosphorylation and failed to attenuate the upregulation of TNF- α , IL-1 α and Cox-2 in response to inflammatory stimuli (Abraham et al., 2006, Furst et al., 2007). Importantly, dexamethasone treatment did not protect MKP-1^{-/-} mice from LPS induced mortality (Abraham et al., 2006, Wang et al., 2008). These studies thus confirm the data presented here and show further that MKP-1 may be central to the pharmacology of widely prescribed anti-inflammatory drugs.

Taken together, these results implicate MKP-1 as a central player in the control of innate immune responses. MKP-1 activity influences the expression of a myriad of cytokines and its deficiency has profound implications in the setting of inflammatory pathology. To date no genetic study has reported an association between MKP-1 polymorphisms and inflammatory disease but in light of its new role as an immunoregulatory factor, it would be of great interest to examine if such polymorphisms exist. In the future it will be of great interest to develop MKP-1 modulating compounds as a therapeutic strategy for regulating MAPK signaling in inflammatory diseases such as RA and multiple sclerosis. The finding that MKP-1 plays a central role in two medically relevant conditions, multiple sclerosis and toxic shock suggests that targeting MKPs activity may be therapeutically beneficial. The recent finding that many of the anti-inflammatory actions of glucocorticoids are mediated through MKP-1 should also pave the way for further research into MKP-1 signalling to facilitate the rational design of next generation steroid drugs which are more specific with fewer side effects.

Chapter 7: General Discussion and Future Work

STAT3 was found to be active during I/R injury where it was responsible for limiting the extent of I/R mediated cell death. This adds to earlier work which had shown that the related transcription factor STAT1 is a pro-apoptotic mediator of I/R injury. Anti-oxidant treatment using tempol was found to limit the phosphorylation of STAT1 and STAT3 during I/R injury. This inhibition of STAT1 activity was shown to be physiologically relevant, since increased STAT1 phosphorylation following IFN- γ treatment counteracted the cardio-protective activity of tempol. These studies add to the emerging body of work which places STAT transcription factors at the centre of apoptotic control during I/R injury. Although manipulation of STAT transcription factors during I/R injury might theoretically be of clinical benefit, the pleiotropic role of these proteins may preclude direct modulation. Therefore it is of great interest to understand the downstream signaling whereby STAT3 mediates its anti-apoptotic effect in the myocardium. This effect is unlikely to reside in a single STAT3 dependent target but rather may involve several factors working in concert. STAT3 is upregulated in several cancers and in these cases the anti-apoptotic effects have been attributed to STAT3 dependent genes such as Bcl-2, Mcl-1, Bcl- and SOD2. Expression of these genes could be inhibited in turn in cardiac myocytes using RNAi and then assessed if overexpression of STAT3 could still confer cardioprotection.

Several studies have shown that administration of green tea and amino acid supplements modulate STAT1 and STAT3 phosphorylation. To further clarify the contribution of STATs to these cardioprotective effects they could be administered to STAT1 and/or STAT3 deficient mice and assessed for cardioprotective activity. The STAT3 antagonist GRIM-19 was found to be downregulated by I/R injury, how this influences STAT3 activity is currently unknown. Overexpression of GRIM-19 may abrogate the protective effects of STAT3 and this could be tested directly in transfection experiments. Another unanswered question is to what extent is the serine 727 residue of STAT3 critical for cardio-protection. The recent generation of STAT3 S727A mice (Shen et al., 2004) would be ideal to examine infarct sizes following *in vivo* I/R injury. Another unresolved question is whether phosphorylation of STAT1 and STAT3 following I/R injury is mediated through growth factor/cytokine release and JAK phosphorylation or through intracellular mechanisms such as via non-receptor tyrosine kinases. This question could be approached by taking conditioned medium from cardiac myocytes following I/R injury, adding it to a separate culture of myocytes and assessing STAT phosphorylation. If cytokine release occurs rapidly after reperfusion, this

conditioned medium should be capable of rapidly inducing STAT phosphorylation in a new culture.

STAT3 also appears to be necessary for a fully fledged DNA damage response; the absence of STAT3 renders cells less efficient in DNA repair. Several possible mediators of this were identified and included ATM, H2AX and MDC1. It is unclear precisely how STAT3 controls the DNA damage response. STAT3 was found to be able to upregulate expression of MDC1, however it is unknown whether this is through direct binding or indirectly via another STAT3 target gene. Direct ChIP assay of the MKP-1 promoter region would allow further characterization of STAT3 dependent transactivation. Increased levels of STAT3 were found to promote more efficient DNA repair which has implications for chemoresistance in cancer. If STAT3 overexpressing tumors can more readily repair damaged DNA it follows that STAT3 overexpression might directly contribute to increased resistance to chemotherapeutic drugs. DNA repair capacity could be tested directly in STAT3 overexpressing cancers and compared to the level of repair after treatment with one of the new class of STAT3 inhibiting drugs.

Microarray analysis identified several novel transcriptional changes which occurred during I/R injury *in vivo*. Further characterization of these effects may give novel insight to I/R injury. A major first step would be to assess if these gene expression changes are also seen at the protein level. The reduced expression of mitochondrial transport proteins is intriguing. It is currently unknown if mitochondrial transport is altered during I/R injury but the reduced expression of specific mitochondrial transport proteins would argue that transport into the mitochondria may be compromised during I/R injury. Experiments could be carried out to directly examine mitochondrial transport of proteins during I/R. This could be achieved using an immunofluorescence approach, transfecting a GFP construct tagged with a mitochondrial target sequence into cardiac myocytes, subjecting them to I/R injury and then examination of the subcellular localization of GFP. Another approach would be to load cells with a radioactively labeled mitochondrial bound protein. Following I/R injury, cardiac myocytes could be subjected to subcellular fractionation and levels of radioactivity in control mitochondrial fractions compared to that of I/R fractions. If indeed mitochondrial transport is reduced during I/R injury, it may affect mitochondrial respiration. This could be assessed by overexpressing components of the mitochondrial transport machinery and examining their effect on mitochondrial respiration during I/R.

Both Ucn1 and Ucn2 were found to lower oxidative stress during I/R injury, however the exact mechanism is unknown. Ucn1 and Ucn2 were both found to upregulate expression of the anti-oxidant gene Nrf-1. Again, examination of Nrf-1 protein levels following urocortin administration would clarify if Nrf-1 is a true target of urocortins and examination of both the anti-oxidant and cardio-protective activity of Ucn1 and Ucn2 in the absence of Nrf-1 would determine to what extent it mediates these effects. Another potential mediator of urocortin cardioprotection is XIAP, which has previously been shown to be necessary for upregulation of anti-oxidants (Resch et al., 2008). Caspase activity and apoptosis levels could be examined following urocortin treatment during I/R in the absence of XIAP to ascertain if XIAP is an absolute requirement for Ucn-mediated cardioprotection.

The finding that the IL-17 cytokines and the IL-17 receptor are upregulated during I/R may represent an important point of cross talk between the immune system and the cardiovascular system during I/R injury. Many questions remain to be answered concerning the regulation and biological effect of IL-17 during I/R injury. Firstly, IL-17 cytokine and receptor levels need to be measured directly by flow cytometry to show that increased mRNA levels are recapitulated by increased protein expression. Measurements of serum IL-17 levels following experimental I/R and in patients would strengthen these findings. Detailed examination of signalling pathways induced by IL-17 in cardiac myocytes both in the presence and absence of I/R injury could be conducted to tease apart the effect of IL-17 on cardiac myocyte physiology. Fundamentally it is still unknown whether elevated IL-17 signalling represents a deleterious or beneficial phenomenon in I/R injury.

The finding that MKP-1 serves as a rheostat for inflammatory responses is an important addition to the growing body of literature concerning the resolution phase of inflammation. Traditionally, the major focus of inflammatory research has been centered on understanding the signals which induce the inflammatory response with less regard given to how inflammation is switched off. Over the last five years however, there has been much greater scientific focus on this resolution phase of inflammation (Serhan et al., 2007). The findings presented here place MKP-1 as a central modulator of inflammatory resolution, in the absence of MKP-1, exuberant cytokine production ensues, leading to deleterious consequences in the case of toxic shock. Increasing cellular availability of MKP-1 might represent a novel approach to limit pro-inflammatory cytokine production which lies at the

heart of an abundance of human pathologies. Although direct administration of MKP-1 is not feasible, more detailed understanding of MKP-1 protein biochemistry might allow small molecule targeting of proteins which inhibit MKP-1 activity. Emerging evidence suggests that one aspect of glucocorticoid mediated inflammatory suppression lies in their ability to induce MKP-1 expression. Although glucocorticoids are a widely prescribed and highly efficacious drug class, one of the major drawbacks of treatment is the resulting side effects such as osteoporosis, stomach ulcers and poor skin healing. Dissecting out the molecular pathways of the MKP-1 - dependent versus the MKP-1 - independent activity of glucocorticoids might pave the way for rational design of next generation anti-inflammatory drugs which might have reduced side effects.

Many questions still remain to be answered regarding the immune response and MKP-1. While this study focused exclusively on MKP-1, there are several other MKPs which may exert control over the immune system in a parallel manner to MKP-1. At the moment only single knockouts of each phosphatase exist, but in the future, generation of double and triple knockouts will allow a greater understanding of how each phosphatase in turn and in concert influence inflammatory responses. The main cell types examined in these studies were macrophages, T cells and to a lesser extent dendritic cells. There are a range of other cell types central to immune function including B cells, neutrophils and mast cells. Examination of the role of MKP-1 in these additional cell types will provide a more holistic picture of its place in the immune system.

An exciting finding of this study was that MKP-1 deficient mice fail to recover from a mouse model of multiple sclerosis and this may have direct implications in understanding MS pathology. The study did not address the mechanism whereby MKP-1 contributes to the EAE phenotype and it is yet unclear as to whether MKP-1 regulates pathological T cell function intrinsically or through its impact on the innate immune system. Since macrophages and DCs deficient in MKP-1 produce altered cytokine responses, there is a good possibility that these cells might contribute to the generation of altered T cell repertoires.

This can be addressed in several ways. Firstly by using OT-II transgenic mice in which T cells express a V α 2/V β 5 TCR specific for an ovalbumin (Ova). MKP-1^{+/+} and MKP-1^{-/-} DC would be incubated with ₋₃₃₉ peptide in the presence and absence of LPS, and then mixed with OT-II CD4 T cells (TCR-transgenic T cells that recognize ₋₃₃₉). T cell proliferation and

cytokine production (IL-2, IL-4, IFN- γ , and IL-17) would then be assayed by 3 H-thymidine proliferation and ELISA, respectively. Indeed initial studies have suggested that lack of MKP-1 in antigen presenting cells may lead to a skewed Th1 phenotype although the experiments were too preliminary to include in this thesis. An alternative *in vivo* approach would be to label OT-II CD4 T cells with CFSE and transfer them into MKP-1^{+/+} and MKP-1^{-/-} mice. The mice would then be immunized with OVA emulsified in Complete Freund's Adjuvant (CFA). CFSE dilution would then be used to measure T cell proliferation and production of T cell cytokines assayed by intracellular staining. These assays would reveal the effect of MKP-1 deficiency in DC on the control of T cell activity *in vitro* and *in vivo*.

It has recently become clear that IL-17 producing cells are central to the pathogenesis of EAE, however this study did not examine the effect of MKP-1 on Th17 cell production. To address this, naïve T cells could be purified from the spleen and lymph nodes of MKP-1^{+/+} and MKP-1^{-/-} mice and stimulated with plate bound α -CD3, α -CD28, IL-6 and TGF- β for five days and the production of IL-17 measured by ELISA and qPCR. In addition, EAE could be induced in MKP-1^{+/+} and MKP-1^{-/-} mice, and production of IL-17 by infiltrating T cells in the brain could be determined by intracellular staining.

To address which cell type requires MKP-1 for the regulation of EAE *in vivo*, an adoptive transfer approach could be employed using MKP-1/RAG1 double knockout mice. WT CD4 T cells would be transferred into MKP-1^{+/+}/RAG1^{-/-} or MKP-1^{-/-}/RAG1^{-/-} mice before MOG immunization – this would reveal whether lack of MKP-1 in APC but not T cells regulates EAE. Conversely, WT CD4 T cells or MKP-1^{-/-} CD4 T cells could be transferred into MKP-1^{+/+}/RAG1^{-/-} mice before immunization – this would determine whether lack of MKP-1 in T cells but not APC regulates EAE. Altogether, these three approaches will allow one to explicitly address whether the protective role of MKP-1 in EAE is mediated through intrinsic effects in the adaptive immune system or through crosstalk between the innate and adaptive immune compartments.

Another important question is whether MKP-1 regulates T cell-dependent immune responses and autoimmune inflammation through negatively modulating JNK or p38 activity. In order to ascertain if the non-remitting phenotype seen in the MKP-1 deficient mice is due to overt activation of p38 or JNK, EAE would be induced in the presence of pharmacological inhibitors of p38 and JNK. These compounds are in clinical trials for the treatment of arthritis

but have yet to be tested in neuro-inflammatory conditions. Although MKP-1 preferentially inactivates p38 and JNK in cell culture, the physiologically relevant substrate in a disease model is unknown. One could pursue this line of inquiry further by generating JNK1/JNK2 or MKK3/MKK6 double knockouts which would definitively reveal the contribution of JNK and p38 to EAE pathology.

Relatively few MKP-1 binding partners have been thus far identified; it would therefore be of potential interest to characterize MKP-1 interactors in cells following LPS treatment. This could be done using an *in vitro* purification/immunoprecipitation and mass spectrometry approach. Identification of novel MKP-1 binding partners would aid in developing novel MKP-1 modulatory agents. One final caveat to the data presented here is that the studies were all conducted in total MKP-1 knockout mice; however a clearer understanding of how MKP-1 affects the innate and T cell compartments could be gleaned from macrophage and T cell specific knockouts.

Appendix 1

(A) Table of Antibodies

Antibody	Company	Species	Catalogue No.
Actin	Santa Cruz	Mouse	Sc-8438
p42/44 ERK	Cell Signaling	Rabbit	9102
GAPDH	Chemicon	Mouse	374
JNK	Cell Signaling	Rabbit	9252
MKP-1	Actin	Rabbit	sc-370
	Upstate	Rabbit	07-164
pERK1/ /Y185	Santa Cruz	Mouse	sc-7383
	Cell Signaling	Rabbit	9251
p38 MAPK	Cell Signaling	Rabbit	9212
pp38 ^{/Y182}	Cell Signaling	Mouse	9216
STAT1	Santa Cruz	Rabbit	sc-346
STAT3	Santa Cruz	Rabbit	sc-482
p-	Zymed	Mouse	33-3400
p-	Upstate	Rabbit	07-714
p-	Cell Signalling	Rabbit	9135
p-	Cell Signalling	Rabbit	9134
Caspase-9	Santa Cruz	Rabbit	sc8355
p-	Cell Signalling	Rabbit	2341
p-	Cell Signalling	Mouse	9286
GRIM-19	Gift from Dhan Kalvakolanu	Mouse	

(B) Table of constructs

Construct	Vector backbone	Obtained From	Institute
STAT3	pcDNA3	James Darnell	Rockefeller Institute
STAT3 β	pSG5	Betty Pace	University of Texas
STAT3 Y705F	pRc/CMV	James Darnell	Rockefeller Institute
STAT3 S727A	pRc/CMV	James Darnell	Rockefeller Institute
STAT3 Y705F/S727A	pRc/CMV	Xinmin Cao	National University of Singapore
STAT3C	pRc/CMV	James Darnell	Rockefeller Institute
p21-Luc	pGL3	Wafik El-Deiry	University of Pennsylvania
3 x Ly-6E	pZLuc	James Darnell	Rockefeller Institute
pEGFP-C1	pUC	Clontech	

(c) Table of cell lines

Cell Line	Obtained From	Institute
Mouse embryonic fibroblasts	Valeria Poli	University of Turin
2FTGH	George Stark	Cleveland Clinic Foundation
U3A	George Stark	Cleveland Clinic Foundation
Chinese Hamster Ovary Cells	American Tissue Culture Collection	Virginia

Appendix 2: List of Primers

Actin-F	AGATGACCCAGATCATGTTTGAG
Actin- R	AGGTCCAGACGCAGGATG
Beta2-micro-F	GTCTTTCTGGTGCTTGTCTCA
Beta2-micro-R	GTGAGCCAGGATATAGAAAGA
Bcl-2_F	GGGAGATCGTGATGAAGTAC
Bcl-2_R	ACATCTCTGCGAAGTCACGA
BNip3_F	GTTCCAGCTTCCGTCTCTAT
BNip3_R	CGCTTGTGTTTCTCATGCTG
c-fos_F	GCCTTTCCTACTACCATTCC
c-fos_R	CCGTTTCTCTTCCTCTTCAG
DUSP1_F	TACAGGAAGGACAGGATCTC
DUSP1_R	AGTGCACAAACACCCTTCCT
DUT-F	TCTGGGTGCTATGGAAGAGT
DUT-R	AAGCCTCCTGAGCCTCTCTC
HPRT_F	CTCATGGACTGATTATGGACAGGAC
HPRT_R	GCAGGTCAGCAAAGAACTTATAGCC
HSP70_F	ACATGAAGCACTGGCCCTT
HSP70_R	AAGATGAGCACGTTGCGCT
Icos_F	CGGTGTCCATCAAGAATCCA
ICOS_R	ACGGGTAACCAAAGCTTCAG
IFNg_F	GTCTTGGTTTTGCAGCTCTG
IFNg_R	TGGTGACAGCTGGTGAATCA
IL-1B_R	CGTTGCTTGGTTCTCCTTGT
IL-1B_R	CGTTGCTTGTCTCTCCTTGT
IL-17A-F	AGGCCCTCAGACTACCTCA
IL-17A-R	TCTCAGGCTCCCTCTTCAG
IL-17F-F	GGCATTCTGTCCCACGTG
IL-17F-R	CTCCAACCTGAAGGAATTAGA
IL-17R-F	GGGTGTATGGCCTCATCAC
IL-17R-R	ACAGGCAGTGATCAGGAACT

IL-6_F	ACTGCCTTCCCTACTTCACA
IL-6_R	GCTCTGAATGACTCTGGCTT
iNOS_F	AGCGGCTCCATGACTCTCA
iNOS_R	TGCACCCAAACACCAAGGT
MAP4K2_F	CCGCTTGTGGATATGTATGG
MAP4K2_R	ATTGTAGCCACCCTTGCCTT
Mdc1_F	AGGTGATTGACTGGGATGCT
Mdc1_R	GATGGTACTGGCAGGGAAA
MMP8_F	ATCTGGAGTGTGCCATCAAC
MMP8_R	GCTGGGTTCTCTGTAAGCAT
MMP9_F	GAAGACGACATAAAAAGGCATCC
MMP9_R	TCAGAAGGACCAGCAGTAG
Nfe2l1-F	AGAGCCCGAGCCATGAAGA
Nfe2l1-R	TCAGTCACGGTCCTGTAAATT
SOCS3_F	TGGTCACCCACAGCAAGTTT
SOCS3_R	ACCAGCTTGAGTACACAGTC
STAT3_F	TCCTCTATCAGCACAACCTG
STAT3_R	CTCCTTGACTCTTGAGGGTT
Timm8a_F	CATTTTCATCGAGGTGGAGAC
Timm8a-R	CTTGTATCAATGAAAGCGTTC
Timm8b_F	AAGCGGAGTTACAACGCCT
Timm8b_R	GTGATGGCAAGAGTAGTGTC
Timm13-F	ATGACGGACAAGTGTTTCC
Timm13-R	TCACATGTTGGCTCGTTCC
Timm23_F	GTCCCGCTGACTGGTATGAA
Timm23_R	GAGCCTAGAGTATTAGCCCA
Timm44_F	TAGAAGAGTCGGATGCCCTT
Timm44_R	CTCCTTCTTCACCGACTCTA
Tom20-F	CTTCAAGAACAGGCTTCGAG
Tom20-R	CCAAGCTGTATCTCTTCAAGG
XIAP-F	GAGGGCTCACGGATTGGAA
XIAP-R	ACTCACAAGATCTGCAATCAG

References

- Abbate A, Bussani R, Biondi-Zoccai GG, Rossiello R, Silvestri F, Baldi F, Biasucci LM, Baldi A: Persistent infarct-related artery occlusion is associated with an increased myocardial apoptosis at postmortem examination in humans late after an acute myocardial infarction. *Circulation*. 2002, 106:1051-4.
- Abbate A, Salloum FN, Vecile E, Das A, Hoke NN, Straino S, Biondi-Zoccai GG, Houser JE et al: Anakinra, a recombinant human interleukin-1 receptor antagonist, inhibits apoptosis in experimental acute myocardial infarction. . 2008, 117:2670-83.
- Abe J, Berk BC: Fyn and JAK2 mediate Ras activation by reactive oxygen species. *J Biol Chem*. 1999, 274:21003-10.
- Abe J, Okuda M, Huang Q, Yoshizumi M, Berk BC: Reactive oxygen species activate p90 ribosomal S6 kinase via Fyn and Ras. *J Biol Chem*. 2000, 275:1739-48.
- Abe K, Hayashi N, Terada H.: Effect of endogenous nitric oxide on energy metabolism of rat heart mitochondria during ischemia and reperfusion. *Free Radic Biol Med*. 1999, 26:379-87.
- Abraham SM, Lawrence T, Kleiman A, Warden P, Medghalchi M, Tuckermann J, Saklatvala J, Clark AR: Antiinflammatory effects of dexamethasone are partly dependent on induction of dual specificity phosphatase 1. *J Exp.Med* 2006, 203:1883-1889.
- Adachi N, Ishino T, Ishii Y, Takeda S, Koyama H: DNA ligase IV-deficient cells are more resistant to ionizing radiation in the absence of Ku70: Implications for DNA double-strand break repair. *Proc Natl Acad Sci U S A*. 2001, 98:12109-13
- Adachi O, Kawai T, Takeda K, Matsumoto M, Tsutsui H, Sakagami M, Nakanishi K, Akira S: Targeted disruption of the MyD88 gene results in loss of IL-1- and IL-18-mediated function. *Immunity*. 1998, 9:143-150.
- Adrain C, Brumatti G, Martin SJ: Apoptosomes: protease activation platforms to die from. *Trends Biochem.Sci*. 2006, 31:243-247.
- Agnello D, Lankford CS, Bream J, Morinobu A, Gadina M, O'Shea JJ, Frucht DM: Cytokines and transcription factors that regulate T helper cell differentiation: new players and new insights. *J Clin.Immunol*. 2003, 23:147-161.
- Aikawa M, Libby P: The vulnerable atherosclerotic plaque: pathogenesis and therapeutic approach. *Pathol*. 2004,13:125-38.
- Aikawa R, Komuro I, Yamazaki T, Zou Y, Kudoh S, Tanaka M, Shiojima I, Hiroi Y, Yazaki Y: Oxidative stress activates extracellular signal-regulated kinases through Src and Ras in cultured cardiac myocytes of neonatal rats. *J Clin Invest*. 1997,100:1813-21.
- Albanesi C, Cavani A, Girolomoni G. IL-17 is produced by nickel-specific T lymphocytes and regulates ICAM-1 expression and chemokine production in human keratinocytes: synergistic or antagonist effects with IFN-gamma and TNF-alpha. *J Immunol*. 1999, 162:494-502.
- Adderley SR, Fitzgerald DJ: Oxidative damage of cardiomyocytes is limited by extracellular regulated kinases 1/2-mediated induction of cyclooxygenase-2. *J Biol Chem*. 1999, 274:5038-46.

Alexander WS, Starr R, Fenner JE, Scott CL, Handman E, Sprigg NS, Corbin JE, Cornish AL, Darwiche R, Owczarek CM, Kay TW, Nicola NA, Hertzog PJ, Metcalf D, Hilton DJ: SOCS1 is a critical inhibitor of interferon gamma signaling and prevents the potentially fatal neonatal actions of this cytokine. *Cell*. 1999, 98:597-608.

Allen DG, Xiao XH: Role of the cardiac Na⁺/H⁺ exchanger during ischemia and reperfusion. *Cardiovasc Res*. 2003, 57:934-41.

Alonzi T, Maritano D, Gorgoni B, Rizzuto G, Libert C, Poli V: Essential role of STAT3 in the control of the acute-phase response as revealed by inducible gene inactivation [correction of activation] in the liver. *Mol.Cell Biol* 2001, 21:1621-1632.

Alvarez JV, Febbo PG, Ramaswamy S, Loda M, Richardson A, Frank DA. Identification of a genetic signature of activated signal transducer and activator of transcription 3 in human tumors. *Cancer Res*. 2005, 65:5054-62.

Ancey C, Menet E, Corbi P, Fredj S, Garcia M, Rucker-Martin C, Bescond J, Morel F, Wijdenes J, Lecron JC, Potreau D: Human cardiomyocyte hypertrophy induced in vitro by gp130 stimulation. *Cardiovasc.Res*. 2003, 59:78-85.

Angell JE, Lindner DJ, Shapiro PS, Hofmann ER, Kalvakolanu DV: Identification of GRIM-19, a novel cell death-regulatory gene induced by the interferon-beta and retinoic acid combination, using a genetic approach. *J Biol Chem*. 2000, 275:33416-26.

Annacker O, Asseman C, Read S, Powrie F: Interleukin-10 in the regulation of T cell-induced colitis. *J Autoimmun*. 2003, 20:277-9.

Archer KJ, Dumur CI, Joel SE, Ramakrishnan V: quality of hybridized RNA in Affymetrix GeneChip experiments using mixed-effects models: *Biostatistics*. 2006, 7:198-212.

Armstrong LC, Saenz AJ, Bornstein P: Metaxin 1 interacts with metaxin 2, a novel related protein associated with the mammalian mitochondrial outer membrane. *J Cell Biochem*. 1999, 74:11-22.

Arnoult D, Gaume B, Karbowski M, Sharpe JC, Cecconi F, Youle RJ.: Mitochondrial release of AIF and EndoG requires caspase activation downstream of Bax/Bak-mediated permeabilization. *EMBO J*. 2003, 22:4385-99.

Arnoult D, Rismanchi N, Grodet A, Roberts RG, Seeburg DP, Estaquier J, Sheng M, Blackstone C: Bax/Bak-dependent release of DDP/TIMM8a promotes Drp1-mediated mitochondrial fission and mitoptosis during programmed cell death. *Curr Biol*. 2005, 15:2112-8.

Ashwell JD: The many paths to p38 mitogen-activated protein kinase activation in the immune system. *Nat.Rev.Immunol*. 2006, 6:532-540.

R, J, S, J, T, S, M, B et al: Blockade of interleukin 6 trans signaling suppresses T-cell resistance against apoptosis in chronic intestinal inflammation: evidence in crohn disease and experimental colitis in vivo. *Med*. 2000, 6:583-8.

Badger AM, Bradbeer JN, Votta B, Lee JC, Adams JL, Griswold DE: Pharmacological profile of SB 203580, a selective inhibitor of cytokine suppressive binding protein/p38 kinase, in animal

models of arthritis, bone resorption, endotoxin shock and immune function. *J Pharmacol Exp. Ther.* 1996, 279:1453-1461.

Bahi N, Zhang J, Llovera M, Ballester M, Comella JX, Sanchis D: Switch from caspase-dependent to caspase-independent death during heart development: essential role of endonuclease G in ischemia-induced DNA processing of differentiated cardiomyocytes. *Biol Chem.* 2006, 281:22943-52.

Baines CP, Kaiser RA, Purcell NH, Blair NS, Osinska H, Hambleton MA, Brunskill EW, Sayen MR, Gottlieb RA, Dorn GW, Robbins J, Molkentin JD: Loss of cyclophilin D reveals a critical role for mitochondrial permeability transition in cell death. *Nature.* 2005, 434:658-62.

Baines CP: The mitochondrial permeability transition pore as a target of cardioprotective signaling. *Am J Physiol Heart Circ Physiol.* 2007 293:H903-4.

Bakhshi A, Jensen JP, Goldman P, Wright JJ, McBride OW, Epstein AL, Korsmeyer SJ: Cloning the chromosomal breakpoint of t(14;18) human lymphomas: clustering around JH on chromosome 14 and near a transcriptional unit on 18. *Cell.* 1985, 41:899-906.

Bale TL, Hoshijima M, Gu Y, Dalton N, Anderson KR, Lee KF, Rivier J, Chien KR, Vale WW, Peterson KL: The cardiovascular physiologic actions of urocortin II: acute effects in murine heart failure. *Proc Natl Acad Sci U S A.* 2004, 101:3697-702.

Barnes E, Khan MA: Myocardial stunning in man. *Fail Rev.* 2003, 8:155-60.

Baron M, Davignon JL: Inhibition of IFN-gamma-induced STAT1 tyrosine phosphorylation by human CMV is mediated by SHP2. *J Immunol.* 2008, 181:5530-6.

Becker LB, vanden Hoek TL, Shao ZH, Li CQ, Schumacker PT: Generation of superoxide in cardiomyocytes during ischemia before reperfusion. *Am J Physiol.* 1999, 277:H2240-6.

Becker LB: New concepts in reactive oxygen species and cardiovascular reperfusion physiology. *Cardiovasc. Res.* 2004, 61:461-470.

Bellot G, Cartron PF, Er E, Oliver L, Juin P, Armstrong LC, Bornstein P, Mihara K, Manon S, Vallette FM: TOM22, a core component of the mitochondria outer membrane protein translocation pore, is a mitochondrial receptor for the proapoptotic protein Bax. *Death Differ.* 2007, 14:785-94.

Benjamini Y, Yekutieli D: False discovery rate-adjusted multiple confidence intervals for selected parameters. *Journal of the American Statistical Association* 2005, 100:71-81.

Berg DJ, Lynch NA, Lynch RG, Lauricella DM: Rapid development of severe hyperplastic gastritis with gastric epithelial dedifferentiation in *Helicobacter felis*-infected IL-10(-/-) mice. *Am. J Pathol.* 1998, 152:1377-1386.

Bettelli E, Das MP, Howard ED, Weiner HL, Sobel RA, Kuchroo VK: IL-10 is critical in the regulation of autoimmune encephalomyelitis as demonstrated by studies of IL-10- and IL-4-deficient and transgenic mice. *J Immunol.* 1998, 161:3299-3306.

Bettelli E, Nicholson LB, Kuchroo VK: IL-10, a key effector regulatory cytokine in experimental autoimmune encephalomyelitis. *J Autoimmun.* 2003, 20:265-267.

- Bevan MJ: Helping the CD8(+) T-cell response. *Rev Immunol.* 2004, 4:595-602.
- Bolli R, Becker L, Gross G, Mentzer R Jr, Balshaw D, Lathrop DA: Myocardial protection at a crossroads: the need for translation into clinical therapy. *Res.* 2004, 95:125-34.
- Bolli R, Marbán E: Molecular and cellular mechanisms of myocardial stunning. *Rev.* 1999, 79:609-34.
- KS, DL, RM, M, MK, JB Jr, RL: Nitric oxide produced during murine listeriosis is protective. *Immun.* 1994, 62:1089-100.
- Boonprasert P, Lailerd N, Chattipakorn N. Urocortins in heart failure and ischemic heart disease. *J Cardiol.* 2008 Jul 21;127(3):307-12.
- Bradley JR: TNF-mediated inflammatory disease. *J Pathol.* 2008, 214:149-60.
- Branger J, van den BB, Weijer S, Madwed J, Bos CL, Gupta A, Yong CL, Polmar SH, Olszyna DP, Hack CE, van Deventer SJ, Peppelenbosch MP, van der PT: Anti-inflammatory effects of a p38 mitogen-activated protein kinase inhibitor during human endotoxemia. *J Immunol.* 2002, 168:4070-4077.
- Brar BK, Jonassen AK, Egorina EM, Chen A, Negro A, Perrin MH, Mjøs OD, Latchman DS, Lee KF, Vale W: Urocortin-II and urocortin-III are cardioprotective against ischemia reperfusion injury: an essential endogenous cardioprotective role for corticotropin releasing factor receptor type 2 in the murine heart. *Endocrinology.* 2004, 145:24-35.
- Brar BK, Jonassen AK, Stephanou A, Santilli G, Railson J, Knight RA, Yellon DM, Latchman DS: Urocortin protects against ischemic and reperfusion injury via a MAPK-dependent pathway. *J.Biol.Chem.* 2000, 275:8508-8514.
- Brar BK, Stephanou A, Knight R, Latchman DS: Activation of protein kinase B/Akt by urocortin is essential for its ability to protect cardiac cells against hypoxia/reoxygenation-induced cell death. *J Mol.Cell Cardiol.* 2002, 34:483-492.
- Brar BK, Stephanou A, Knight R, Latchman DS: Activation of protein kinase B/Akt by urocortin is essential for its ability to protect cardiac cells against hypoxia/reoxygenation-induced cell death. *J Mol Cell Cardiol.* 2002, 34:483-92.
- Brar BK, Stephanou A, Okosi A, Lawrence KM, Knight RA, Marber MS, Latchman DS: CRH-like peptides protect cardiac myocytes from lethal ischaemic injury. *Mol Cell Endocrinol.* 1999, 158:55-63.
- Braunwald E: Application of current guidelines to the management of unstable angina and non-ST-elevation myocardial infarction. . 2003, 108(16 Suppl 1):III28-37.
- V, AA, A, M, VO, M, M, A, P, H: Cardiac functional improvement by a human Bcl-2 transgene in a mouse model of ischemia/reperfusion injury. *Gene Med.* 2000, 2:326-33.
- Bromberg JF, Horvath CM, Besser D, Lathem WW, Darnell JE Jr: Stat3 activation is required for cellular transformation by v-src. *Mol Cell Biol.* 1998, 18:2553-8.

- Bromberg JF, Wrzeszczynska MH, Devgan G, Zhao Y, Pestell RG, Albanese C, Darnell JE, Jr.: Stat3 as an oncogene. *Cell* 1999, 98:295-303.
- Brondello JM, Pouyssegur J, McKenzie FR: Reduced MAP kinase phosphatase-1 degradation after p42/p44MAPK-dependent phosphorylation. *Science* 1999, 286:2514-2517.
- Burke WM, Jin X, Lin HJ, Huang M, Liu R, Reynolds RK, Lin J: Inhibition of constitutively active Stat3 suppresses growth of human ovarian and breast cancer cells. *Oncogene*. 2001, 20:7925-34.
- Burma S, Chen BP, Murphy M, Kurimasa A, Chen DJ: ATM phosphorylates histone H2AX in response to DNA double-strand breaks. *J Biol Chem*. 2001, 276:42462-7.
- Carballo E, Lai WS, Blackshear PJ: Feedback inhibition of macrophage tumor necrosis factor-alpha production by tristetraprolin. *Science* 1998, 281:1001-1005.
- Falcone R, TH, MM, J, A, R, G, L, -Luna JL, -G, WS, R: Constitutive activation of Stat3 signaling confers resistance to apoptosis in human U266 myeloma cells. . 1999, 10:105-15.
- Chacinska A, Lind M, Frazier AE, Dudek J, Meisinger C, Geissler A, Sickmann A, Meyer HE, Truscott KN, Guiard B, Pfanner N, Rehling P: Mitochondrial presequence translocase: switching between TOM tethering and motor recruitment involves Tim21 and Tim17. *Cell*. 2005, 120:817-29.
- Chan ED, Riches DW: IFN-gamma + LPS induction of iNOS is modulated by ERK, JNK/SAPK, and p38(mapk) in a mouse macrophage cell line. *Am J Physiol Cell Physiol*. 2001, 280:C441-50.
- Chanalaris A, Lawrence KM, Stephanou A, Knight RD, Hsu SY, Hsueh AJ, Latchman DS: Protective effects of the urocortin homologues stresscopin (SCP) and stresscopin-related peptide (SRP) against hypoxia/reoxygenation injury in rat neonatal cardiomyocytes. *J Mol Cell Cardiol*. 2003, 35:1295-305.
- Chang L, Karin M: Mammalian MAP kinase signalling cascades. *Nature* 2001, 410:37-40.
- Charriaut-Marlangue C, Ben Ari Y: A cautionary note on the use of the TUNEL stain to determine apoptosis. *Neuroreport* 1995, 7:61-64.
- Chatterjee-Kishore M, Wright KL, Ting JP, Stark GR: How Stat1 mediates constitutive gene expression: a complex of unphosphorylated Stat1 and IRF1 supports transcription of the LMP2 gene. *EMBO J*. 2000, 19:4111-22.
- Chen C, Chen YH, Lin WW: Involvement of p38 mitogen-activated protein kinase in lipopolysaccharide-induced iNOS and COX-2 expression in J774 macrophages. *Immunology*. 1999, 97:124-9.
- Chen EP, Bittner HB, Davis RD, Folz RJ, Van Trigt P: Extracellular superoxide dismutase transgene overexpression preserves postischemic myocardial function in isolated murine hearts. *Circulation*. 1996, 94:II412-7.

Chen P, Li J, Barnes J, Kokkonen GC, Lee JC, Liu Y: Restraint of proinflammatory cytokine biosynthesis by mitogen-activated protein kinase phosphatase-1 in lipopolysaccharide-stimulated macrophages. *J Immunol.* 2002, 169:6408-6416.

Q, EJ, S, CL, EJ: Production of reactive oxygen species by mitochondria: central role of complex III. *Biol Chem.* 2003, 278:36027-31.

Chen X, Vinkemeier U, Zhao Y, Jeruzalmi D, Darnell JE Jr, Kuriyan J: Crystal structure of a tyrosine phosphorylated STAT-1 dimer bound to DNA. . 1998, 93:827-39.

Chen Z, Siu B, Ho YS, Vincent R, Chua CC, Hamdy RC, Chua BH: Overexpression of MnSOD protects against myocardial ischemia/reperfusion injury in transgenic mice. *J Mol Cell Cardiol.* 1998, 30:2281-9.

Chapman RS, Lourenco PC, Tonner E, Flint DJ, Selbert S, Takeda K, Akira S, Clarke AR, Watson CJ: Suppression of epithelial apoptosis and delayed mammary gland involution in mice with a conditional knockout of Stat3. *Genes Dev.* 1999, 13:2604-16.

Chin YE, Kitagawa M, Kuida K, Flavell RA, Fu XY: Activation of the STAT signaling pathway can cause expression of caspase 1 and apoptosis. *Mol. Cell Biol.* 1997, 17:5328-5337.

Chipuk JE, Bouchier-Hayes L, Green DR: Mitochondrial outer membrane permeabilization during apoptosis: the innocent bystander scenario. *Cell Death Differ.* 2006, 13:1396-402.

Chipuk JE, Green DR: How do BCL-2 proteins induce mitochondrial outer membrane permeabilization? *Trends Cell Biol.* 2008, 18:157-64.

Chipuk JE, Kuwana T, Bouchier-Hayes L, Droin NM, Newmeyer DD, Schuler M, Green DR: Direct activation of Bax by p53 mediates mitochondrial membrane permeabilization and apoptosis. *Science.* 2004, 303:1010-4.

Christova R, Jones T, Wu PJ, Bolzer A, Costa-Pereira AP, Watling D, Kerr IM, Sheer D: P-STAT1 mediates higher-order chromatin remodelling of the human MHC in response to IFN γ . *J Cell Sci.* 2007, 120:3262-70.

Chung CD, Liao J, Liu B, Rao X, Jay P, Berta P, Shuai K: Specific inhibition of Stat3 signal transduction by PIAS3. *Science.* 1997, 278:1803-5.

Chung J, Uchida E, Grammer TC, Blenis J. STAT3 serine phosphorylation by ERK-dependent and -independent pathways negatively modulates its tyrosine phosphorylation. *Mol Cell Biol.* 1997;17:6508-6516.

SA, JC, K, C, R, E, J, KC, P, CJ, GJ, CJ, JJ. Small-molecule XIAP antagonist restores caspase-9 mediated apoptosis in XIAP-positive diffuse large B-cell lymphoma cells. . 2008, 111:369-75.

Clerk A, Cole SM, Cullingford TE, Harrison JG, Jormakka M, Valks DM: Regulation of cardiac myocyte cell death. *Pharmacol Ther.* 2003, 97:223-261.

Compston A, Coles A: Multiple sclerosis. *Lancet* 2002, 359:1221-1231.

- Cook SA, Sugden PH, Clerk A. Regulation of bcl-2 family proteins during development and in response to oxidative stress in cardiac myocytes: association with changes in mitochondrial membrane potential. *Res.* 1999, 85:940-9.
- Cortez DM, Feldman MD, Mummidi S, Valente AJ, Steffensen B, Vincenti M, Barnes JL, Chandrasekar B: IL-17 stimulates MMP-1 expression in primary human cardiac fibroblasts via p38 MAPK- and ERK1/2-dependent C/EBP-beta, NF-kappaB, and AP-1 activation. *J Physiol Heart Circ Physiol.* 2007, 293:H3356-65.
- Costa-Pereira AP, Tininini S, Strobl B, Alonzi T, Schlaak JF, Is'harc H, Gesualdo I, Newman SJ, Kerr IM, Poli V: Mutational switch of an IL-6 response to an interferon-gamma-like response. *Proc.Natl.Acad.Sci.U.S.A* 2002, 99:8043-8047.
- Couper KN, Blount DG, Riley EM. IL-10: the master regulator of immunity to infection. *Immunol.* 2008, 180:5771-7.
- Creagh EM, Murphy BM, Duriez PJ, Duckett CS, Martin SJ: Smac/Diablo antagonizes ubiquitin ligase activity of inhibitor of apoptosis proteins. *Biol Chem.* 2004, 279:26906-14.
- Cua DJ, Sherlock J, Chen Y, Murphy CA, Joyce B, Seymour B, Lucian L, To W et al.: Interleukin-23 rather than interleukin-12 is the critical cytokine for autoimmune inflammation of the brain. . 2003, 421:744-8.
- d'Adda di Fagagna F: Living on a break: cellular senescence as a DNA-damage response. *Rev Cancer.* 2008, 8:512-22.
- Darmon AJ, Nicholson DW, Bleackley RC: Activation of the apoptotic protease CPP32 by cytotoxic T-cell-derived granzyme B. *Nature.* 1995, 377:446-8.
- Davidson NJ, Hudak SA, Lesley RE, Menon S, Leach MW, Rennick DM: IL-12, but not IFN-gamma, plays a major role in sustaining the chronic phase of colitis in IL-10-deficient mice. *Immunol.* 1998, 161:3143-9.
- Dawn B, Xuan YT, Guo Y, Rezazadeh A, Stein AB, Hunt G, Wu WJ, Tan W, Bolli R: IL-6 plays an obligatory role in late preconditioning via JAK-STAT signaling and upregulation of iNOS and COX-2. *Cardiovasc.Res.* 2004, 64:61-71.
- Dean JL, Sarsfield SJ, Tsounakou E, Saklatvala J: p38 Mitogen-activated protein kinase stabilizes mRNAs that contain cyclooxygenase-2 and tumor necrosis factor AU-rich elements by inhibiting deadenylation. *Biol Chem.* 2003, 278:39470-6.
- Dean JL, Sully G, Clark AR, Saklatvala J: The involvement of AU-rich element-binding proteins in p38 mitogen-activated protein kinase pathway-mediated mRNA stabilisation. *Cell Signal.* 2004, 16:1113-1121.
- Decker T, Kovarik P: Serine phosphorylation of STATs. *Oncogene* 2000, 19:2628-2637.
- Dérijard B, Hibi M, Wu IH, Barrett T, Su B, Deng T, Karin M, Davis RJ: JNK1: a protein kinase stimulated by UV light and Ha-Ras that binds and phosphorylates the c-Jun activation domain. *Cell.* 1994, 76:1025-37.

- Deveraux QL, Takahashi R, Salvesen GS, Reed JC. X-linked IAP is a direct inhibitor of cell-death proteases. *Nature*. 1997, 388:300-4.
- DeVries TA, Kalkofen RL, Matassa AA, Reyland ME: Protein kinase Cdelta regulates apoptosis via activation of STAT1. *J.Biol.Chem.* 2004, 279:45603-45612.
- Dolezal P, Likic V, Tachezy J, Lithgow T: Evolution of the molecular machines for protein import into mitochondria. *Science*. 2006, 313:314-8.
- Donà F, Prosperi E, Savio M, Coppa T, Scovassi AI, Mondello C. Loss of histone H2AX increases sensitivity of immortalized mouse fibroblasts to the topoisomerase II inhibitor etoposide. *J Oncol.* 2008, 33:613-21.
- Dong C, Davis RJ, Flavell RA: MAP kinases in the immune response. *Annu.Rev.Immunol.* 2002, 20:55-72.
- Dong C, Yang DD, Tournier C, Whitmarsh AJ, Xu J, Davis RJ, Flavell RA: JNK is required for effector T-cell function but not for T-cell activation. *Nature* 2000, 405:91-94.
- Dong C, Yang DD, Wysk M, Whitmarsh AJ, Davis RJ, Flavell RA: Defective T cell differentiation in the absence of Jnk1. *Science* 1998, 282:2092-2095.
- Dong C: TH17 cells in development: an updated view of their molecular identity and genetic programming. *Nat Rev Immunol.* 2008, 8:337-48.
- Dorfman K, Carrasco D, Gruda M, Ryan C, Lira SA, Bravo R: Disruption of the erp/mkp-1 gene does not affect mouse development: normal MAP kinase activity in ERP/MKP-1-deficient fibroblasts. *Oncogene* 1996, 13:925-931.
- Du C, Fang M, Li Y, Li L, Wang X: Smac, a mitochondrial protein that promotes cytochrome c-dependent caspase activation by eliminating IAP inhibition. *Cell*. 2000, 102:33-42.
- Dumitru CD, Ceci JD, Tsatsanis C, Kontoyiannis D, Stamatakis K, Lin JH, Patriotis C, Jenkins NA, Copeland NG, Kollias G, Tsichlis PN: TNF-alpha induction by LPS is regulated posttranscriptionally via a Tpl2/ERK-dependent pathway. *Cell* 2000, 103:1071-1083.
- Dunne A, O'Neill LA: Adaptor usage and Toll-like receptor signaling specificity. *FEBS Lett.* 2005, 579:3330-3335.
- Eefting F: Role of apoptosis in reperfusion injury. *Cardiovasc.Res.* 2004, 61:414-426.
- Ekert PG, Silke J, Hawkins CJ, Verhagen AM, Vaux DL: DIABLO promotes apoptosis by removing MIHA/XIAP from processed caspase 9. *J Cell Biol.* 2001, 152:483-90.
- El Behi M, Dubucquoi S, Lefranc D, Zephir H, De Seze J, Vermersch P, Prin L: New insights into cell responses involved in experimental autoimmune encephalomyelitis and multiple sclerosis. *Immunol.Lett.* 2005, 96:11-26.
- El Kasmi KC, Holst J, Coffre M, Mielke L, de Pauw A, Lhocine N, Smith AM, Rutschman R, Kaushal D, Shen Y, Suda T, Donnelly RP, Myers MG Jr, Alexander W, Vignali DA, Watowich SS, Ernst M, Hilton DJ, Murray PJ: General nature of the STAT3-activated anti-inflammatory response. *J Immunol.* 2006, 177:7880-8.

- Ellerman KE, Powers JM, Brostoff SW: A suppressor T-lymphocyte cell line for autoimmune encephalomyelitis. *Nature*. 1988, 331:265-7.
- Enari M, Sakahira H, Yokoyama H, Okawa K, Iwamatsu A, Nagata S: A caspase-activated DNase that degrades DNA during apoptosis, and its inhibitor ICAD. *Nature*. 1998, 391:43-50
- Endo T, Kohda D: Functions of outer membrane receptors in mitochondrial protein import.
- Burnette PK, JH, -Falcone R, J, M, R, Y, JM, -Yen HF, J, R, TP Jr: Inhibition of STAT3 signaling leads to apoptosis of leukemic large granular lymphocytes and decreased Mcl-1 expression. *Clin Invest*. 2001, 107:351-62.
- Esumi K, Nishida M, Shaw D, Smith TW, Marsh JD: NADH measurements in adult rat myocytes during simulated ischemia. *Am.J Physiol* 1991, 260:H1743-H1752.
- Fearnley IM, Carroll J, Shannon RJ, Runswick MJ, Walker JE, Hirst J: GRIM-19, a cell death regulatory gene product, is a subunit of bovine mitochondrial NADH:ubiquinone oxidoreductase (complex I). *J Biol Chem*. 2001, 276:38345-8.
- Fillatreau S, Sweeney CH, McGeachy MJ, Gray D, Anderton SM: B cells regulate autoimmunity by provision of IL-10. *Nat.Immunol*. 2002, 3:944-950.
- Fiorentino DF, Zlotnik A, Vieira P, Mosmann TR, Howard M, Moore KW, O'Garra A: IL-10 acts on the antigen-presenting cell to inhibit cytokine production by Th1 cells. *J Immunol*. 1991, 146:3444-51.
- P, Hilfiker-Kleiner D. Survival pathways in hypertrophy and heart failure: the gp130-STAT axis. *Basic Res Cardiol*. 2007, 102:393-411.
- Flaherty JT, Pitt B, Gruber JW, Heuser RR, Rothbaum DA, Burwell LR, George BS, Kereiakes DJ, Deitchman D, Gustafson N, et al.: Recombinant human superoxide dismutase (h-SOD) fails to improve recovery of ventricular function in patients undergoing coronary angioplasty for acute myocardial infarction. . 1994, 89:1982-91.
- Foey AD, Parry SL, Williams LM, Feldmann M, Foxwell BM, Brennan FM: Regulation of monocyte IL-10 synthesis by endogenous IL-1 and TNF-alpha: role of the p38 and p42/44 mitogen-activated protein kinases. *J Immunol*. 1998, 160:920-928.
- Franklin CC, Kraft AS: Conditional expression of the mitogen-activated protein kinase (MAPK) phosphatase MKP-1 preferentially inhibits p38 MAPK and stress-activated protein kinase in U937 cells. *J Biol Chem*. 1997, 272:16917-16923.
- Frey N, Katus HA, Olson EN, Hill JA: Hypertrophy of the heart: a new therapeutic target? *Circulation* 2004, 109:1580-1589.
- Fu AK, Fu WY, Ng AK et al. Cyclin-dependent kinase 5 phosphorylates signal transducer and activator of transcription 3 and regulates its transcriptional activity. *Proc Natl Acad Sci U S A*. 2004;101:6728-6733.
- Gao B, Shen X, Kunos G, Meng Q, Goldberg ID, Rosen EM, Fan S: Constitutive activation of JAK-STAT3 signaling by BRCA1 in human prostate cancer cells. *FEBS Lett*. 2001, 488:179-84.

Garcia R, Bowman TL, Niu G, Yu H, Minton S, Muro-Cacho CA, Cox CE, Falcone R, Fairclough R, Parsons S, Laudano A, Gazit A, Levitzki A, Kraker A, Jove R: Constitutive activation of Stat3 by the Src and JAK tyrosine kinases participates in growth regulation of human breast carcinoma cells. *Oncogene*. 2001, 20:2499-513.

Gavrieli Y, Sherman Y, Ben-Sasson SA: Identification of programmed cell death in situ via specific labeling of nuclear DNA fragmentation. *J Cell Biol*. 1992,119:493-501.

S, SH, KM, S: Sensitization of pancreatic carcinoma cells for gamma-irradiation-induced apoptosis by XIAP inhibition. . 2007, 26:7006-16.

S, A, S, Coqueret O: Implication of BRG1 and cdk9 in the STAT3-mediated activation of the p21waf1 gene. . 2004, 23:7391-8.

Goldberg M, Stucki M, Falck J, D'Amours D, Rahman D, Pappin D, Bartek J, Jackson SP: MDC1 is required for the intra-S-phase DNA damage checkpoint. *Nature*. 2003, 421:952-6.

SK, Maulik N, Das DK. Ischemia-reperfusion and cardioprotection: a delicate balance between reactive oxygen species generation and redox homeostasis. *Ann Med*. 2007, 39:275-89.

Gran B, Zhang GX, Yu S, Li J, Chen XH, Ventura ES, Kamoun M, Rostami A: IL-12p35-deficient mice are susceptible to experimental autoimmune encephalomyelitis: evidence for redundancy in the IL-12 system in the induction of central nervous system autoimmune demyelination. *J Immunol*. 2002, 169:7104-7110.

Grandis JR, Drenning SD, Zeng Q, Watkins SC, Melhem MF, Endo S, Johnson DE, Huang L, He Y, Kim JD: Constitutive activation of Stat3 signaling abrogates apoptosis in squamous cell carcinogenesis in vivo. *Proc Natl Acad Sci U S A*. 2000, 97:4227-32.

Grey JY, Connor MK, Gordon JW, Yano M, Mori M, Hood DA: Tom20-mediated mitochondrial protein import in muscle cells during differentiation. *J Physiol Cell Physiol*. 2000, 279:C1393-400.

Griffiths EJ, Halestrap AP: Mitochondrial non-specific pores remain closed during cardiac ischaemia, but open upon reperfusion. *Biochem J*. 1995, 307 :93-8.

Guégan C, Braudeau J, Couriaud C, Dietz GP, Lacombe P, Bähr M, Nosten-Bertrand M, Onténiente B. PTD-XIAP protects against cerebral ischemia by anti-apoptotic and transcriptional regulatory mechanisms. *Dis*. 2006, 22:177-86

AB, Gottlieb RA. Heart mitochondria: gates of life and death. *Cardiovasc Res*. 2008, 77:334-43

Gustafsson AB, Gottlieb RA: Recycle or die: the role of autophagy in cardioprotection. *J Mol Cell Cardiol*. 2008, 44:654-61.

Haddad JJ, Saade NE, Safieh-Garabedian B: Interleukin-10 and the regulation of mitogen-activated protein kinases: are these signalling modules targets for the anti-inflammatory action of this cytokine? *Cell Signal*. 2003, 15:255-267.

Haga S, Terui K, Zhang HQ, Enosawa S, Ogawa W, Inoue H, Okuyama T, Takeda K, Akira S, Ogino T, Irani K, Ozaki M: Stat3 protects against Fas-induced liver injury by redox-dependent and -independent mechanisms. *J.Clin.Invest* 2003, 112:989-998.

- Hammer M, Mages J, Dietrich H, Schmitz F, Striebel F, Murray PJ, Wagner H, Lang R: Control of dual-specificity phosphatase-1 expression in activated macrophages by IL-10. *Eur.J Immunol.* 2005, 35:2991-3001.
- Hammer M, Mages J, Dietrich H, Servatius A, Howells N, Cato AC, Lang R: specificity phosphatase 1 (DUSP1) regulates a subset of LPS-induced genes and protects mice from lethal endotoxin shock. *J Exp Med.* 2006, 203:15-20.
- Hansson GK, Libby P: The immune response in atherosclerosis: a double-edged sword. *Nat Rev Immunol.* 2006, 6:508-19.
- Harada M, Qin Y, Takano H, Minamino T, Zou Y, Toko H, Ohtsuka M, Matsuura K, Sano M, Nishi J, Iwanaga K, Akazawa H, Kunieda T, Zhu W, Hasegawa H, Kunisada K, Nagai T, Nakaya H, Yamauchi-Takahara K, Komuro I: G-CSF prevents cardiac remodeling after myocardial infarction by activating the Jak-Stat pathway in cardiomyocytes. *Nat.Med.* 2005, 11:305-311.
- Hardwick JS, Sefton BM: Activation of the Lck tyrosine protein kinase by hydrogen peroxide requires the phosphorylation of Tyr-394. *Proc Natl Acad Sci U S A.* 1995, 92:4527-31.
- Harlin H, Reffey SB, Duckett CS, Lindsten T, Thompson CB: Characterization of XIAP-deficient mice. *Cell Biol.* 2001, 21:3604-8.
- Harris TJ, Grosso JF, Yen HR, Xin H, Kortylewski M, Albesiano E, Hipkiss EL, Getnet D, et al.: Cutting edge: An in vivo requirement for STAT3 signaling in TH17 development and TH17-dependent autoimmunity. *J Immunol.* 2007, 179:4313-7.
- Hattori R, Maulik N, Otani H, Zhu L, Cordis G, Engelman RM, Siddiqui MA, Das DK: Role of STAT3 in ischemic preconditioning. *J Mol.Cell Cardiol.* 2001, 33:1929-1936.
- Hausenloy DJ, Duchen MR, Yellon DM: Inhibiting mitochondrial permeability transition pore opening at reperfusion protects against ischaemia-reperfusion injury. *Res.* 2003 60:617-25.
- S, B: Quality assessment of Affymetrix GeneChip data: OMICS. 2006, 10:358-68.
- Hess J, Angel P, Schorpp-Kistner M: AP-1 subunits: quarrel and harmony among siblings. *J Cell Sci.* 2004, 117:5965-73.
- Heyndrickx GR, Millard RW, McRitchie RJ, Maroko PR, Vatner SF: Regional myocardial functional and electrophysiological alterations after brief coronary artery occlusion in conscious dogs. *J Clin Invest.* 1975, 56:978-85.
- Hilfiker-Kleiner D, Hilfiker A, Fuchs M, Kaminski K, Schaefer A, Schieffer B, Hillmer A, Schmiedl A, Ding Z, Podewski E, Podewski E, Poli V, Schneider MD, Schulz R, Park JK, Wollert KC, Drexler H: Signal transducer and activator of transcription 3 is required for myocardial capillary growth, control of interstitial matrix deposition, and heart protection from ischemic injury. *Circ.Res.* 2004, 95:187-195.
- Hill MM, Adrain C, Duriez PJ, Creagh EM, Martin SJ: Analysis of the composition, assembly kinetics and activity of native Apaf-1 apoptosomes. *EMBO J.* 2004, 23:2134-45.
- Hirota H, Chen J, Betz UA, Rajewsky K, Gu Y, Ross J, Jr., Muller W, Chien KR: Loss of a gp130 cardiac muscle cell survival pathway is a critical event in the onset of heart failure during biomechanical stress. *Cell* 1999, 97:189-198.

Hirota H, Izumi M, Hamaguchi T, Sugiyama S, Murakami E, Kunisada K, Fujio Y, Oshima Y, Nakaoka Y, Yamauchi-Takahara K: Circulating interleukin-6 family cytokines and their receptors in patients with congestive heart failure. *Heart Vessels*. 2004, 19:237-41.

Hirota H, Yoshida K, Kishimoto T, Taga T: Continuous activation of gp130, a signal-transducing receptor component for interleukin 6-related cytokines, causes myocardial hypertrophy in mice. *Proc.Natl.Acad.Sci.U.S.A* 1995, 92:4862-4866.

E, Kivity S, Offen D, Maulik N, Otani H, Barhum Y, Pannet H, Shneyvays V, Shainberg A, Goldshtaub V, Tobar A, Vidne BA. Bax ablation protects against myocardial ischemia-reperfusion injury in transgenic mice. *Am J Physiol Heart Circ Physiol*. 2003, 284:H2351-9.

Hoebe K, Du X, Georgel P, Janssen E, Tabeta K, Kim SO, Goode J, Lin P, Mann N, Mudd S, Crozat K, Sovath S, Han J, Beutler B: Identification of Lps2 as a key transducer of MyD88-independent TIR signalling. *Nature* 2003, 424:743-748.

Hoentjen F, Sartor RB, Ozaki M, Jobin C: STAT3 regulates NF-kappaB recruitment to the IL-12p40 promoter in dendritic cells. *Blood* 2005, 105:689-696.

HH, SM, D, N, A, KV, R. Therapeutic efficacy of IL-17 neutralization in murine experimental autoimmune encephalomyelitis. *Immunol*. 2005, 237:123-30.

Högberg J, Orrenius S, Larson RE: Lipid peroxidation in isolated hepatocytes. *Eur J Biochem*. 1975, 50:595-602

C, Ansel A, Altschuld R, Brierley GP. Contracture of isolated rat heart cells on anaerobic to aerobic transition. *Am J Physiol*. 1982, 242:H1022-30.

Holly TA, Drincic A, Byun Y, Nakamura S, Harris K, Klocke FJ, Cryns VL: Caspase inhibition reduces myocyte cell death induced by myocardial ischemia and reperfusion in vivo. *J Mol Cell Cardiol*. 1999, 31:1709-15

Hommes D, van den BB, Plasse T, Bartelsman J, Xu C, Macpherson B, Tytgat G, Peppelenbosch M, Van Deventer S: Inhibition of stress-activated MAP kinases induces clinical improvement in moderate to severe Crohn's disease. *Gastroenterology* 2002, 122:7-14.

KP, L, G, RA, T, BA, A, B, JL, CT, JP, JH, JA: The Rad50 zinc-hook is a structure joining Mre11 complexes in DNA recombination and repair. . 2002, 418:562-6.

Hou T, Ray S, Lee C, Brasier AR: The STAT3 NH2-terminal domain stabilizes enhanceosome assembly by interacting with the p300 bromodomain. *J Biol Chem*. 2008 Sep 9. [Epub ahead of print]

Huang JQ, Radinovic S, Rezaiefar P, Black SC: In vivo myocardial infarct size reduction by a caspase inhibitor administered after the onset of ischemia. *J Pharmacol*. 2000, 402:139-42.

Hutter D, Chen P, Li J, Barnes J, Liu Y: The carboxyl-terminal domains of MKP-1 and MKP-2 have inhibitory effects on their phosphatase activity. *Mol.Cell Biochem*. 2002, 233:107-117.

Ikura T, Tashiro S, Kakino A, Shima H, Jacob N, Amunugama R, Yoder K, Izumi S et al.: DNA damage-dependent acetylation and ubiquitination of H2AX enhances chromatin dynamics. *Cell Biol*. 2007, 27:7028-40.

- Ito H, Maruyama A, Iwakura K, Takiuchi S, Masuyama T, Hori M, Higashino Y, Fujii K, Minamino T. Clinical implications of the 'no reflow' phenomenon. A predictor of complications and left ventricular remodeling in reperfused anterior wall myocardial infarction. *Circulation*. 1996, 93:223-8.
- Jacobs CA, Baker PE, Roux ER, Picha KS, Toivola B, Waugh S, Kennedy MK: Experimental autoimmune encephalomyelitis is exacerbated by IL-1 alpha and suppressed by soluble IL-1 receptor. *J Immunol*. 1991, 146:2983-2989.
- Javadov SA, Clarke S, Das M, Griffiths EJ, Lim KH, Halestrap AP: Ischaemic preconditioning inhibits opening of mitochondrial permeability transition pores in the reperfused rat heart. *Physiol*. 2003 549:513-24.
- Jazayeri A, Balestrini A, Garner E, Haber JE, Costanzo V: Mre11-Rad50-Nbs1-dependent processing of DNA breaks generates oligonucleotides that stimulate ATM activity. *J*. 2008, 27:1953-62.
- Jennings RB, Sommers HM, Smyth GA, Flack HA, Linn H: Myocardial necrosis induced by temporary occlusion of a coronary artery in the dog. *Arch Pathol*. 1960, 70:68-78.
- Jensen RE, Dunn CD: Protein import into and across the mitochondrial inner membrane: role of the TIM23 and TIM22 translocons. *Biochim Biophys Acta*. 2002, 1592:25-34.
- Jin H, May M, Tranebjaerg L, Kendall E, Fontán G, Jackson J, Subramony SH, Arena F, Lubs H, Smith S, Stevenson R, Schwartz C, Vetrie D: A novel X-linked gene, DDP, shows mutations in families with deafness (DFN-1), dystonia, mental deficiency and blindness. *Nat Genet*. 1996, 14:177-80.
- Juedes AE, Hjelmstrom P, Bergman CM, Neild AL, Ruddle NH: Kinetics and cellular origin of cytokines in the central nervous system: insight into mechanisms of myelin oligodendrocyte glycoprotein-induced experimental autoimmune encephalomyelitis. *J Immunol*. 2000, 164:419-426.
- Kalakonda S, Nallar SC, Lindner DJ, Hu J, Reddy SP, Kalvakolanu D: Tumor-suppressive activity of the cell death activator GRIM-19 on a constitutively active signal transducer and activator of transcription 3. *Cancer Res*. 2007, 67:6212-20.
- M, ST, YY, FS, -Tejero M, JE, E, RA: Expression of interleukin-10 in intestinal lymphocytes detected by an interleukin-10 reporter knockin tiger mouse. . 2006, 25:941-52.
- Kaminska B: MAPK signalling pathways as molecular targets for anti-inflammatory therapy--from molecular mechanisms to therapeutic benefits. *Biochim.Biophys.Acta* 2005, 1754:253-262.
- Kamura T, Sato S, Haque D, Liu L, Kaelin WG Jr, Conaway RC, Conaway JW: The Elongin BC complex interacts with the conserved SOCS-box motif present in members of the SOCS, ras, WD-40 repeat, and ankyrin repeat families. *Dev*. 1998, 12:3872-81.
- Kang BY, Kim E, Kim TS: Regulatory mechanisms and their therapeutic implications of interleukin-12 production in immune cells. *Cell Signal*. 2005, 17:665-673.
- Kang PM, Izumo S: Apoptosis and heart failure: A critical review of the literature. *Circ.Res*. 2000, 86:1107-1113.

Kassel O, Sancono A, Kratzschmar J, Kreft B, Stassen M, Cato AC: Glucocorticoids inhibit MAP kinase via increased expression and decreased degradation of MKP-1. *EMBO J* 2001, 20:7108-7116.

Kato H, Mihara K: Identification of Tom5 and Tom6 in the preprotein translocase complex of human mitochondrial outer membrane. *Biochem Biophys Res Commun.* 2008, 369:958-63.

Kaul P, Armstrong PW, Chang WC, Naylor CD, Granger CB, Lee KL, Peterson ED, Califf RM, Topol EJ, Mark DB: Long-term mortality of patients with acute myocardial infarction in the United States and Canada: comparison of patients enrolled in Global Utilization of Streptokinase and t-PA for Occluded Coronary Arteries (GUSTO)-I. . 2004, 110:1754-60.

Kawai T, Akira S: Pathogen recognition with Toll-like receptors. *Curr.Opin.Immunol.* 2005, 17:338-344.

Keeley EC, Boura JA, Grines CL: Primary angioplasty versus intravenous thrombolytic therapy for acute myocardial infarction: a quantitative review of 23 randomised trials: *Lancet.* 2003. 361:13-20.

Khan SQ, Kelly D, Quinn P, Davies JE, Ng LL.: Cardiotrophin-1 predicts death or heart failure following acute myocardial infarction. *J Card Fail.* 2006, 12:635-40.

Khan KD, Shuai K, Lindwall G, Maher SE, Darnell JE Jr, Bothwell AL: Induction of the Ly-6A/E gene by interferon alpha/beta and gamma requires a DNA element to which a tyrosine-phosphorylated 91-kDa protein binds. *Proc Natl Acad Sci U S A.* 1993, 90:6806-10.

Kim JS, Jin Y, Lemasters JJ: Reactive oxygen species, but not Ca²⁺ overloading, trigger pH- and mitochondrial permeability transition-dependent death of adult rat myocytes after ischemia-reperfusion. *Am J Physiol Heart Circ Physiol.* 2006, 290:H2024-34.

Kloner RA, Rude RE, Carlson N, Maroko PR, DeBoer LW, Braunwald E: Ultrastructural evidence of microvascular damage and myocardial cell injury after coronary artery occlusion: which comes first? *Circulation.* 1980, 62:945-52.

Kloner RA. Does reperfusion injury exist in humans? *Am Coll Cardiol.* 1993 Feb;21(2):537-45.

Koehler CM: New developments in mitochondrial assembly. *Rev Cell Dev Biol.* 2004, 20:309-35.

Kojima H, Sasaki T, Ishitani T et al. STAT3 regulates Nemo-like kinase by mediating its interaction with IL-6-stimulated TGFbeta-activated kinase 1 for STAT3 Ser-727 phosphorylation. *Proc Natl Acad Sci U S A.* 2005;102:4524-4529.

Komine-Kobayashi M, Zhang N, Liu M, Tanaka R, Hara H, Osaka A, Mochizuki H, Mizuno Y, Urabe T: Neuroprotective effect of recombinant human granulocyte colony-stimulating factor in transient focal ischemia of mice. *J.Cereb.Blood Flow Metab* 2006, 26:402-413.

Komiyama Y, Nakae S, Matsuki T, Nambu A, Ishigame H, Kakuta S, Sudo K, Iwakura Y: IL-17 plays an important role in the development of experimental autoimmune encephalomyelitis. *Immunol.* 2006, 177:566-73.

- Kontoyiannis D, Pasparakis M, Pizarro TT, Cominelli F, Kollias G: Impaired on/off regulation of TNF biosynthesis in mice lacking TNF AU-rich elements: implications for joint and gut-associated immunopathologies. *Immunity*. 1999, 10:387-398.
- Koopman G, Reutelingsperger CP, Kuijten GA, Keehnen RM, Pals ST, van Oers MH: Annexin V for flow cytometric detection of phosphatidylserine expression on B cells undergoing apoptosis. *Blood* 1994, 84:1415-1420.
- Kopp E, Medzhitov R: Recognition of microbial infection by Toll-like receptors. *Curr Opin Immunol*. 2003, 15:396-401.
- Korner H, Riminton DS, Strickland DH, Lemckert FA, Pollard JD, Sedgwick JD: Critical points of tumor necrosis factor action in central nervous system autoimmune inflammation defined by gene targeting. *J Exp.Med* 1997, 186:1585-1590.
- Kotlyarov A, Neininger A, Schubert C, Eckert R, Birchmeier C, Volk HD, Gaestel M: MAPKAP kinase 2 is essential for LPS-induced TNF-alpha biosynthesis. *Nat.Cell Biol* 1999, 1:94-97.
- Kovarik P, Mangold M, Ramsauer K, Heidari H, Steinborn R, Zotter A, Levy DE, Muller M, Decker T: Specificity of signaling by STAT1 depends on SH2 and C-terminal domains that regulate Ser727 phosphorylation, differentially affecting specific target gene expression. *EMBO J*. 2001, 20:91-100.
- Kovarik P, Stoiber D, Eyers PA, Menghini R, Neininger A, Gaestel M, Cohen P, Decker T: Stress-induced phosphorylation of STAT1 at Ser727 requires p38 mitogen-activated protein kinase whereas IFN-gamma uses a different signaling pathway. *Proc.Natl.Acad.Sci.U.S.A* 1999, 96:13956-13961.
- Kramer OH, Baus D, Knauer SK, Stein S, Jager E, Stauber RH, Grez M, Pfitzner E, Heinzl T: Acetylation of Stat1 modulates NF-kappaB activity. *Genes Dev*. 2006, 20:473-485.
- Kühn R, Löhler J, Rennick D, Rajewsky K, Müller W: Interleukin-10-deficient mice develop chronic enterocolitis. *Cell* 1993, 75:263-74.
- Kunisada K, Negoro S, Tone E, Funamoto M, Osugi T, Yamada S, Okabe M, Kishimoto T, Yamauchi-Takahara K: Signal transducer and activator of transcription 3 in the heart transduces not only a hypertrophic signal but a protective signal against doxorubicin-induced cardiomyopathy. *Proc.Natl.Acad.Sci.U.S.A* 2000, 97:315-319.
- Kunisada K, Tone E, Fujio Y, Matsui H, Yamauchi-Takahara K, Kishimoto T: Activation of gp130 transduces hypertrophic signals via STAT3 in cardiac myocytes. *Circulation* 1998, 98:346-352.
- Kuroki M, O'Flaherty JT: Extracellular signal-regulated protein kinase (ERK)-dependent and ERK-independent pathways target STAT3 on serine-727 in human neutrophils stimulated by chemotactic factors and cytokines. *Biochem.J* 1999, 341 (Pt 3):691-696.
- Kutik S, Stojanovski D, Becker L, Becker T, Meinecke M, Krüger V, Prinz C, Meisinger C, Guiard B, Wagner R, Pfanner N, Wiedemann N: Dissecting membrane insertion of mitochondrial beta-barrel proteins. *Cell*. 2008, 132:1011-24.
- Kuwana T, Bouchier-Hayes L, Chipuk JE, Bonzon C, Sullivan BA, Green DR, Newmeyer DD: BH3 domains of BH3-only proteins differentially regulate Bax-mediated mitochondrial membrane permeabilization both directly and indirectly. *Cell*. 2005, 17:525-35

- Kuwata H, Watanabe Y, Miyoshi H, Yamamoto M, Kaisho T, Takeda K, Akira S: IL-10-inducible Bcl-3 negatively regulates LPS-induced TNF-alpha production in macrophages. *Blood* 2003, 102:4123-4129.
- Lang R, Hammer M, Mages J: DUSP meet immunology: dual specificity MAPK phosphatases in control of the inflammatory response. *Immunol.* 2006, 177:7497-504.
- Lang R, Pauleau AL, Parganas E, Takahashi Y, Mages J, Ihle JN, Rutschman R, Murray PJ: SOCS3 regulates the plasticity of gp130 signaling. *Nat.Immunol.* 2003, 4:546-550.
- Latchman DS: Urocortin. *Int.J Biochem.Cell Biol* 2002, 34:907-910.
- Lawrence KM, Chanalaris A, Scarabelli T, Hubank M, Pasini E, Townsend PA, Comini L, Ferrari R, Tinker A, Stephanou A, Knight RA, Latchman DS: K(ATP) channel gene expression is induced by urocortin and mediates its cardioprotective effect. *Circulation* 2002, 106:1556-1562.
- Lawrence KM, Kabir AM, Bellahcene M, Davidson S, Cao XB, McCormick J, Mesquita RA, Carroll CJ, Chanalaris A, Townsend PA, Hubank M, Stephanou A, Knight RA, Marber MS, Latchman DS: Cardioprotection mediated by urocortin is dependent on PKCepsilon activation. *FASEB J* 2005, 19:831-833.
- Lawrence KM, Scarabelli TM, Turtle L, Chanalaris A, Townsend PA, Carroll CJ, Hubank M, Stephanou A, Knight RA, Latchman DS: Urocortin protects cardiac myocytes from ischemia/reperfusion injury by attenuating calcium-insensitive phospholipase A2 gene expression. *FASEB J.* 2003, 17:2313-5.
- Lawrence KM, Townsend PA, Davidson SM, Carroll CJ, Eaton S, Hubank M, Knight RA, Stephanou A, Latchman DS: The cardioprotective effect of urocortin during ischaemia/reperfusion involves the prevention of mitochondrial damage. *Biochem Biophys Res Commun.* 2004, 321:479-86.
- Lecour S, Suleman N, Deuchar GA, Somers S, Lacerda L, Huisamen B, Opie LH: Pharmacological preconditioning with tumor necrosis factor-alpha activates signal transducer and activator of transcription-3 at reperfusion without involving classic prosurvival kinases (Akt and extracellular signal-regulated kinase). *Circulation* 2005, 112:3911-3918.
- P, M, DJ, SM, K, RN: Fas pathway is a critical mediator of cardiac myocyte death and MI during ischemia-reperfusion in vivo. *J Physiol Heart Circ Physiol.* 2003, 284:H456-63.
- Leonard JP, Waldburger KE, Goldman SJ: Prevention of experimental autoimmune encephalomyelitis by antibodies against interleukin 12. *J Exp.Med* 1995, 181:381-386.
- Leong PL, Andrews GA, Johnson DE, Dyer KF, Xi S, Mai JC, Robbins PD, Gadiparthi S, Burke NA, Watkins SF, Grandis JR: Targeted inhibition of Stat3 with a decoy oligonucleotide abrogates head and neck cancer cell growth. *Proc Natl Acad Sci U S A.* 2003, 100:4138-43.
- Lerner L, Henriksen MA, Zhang X, Darnell JE, Jr.: STAT3-dependent enhanceosome assembly and disassembly: synergy with GR for full transcriptional increase of the alpha 2-macroglobulin gene. *Genes Dev.* 2003, 17:2564-2577.
- Levy DE, Darnell JE, Jr.: Stats: transcriptional control and biological impact. *Nat.Rev.Mol.Cell Biol.* 2002, 3:651-662.

- Ley R, Balmanno K, Hadfield K, Weston C, Cook SJ: Activation of the ERK1/2 signaling pathway promotes phosphorylation and proteasome-dependent degradation of the BH3-only protein, Bim. *J Biol Chem.* 2003, 278:18811-6.
- Li J, Gorospe M, Hutter D, Barnes J, Keyse SM, Liu Y: Transcriptional induction of MKP-1 in response to stress is associated with histone H3 phosphorylation-acetylation. *Mol. Cell Biol* 2001, 21:8213-8224.
- Li P, Nijhawan D, Budihardjo I, Srinivasula SM, Ahmad M, Alnemri ES, Wang X: Cytochrome c and dATP-dependent formation of Apaf-1/caspase-9 complex initiates an apoptotic protease cascade: *Cell.* 1997, 91:479-89.
- Li Q, Guo Y, Xuan YT, Lowenstein CJ, Stevenson SC, Prabhu SD, Wu WJ, Zhu Y, Bolli R: Gene therapy with inducible nitric oxide synthase protects against myocardial infarction via a cyclooxygenase-2-dependent mechanism. *Circ. Res.* 2003, 92:741-748.
- Lim CP, Cao X. Serine phosphorylation and negative regulation of Stat3 by JNK. *J Biol Chem.* 1999;274:31055-31061.
- Lin YW, Yang JL: Cooperation of ERK and SCFSkp2 for MKP-1 destruction provides a positive feedback regulation of proliferating signaling. *J Biol Chem.* 2006, 281:915-926.
- Lindsten T, Ross AJ, King A, Zong WX, Rathmell JC, Shiels HA, Ulrich E, Waymire KG et al.: The combined functions of proapoptotic Bcl-2 family members bak and bax are essential for normal development of multiple tissues. *Cell.* 2000, 6:1389-99.
- B, Liao J, Rao X, Kushner SA, Chung CD, Chang DD, Shuai K. Inhibition of Stat1-mediated gene activation by PIAS1. *Proc Natl Acad Sci U S A.* 1998, 95:10626-31.
- B, S, KA, N, C, PW, H, K: PIAS1 selectively inhibits interferon-inducible genes and is important in innate immunity. *Immunol.* 2004, 5:891-8.
- Liu CN, Yang C, Liu XY, Li S: In vivo protective effects of urocortin on ischemia-reperfusion injury in rat heart via free radical mechanisms. *Can J Physiol Pharmacol.* 2005, 83:459-65.
- Liu Q, D'Silva P, Walter W, Marszalek J, Craig EA: Regulated cycling of mitochondrial Hsp70 at the protein import channel. *Science.* 2003, 300:139-41.
- Livak KJ, Schmittgen TD. Analysis of relative gene expression data using real-time quantitative PCR and the 2⁻($\Delta\Delta C(T)$) Method. *Methods.* 2001, 25: 402–408.
- Lu C, Zhu F, Cho YY, Tang F, Zykova T, Ma WY, Bode AM, Dong Z. Cell apoptosis: requirement of H2AX in DNA ladder formation, but not for the activation of caspase-3. *Cell.* 2006, 23:121-32.
- Lu HT, Yang DD, Wusk M, Gatti E, Mellman I, Davis RJ, Flavell RA: Defective IL-12 production in mitogen-activated protein (MAP) kinase kinase 3 (Mkk3)-deficient mice. *EMBO J* 1999, 18:1845-1857.
- Lu Y, Fukuyama S, Yoshida R, Kobayashi T, Saeki K, Shiraishi H, Yoshimura A, Takaesu G: Loss of SOCS3 gene expression converts STAT3 function from anti-apoptotic to pro-apoptotic. *J Biol Chem.* 2006, 281:36683-90

Lufe C, Ma J, Huang G, Zhang T, Novotny-Diermayr V, Ong CT, Cao X: GRIM-19, a death-regulatory gene product, suppresses Stat3 activity via functional interaction. *EMBO J.* 2003, 22:1325-35.

Lund TC, Coleman C, Horvath E, Sefton BM, Jove R, Medveczky MM, Medveczky PG: The Src-family kinase Lck can induce STAT3 phosphorylation and DNA binding activity. *Cell Signal.* 1999, 11:789-96.

Ma J, Zhang T, Novotny-Diermayr V, Tan AL, Cao X: A novel sequence in the coiled-coil domain of Stat3 essential for its nuclear translocation. *J.Biol.Chem.* 2003, 278:29252-29260.

JD, C, G, N, DS, M, K, QW, K, N, et al. Altered responses to bacterial infection and endotoxic shock in mice lacking inducible nitric oxide synthase. . 1995, 81:641-50.

Mahaffey KW, Puma JA, Barbagelata NA, DiCarli MF, Leeser MA, Browne KF, Eisenberg PR, Bolli R, Casas AC, Molina-Viamonte V, Orlandi C, Blevins R, Gibbons RJ, Califf RM, Granger CB: Adenosine as an adjunct to thrombolytic therapy for acute myocardial infarction: results of a multicenter, randomized, placebo-controlled trial: the Acute Myocardial Infarction Study of Adenosine (AMISTAD) trial. *J.Am.Coll.Cardiol.* 1999, 34:1711-1720.

Mani K: Programmed cell death in cardiac myocytes: strategies to maximize post-ischemic salvage. *Heart Fail Rev.* 2008 ,13:193-209.

GD, Thomas PD, Lopaschuk GD, Poznansky MJ. Superoxide dismutase (SOD)-catalase conjugates. Role of hydrogen peroxide and the Fenton reaction in SOD toxicity. *J Biol Chem.* 1993, 68:416-20

Mao X, Ren Z, Parker GN, Sondermann H, Pastorello MA, Wang W, McMurray JS, Demeler B, Darnell JE, Jr., Chen X: Structural bases of unphosphorylated STAT1 association and receptor binding. *Mol.Cell* 2005, 17:761-771.

Mandl M, Slack DN, Keyse SM: Specific inactivation and nuclear anchoring of extracellular signal-regulated kinase 2 by the inducible dual-specificity protein phosphatase DUSP5. *Mol Cell Biol.* 2005, 25:1830-45.

Marg A, Shan Y, Meyer T, Meissner T, Brandenburg M, Vinkemeier U: Nucleocytoplasmic shuttling by nucleoporins Nup153 and Nup214 and CRM1-dependent nuclear export control the subcellular distribution of latent Stat1. *J.Cell Biol.* 2004, 165:823-833.

MB, Schieffer B, Paxton WG, Heerdt L, Berk BC, Delafontaine P, Bernstein KE. Direct stimulation of Jak/STAT pathway by the angiotensin II AT1 receptor. *Nature.* 1995, 375:247-50.

Martin GS, Mannino DM, Eaton S, Moss M: The epidemiology of sepsis in the United States from 1979 through 2000. *N.Engl.J Med* 2003, 348:1546-1554.

Martin GS, Mannino DM, Eaton S, Moss M: The epidemiology of sepsis in the United States from 1979 through 2000. *N.Engl.J Med* 2003, 348:1546-1554.

Mascareno E, Beckles DL, Siddiqui MA: Janus kinase-2 signaling mediates apoptosis in rat cardiomyocytes. *Vascul Pharmacol.* 2005, 43:327-35.

Matthews JR, Clarke AR: p53 mediates a default programme of mammary gland involution in the absence of STAT. *Oncogene.* 2005, 24:3083-90.

Matsuoka T, Wada J, Hashimoto I, Zhang Y, Eguchi J, Ogawa N, Shikata K, Kanwar YS, Makino H: Gene delivery of Tim44 reduces mitochondrial superoxide production and ameliorates neointimal proliferation of injured carotid artery in diabetic rats. . 2005, 54:2882-90.

McBride KM, McDonald C, Reich NC: Nuclear export signal located within the DNA-binding domain of the STAT1 transcription factor. *EMBO J.* 2000, 19:6196-206.

McDonald MC, Zacharowski K, Bowes J, Cuzzocrea S, Thiemermann C: Tempol reduces infarct size in rodent models of regional myocardial ischemia and reperfusion. *Free Radic Biol Med* 1999, 27:493-503.

McFarland HF, Martin R: Multiple sclerosis: a complicated picture of autoimmunity. *Nat Immunol.* 2007, 8:913-9.

McGeachy MJ, Anderson SM: Cytokines in the induction and resolution of experimental autoimmune encephalomyelitis. *Cytokine* 2005, 32:81-84.

McGeachy MJ, Stephens LA, Anderson SM: Natural recovery and protection from autoimmune encephalomyelitis: contribution of CD4+CD25+ regulatory cells within the central nervous system. *J Immunol.* 2005, 175:3025-3032.

Meers P, Daleke D, Hong K, Papahadjopoulos D: Interactions of annexins with membrane phospholipids. *Biochemistry.* 1991, 30:2903-8.

Meinecke M, Wagner R, Kovermann P, Guiard B, Mick DU, Hutu DP, Voos W, Truscott KN, Chacinska A, Pfanner N, Rehling P: Tim50 maintains the permeability barrier of the mitochondrial inner membrane. *Science.* 2006, 312:1523-6.

Mertens C, Zhong M, Krishnaraj R, Zou W, Chen X, Darnell JE Jr: Dephosphorylation of phosphotyrosine on STAT1 dimers requires extensive spatial reorientation of the monomers facilitated by the N-terminal domain. *Dev.* 2006, 20:3372-81.

Meyaard L, Hovenkamp E, Otto SA, Miedema F: IL-12-induced IL-10 production by human T cells as a negative feedback for IL-12-induced immune responses. *J Immunol.* 1996, 156:2776-82.

Meyer T, Hendry L, Begitt A, John S, Vinkemeier U: A single residue modulates tyrosine dephosphorylation, oligomerization, and nuclear accumulation of stat transcription factors. *J.Biol.Chem.* 2004, 279:18998-19007.

Meyer T, Marg A, Lemke P, Wiesner B, Vinkemeier U: DNA binding controls inactivation and nuclear accumulation of the transcription factor Stat1. *Genes Dev.* 2003, 17:1992-2005.

Meyer T, Vinkemeier U: Nucleocytoplasmic shuttling of STAT transcription factors. *Eur.J.Biochem.* 2004, 271:4606-4612.

Milenkovic D, Kozjak V, Wiedemann N, Lohaus C, Meyer HE, Guiard B, Pfanner N, Meisinger C: Sam35 of the mitochondrial protein sorting and assembly machinery is a peripheral outer membrane protein essential for cell viability. *J Biol Chem.* 2004, 279:22781-5.

Ming L, Wang P, Bank A, Yu J, Zhang L: PUMA Dissociates Bax and Bcl-X(L) to induce apoptosis in colon cancer cells. *J Biol Chem.* 2006, 281:16034-42.

Minners J, McLeod CJ, Sack MN: Mitochondrial plasticity in classical ischemic preconditioning—moving beyond the mitochondrial KATP channel. *Res.* 2003, 59:1-6.

Mo W, Zhang L, Yang G, Zhai J, Hu Z, Chen Y, Chen X, Hui L, Huang R, Hu: Nuclear beta-arrestin1 functions as a scaffold for the dephosphorylation of STAT1 and moderates the antiviral activity of IFN-gamma. *Mol Cell.* 2008, 31:695-707.

Mocanu MM, Baxter GF, Yellon DM: Caspase inhibition and limitation of myocardial infarct size: protection against lethal reperfusion injury. *Br.J.Pharmacol.* 2000, 130:197-200.

Y, Naka T, Kawazoe Y, Fujimoto M, Narazaki M, Nakagawa R, Fukuyama H, Nagata S, Kishimoto T. Signals transducers and activators of transcription (STAT)-induced STAT inhibitor-1 (SSI-1)/suppressor of cytokine signaling-1 (SOCS-1) suppresses tumor necrosis factor alpha-induced cell death in fibroblasts. *Proc Natl Acad Sci U S A.* 2000, 97:5405-10.

Moro F, Okamoto K, Donzeau M, Neupert W, Brunner M: Mitochondrial protein import: molecular basis of the ATP-dependent interaction of MtHsp70 with Tim44. *J Biol Chem.* 2002, 277:6874-80.

Motta M, Accornero P, Taulli R, Bernabei P, Desrivieres S, Baratta M: Leptin enhances STAT-3 phosphorylation in HC11 cell line: effect on cell differentiation and cell viability. *Mol Cell Endocrinol.* 2007, 263:149-55.

Mowen KA, Glimcher LH: Signaling pathways in Th2 development. *Immunol.Rev.* 2004, 202:203-222.

KA, Tang J, Zhu W, Schurter BT, Shuai K, Herschman HR, David M. Arginine methylation of STAT1 modulates IFNalpha/beta-induced transcription. *Cell.* 2000, 104:731-41.

Muda M, Boschert U, Dickinson R, Martinou JC, Martinou I, Camps M, Schlegel W, Arkinstall S: MKP-3, a novel cytosolic protein-tyrosine phosphatase that exemplifies a new class of mitogen-activated protein kinase phosphatase. *J Biol Chem.* 1996, 271:4319-4326.

Muda M, Theodosiou A, Rodrigues N, Boschert U, Camps M, Gillieron C, Davies K, Ashworth A, Arkinstall S: The dual specificity phosphatases M3/6 and MKP-3 are highly selective for inactivation of distinct mitogen-activated protein kinases. *J Biol Chem.* 1996, 271:27205-27208.

Muniyappa H, Das KC: Activation of c-Jun N-terminal kinase (JNK) by widely used specific p38 MAPK inhibitors SB202190 and SB203580: a MLK-3-MKK7-dependent mechanism. *Cell Signal.* 2008, 20:675-83.

Murphy KM, Reiner SL: The lineage decisions of helper T cells. *Nat.Rev.Immunol.* 2002, 2:933-944.

J, Zhang B, Taylor SW, Oglesbee D, Fahy E, Marusich MF, Ghosh SS, Capaldi RA. The subunit composition of the human NADH dehydrogenase obtained by rapid one-step immunopurification. *J Biol Chem.* 2003, 278:13619-22.

PJ. The JAK-STAT signaling pathway: input and output integration. *J Immunol.* 2007, 178:2623-9.

Murray PJ: The primary mechanism of the IL-10-regulated antiinflammatory response is to selectively inhibit transcription. *Proc.Natl.Acad.Sci.U.S.A* 2005, 102:8686-8691.

Muruve DA, Pétrilli V, Zaiss AK, White LR, Clark SA, Ross PJ, Parks RJ, Tschopp J: The inflammasome recognizes cytosolic microbial and host DNA and triggers an innate immune response. *Nature*. 2008, 452:103-7.

Muzio M, Ni J, Feng P, Dixit VM: IRAK (Pelle) family member IRAK-2 and MyD88 as proximal mediators of IL-1 signaling. *Science* 1997, 278:1612-1615.

Nair JS, DaFonseca CJ, Tjernberg A, Sun W, Darnell JE, Jr., Chait BT, Zhang JJ: Requirement of Ca²⁺ and CaMKII for Stat1 Ser-727 phosphorylation in response to IFN-gamma. *Proc.Natl.Acad.Sci.U.S.A* 2002, 99:5971-5976.

T, Matsumoto T, Narazaki M, Fujimoto M, Morita Y, Ohsawa Y, Saito H, Nagasawa T, Uchiyama Y, Kishimoto T. Accelerated apoptosis of lymphocytes by augmented induction of Bax in SSI-1 (STAT-induced STAT inhibitor-1) deficient mice. *Proc Natl Acad Sci U S A*. 1998, 95:15577-82.

Nakagawa T, Shimizu S, Watanabe T, Yamaguchi O, Otsu K, Yamagata H, Inohara H, Kubo T, Tsujimoto Y: Cyclophilin D-dependent mitochondrial permeability transition regulates some necrotic but not apoptotic cell death. *Nature*. 2005, 434:652-8.

Nakano K, Vousden KH. PUMA, a novel proapoptotic gene, is induced by p53. *Mol Cell*. 2001, 7:683-94.

Nam S, Buettner R, Turkson J, Kim D, Cheng JQ, Muehlbeyer S, Hippe F, Vatter S, Merz KH, Eisenbrand G, Jove R: Indirubin derivatives inhibit Stat3 signaling and induce apoptosis in human cancer cells. *Proc.Natl.Acad.Sci.U.S.A* 2005, 102:5998-6003.

Narazaki M, Fujimoto M, Matsumoto T, Morita Y, Saito H, Kajita T, Yoshizaki K, Naka T, Kishimoto T: Three distinct domains of SSI-1/SOCS-1/JAB protein are required for its suppression of interleukin 6 signaling. *Proc Natl Acad Sci U S A*. 1998, 95:13130-4.

Narula J, Pandey P, Arbustini E, Haider N, Narula N, Kolodgie FD, Dal Bello B, Semigran MJ, Bielsa-Masdeu A, Dec GW, Israels S, Ballester M, Virmani R, Saxena S, Kharbanda S: Apoptosis in heart failure: release of cytochrome c from mitochondria and activation of caspase-3 in human cardiomyopathy. *Proc.Natl.Acad.Sci.U.S.A* 1999, 96:8144-8149.

Ndubuisi MI, Guo GG, Fried VA, Etlinger JD, Sehgal PB: Cellular physiology of STAT3: Where's the cytoplasmic monomer? *Biol Chem*. 1999, 274:25499-509.

Negoro S, Kunisada K, Tone E, Funamoto M, Oh H, Kishimoto T, Yamauchi-Takahara K: Activation of JAK/STAT pathway transduces cytoprotective signal in rat acute myocardial infarction. *Cardiovasc.Res*. 2000, 47:797-805.

Neininger A, Kontoyiannis D, Kotlyarov A, Winzen R, Eckert R, Volk HD, Holtmann H, Kollias G, Gaestel M: MK2 targets AU-rich elements and regulates biosynthesis of tumor necrosis factor and interleukin-6 independently at different post-transcriptional levels. *J Biol Chem*. 2002, 277:3065-3068.

KL, JA, TL, R, TE: Activation of STAT3 by the c-Fes protein-tyrosine kinase. *Biol Chem.* 1998, 273:7072-7.

Neupert W, Herrmann JM: Translocation of proteins into mitochondria. *Annu Rev Biochem.* 2007, 76:723-49.

Ng LL, Loke IW, O'Brien RJ, Squire IB, Davies JE: Plasma urocortin in human systolic heart failure. *Clin Sci (Lond).* 2004, 106:383-8.

Nielsen M, Kaestel CG, Eriksen KW, Woetmann A, Stokkedal T, Kaltoft K, Geisler C, Röpke C, Odum N: Inhibition of constitutively activated Stat3 correlates with altered Bcl-2/Bax expression and induction of apoptosis in mycosis fungoides tumor cells. *Leukemia.* 1999, 13:735-8.

Nishikimi T, Miyata A, Horio T, Yoshihara F, Nagaya N, Takishita S, Yutani C, Matsuo H, Matsuoka H, Kangawa K: Urocortin, a member of the corticotropin-releasing factor family, in normal and diseased heart. *Am.J Physiol Heart Circ.Physiol* 2000, 279:H3031-H3039.

Niu G, Wright KL, Ma Y, Wright GM, Huang M, Irby R, Briggs J, Karras J, Cress WD, Pardoll D, Jove R, Chen J, Yu H: Role of Stat3 in regulating p53 expression and function. *Mol.Cell Biol* 2005, 25:7432-7440.

Niu G, Heller R, Catlett-Falcone R, Coppola D, Jaroszeski M, Dalton W, Jove R, Yu H: Gene therapy with dominant-negative Stat3 suppresses growth of the murine melanoma B16 tumor in vivo. *Cancer Res.* 1999, 59:5059-63.

Oda E, Ohki R, Murasawa H, Nemoto J, Shibue T, Yamashita T, Tokino T, Taniguchi T, Tanaka N. Noxa, a BH3-only member of the Bcl-2 family and candidate mediator of p53-induced apoptosis. *Science.* 2000, 288:1053-8.

Olivetti G, Quaini F, Sala R, Lagrasta C, Corradi D, Bonacina E, Gambert SR, Cigola E, Anversa P: Acute myocardial infarction in humans is associated with activation of programmed myocyte cell death in the surviving portion of the heart. *Mol Cell Cardiol.* 1996, 28:2005-16.

O'Neill LA, Bowie AG: The family of five: TIR-domain-containing adaptors in Toll-like receptor signalling. *Nat Rev Immunol.* 2007, 7:353-64.

O'Neill LA: How Toll-like receptors signal: what we know and what we don't know. *Curr.Opin.Immunol.* 2006, 18:3-9.

O'Neill LA: TLRs: Professor Mechnikov, sit on your hat. *Trends Immunol.* 2004, 25:687-693.

O'Rourke L, Shepherd PR. Biphasic regulation of extracellular-signal-regulated protein kinase by leptin in macrophages: role in regulating STAT3 Ser727 phosphorylation and DNA binding. *Biochem J.* 2002;364:875-879.

O'Shea JJ, Gadina M, Schreiber RD: Cytokine signaling in 2002: new surprises in the Jak/Stat pathway. *Cell* 2002, 109 Suppl:S121-S131.

Oshima Y, Fujio Y, Nakanishi T, Itoh N, Yamamoto Y, Negoro S, Tanaka K, Kishimoto T, Kawase I, Azuma J: STAT3 mediates cardioprotection against ischemia/reperfusion injury through metallothionein induction in the heart. *Cardiovasc.Res.* 2005, 65:428-435.

- Ott M, Norberg E, Walter KM, Schreiner P, Kemper C, Rapaport D, Zhivotovsky B, Orrenius S: The mitochondrial TOM complex is required for tBid/Bax-induced cytochrome c release. *J Biol Chem.* 2007, 282:27633-9.
- Palazzo AJ, Jones SP, Girod WG, Anderson DC, Granger DN, Lefer DJ: Myocardial ischemia-reperfusion injury in. *Am.J.Physiol* 1998, 275:H2300-H2307.
- Pamer EG: Immune responses to *Listeria monocytogenes*. *Nat.Rev.Immunol.* 2004, 4:812-823.
- Pan J, Fukuda K, Saito M, Matsuzaki J, Kodama H, Sano M, Takahashi T, Kato T, Ogawa S: Mechanical stretch activates the JAK/STAT pathway in rat cardiomyocytes. *Circ.Res.* 1999, 84:1127-1136.
- Pargellis C, Regan J: Inhibitors of p38 mitogen-activated protein kinase for the treatment of rheumatoid arthritis. *Curr.Opin.Investig.Drugs* 2003, 4:566-571.
- Parkes DG, Vaughan J, Rivier J, Vale W, May CN: Cardiac inotropic actions of urocortin in conscious sheep. *Am J Physiol.* 1997, 272:H2115-22.
- Paschen SA, Rothbauer U, Káldi K, Bauer MF, Neupert W, Brunner M: The role of the TIM8-13 complex in the import of Tim23 into mitochondria. *EMBO J.* 2000, 19:6392-400.
- Pelletier S, Duhamel F, Coulombe P, Popoff MR, Meloche S: Rho family GTPases are required for activation of Jak/STAT signaling by G protein-coupled receptors. *Mol Cell Biol.* 2003, 23:1316-33.
- Peterson GL: A simplification of the protein assay method of Lowry et al. which is more generally applicable: *Biochem.* 1977, 83:346-56.
- Peyrin-Biroulet L, Desreumaux P, Sandborn WJ, Colombel JF: Crohn's disease: beyond antagonists of tumour necrosis factor: *Lancet* 2008, 372:67-81.
- Piot C, Croisille P, Staat P, Thibault H, Rioufol G, Mewton N, Elbelghiti R, Cung TT, Bonnefoy E et al., Effect of cyclosporine on reperfusion injury in acute myocardial infarction. *N Engl J Med.* 2008, 359:473-81.
- Piper HM, García-Dorado D, Ovize M: A fresh look at reperfusion injury. *Res.* 1998, 38:291-300.
- Podewski EK, Hilfiker-Kleiner D, Hilfiker A, Morawietz H, Lichtenberg A, Wollert KC, Drexler H: Alterations in Janus kinase (JAK)-signal transducers and activators of transcription (STAT) signaling in patients with end-stage dilated cardiomyopathy. *Circulation* 2003, 107:798-802.
- Potts MB, Vaughn AE, McDonough H, Patterson C, Deshmukh M: Reduced Apaf-1 levels in cardiomyocytes engage strict regulation of apoptosis by endogenous XIAP. *J Cell Biol.* 2005, 171:925-30.
- Priel-Halachmi S, Ben-Dor I, Shpungin S, Tennenbaum T, Molavani H, Bachrach M, Salzberg S, Nir U: FER kinase activation of Stat3 is determined by the N-terminal sequence. *J Biol Chem.* 2000, 275:28902-10.

- F, Y, D, C, SB, PT, RJ, Monte F. Prevention of ventricular arrhythmias with sarcoplasmic reticulum Ca²⁺ ATPase pump overexpression in a porcine model of ischemia. . 2008, 118:614-24.
- Rademaker MT, Cameron VA, Charles CJ, Richards AM: Integrated hemodynamic, hormonal, and renal actions of urocortin 2 in normal and paced sheep: beneficial effects in heart failure. *Circulation*. 2005, 112:3624-32.
- Rademaker MT, Charles CJ, Espiner EA, Fisher S, Frampton CM, Kirkpatrick CM, Lainchbury JG, Nicholls MG, Richards AM, Vale WW: Beneficial hemodynamic, endocrine, and renal effects of urocortin in experimental heart failure: comparison with normal sheep. *J Am Coll Cardiol*. 2002, 40:1495-505.
- Rademaker MT, Charles CJ, Espiner EA, Frampton CM, Lainchbury JG, Richards AM: Four-day urocortin-I administration has sustained beneficial haemodynamic, hormonal, and renal effects in experimental heart failure. *Eur Heart J*. 2005, 26:2055-62.
- Rademaker MT, Charles CJ, Richards AM: Urocortin 1 administration from onset of rapid left ventricular pacing represses progression to overt heart failure. *Am J Physiol Heart Circ Physiol*. 2007, 293:H1536-44.
- Raivich G, Banati R: Brain microglia and blood-derived macrophages: molecular profiles and functional roles in multiple sclerosis and animal models of autoimmune demyelinating disease. *Brain Res. Brain Res. Rev.* 2004, 46:261-281.
- Ramsauer K, Farlik M, Zupkovitz G, Seiser C, Kröger A, Hauser H, Decker T: Distinct modes of action applied by transcription factors STAT1 and IRF1 to initiate transcription of the IFN-gamma-inducible gbp2 gene. *Proc Natl Acad Sci U S A*. 2007, 104:2849-54.
- Ramsauer K, Sadzak I, Porras A, Pilz A, Nebreda AR, Decker T, Kovarik P: p38 MAPK enhances STAT1-dependent transcription independently of Ser-727 phosphorylation. *Proc. Natl. Acad. Sci. U.S.A* 2002, 99:12859-12864.
- Randolph GJ, Angeli V, Swartz MA: Dendritic-cell trafficking to lymph nodes through lymphatic vessels. *Rev Immunol*. 2005, 5:617-28.
- Rangachari M, Mauermann N, Marty RR, Dirnhofer S, Kurrer MO, Komnenovic V, Penninger JM, Eriksson U: T-bet negatively regulates autoimmune myocarditis by suppressing local production of interleukin 17. *J Exp Med*. 2006, 203:2009-19
- JM, Virtamo J, Ripatti S, Huttunen JK, Albanes D, Taylor PR, Heinonen OP: Randomised trial of alpha-tocopherol and beta-carotene supplements on incidence of major coronary events in men with previous myocardial infarction. *Lancet*. 1997, 349:1715-20.
- Rathmell JC, Lindsten T, Zong WX, Cinalli RM, Thompson CB. Deficiency in Bak and Bax perturbs thymic selection and lymphoid homeostasis. *Nat Immunol*. 2002, 3:932-9.
- Redford EJ, Kapoor R, Smith KJ. Nitric oxide donors reversibly block axonal conduction: demyelinated axons are especially susceptible. *Brain*. 1997, 120:2149-57.

- Redford EJ, Smith KJ, Gregson NA, Davies M, Hughes P, Gearing AJ, Miller K, Hughes RA: A combined inhibitor of matrix metalloproteinase activity and tumour necrosis factor- α processing attenuates experimental autoimmune neuritis. *Brain* 1997, 120 (Pt 10):1895-1905.
- Resch U, Schichl YM, Sattler S, de Martin R: XIAP regulates intracellular ROS by enhancing antioxidant gene expression. *Biophys Res Commun.* 2008, 375:156-61.
- Riley JK, Takeda K, Akira S, Schreiber RD: Interleukin-10 receptor signaling through the JAK-STAT pathway. Requirement for two distinct receptor-derived signals for anti-inflammatory action. *J Biol Chem.* 1999, 274:16513-16521.
- Rincon M, Enslen H, Raingeaud J, Recht M, Zapton T, Su MS, Penix LA, Davis RJ, Flavell RA: Interferon- γ expression by Th1 effector T cells mediated by the p38 MAP kinase signaling pathway. *EMBO J* 1998, 17:2817-2829.
- Rincon M, Pedraza-Alva G: JNK and p38 MAP kinases in CD4+ and CD8+ T cells. *Immunol.Rev.* 2003, 192:131-142.
- Robinson GW, Pacher-Zavisin M, Zhu BM, Yoshimura A, Hennighausen L: Socs 3 modulates the activity of the transcription factor Stat3 in mammary tissue and controls alveolar homeostasis. *Dev Dyn.* 2007, 236:654-61.
- Rödel B, Tavassoli K, Karsunky H, Schmidt T, Bachmann M, Schaper F, Heinrich P, Shuai K, Elsässer HP, Möröy T.: The zinc finger protein Gfi-1 can enhance STAT3 signaling by interacting with the STAT3 inhibitor PIAS3. *EMBO J.* 2000, 19:5845-55.
- Rogakou EP, Pilch DR, Orr AH, Ivanova VS, Bonner WM: DNA double-stranded breaks induce histone H2AX phosphorylation on serine 139. *J Biol Chem.* 1998, 273:5858-68.
- RS, CM, MJ: SUMO modification of STAT1 and its role in PIAS-mediated inhibition of gene activation. *Biol Chem.* 2003, 278:30091-7.
- Röhn TA, Jennings GT, Hernandez M, Grest P, Beck M, Zou Y, Kopf M, Bachmann MF: Vaccination against IL-17 suppresses autoimmune arthritis and encephalomyelitis. *J Immunol.* 2006, 36:2857-67.
- E, Orús J, Paré C, Azqueta M, Filella X, Perez-Villa F, Heras M, Sanz G. Serum interleukin-6 in congestive heart failure secondary to idiopathic dilated cardiomyopathy. *Am J Cardiol.* 1998, 82:688-90, A8.
- Rosamond W, Flegal K, Furie K, Go A, Greenlund K, Haase N, Hailpern SM, Ho M, Howard V, Kissela B, Kittner S, Lloyd-Jones D, McDermott M, Meigs J, Moy C, Nichol G, O'Donnell C, Roger V, Sorlie P, Steinberger J, Thom T, Wilson M, Hong Y; American Heart Association Statistics Committee and Stroke Statistics Subcommittee: Heart disease and stroke statistics--2008 update: a report from the American Heart Association Statistics Committee and Stroke Statistics Subcommittee. *Circulation.* 2008, 117:e25-146.
- Rossé T, Olivier R, Monney L, Rager M, Conus S, Fellay I, Jansen B, Borner C: Bcl-2 prolongs cell survival after Bax-induced release of cytochrome c. *Nature.* 1998, 391:496-9.

Roucou X, Montessuit S, Antonsson B, Martinou JC: Bax oligomerization in mitochondrial membranes requires tBid (caspase-8-cleaved Bid) and a mitochondrial protein. *Biochem J.* 2002, 368:915-21.

Rupnik A, Grenon M, Lowndes N: The MRN complex. *Biol.* 2008, 18:R455-7.

Sabelko-Downes KA, Cross AH, Russell JH: Dual role for Fas ligand in the initiation of and recovery from experimental allergic encephalomyelitis. *J Exp Med.* 1999, 189:1195-205.

Sadzak I, Schiff M, Gattermeier I, Glinitzer R, Sauer I, Saalmüller A, Yang E, Schaljo B, Kovarik P: Recruitment of Stat1 to chromatin is required for interferon-induced serine phosphorylation of Stat1 transactivation domain. *Proc Natl Acad Sci U S A.* 2008, 105:8944-9.

Saklatvala J: The p38 MAP kinase pathway as a therapeutic target in inflammatory disease. *Curr.Opin.Pharmacol* 2004, 4:372-377.

Samoilova EB, Horton JL, Chen Y: Acceleration of experimental autoimmune encephalomyelitis in interleukin-10-deficient mice: roles of interleukin-10 in disease progression and recovery. *Cell Immunol.* 1998, 188:118-124.

_PL, _Avilés F: Appropriate invasive and conservative treatment strategies for patients with ST elevation myocardial infarction. *Opin Cardiol.* 2005, 20:530-5.

Sanchis D, Mayorga M, Ballester M, Comella JX: Lack of Apaf-1 expression confers resistance to cytochrome c-driven apoptosis in cardiomyocytes. *Cell Death Differ.* 2003, 10:977-86.

Saraste A, Pulkki K, Kallajoki M, Henriksen K, Parvinen M, Voipio-Pulkki LM: Apoptosis in human acute myocardial infarction. *Circulation.* 1997, 95:320-3.

Sasaki A, Yasukawa H, Suzuki A, Kamizono S, Syoda T, Kinjyo I, Sasaki M, Johnston JA, Yoshimura A.: Cytokine-inducible SH2 protein-3 (CIS3/SOCS3) inhibits Janus tyrosine kinase by binding through the N-terminal kinase inhibitory region as well as SH2 domain. *Genes Cells.* 1999, 4:339-51.

M, JM, MH, P, Y, T, T, JS: Reversal of experimental colitis disease activity in mice following administration of an adenoviral IL-10 vector. *Inflamm (Lond).* 2005, 31:13.

Sato S, Sugiyama M, Yamamoto M, Watanabe Y, Kawai T, Takeda K, Akira S.: Toll/IL-1 receptor domain-containing adaptor inducing IFN-beta (TRIF) associates with TNF receptor-associated factor 6 and TANK-binding kinase 1, and activates two distinct transcription factors, NF-kappa B and IFN-regulatory factor-3, in the Toll-like receptor signaling. *J Immunol.* 2003, 171:4304-10.

Savitsky K, Bar-Shira A, Gilad S, Rotman G, Ziv Y, Vanagaite L, Tagle DA, Smith S et al.: A single ataxia telangiectasia gene with a product similar to PI-3 kinase. . 1995, 268:1749-53.

Scaffidi P, Misteli T, Bianchi ME: Release of chromatin protein HMGB1 by necrotic cells triggers inflammation. *Nature.* 2002, 418:191-5.

Scarabelli TM, Pasini E, Stephanou A, Comini L, Curello S, Raddino R, Ferrari R, Knight R, Latchman DS: Urocortin promotes hemodynamic and bioenergetic recovery and improves cell survival in the isolated rat heart exposed to ischemia/reperfusion. *J Am Coll Cardiol.* 2002, 40:155-61.

Scheubel RJ, Bartling B, Simm A, Silber RE, Drogaris K, Darmer D, Holtz J: Apoptotic pathway activation from mitochondria and death receptors without caspase-3 cleavage in failing human myocardium: fragile balance of myocyte survival? *J.Am.Coll.Cardiol.* 2002, 39:481-488.

Scheubel RJ, Bartling B, Simm A, Silber RE, Drogaris K, Darmer D, Holtz J: Apoptotic pathway activation from mitochondria and death receptors without caspase-3 cleavage in failing human myocardium: fragile balance of myocyte survival? *J Am Coll Cardiol.* 2002, 39:481-8.

Schile AJ, García-Fernández M, Steller H. Regulation of apoptosis by XIAP ubiquitin-ligase activity. *Dev.* 2008, 22:2256-66.

Schmittgen TD, Livak KJ: Analyzing real-time PCR data by the comparative C(T) method. *Nat Protoc.* 2008, 3:1101-8.

Schnare M, Barton GM, Holt AC, Takeda K, Akira S, Medzhitov R: Toll-like receptors control activation of adaptive immune responses. *Nat.Immunol.* 2001, 2:947-950.

Schulman D, Latchman DS, Yellon DM: Urocortin protects the heart from reperfusion injury via upregulation of p42/p44 MAPK signaling pathway. *J Physiol Heart Circ Physiol.* 2002, 283:H1481-8

Schuringa JJ, Jonk LJ, Dokter WH, Vellenga E, Kruijer W: Interleukin-6-induced STAT3 transactivation and Ser727 phosphorylation involves Vav, Rac-1 and the kinase SEK-1/MKK-4 as signal transduction components. *Biochem.J.* 2000, 347 Pt 1:89-96.

Schuringa JJ, Dekker LV, Vellenga E, Kruijer W. Sequential activation of Rac-1, SEK-1/MKK-4, and protein kinase Cdelta is required for interleukin-6-induced STAT3 Ser-727 phosphorylation and transactivation. *J Biol Chem.* 2001;276:27709-27715.

Segal BM, Dwyer BK, Shevach EM: An interleukin (IL)-10/IL-12 immunoregulatory circuit controls susceptibility to autoimmune disease. *J Exp.Med* 1998, 187:537-546.

Sellon RK, Tonkonogy S, Schultz M, Dieleman LA, Grenther W, Balish E, Rennick DM, Sartor RB: Resident enteric bacteria are necessary for development of spontaneous colitis and immune system activation in interleukin-10-deficient mice. *Infect.Immun.* 1998, 66:5224-5231.

SR, CP, DS, CM: Reperfusion strategies for ST-elevation myocardial infarction. *Cardiol Rep.* 2007, 9:281-8.

YD, R. The MEK/ERK cascade: from signaling specificity to diverse functions. *Biophys Acta.* 2007, 1773:1213-26.

Shen Y, Devgan G, Darnell JE, Jr., Bromberg JF: Constitutively activated Stat3 protects fibroblasts from serum withdrawal and UV-induced apoptosis and antagonizes the proapoptotic effects of activated Stat1. *Proc.Natl.Acad.Sci.U.S.A* 2001, 98:1543-1548.

Shen Y, La Perle KM, Levy DE, Darnell JE, Jr.: Reduced STAT3 activity in mice mimics clinical disease syndromes. *Biochem.Biophys.Res.Commun.* 2005, 330:305-309.

Shen Y, Schlessinger K, Zhu X, Meffre E, Quimby F, Levy DE, Darnell JE, Jr.: Essential role of STAT3 in postnatal survival and growth revealed by mice lacking STAT3 serine 727 phosphorylation. *Mol.Cell Biol.* 2004, 24:407-419.

Shepherd EG, Zhao Q, Welty SE, Hansen TN, Smith CV, Liu Y: The function of mitogen-activated protein kinase phosphatase-1 in peptidoglycan-stimulated macrophages. *J Biol Chem.* 2004, 279:54023-54031.

Shi S, Calhoun HC, Xia F, Li J, Le L, Li WX: JAK signaling globally counteracts heterochromatic gene silencing. *Genet.* 2006, 38:1071-6.

Shi S, Larson K, Guo D, Lim SJ, Dutta P, Yan SJ, Li WX: Drosophila STAT is required for directly maintaining HP1 localization and heterochromatin stability. *Cell Biol.* 2008, 10:489-96.

Shi X, Zhang H, Paddon H et al. Phosphorylation of STAT3 serine-727 by cyclin-dependent kinase 1 is critical for nocodazole-induced mitotic arrest. *Biochemistry.* 2006;45:5857-5867.

Shi Y, Evans JE, Rock KL: Molecular identification of a danger signal that alerts the immune system to dying cells. *J Biol Chem.* 2003, 278:516-21.

Shidoji Y, Hayashi K, Komura S, Ohishi N, Yagi K: Loss of molecular interaction between cytochrome c and cardiolipin due to lipid peroxidation. *Biochem.Biophys.Res.Comm.* 1999, 264:343-347.

Shrivastav M, De Haro LP, Nickoloff JA: Regulation of DNA double-strand break repair pathway choice. *Cell Res.* 2008, 18:134-47.

Simon AR, Rai U, Fanburg BL, Cochran BH: Activation of the JAK-STAT pathway by reactive oxygen species. *Am.J.Physiol* 1998, 275:C1640-C1652.

Slee EA, Harte MT, Kluck RM, Wolf BB, Casiano CA, Newmeyer DD, Wang HG, Reed JC, Nicholson DW, Alnemri ES, Green DR, Martin SJ: Ordering the cytochrome c-initiated caspase cascade: hierarchical activation of caspases-2, -3, -6, -7, -8, and -10 in a caspase-9-dependent manner. *Cell Biol.* 1999, 144:281-92.

Smith RM, Suleman N, Lacerda L, Opie LH, Akira S, Chien KR, Sack MN: Genetic depletion of cardiac myocyte STAT-3 abolishes classical preconditioning. *Cardiovasc.Res.* 2004, 63:611-616.

Smith RM: Classic ischemic but not pharmacologic preconditioning is abrogated following genetic ablation of the TNF- α gene. *Cardiovasc.Res.* 2002, 55:553-560.

Srinivasula SM, Ahmad M, Fernandes-Alnemri T, Litwack G, Alnemri ES: Molecular ordering of the Fas-apoptotic pathway: the Fas/APO-1 protease Mch5 is a CrmA-inhibitable protease that activates multiple Ced-3/ICE-like cysteine proteases. *Proc Natl Acad Sci U S A.* 1996, 93:14486-91.

Stamler J, Shekelle R. Dietary cholesterol and human coronary heart disease. The epidemiologic evidence. *Arch Pathol Lab Med,* 1988, 112:1032-40.

Steidler L, Hans W, Schotte L, Neiryneck S, Obermeier F, Falk W, Fiers W, Remaut E: Treatment of murine colitis by *Lactococcus lactis* secreting interleukin-10. *Science* 2000, 289:1352-1355.

Steinman L, Zamvil SS: Virtues and pitfalls of EAE for the development of therapies for multiple sclerosis. *Trends Immunol.* 2005, 26:565-71.

Stephanou A, Brar BK, Scarabelli TM, Jonassen AK, Yellon DM, Marber MS, Knight RA, Latchman DS: Ischemia-induced STAT-1 expression and activation play a critical role in cardiomyocyte apoptosis. *J.Biol.Chem.* 2000, 275:10002-10008.

Stephanou A, Brar B, Liao Z, Scarabelli T, Knight RA, Latchman DS: Distinct initiator caspases are required for the induction of apoptosis in cardiac myocytes during ischaemia versus reperfusion injury. *Cell Death Differ.* 2001, 8:434-5

Stephanou A, Scarabelli TM, Brar BK, Nakanishi Y, Matsumura M, Knight RA, Latchman DS: Induction of apoptosis and Fas receptor/Fas ligand expression by ischemia/reperfusion in cardiac myocytes requires serine 727 of the STAT-1 transcription factor but not tyrosine 701. *J.Biol.Chem.* 2001, 276:28340-28347.

Stephanou A, Scarabelli TM, Townsend PA, Bell R, Yellon D, Knight RA, Latchman DS: The carboxyl-terminal activation domain of the STAT-1 transcription factor enhances ischemia/reperfusion-induced apoptosis in cardiac myocytes. *FASEB J.* 2002, 16:1841-1843.

Stewart GS, Wang B, Bignell CR, Taylor AM, Elledge SJ: MDC1 is a mediator of the mammalian DNA damage checkpoint. *Nature.* 2003, 421:961-6.

Stokkers PC, Hommes DW: New cytokine therapeutics for inflammatory bowel disease. *Cytokine* 2004, 28:167-173.

Sun H, Charles CH, Lau LF, Tonks NK: MKP-1 (3CH134), an immediate early gene product, is a dual specificity phosphatase that dephosphorylates MAP kinase in vivo. *Cell.* 1993, 75:487-93.

Sun X, Majumder P, Shioya H, Wu F, Kumar S, Weichselbaum R, Kharbanda S, Kufe D: Activation of the cytoplasmic c-Abl tyrosine kinase by reactive oxygen species. *J Biol Chem.* 2000, 275:17237-40.

Sunters A, Fernández de Mattos S, Stahl M, Brosens JJ, Zoumpoulidou G, Saunders CA, Coffey PJ, Medema RH, Coombes RC, Lam EW: FoxO3a transcriptional regulation of Bim controls apoptosis in paclitaxel-treated breast cancer cell lines. *Biol Chem.* 2003, 278:49795-805.

Sutherland KD, Vaillant F, Alexander WS, Wintermantel TM, Forrest NC, Holroyd SL, McManus EJ, Schutz G, Watson CJ, Chodosh LA, Lindeman GJ, Visvader JE: c-myc as a mediator of accelerated apoptosis and involution in mammary glands lacking Socs3. *EMBO J.* 2006, 25:5805-15.

Suzuki Y, Imai Y, Nakayama H, Takahashi K, Takio K, Takahashi R: A serine protease, HtrA2, is released from the mitochondria and interacts with XIAP, inducing cell death. *Mol Cell.* 2001, 8:613-21.

Swantek JL, Cobb MH, Geppert TD: Jun N-terminal kinase/stress-activated protein kinase (JNK/SAPK) is required for lipopolysaccharide stimulation of tumor necrosis factor alpha (TNF-alpha) translation: glucocorticoids inhibit TNF-alpha translation by blocking JNK/SAPK. *Mol.Cell Biol* 1997, 17:6274-6282.

Szabo SJ, Sullivan BM, Peng SL, Glimcher LH. Molecular mechanisms regulating Th1 immune responses. *Rev Immunol.* 2003, 21:713-58.

Takagi Y, Harada J, Chiarugi A, Moskowitz MA: STAT1 is activated in neurons after ischemia and contributes to ischemic brain injury. *J.Cereb.Blood Flow Metab* 2002, 22:1311-1318.

Takahashi H, Numasaki M, Lotze MT, Sasaki H: Interleukin-17 enhances bFGF-, HGF- and VEGF-induced growth of vascular endothelial cells. *Immunol Lett.* 2005, 98:189-93.

Takeda K, Noguchi K, Shi W, Tanaka T, Matsumoto M, Yoshida N, Kishimoto T, Akira S: Targeted disruption of the mouse Stat3 gene leads to early embryonic lethality. *Proc.Natl.Acad.Sci.U.S.A* 1997, 94:3801-3804.

Takeda K, Kaisho T, Yoshida N, Takeda J, Kishimoto T, Akira S: Stat3 activation is responsible for IL-6-dependent T cell proliferation through preventing apoptosis: generation and characterization of T cell-specific Stat3-deficient mice. *J Immunol.* 1998, 161:4652-60.

Takeda K, Clausen BE, Kaisho T, Tsujimura T, Terada N, Forster I, Akira S: Enhanced Th1 activity and development of chronic enterocolitis in mice devoid of Stat3 in macrophages and neutrophils. *Immunity.* 1999, 10:39-49.

Takenaka H, Maruo S, Yamamoto N, Wysocka M, Ono S, Kobayashi M, Yagita H, Okumura K, et al.: Regulation of T cell-dependent and -independent IL-12 production by the three Th2-type cytokines IL-10, IL-6, and IL-4. *Leukoc Biol.* 1997, 61:80-7.

Taneja N, Davis M, Choy JS, Beckett MA, Singh R, Kron SJ, Weichselbaum RR: Histone H2AX phosphorylation as a predictor of radiosensitivity and target for radiotherapy. *Biol Chem.* 2004, 279:2273-80.

Tang XL, Takano H, Rizvi A, Turrens JF, Qiu Y, Wu WJ, Zhang Q, Bolli R.: Oxidant species trigger late preconditioning against myocardial stunning in conscious rabbits. *Am J Physiol Heart Circ Physiol* 2002, 282:H281– 91.

Tao J, Li S: Urocortin: a cardiac protective peptide? *Biochem.Biophys.Res.Commun.* 2005, 332:923-926.

Taylor RC, Cullen SP, Martin SJ: Apoptosis: controlled demolition at the cellular level. *Nat Rev Mol Cell Biol.* 2008, 9:231-41

ten Hoeve J, de Jesus Ibarra-Sanchez M, Fu Y, Zhu W, Tremblay M, David M, Shuai K.: Identification of a nuclear Stat1 protein tyrosine phosphatase. *Mol Cell Biol.* 2002, 22:5662-8.

Terrones O, Etxebarria A, Landajuela A, Landeta O, Antonsson B, Basañez G: BIM and tBID are not mechanistically equivalent when assisting BAX to permeabilize bilayer membranes. *J Biol Chem.* 2008, 283:7790-803.

Thangaraju M, Rudelius M, Bierie B, Raffeld M, Sharan S, Hennighausen L, Huang AM, Sterneck E: C/EBPdelta is a crucial regulator of pro-apoptotic gene expression during mammary gland involution. *Development.* 2005, 132:4675-85.

Toh ML, Yang Y, Leech M, Santos L, Morand EF: Expression of mitogen-activated protein kinase phosphatase 1, a negative regulator of the mitogen-activated protein kinases, in rheumatoid

arthritis: up-regulation by interleukin-1beta and glucocorticoids. *Arthritis Rheum.* 2004, 50:3118-3128.

Torre-Amione G, Kapadia S, Benedict C, Oral H, Young JB, Mann DL: Proinflammatory cytokine levels in patients with depressed left ventricular ejection fraction: a report from the Studies of Left Ventricular Dysfunction (SOLVD). *J Am Coll Cardiol.* 1996, 27:1201-6.

A, Jeffers JR, Nickson P, Min JY, Morgan JP, Zambetti GP, Erhardt P. Targeted deletion of Puma attenuates cardiomyocyte death and improves cardiac function during ischemia-reperfusion. *Am J Physiol Heart Circ Physiol.* 2006, 291:H52-60

Townsend PA, Cragg MS, Davidson SM, McCormick J, Barry S, Lawrence KM, Knight RA, Hubank M, Chen PL, Latchman DS, Stephanou A: STAT-1 facilitates the ATM activated checkpoint pathway following DNA damage. *J.Cell Sci.* 2005, 118:1629-1639.

Townsend PA, Scarabelli TM, Davidson SM, Knight RA, Latchman DS, Stephanou A: STAT-1 interacts with p53 to enhance DNA damage-induced apoptosis. *J.Biol.Chem.* 2004, 279:5811-5820.

Townsend PA, Scarabelli TM, Pasini E, Gitti G, Menegazzi M, Suzuki H, Knight RA, Latchman DS, Stephanou A: Epigallocatechin-3-gallate inhibits STAT-1 activation and protects cardiac myocytes from ischemia/reperfusion-induced apoptosis. *FASEB J.* 2004, 18:1621-1623.

Trinchieri G, Pflanz S, Kastelein RA: The IL-12 family of heterodimeric cytokines: new players in the regulation of T cell responses. *Immunity.* 2003, 19:641-644.

Trinchieri G. Interleukin-12 and the regulation of innate resistance and adaptive immunity. *Nat Rev Immunol.* 2003, 3:133-46.

Tsujimura H, Tamura T, Kong HJ, Nishiyama A, Ishii KJ, Klinman DM, Ozato K: Toll-like receptor 9 signaling activates NF-kappaB through IFN regulatory factor-8/IFN consensus sequence binding protein in dendritic cells. *J Immunol.* 2004, 172:6820-6827.

Turkson J, Zhang S, Mora LB, Burns A, Sebt S, Jove R: A novel platinum compound inhibits constitutive Stat3 signaling and induces cell cycle arrest and apoptosis of malignant cells. *J.Biol.Chem.* 2005, 280:32979-32988.

Uddin S, Sassano A, Deb DK, Verma A, Majchrzak B, Rahman A, Malik AB, Fish EN, Plataniias LC: Protein kinase C-delta (PKC-delta) is activated by type I interferons and mediates phosphorylation of Stat1 on serine 727. *J.Biol.Chem.* 2002, 277:14408-14416.

Ungureanu D, Saharinen P, Junttila I, Hilton DJ, Silvennoinen O: Regulation of Jak2 through the ubiquitin-proteasome pathway involves phosphorylation of Jak2 on Y1007 and interaction with SOCS-1. *Mol Cell Biol.* 2002, 22:3316-26.

D, S, N, J, S, OA, JJ, O: PIAS proteins promote SUMO-1 conjugation to STAT1. . *J Biol Chem.* 2003, 278:3311-3.

T, Y, L, Y, L, Y: Requirement of the MRN complex for ATM activation by DNA damage. *J Biol Chem.* 2003, 278:5612-21.

Valledor AF, Xaus J, Comalada M, Soler C, Celada A: Protein kinase C epsilon is required for the induction of mitogen-activated protein kinase phosphatase-1 in lipopolysaccharide-stimulated macrophages. *J Immunol.* 2000, 164:29-37.

Vanden Hoek TL, Becker LB, Shao Z, Li C, Schumacker PT. Preconditioning in cardiomyocytes protects by attenuating oxidant stress at reperfusion. *Circ Res* 2000, 86:534-40.

Vanden Hoek TL, Li C, Shao Z, Schumacker PT, Becker LB. Significant levels of oxidants are generated by isolated cardiomyocytes. *J Mol Cell Cardiol.* 1997, 29:2571-83.

S, D, M, O: MAPK-induced Ser727 phosphorylation promotes SUMOylation of STAT1. *J.* 2008, 409:179-85.

Varinou L, Ramsauer K, Karaghiosoff M, Kolbe T, Pfeffer K, Muller M, Decker T: Phosphorylation of the Stat1 transactivation domain is required for full-fledged IFN-gamma-dependent innate immunity. *Immunity.* 2003, 19:793-802.

Vaux DL, Cory S, Adams JM: Bcl-2 gene promotes haemopoietic cell survival and cooperates with c-myc to immortalize pre-B cells. *Nature.* 1988, 335:440-2.

Verhagen AM, Ekert PG, Pakusch M, Silke J, Connolly LM, Reid GE, Moritz RL, Simpson RJ, Vaux DL: Identification of DIABLO, a mammalian protein that promotes apoptosis by binding to and antagonizing IAP proteins. *Cell.* 2000, 7:102:43-53.

BQ, Arenzana TL, Showalter BM, Losman J, Chen XP, Mosteck J, Banks AS, Limnander A, Fernandez N, Rothman PB. SOCS-1 localizes to the microtubule organizing complex-associated 20S proteasome. *Mol Cell Biol.* 2004, 24:9092-101.

Wada T, Penninger JM: Mitogen-activated protein kinases in apoptosis regulation. *Oncogene* 2004, 23:2838-2849.

Wang Y, Meyer JW, Ashraf M, Shull GE.: Mice with a null mutation in the NHE1 Na⁺-H⁺ exchanger are resistant to cardiac ischemia-reperfusion injury. *Circ Res.* 2003, 93:776-82

Wang Y, Wu TR, Cai S, Welte T, Chin YE: Stat1 as a component of tumor necrosis factor alpha receptor 1-TRADD signaling complex to inhibit NF-kappaB activation. *Mol. Cell Biol.* 2000, 20:4505-4512.

Welte T, Zhang SS, Wang T, Zhang Z, Hesslein DG, Yin Z, Kano A, Iwamoto Y, et al.: STAT3 deletion during hematopoiesis causes Crohn's disease-like pathogenesis and lethality: a critical role of STAT3 in innate immunity. *Natl Acad Sci U S A.* 2003, 100:1879-84.

Wen X, Lin HH, Shih HM, Kung HJ, Ann DK: Kinase activation of the non-receptor tyrosine kinase Etk/BMX alone is sufficient to transactivate STAT-mediated gene expression in salivary and lung epithelial cells. *J Biol Chem.* 1999, 274:38204-10.

Wencker D, Chandra M, Nguyen K, Miao W, Garantziotis S, Factor SM, Shirani J, Armstrong RC, Kitsis RN: A mechanistic role for cardiac myocyte apoptosis in heart failure. *J.Clin.Invest* 2003, 111:1497-1504.

Wenta N, Strauss H, Meyer S, Vinkemeier U: Tyrosine phosphorylation regulates the partitioning of STAT1 between different dimer conformations. *Natl Acad Sci U S A.* 2008, 105:9238-43.

- Weston CR, Davis RJ: The JNK signal transduction pathway. *Curr Opin Genet Dev.* 2002, 12:14-21.
- Wiedemann N, van der Laan M, Hutu DP, Rehling P, Pfanner N: Sorting switch of mitochondrial presequence translocase involves coupling of motor module to respiratory chain. *J Cell Biol.* 2007, 179:1115-22.
- Wierenga AT, Vogelzang I, Eggen BJ, Vellenga E. Erythropoietin-induced serine 727 phosphorylation of STAT3 in erythroid cells is mediated by a MEK-, ERK-, and MSK1-dependent pathway. *Exp Hematol.* 2003;31:398-405.
- Williams L, Bradley L, Smith A, Foxwell B: Signal transducer and activator of transcription 3 is the dominant mediator of the anti-inflammatory effects of IL-10 in human macrophages. *J.Immunol.* 2004, 172:567-576.
- Williams LM, Ricchetti G, Sarma U, Smallie T, Foxwell BM: Interleukin-10 suppression of myeloid cell activation--a continuing puzzle. *Immunology* 2004, 113:281-292.
- Williams LM, Sarma U, Willets K, Smallie T, Brennan F, Foxwell BM: Expression of constitutively active STAT3 can replicate the cytokine-suppressive activity of interleukin-10 in human primary macrophages. *J Biol Chem.* 2007, 282:6965-75.
- Xu B, Bhattacharjee A, Roy B et al. Interleukin-13 induction of 15-lipoxygenase gene expression requires p38 mitogen-activated protein kinase-mediated serine 727 phosphorylation of Stat1 and Stat3. *Mol Cell Biol.* 2003;23:3918-3928.
- Wu TR, Hong YK, Wang XD, Ling MY, Dragoi AM, Chung AS, Campbell AG, Han ZY, Feng GS, Chin YE: SHP-2 is a dual-specificity phosphatase involved in Stat1 dephosphorylation at both tyrosine and serine residues in nuclei. *J Biol Chem.* 2002, 277:47572-8
- Xia Z, Dickens M, Raingeaud J, Davis RJ, Greenberg ME: Opposing effects of ERK and JNK-p38 MAP kinases on apoptosis. *Science.* 1995, 270:1326-31.
- Xu B, Bhattacharjee A, Roy B et al. Interleukin-13 induction of 15-lipoxygenase gene expression requires p38 mitogen-activated protein kinase-mediated serine 727 phosphorylation of Stat1 and Stat3. *Mol Cell Biol.* 2003;23:3918-3928.
- Xuan YT, Guo Y, Han H, Zhu Y, Bolli R: An essential role of the JAK-STAT pathway in ischemic preconditioning. *Proc.Natl.Acad.Sci.U.S.A* 2001, 98:9050-9055.
- Xuan YT, Guo Y, Zhu Y, Han H, Langenbach R, Dawn B, Bolli R: Mechanism of cyclooxygenase-2 upregulation in late preconditioning. *J.Mol.Cell Cardiol.* 2003, 35:525-537.
- Xuan YT, Guo Y, Zhu Y, Wang OL, Rokosh G, Messing RO, Bolli R: Role of the protein kinase C-epsilon-Raf-1-MEK-1/2-p44/42 MAPK signaling cascade in the activation of signal transducers and activators of transcription 1 and 3 and induction of cyclooxygenase-2 after ischemic preconditioning. *Circulation* 2005, 112:1971-1978.
- Xuan YT, Tang XL, Banerjee S, Takano H, Li RC, Han H, Qiu Y, Li JJ, Bolli R: Nuclear factor-kappaB plays an essential role in the late phase of ischemic preconditioning in conscious rabbits. *Circ.Res.* 1999, 84:1095-1109.

- Yamamoto M, Sato S, Hemmi H, Hoshino K, Kaisho T, Sanjo H, Takeuchi O, Sugiyama M, Okabe M, Takeda K, Akira S: Role of adaptor TRIF in the MyD88-independent toll-like receptor signaling pathway. *Science* 2003, 301:640-643.
- Yamamoto M, Takeda K, Akira S: TIR domain-containing adaptors define the specificity of TLR signaling. *Mol Immunol.* 2004, 40:861-8.
- Yamamoto T, Sekine Y, Kashima K, Kubota A, Sato N, Aoki N, Matsuda T: The nuclear isoform of protein-tyrosine phosphatase TC-PTP regulates interleukin-6-mediated signaling pathway through STAT3 dephosphorylation. *Biophys Res Commun.* 2002, 297:811-7.
- Yamano K, Yatsukawa Y, Esaki M, Hobbs AE, Jensen RE, Endo T: Tom20 and Tom22 share the common signal recognition pathway in mitochondrial protein import. *J Biol Chem.* 2008, 283:3799-807.
- Yang E, Lerner L, Besser D, Darnell JE Jr: Independent and cooperative activation of chromosomal c-fos promoter by STAT3. *J Biol Chem.* 2003, 278:15794-9.
- L, DE, SJ, H, M, WH, G, Y, J, SF. Autophagy in chronically ischemic myocardium. *Natl Acad Sci U S A.* 2005, 102:13807-12.
- J, -Kishore M, SM, H, K, DE, GR: Novel roles of unphosphorylated STAT3 in oncogenesis and transcriptional regulation. *Res.* 2005, 65:939-47.
- J, X, MK, L, PE, GR: Unphosphorylated STAT3 accumulates in response to IL-6 and activates transcription by binding to NFkappaB. *Dev.* 2007, 21:1396-408.
- Yang JC, Cortopassi GA: Induction of the mitochondrial permeability transition causes release of the apoptogenic factor cytochrome c. *Free Radic Biol Med.* 1998, 24:624-31.
- Yang LZ, Kockskämper J, Heinzel FR, Hauber M, Walther S, Spiess J, Pieske B: Urocortin II enhances contractility in rabbit ventricular myocytes via CRF(2) receptor-mediated stimulation of protein kinase A. *Cardiovasc Res.* 2006, 69:402-11.
- Yang XO, Panopoulos AD, Nurieva R, Chang SH, Wang D, Watowich SS, Dong C: STAT3 regulates cytokine-mediated generation of inflammatory helper T cells. *J Biol Chem.* 2007, 282:9358-63.
- Yang XP, Irani K, Mattagajasingh S, Dipaula A, Khanday F, Ozaki M, Fox-Talbot K, Baldwin WM, III, Becker LC: Signal transducer and activator of transcription 3alpha and specificity protein 1 interact to upregulate intercellular adhesion molecule-1 in ischemic-reperfused myocardium and vascular endothelium. *Arterioscler.Thromb.Vasc.Biol.* 2005, 25:1395-1400.
- Yaoita H, Ogawa K, Maehara K, Maruyama Y: Attenuation of ischemia/reperfusion injury in rats by a caspase inhibitor. *Circulation.* 1998, 97:276-81.
- Yasukawa H, Hoshijima M, Gu Y, Nakamura T, Pradervand S, Hanada T, Hanakawa Y, Yoshimura A, Ross J, Jr., Chien KR: Suppressor of cytokine signaling-3 is a biomechanical stress-inducible gene that suppresses gp130-mediated cardiac myocyte hypertrophy and survival pathways. *J.Clin.Invest* 2001, 108:1459-1467.

Yasukawa H, Misawa H, Sakamoto H, Masuhara M, Sasaki A, Wakioka T, Ohtsuka S, Imaizumi T, Matsuda T, Ihle JN, Yoshimura A: The JAK-binding protein JAB inhibits Janus tyrosine kinase activity through binding in the activation loop. *EMBO J.* 1999, 18:1309-20.

Yasukawa H, Ohishi M, Mori H, Murakami M, Chinen T, Aki D, Hanada T, Takeda K, Akira S, Hoshijima M, Hirano T, Chien KR, Yoshimura A: IL-6 induces an anti-inflammatory response in the absence of SOCS3 in macrophages. *Nat.Immunol.* 2003, 4:551-556.

Yellon DM, Hausenloy DJ: Myocardial reperfusion injury. *Engl J Med.* 2007, 357:1121-35.

Yi AK, Yoon JG, Yeo SJ, Hong SC, English BK, Krieg AM: Role of mitogen-activated protein kinases in CpG DNA-mediated IL-10 and IL-12 production: central role of extracellular signal-regulated kinase in the negative feedback loop of the CpG DNA-mediated Th1 response. *J Immunol.* 2002, 168:4711-4720.

Yi AK, Yoon JG, Yeo SJ, Hong SC, English BK, Krieg AM: Role of mitogen-activated protein kinases in CpG DNA-mediated IL-10 and IL-12 production: central role of extracellular signal-regulated kinase in the negative feedback loop of the CpG DNA-mediated Th1 response. *J Immunol.* 2002, 168:4711-4720.

Yokogami K, Wakisaka S, Avruch J, Reeves SA. Serine phosphorylation and maximal activation of STAT3 during CNTF signaling is mediated by the rapamycin target mTOR. *Curr Biol.* 2000;10:47-50.

Yoshimura A, Naka T, Kubo M: SOCS proteins, cytokine signalling and immune regulation. *Nat Rev Immunol.* 2007, 7:454-65.

CL, R, SJ: Constitutive activation of the Janus kinase-STAT pathway in T lymphoma overexpressing the Lck protein tyrosine kinase. *Immunol.* 1997, 159:5206-10.

CL, DJ, GS, AC, -Su C, J, R: Enhanced DNA-binding activity of a Stat3-related protein in cells transformed by the Src oncoprotein. . 1995, 269:81-3.

Yue TL, Wang C, Gu JL, Ma XL, Kumar S, Lee JC, Feuerstein GZ, Thomas H, Maleeff B, Ohlstein EH: Inhibition of extracellular signal-regulated kinase enhances Ischemia/Reoxygenation-induced apoptosis in cultured cardiac myocytes and exaggerates reperfusion injury in isolated perfused heart. *Circ Res.* 2000, 86:692-9.

Yusuf S, Hawken S, Ounpuu S, Dans T, Avezum A, Lanan F, McQueen M, Budaj A, Pais P, Varigos J, Lisheng L; INTERHEART Study Investigators: Effect of potentially modifiable risk factors associated with myocardial infarction in 52 countries (the INTERHEART study): case-control study. . 2004, 364:937-52.

Zarubin T, Han J: Activation and signaling of the p38 MAP kinase pathway. *Cell Res.* 2005, 15:11-18.

Zha J, Harada H, Yang E, Jockel J, Korsmeyer SJ: Serine phosphorylation of death agonist BAD in response to survival factor results in binding to 14-3-3 not BCL-X(L). *Cell.* 1996, 87:619-28.

Zhang J, Yang J, Roy SK, Tininini S, Hu J, Bromberg JF, Poli V, Stark GR, Kalvakolanu DV: The cell death regulator GRIM-19 is an inhibitor of signal transducer and activator of transcription 3. *Proc Natl Acad Sci U S A*. 2003, 100:9342-7.

JG, Farley A, Nicholson SE, Willson TA, Zugaro LM, Simpson RJ, Moritz RL, Cary D, Richardson R, Hausmann G, Kile BJ, Kent SB, Alexander WS, Metcalf D, Hilton DJ, Nicola NA, Baca M. The conserved SOCS box motif in suppressors of cytokine signaling binds to elongins B and C and may couple bound proteins to proteasomal degradation. *Proc Natl Acad Sci U S A*. 1999, 96:2071-6

JG, Metcalf D, Rakar S, Asimakis M, Greenhalgh CJ, Willson TA, Starr R, Nicholson SE, Carter W, Alexander WS, Hilton DJ, Nicola NA. The SOCS box of suppressor of cytokine signaling-1 is important for inhibition of cytokine action in vivo: *Proc Natl Acad Sci U S A*. 2001, 98:13261-5.

Zhang X, Guo A, Yu J, Possemato A, Chen Y, Zheng W, Polakiewicz RD, Kinzler KW, Vogelstein B, Velculescu VE, Wang ZJ: Identification of STAT3 as a substrate of receptor protein tyrosine phosphatase T. *Proc Natl Acad Sci U S A*. 2007, 104:4060-4.

Zhang X, Shan P, Alam J, Fu XY, Lee PJ: Carbon monoxide differentially modulates STAT1 and STAT3 and inhibits apoptosis via a phosphatidylinositol 3-kinase/Akt and p38 kinase-dependent STAT3 pathway during anoxia-reoxygenation injury. *J Biol Chem*. 2005, 280:8714-8721.

Zhang Y, Blattman JN, Kennedy NJ, Duong J, Nguyen T, Wang Y, Davis RJ, Greenberg PD, Flavell RA, Dong C: Regulation of innate and adaptive immune responses by MAP kinase phosphatase 5. *Nature* 2004, 430:793-797.

Zhang Y, Cho YY, Petersen BL et al. Ataxia telangiectasia mutated proteins, MAPKs, and RSK2 are involved in the phosphorylation of STAT3. *J Biol Chem*. 2003;278:12650-12659.

Zhang Y, Wada J, Hashimoto I, Eguchi J, Yasuhara A, Kanwar YS, Shikata K, Makino H: Therapeutic approach for diabetic nephropathy using gene delivery of translocase of inner mitochondrial membrane 44 by reducing mitochondrial superoxide production. *Am Soc Nephrol*. 2006, 17:1090-101.

Zhao Q, Shepherd EG, Manson ME, Nelin LD, Sorokin A, Liu Y: The role of mitogen-activated protein kinase phosphatase-1 in the response of alveolar macrophages to lipopolysaccharide: attenuation of proinflammatory cytokine biosynthesis via feedback control of p38. *J Biol Chem*. 2005, 280:8101-8108.

Zhao Q, Wang X, Nelin LD, Yao Y, Matta R, Manson ME, Baliga RS, Meng X, Smith CV, Bauer JA, Chang CH, Liu Y: MAP kinase phosphatase 1 controls innate immune responses and suppresses endotoxic shock. *J Exp.Med* 2006, 203:131-140.

Zhao Q, Wang X, Nelin LD, Yao Y, Matta R, Manson ME, Baliga RS, Meng X, Smith CV, Bauer JA, Chang CH, Liu Y. MAP kinase phosphatase 1 controls innate immune responses and suppresses endotoxic shock. *J Exp Med*, 2006, 203:131-40.

Zhao ZQ: Oxidative stress-elicited myocardial apoptosis during reperfusion. *Curr.Opin.Pharmacol* 2004, 4:159-165.

Zhong M, Henriksen MA, Takeuchi K, Schaefer O, Liu B, ten Hoeve J, Ren Z, Mao X, Chen X, Shuai K, Darnell JE, Jr.: Implications of an antiparallel dimeric structure of nonphosphorylated STAT1 for the activation-inactivation cycle. *Proc.Natl.Acad.Sci.U.S.A* 2005, 102:3966-3971.

M, Henriksen MA, Takeuchi K, Schaefer O, Liu B, ten Hoeve J, Ren Z, Mao X, Chen X, Shuai K, Darnell JE Jr.: Implications of an antiparallel dimeric structure of nonphosphorylated STAT1 for the activation-inactivation cycle. *Proc Natl Acad Sci U S A*. 2005, 102:3966-71.

Zhou XM, Liu Y, Payne G, Lutz RJ, Chittenden T: Growth factors inactivate the cell death promoter BAD by phosphorylation of its BH3 domain on Ser155. *Biol Chem*. 2000, 275:25046-51.

M, -Porenta O, -Pleskovic R, N, D. Apoptosis of myocytes and proliferation markers as prognostic factors in end-stage dilated cardiomyopathy. *Pathol*. 2003, 12:36-9.

Zorov DB, Filburn CR, Klotz LO, Zweier JL, Sollott SJ: Reactive oxygen species (ROS)-induced ROS release: a new phenomenon accompanying induction of the mitochondrial permeability transition in cardiac myocytes. *Exp Med*. 2000, 192:1001-14.

Zou H, Henzel WJ, Liu X, Lutschg A, Wang X: Apaf-1, a human protein homologous to *C. elegans* CED-4, participates in cytochrome c-dependent activation of caspase-3. *Cell*. 1997, 90:405-13.

Zweier JL, Flaherty JT, Weisfeldt ML: Direct measurement of free radical generation following reperfusion of ischemic myocardium. *Proc Natl Acad Sci U S A*. 1987, 84:1404-7